UNIVERSITEIT VAN PRETORIA
UNIVERSITY OF PRETORIA
YUNIBESITHI YA PRETORIA

DIAGNOSTIC IMAGING ASPECTS OF *Spirocerca lupi* INFECTION IN THE DOG

By

ROBERT MURCO KIRBERGER

Submitted in fulfilment of the requirements for the degree

DOCTOR OF VETERINARY SCIENCE

in the

DEPARTMENT OF COMPANION ANIMAL CLINICAL STUDIES
FACULTY OF VETERINARY SCIENCE
UNIVERSITY OF PRETORIA
2013

DECLARATION

I hereby declare that

This collection of publications has not previously been submitted to this or any other tertiary institution for such a doctoral degree.

These publications, in which I am the senior or co-author, were prepared as a member of a team of investigators with my contribution being primarily the diagnostic imaging components of the papers or intellectual contributions.

The collection of publications making up this dissertation is submitted with the permission of the copyright holders of the various papers and the book chapter is reproduced with the permission of Wiley-Blackwell, the publishers.

R M Kirberger

2013:02:05

ACKNOWLEDGEMENTS

My thanks to the following:

To my wife Melinda, who over the span of my academic career of more than 25 years, has consistently supported the development of my university career. This was not always plain sailing because as a clinician with a heavy clinical load, a lot of research writing had to be, and still is, done after hours at home. You had to share your husband with a computer which has not always been easy. Your indirect contribution to this dissertation is much appreciated and has made me love you even more.

Eran Dvir, who together with me, has been the main driving force of *Spirocerca lupi* research and publications within our Faculty over the last 12 years. We have been sounding boards for each other and have been involved together in most of the research projects and without him many of the publications in this dissertation would not have materialized and the degree would not have been possible. It is only fitting that he received his PhD in 2012 for his work on spirocercosis.

Liesel van der Merwe who initiated the spirocercosis study group at Onderstepoort and the prospective clinical trial which generated the material for all the publications post 2007, as well as being senior or co-author of many of these publications.

My sincere thanks are extended to all my co-workers who made many of the publications possible. My association with the following co-authors was peripheral and I hereby acknowledge their contributions to the publications making up this dissertation: Ann Carstens, Jevan Christie, Ninette Keller, Vari Mukorera, Vinny Naidoo, Samantha Thompkins and Mark Williams. I had a much closer association with the following co-workers which were either senior authors publishing under my guidance or played a significant role in the collection of data or sample interpretation: Avi Avner, Nicky Cassel, Sarah Clift, Dieter Malleczek, Nerissa Stander, Paolo Pazzi, Audrey Petite, Erna von Wilpe and Anthony Zambelli. I appreciate your significant contributions to this dissertation.

Prof Sybrand van den Berg, head of the former Department of Surgery, the department in which I started my academic career, for his support during those early years in giving me free reign to develop my research interests.

Over my many years at Onderstepoort I have always had the support and help of the hospital radiographers. More recently, special thanks to Bev Olivier and Lizette Neethling for their assistance. A special thanks to Melanie McLean who was and is always willing to help with my research projects. This is particularly so in more recent years with the acquisition of the hospital CT machine. Many times after work she has had to upload saved research data back on the CT machine for me to collect data from old cases. Thanks Melanie!

Antoinette Lourens from the Department of Library Services for always being prepared to assist with my queries and requests.

Prof Johan Schoeman for his support, advice and proofreading of the manuscript.

Sandra Wilkinson for formatting and printing this dissertation.

The National Research Foundation which supplied funding for the prospective spirocercosis trial.

It has been a rewarding 12 years working on the diagnostic imaging aspects of spirocercosis. The group of clinicians working in the Onderstepoort Veterinary Academic Hospital have over this period made a significant contribution to our understanding of this unique disease, particularly its clinical diagnosis and the determination of whether oesophageal nodules have undergone malignant transformation and the pathophysiology of this transformation. I believe the Onderstepoort *S. lupi* study group are world leaders in this field and I am grateful that I could have made a diagnostic imaging contribution to this body of international expertise.

SUMMARY

This collection of one book chapter and 12 peer reviewed scientific papers comprises of 7 chapters. The first chapter starts with a 2008 review article as an introduction. This was a comprehensive review of *Spirocerca lupi* with an extensive section on diagnostic imaging, which included the value of computed tomography. The second publication in the first chapter deals with our first paper in 2001 which described in detail the radiographic characteristics of the spondylitis reactions as well as the oesophageal masses, which could be typical or atypical. Aortic aneurysm formation as well as aortic mineralisation visibility was also reported on. Additionally, the value of computed tomography (CT) in spirocercosis was elucidated for the first time. This is the first *S. lupi* article to extensively describe the imaging findings from a radiological viewpoint and to combine these with the clinical findings. To date this paper is still regularly referenced.

The second chapter emphasizes the value of a variety of radiographic techniques, including pneumoesophagography, to optimize the diagnosis of spirocercosis as a primary imaging modality. Radiography remains the cheapest and most readily accessible diagnostic imaging technique and as such making the correct technical decisions, as proven in these 3 papers, optimizes diagnostic capabilities in a cost-effective way for the first time.

The third chapter examines the value of CT and alternative imaging techniques in *S. lupi* associated disorders to diagnose spirocercosis and its complications. These include the limited value of ultrasonography and the very important role CT, as well as CT angiography, has to play. Computed tomography was shown to play a major role in detecting aortic changes, in decision-making for surgical removal of neoplastic oesophageal masses, as well as in detecting and determining the extent of secondary changes associated with spirocercosis. The value of CT, first described by us in 2001, is amplified in these publications and has become an essential imaging tool to manage this disease. Magnetic resonance imaging is not available at the Onderstepoort Veterinary Academic Hospital and as such was not addressed in this dissertation. However, its primary use in spirocercosis is in diagnosing aberrant larval migration to the vertebral canal.

The fourth chapter discusses the perplexing matter of malignant transformation of the *S. lupi* associated benign oesophageal nodule and how to diagnose it. This is an on-going investigation in our department, but this chapter contains the first publication that linked diagnostic imaging findings with clinical parameters in an attempt to determine if malignant transformation of the nodule had taken place. The latter is vitally important in determining prognosis and treatment. Once malignancy is present, metastatic spread can take place to

many parts of the body. Two case reports are presented with hitherto undescribed metastatic spread to the central nervous system from the primary oesophageal neoplasm.

The fifth chapter looks at the pathomechanisms of spondylitis formation in spirocercosis by means of a radiological-pathological investigation. This is the first in-depth veterinary investigation on how vertebral new bone formation takes place and whether inflammation plays a role.

The sixth chapter, consisting of a review paper published in 2010, brought together more recent thoughts on some of the dilemmas still facing clinicians in the diagnosis and treatment of spirocercosis.

The final chapter concludes with a discussion of the most appropriate imaging procedures to use in diagnosing spirocercosis and its complications. Additionally challenges remaining and future research directions are considered.

CONTENTS

Introduction

Spirocerca lupi is a common helminth in many parts of South Africa, including the Onderstepoort area. As such it was and still is commonly diagnosed in dogs in the Onderstepoort Veterinary Academic Hospital's outpatient clinic. These dogs usually present with regurgitation or vomiting and radiography is often the first diagnostic procedure performed to confirm spirocercosis and to rule out an oesophageal foreign body. Over the last 10-15 years it has been the subjective opinion of many clinicians that the disease incidence is increasing. This could be because of environmental factors, but most certainly also because of greater awareness of the disease and improved diagnostic techniques, and in particular, diagnostic imaging techniques.

I joined the Radiology Section of the then Department of Surgery in 1988 to become a specialist radiologist. I achieved this qualification in 1991 and over the years have spent much time being involved in imaging clinical cases of spirocercosis as well as numerous spirocercosis-related research projects with colleagues which has culminated in this dissertation.

I was fortunate that in January 1998 Dr Eran Dvir came to the then Medicine Department, as a clinical assistant to specialize in small animal internal medicine. It was my pleasure to help him with the first 2 articles that he published. The second of these in 2001, which was our publication on the clinical and diagnostic imaging aspects of spirocercosis, is to this day still regularly referenced worldwide by workers in the field. After qualifying as a specialist Dr Dvir left the Faculty, but returned in December 2006 as an associate professor in medicine. Since that time we have worked closely together on many aspects of spirocercosis and he has gone on to obtain a PhD on spirocercosis and became a leading figure internationally on the disease. It has indeed been a pleasure to see Prof Dvir's academic career develop over the years and to see the student exceeding the original master.

With the return of Prof Dvir to Onderstepoort a Spirocercosis study group was established in 2007 under the guidance and chair of Dr Liesel van der Merwe. One of the main objectives of the group, which consisted of physicians, radiologists, pathologists and pharmacologists, was to set up a prospective study involving all *S. lupi* infected clinical cases presented to our hospital. Research projects were identified to make use of this study material in the various disciplines and post graduate students were identified to run some of the projects. Dr van der Merwe left the Faculty at the end of 2011 and Prof Dvir took over the chair of the group. The trial is still ongoing and currently stands at 185 cases enrolled in the study. With the acquisition of a CT machine for the hospital all spirocerca cases admitted to the trial received a comprehensive thoracic CT examination, including angiography, which was funded by my National Research Foundation grant, creating more research material. To date, since the inception of the study group, 18 articles have been published in peer-reviewed ISI-accredited journals, numerous local and international congress presentations have been made and 2 master's degrees and one PhD have been awarded. Currently 2 students are still busy with their dissertations and numerous research projects are still ongoing.

I have been privileged to work with numerous excellent clinicians during my career at Onderstepoort. Many of those were involved in the subject material for this dissertation and

they are acknowledged elsewhere. This dissertation on Diagnostic Imaging Aspects of *Spirocerca lupi* is also a credit to their contributions to the study of this fascinating parasite and its various manifestations.

Chapter 1

Review and the first imaging descriptions

van der Merwe LL, **Kirberger RM,** Clift S, Williams M, Keller N, Naidoo V. *Spirocerca lupi* infection in the dog: A review. *The Veterinary Journal* 2008;176:294-309.

Dvir E, **Kirberger RM,** Malleczek D. Radiographic and computed tomographic changes and clinical presentation of spirocercosis in the dog. *Veterinary Radiology & Ultrasound* 2001;42:119-129.

Prior to the above articles there was minimal information available to radiologists on the imaging aspects of spirocercosis. W S Bailey (Department of Pathology and Parasitology, School of Veterinary Medicine, Auburn University, USA) was the primary worker on spirocercosis and published extensively on its life cycle and pathophysiology from the 1950s through to the 1970s.[1,2] These excellent articles, which also had radiograph illlustrations,[1] formed the basis for many years on what to look for on radiographs - namely a caudal oesophageal mass and spondylitis. The latter, in its typical location, affecting the caudal thoracic vertebra was considered pathognomonic for spirocercosis by Bailey.[1] However at that stage the vertebral reactions appear to have been described using the variable terminology of spondylosis and spondylitis.[2] In 1974 an article described the use of angiography to determine aortic displacement by oesophageal masses but no specific mention was made about the diagnosis of aortic aneurysms or mineralisation.[3] Scarring of the aorta is a typical result of the larval migration via the aorta to the oesophagus. The end result of the aortic migration is often calcification and ossification of the aortic wall.[2] Radiographically this mineralization was first described by Fox in 1998.[4]

The review by v/d Merwe, Kirberger *et al* brought together the current knowledge on *S. lupi* in 2008 and is frequently cited as the standard overview reference on spirocercosis. The review included a lot of the Onderstepoort spirocercosis study group's experiences at that time as well as an extensive section on diagnostic imaging, which included the value of computed tomography. Many of the statements made in the review have subsequently been corroborated and published by the Onderstepoort group.

The second article in this chapter, published in 2001, was the first to describe in detail the radiographic characteristics of the spondylitis reactions as well as the oesophageal masses, which could be typical or atypical. Aortic aneurysm formations as well as aortic mineralisation visibility were also reported on. Additionally, the 3 cases that underwent CT emphasized the value of this modality to better evaluate many of the changes seen in spirocercosis. The cross sectional CT images lend themselves to detailed mass description, increased sensitivity to detect aortic and mass mineralisation, as well as secondary spirocercosis-associated thoracic changes such as metastasis, effusion and pneumonia.

References

1 Bailey WS. Parasites and cancer: sarcoma associated with *Spirocerca lupi*. Ann NY Acad Sci 1963;108:890-923.

2 Bailey WS. *Spirocerca lupi:* A continuing enquiry. Vet Parasitol 1972;58:3-22.

3 Singh J, Bhargava AK, Tyagi RPS. Angiographic findings for the diagnosis of the *Spirocerca* infestations in dogs. Haryana Agr Univ J Res 1974;4:18-21.

4 Fox MS, Bums J, Hawkins J. Spirocercosis in dogs. Comp Cont Ed 1988;10:807-823.

Available online at www.sciencedirect.com
ScienceDirect
The Veterinary Journal 176 (2008) 294–309
The Veterinary Journal
www.elsevier.com/locate/tvjl

Review

Spirocerca lupi infection in the dog: A review

Liesel L. van der Merwe *, Robert M. Kirberger, Sarah Clift, Mark Williams, Ninette Keller, Vinny Naidoo

Department of Companion Animal Clinical Studies, Faculty of Veterinary Science, University of Pretoria, Gauteng 0110, South Africa

Accepted 28 February 2007

Abstract

Spirocercosis is a disease occurring predominantly in Canidae, caused by the nematode *Spirocerca lupi*. Typical clinical signs are regurgitation, vomiting and dyspnoea. The life-cycle involves an intermediate (coprophagous beetle) and a variety of paratenic hosts. Larvae follow a specific migratory route, penetrating the gastric mucosa of the host, migrating along arteries, maturing in the thoracic aorta before eventually moving to the caudal oesophagus. Here the worm lives in nodules and passes larvated eggs which can be detected using zinc sulphate faecal flotation. Histologically, the mature oesophageal nodule is composed mostly of actively dividing fibroblasts.

Spirocerca lupi-associated oesophageal sarcomas may occur and damage to the aorta results in aneurysms. A pathognomonic lesion for spirocercosis is spondylitis of the thoracic vertebrae. Primary radiological lesions include an oesophageal mass, usually in the terminal oesophagus, spondylitis, and undulation of the aortic border. Contrast radiography and computed tomography are helpful additional emerging modalities. Oesophageal endoscopy has a greater diagnostic sensitivity than radiography. Endoscopic biopsies are not sensitive for detecting neoplastic transformation. Doramectin is the current drug of choice, effectively killing adult worms and decreasing egg shedding. Early diagnosis of infection is still a challenge and to date no ideal regimen for prophylaxis has been published.

Keywords: Regurgitation; Dyspnoea; Neoplastic transformation; Oesophageal sarcoma; Spondylitis; Aortic aneurysm; Doramectin

Introduction

Spirocercosis is a disease caused by the nematode *Spirocerca lupi* which has a variety of clinical presentations (Dvir et al., 2001; Lobetti, 2000; Mazaki-Tovi et al., 2002). *S. lupi* is found worldwide especially in tropical and subtropical regions. This nematode has been found in many species, but affects mostly carnivores, especially Canidae (Dvir et al., 2001; Lobetti, 2000; Mazaki-Tovi et al., 2002). Clinical signs are mostly due to the migration and persistence of the larvae or adult worms within the host and secondary bacterial infections. Diagnosis in the early stages can be challenging and, unfortunately, most animals are only diagnosed once advanced disease is present. The most commonly reported clinical signs are regurgitation and vomiting (Mazaki-Tovi et al., 2002; Ranen et al., 2004). The distribution, life-cycle, pathogenesis and pathology, clinical signs, diagnosis, treatment and prevention of *S. lupi* will be discussed in this review.

Distribution

Spirocerca lupi is a nematode with a worldwide distribution in regions with a warm climate. The majority of reports are from Israel (Mazaki-Tovi et al., 2002), Greece (Mylonakis et al., 2001), Turkey, India (Ramachandran et al., 1984), Pakistan (Anataraman and Krishna, 1966), the southern United States (Dixon and McCue, 1967), Brazil (Oliviera-Sequeira et al., 2002), Kenya (Brodey et al., 1977) and South Africa (Lobetti, 2000).

In Israel, the majority (62%) of infections are diagnosed in winter whereas no seasonality was found in South Africa (Lobetti, 2000; Mazaki-Tovi et al., 2002). Spirocercosis is

* Corresponding author. Tel.: +27 12 529 8000; fax: +27 12 529 8307.
E-mail address: liesel.vdmerwe@up.ac.za (L.L. van der Merwe).

1090-0233/$ - see front matter © 2007 Elsevier Ltd. All rights reserved.
doi:10.1016/j.tvjl.2007.02.032

an emerging disease in Tel Aviv with a sevenfold increase in cases in nine years and the disease is more prevalent in urban areas, in contrast to information from the USA where the disease is more common in rural areas (Mazaki-Tovi et al., 2002).

The most important factors affecting prevalence are proximity to intermediate and paratenic (transport) hosts and the population density of infected and intermediate hosts. Prevalence data can, however, be misleading and must be interpreted with reference to the dog population sampled: stray animals versus pets, the region of the country sampled, urban versus rural and the method of diagnosis (necropsy versus faecal flotation). Prevalence data also changes over time in a specific region. These factors have been clearly demonstrated in the various studies performed in Kenya (Brodey et al., 1977; Kagira and Kanyari, 2001; Murray, 1968; Wandera, 1976). The variability in prevalence is attributed to degree of rural development, utilisation of pesticides, efforts at disease control and changing nutritional habits. Faecal surveys have shown prevalences of 57% in Sierra Leone (Kamara, 1964), 56% in Kenya (Brodey et al., 1977), 23% in India (Chandrasekharon et al., 1958), 33.5–47% in the southern United States (Dixon and McCue, 1967) and 5% in Reunion Island (Prunaux and Guignard, 1991). Prevalence based on necropsy results are 23.5% in India (Ramachandran et al., 1984), 3–78% in Kenya and 13% in South Africa (Minnaar et al., 2002). In a necropsy report from Kenya the prevalence was 85% in stray dogs and only 38% in client owned dogs (Brodey et al., 1977).

There is no sex or age predilection for infection although due to the nematode lifecycle, dogs under 6 months of age, although infected, have not yet developed oesophageal disease and the classic clinical signs (Fox et al., 1988; Wandera, 1976). There does however seem to be a breed predilection. Hounds and large breed dogs have a higher incidence of *S. lupi* than other breeds (Bailey, 1963; Lobetti, 2000). A study conducted in Greece showed a disease prevalence of 10% in 260 privately owned dogs (Mylonakis et al., 2001). However, the prevalence in subgroups differed markedly: the prevalence in trace hunting dogs was 21%, scent hunting dogs 5% and pets 0%. This indicates a definite impact of lifestyle and exposure to the intermediate or paratenic host on disease transmission. German Shepherd dogs have been overrepresented in several studies (Dvir et al., 2001; Ramachandran et al., 1984). A study from Brazil determined that poodles were predisposed (Oliviera-Sequeira et al., 2002) and in Israel the Labrador Retriever seems predisposed (Mazaki-Tovi et al., 2002). Spirocercosis has also been reported in domestic cats showing clinical signs of vomiting (Mense et al., 1992) and wild Felidae (Brodey et al., 1977; Upadhye et al., 2001).

Life-cycle

The lifecycle of *S. lupi* involves intermediate and paratenic hosts. The adult worms are found coiled within nodules in the oesophageal wall. *S. lupi* eggs containing larvae (L1) are passed from the oesophagus through the gastrointestinal tract and into the faeces or may be shed in the vomitus. A variety of species of coprophagous beetles act as intermediate hosts. Eggs are ingested by the intermediate host and the larvae encyst within the tissues and develop to infectivity (L3) within 2 months. The beetle is ingested by the final host (dog) or a paratenic host.

Infective larvae are capable of utilising a great variety of paratenic hosts including poultry, wild birds, lizards, rodents, hedgehogs and rabbits (Fox et al., 1988). The larvae can also transfer from one paratenic host to another (Fox et al., 1988). In the paratenic hosts the third stage larvae excyst and then re-encyst within host tissue where they appear as small (0.5×0.4 mm) white nodules (Sen and Anataraman, 1971). The distribution of the L3 within sthe paratenic host varies between species (Sen and Anataraman, 1971). In the lizard, *Calotes versicolor*, the larvae were found throughout the subcutis, thoracic muscles and stomach wall and averaged 54.7 (2–600) per specimen. In the grey shrew, *Suncus murinus*, cysts were mainly found in the stomach wall and were fewer in number, averaging 25.8 per specimen. In poultry and wild birds larvae develop in the wall of the crop (Bhatia et al., 1979; Brodey et al., 1977). Poultry offal has been shown to be a major source of infection in Kenya (Brodey et al., 1977) and the southern United States (Dixon and McCue, 1967). In Madras, India, 88.5% of lizards were found to be infected (Anataraman and Krishna, 1966).

The final host becomes infected by ingesting either the infected beetle or paratenic host. The paratenic host is a more probable source of infection for carnivores (Sharpilo, 1983). The L3 excyst in the stomach and penetrate the gastric mucosa within 2 h of ingestion, evidenced by petechial haemorrhages and erosions on the mucosa (Hu and Hoeppli, 1936). The gastric serosal surface is reached within 24–48 h, resulting again in haemorrhage and inflammation. Larvae migrate within the walls of the gastric and gastroepiploic arteries, where haemorrhagic lesions are evident from day 4. They reach the caudal thoracic aorta via the coeliac artery approximately 10 days after hatching and remain there from days 7 to 109 where they mature to L4 (Hu and Hoeppli, 1936). After their final moult, approximately 3 months post-infection, they migrate as immature adults, from the caudal thoracic aorta to the caudal oesophagus where they are found from days 93–227. Here they live in nodules in the submucosa and adventitia of the oesophagus (Bailey, 1963). Even larvae implanted into the host sites other than the gastrointestinal tract are eventually found in the aorta or oesophagus (Bailey, 1972).

Male and female worms can be differentiated by 60 days post-infection. Mature oesophageal nodules containing adult worms are present by 3–9 months (Bailey, 1963; Sen and Anataraman, 1971). The adult is a large spiralled pink worm with males up to 54 mm and females up to 80 mm in length (Soulsby, 1982). The female worm perforates the mucosa, establishing an opening to the lumen of

the oesophagus through which to pass eggs, then moves back to the submucosa or muscular layers to complete development (Bailey, 1972). A nodule eventually develops around the worm (Fig. 1). The adult worm can remain in the oesophagus for up to 2 years and the female may produce up to 3 million eggs per day (Bailey, 1972). Peak egg production appears to be between 140 and 205 days post-infection with a maximum of 2100 eggs per gram faeces (Sen and Anataraman, 1971).

Only about 47% of ingested larvae eventually establish themselves within the host (Bailey, 1972). In the initial 4 days of infection larval migration is non-directional and they may be found within the veins and lymphatics of the gastric wall. This is hypothesised to result in aberrant migration to other organs (Hu and Hoeppli, 1936). The stimulus for both directional and aberrant migration is still not known.

Pathogenesis and pathology

Larvae cause necrosis, haemorrhage and neutrophil exudation within the vessel walls in which they migrate, but, except for the thoracic aorta, these lesions usually heal completely. In the thoracic aorta, degenerate elastic and muscle tissue becomes fibrotic, and sometimes mineralised to form permanent intimal scars and aneurysms of varying size and number. These result by the sixth month post infection (Fig. 2) (Hu and Hoeppli, 1936; Johnson, 1992). Tissue damage in the aorta can be severe with 13/98 dogs in one experimental study dying 12–102 days post-infection

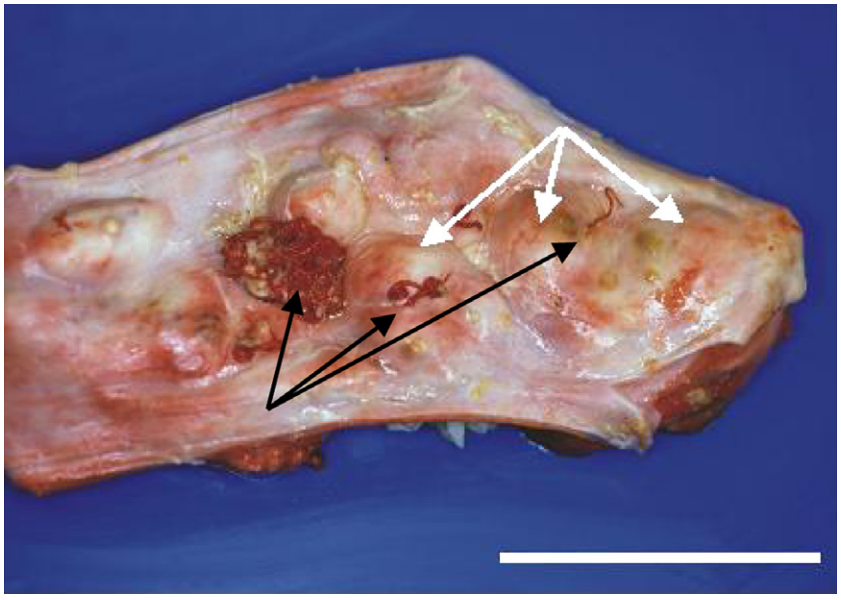

Fig. 1. The caudal oesophagus of a dog showing multiple parasitic nodules (white arrows) with red adult *S lupi* worms (black arrows). Bar = 5.5 cm.

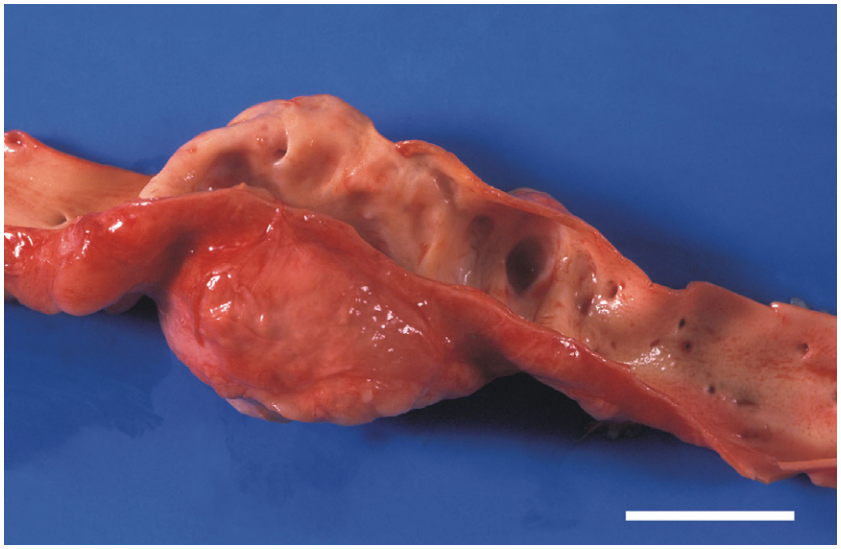

Fig. 2. The thoracic aorta of a dog with widespread *S lupi*-associated aneurysms and mineralisation of the aortic wall. Bar = 2.5 cm.

due to aortic rupture (Bailey, 1972). The severity of damage may be associated with the amount of infective larvae taken in at a single time. Metaplastic ossification of the aorta, to the extent of bone marrow formation, has been reported (Kumar et al., 1981b). Aortic lesions are the most common lesion associated with spirocercosis and are considered pathognomonic (Bailey, 1963; Ramachandran et al., 1984).

Spondylitis of the thoracic vertebrae is an almost invariable finding in spirocercosis but the pathogenesis has not been elucidated (Bailey, 1963; Ramachandran et al., 1984). As only the vertebrae directly adjacent to the descending aorta seem to be involved, aberrant migration or severe peri-aortic inflammation secondary to aortic migration are possible causes. Bailey (1963) recovered three worms embedded in muscle and connective tissue adjacent to the aorta and vertebral bodies in a dog with spondylitis at 90 days post-infection, supporting the theory of aberrant migration.

Usually there are one to four worm-containing nodules in the submucosa of the wall of the oesophagus, a few centimetres cranial to the diaphragm (Bailey, 1963; Chandrasekharon et al., 1958). The nodules vary from <1 to >4 cm in diameter and not only bulge into the lumen of the oesophagus but also distort the oesophageal wall and extend into the surrounding mediastinal tissues. The number of worms present in a nodule varies from a few to >30, but there are typically between three and six. The nodules are usually referred to as granulomas but, histologically, this is inappropriate. Initially the worms are surrounded by highly vascularised loose connective tissue, which contains fibrin-rich fluid, neutrophils and foci of necrosis. Bailey (1963), likens it to granulation tissue. Later, this tissue is composed mostly of actively dividing fibroblasts with an embryonal appearance, sometimes resembling sarcoma (Fig. 3) (Bailey, 1963; Hu and Hoeppli, 1936).

Aberrant migration of larvae is a fairly common occurrence in spirocercosis and may be responsible for the presenting clinical signs. Nodules containing worms have been found in many sites, including the stomach and intestine, mediastinum (Dvir et al., 2001), lumbar fascia (Chandrasekharon et al., 1958), rectum (Georgi et al., 1980), trachea, interdigital tissue (Bailey, 1963), lung (Stephens et al., 1983), thymus (Rajan and Mohiyuddeen, 1974), diaphragm (Harrus et al., 1996), heart (Garg et al., 1989), kidney, subcutis (Singh et al., 1999) and urinary bladder (Thanikachalam et al., 1984). Some experimentally infected dogs have demonstrated spontaneous regression of oesophageal nodules even though pathognomonic aortic lesions were present (Bailey, 1972).

Neoplastic transformation

The association between spirocercosis and neoplasia was first reported by Seibold et al. (1955), with numerous subsequent reports in the literature (Bailey, 1963; Bailey, 1972). Chronic helminthiasis is recognised as a significant factor in cancer development in humans (Herrera and Ostrosky-Wegman, 2001). Oesophageal tumours are rare in dogs and account for only 0.5% of canine neoplasms (Ridgway and Suter, 1979). Bailey (1963) summarised 39 cases diagnosed with oesophageal sarcoma. These cases were extracted from a total of 3148 necropsies. Although only 8% of all the dogs necropsied were infected with *S. lupi*, there was direct or very strong presumptive evidence of *S. lupi* infection in 38/39 dogs diagnosed with oesophageal sarcoma: 15/39 cases had adult *S. lupi* in or around the oesophageal masses, 32/39 cases had characteristic lesions

Fig. 3. Histopathological sample from an oesophageal nodule in a dog. The slide shows a segment of a cross-sectioned *S lupi* adult (white arrow) surrounded by proliferating fibroblasts with multiple small clusters of neutrophils and plasma cells. H&E. Bar = 270 μm.

in the aorta and 26/39 cases had spondylitis, indicating prior infection with *S. lupi*. The oesophageal masses were typically cauliflower like, irregular and pedunculated with a variable amount of superficial necrosis and originated in the portion of the oesophagus where *S. lupi* induced lesions are typically found (Fig. 4). Histopathologically, ossification was found in 26/39 neoplasms. These neoplasms are true malignancies since metastasis, particularly to the lungs, is frequently noted (Bailey, 1963). Osteosarcoma appears to occur more commonly than fibrosarcoma, being present in approximately in 60% of cases (Bailey, 1963).

In a report from Kenya, 42/206 spirocercosis cases had sarcomas, with 17/42 being fibrosarcomas and 25/42 osteosarcomas. Twenty-four of these cases (57%) had worms contained within the sarcomatous tissue (Wandera, 1976). A distinct age predisposition was also noted in this study with dogs younger than 2 years of age having oesophageal fibrosarcoma and those older than 5 years having osteosarcoma. In a more recent report of 15 cases, nine were diagnosed with osteosarcoma, five with fibrosarcoma and one with an undifferentiated sarcoma (Ranen et al., 2004). The vast majority of cases showing neoplastic transformation have occurred in the typical caudal oesophageal region. Three non-oesophageal *S. lupi* associated sarcomas have been reported and involved the aorta, lung and vertebra (Bailey, 1963; Stephens et al., 1983; Wandera, 1976).

A murine xenograft model of spirocerca-associated sarcoma has been established (Stettner et al., 2005). In this study, three tumours lines were established: a typical fibrosarcoma, a moderately aggressive osteosarcoma and a relatively non-aggressive osteosarcoma. This diversity in tumour lines is advantageous as their diverse behaviour patterns mimic the natural situation. This allows comparison between different tumour types, degrees of malignancy and growth rates in dogs.

Clinical signs

The clinical signs of spirocercosis vary greatly, depending on the stage of disease, aberrant migrations and possible complications. Early migration of larvae through the gastric mucosa is associated with acute onset vomition in experimental cases (Bailey, 1972; Hu and Hoeppli, 1936). An uncomplicated infection may be sub-clinical, or show vomiting or regurgitation, weight loss and dysphagia due to the development of a caudal oesophageal mass (Mazaki-Tovi et al., 2002). The dog may also breathe shallowly and sit with its head extended (Evans, 1983). A few studies characterise the clinical signs exhibited by patients affected with *S. lupi*. The data are summarised in Table 1.

Complicated cases may result from normal or aberrant nematode migration. The normal migration route along the gastro-aortic arterial system may result in either rupture of the aorta, causing haemothorax and acute death, or other major blood vessels, resulting in the development of large haematomas (Bailey, 1963; Dvir et al., 2001; Hamir, 1984). Migration through the aortic wall to the oesophagus is via the mediastinum and may result in mediastinitis, pneumomediastinum, pleuritis or pyothorax which will present clinically as dyspnoea of varying magnitudes (Dvir et al., 2001; Hamir, 1986). Some patients may develop aspiration pneumonia secondary to the oesophageal lesion.

Sialoadenosis has been associated with *S. lupi* nodules and results in moderate to severe dysphagia (Schroeder and Berry, 1998). Metastases to the lungs secondary to neoplastic transformation of the nodule may contribute to the dyspnoea. Patients with oesophageal sarcomas have also shown a strong tendency to develop hypertrophic osteopathy with subsequent lameness (Brodey et al., 1977). Concurrent bacterial infection may lead to discospondylitis

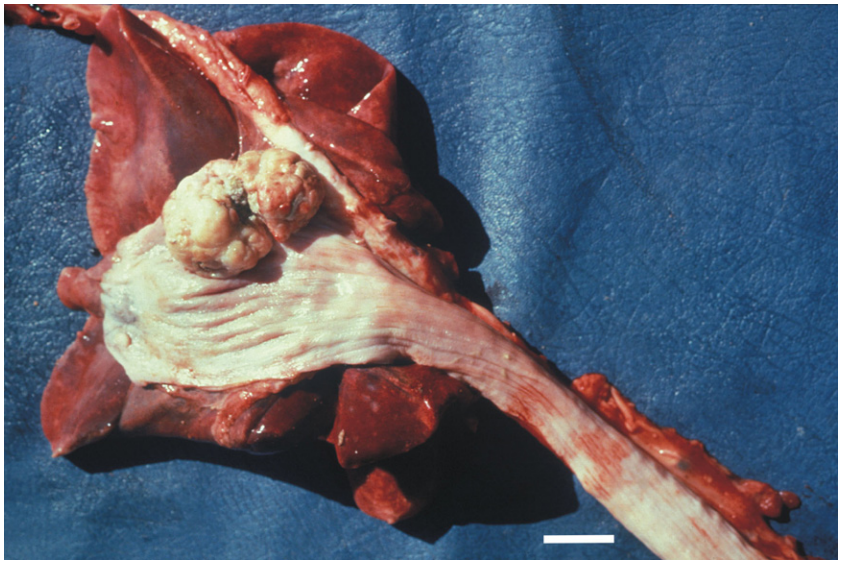

Fig. 4. Caudal oesophagus of a dog showing a cauliflower-like mass which is a *S lupi*-associated osteosarcoma with regional megaoesophagus. Bar = 5 cm.

Table 1
Clinical and clinicopathological signs associated with *S. lupi* infection

Clinical signs	Mazaki-Tovi ($n = 50$)	Dvir ($n = 27$)	Ranen ($n = 17$)
Gastrointestinal	$n = 33$ (66%)	$n = 8$ (30%)	$n = 16$ (94%)
Vomition + regurgitation	30	7	16
Melaena	9	1	5
Hypersalivation	4	5	4
Diarrhoea	4		
Dysphagia		4	
Submandibular salivary gland enlargement			5
Haematemesis			3
Respiratory	$n = 10$ (20%)	$n = 16$ (59%)	$n = 3$ (18%)
Dyspnoea	6	11	
Coughing/retching	5	7	3
Abnormal respiratory sounds		2	
Neurological	$n = 7$ (14%)	$n = 3$ (11%)	
Paraparesis	7		
Seizures		3	
Musculoskeletal	$n = 2$ (4%)	$n = 8$ (30%)	$n = 10$ (59%)
Back pain	2		
Lameness		6	
Weakness/lethargy		3	10
Other			
Pyrexia	12	14	7
Weakness	11	1	
Anorexia	9	18	7
Weight loss	5	20	6
Generalised lymphadenopathy		8	
Acute death		2	
Muffled heart sounds		1	
No clinical signs	2		
Clinical pathology	$n = 47$ (95%)		$n = 14$ (82%)
Anaemia	25		8
Leukocytosis	15		14

A composite of three separate studies (Dvir et al., 2001; Mazaki-Tovi et al., 2002; Ranen et al., 2004). It must be noted that the cases in the Ranen study were all diagnosed with oesophageal sarcoma whereas those in the first two studies were more typical spirocerca cases.

(Bailey, 1963; Fox et al., 1988), septic polyarthritis (Dvir et al., 2001), endocarditis and interstitial nephritis (Harrus et al., 1996). Non-specific clinical signs associated with *S. lupi* are pyrexia, occurring in >50% cases, and mild peripheral lymphadenopathy (Dvir et al., 2001; Mazaki-Tovi et al., 2002). Aberrant migration may result in any form of clinical disease, but the most common presentations include respiratory, neurological and musculoskeletal signs (Dvir et al., 2001).

At our hospital, signs other than regurgitation, which raise a suspicion of *S. lupi*, are dyspnoea; often only a subtle tucking in of the abdomen and flaring of the ribcage, and dysphagia; ranging from mild to severe, often associated with enlarged mandibular salivary glands and hypersalivation.

Additional reported complications of spirocercosis include aortic thromboembolism (Alvarenga and Saliba, 1971; Gal et al., 2005; Wandera, 1976), aberrant migration to the vertebral canal (Smith and Knottenbelt, 1989; Tudury et al., 1995; du Plessis et al., in press), secondary megaoesophagus (Dvir et al., 2001; Londono et al., 2003), haemopericardium (Pereira et al., 1995), oesophageal obstruction or perforation (Chandrasekharon et al., 1958; Hamir, 1986; Klainbart et al., in press) and gastro-oesophageal intussusception (Rallis et al., 1995).

Diagnosis

Faecal flotation

The female worm produces numerous small (35 × 15 μm) thick shelled larvated eggs (Fig. 5). Several factors affect the results of faecal flotation. Passage of eggs occurs for a relatively short period in the lifespan of the worm and is thus unpredictable. Eggs will only be present in the faeces when the female has a patent passage to the oesophageal lumen thus maturation of the nodule is essential. Eggs are difficult to detect in direct faecal preparations and routine flotation techniques using sugar and salt solutions thus requiring special laboratory techniques (Fox et al.,

Fig. 5. A thick-shelled larvated *S lupi* egg 35 × 15 μm. To allow for comparative sizing: *Ancylostoma caninum* eggs are usually 56–65 μm in length.

1988). The modified Stoll technique, is purported to make the solution clearer and facilitates visualisation of the eggs (Cabrera and Bailey, 1964). Flotation with sodium nitrate solution with an SG of 1.36 or supersaturated 33% zinc sulphate will concentrate the eggs. Improved diagnostic sensitivity has been shown with a modified sugar flotation technique (Markovics and Medinski, 1996). It is important to repeat a negative faecal flotation to improve diagnostic accuracy. The sensitivity of faecal flotation in the study by Mazaki-Tovi et al. (2002) was 80% ($n = 40$), with 72% of the positives detected on the first examination and the remainder on a second examination performed a few days later.

Clinical pathology

Mild anaemia is well described and is present in approximately 50% of cases (Mazaki-Tovi et al., 2002; Ranen et al., 2004). Patients whose nodules have transformed into sarcomas showed an increased incidence of microcytic hypochromic anaemia, which was ascribed to chronic blood loss and melaena due to ulceration of the oesophageal mass (Ranen et al., 2004). Patients with early disease were likely to present with normocytic normochromic anaemia (Mazaki-Tovi et al., 2002). Animals presented with advanced disease were also more likely to show leukocytosis. In one study of oesophageal osteosarcomas, 82% of cases presented with a leukocytosis, compared to only 32% of patients with earlier disease (Mazaki-Tovi et al., 2002; Ranen et al., 2004). Monocytosis was also common, whereas eosinophilia was uncommon (Mazaki-Tovi et al., 2002). There was no correlation between the white cell counts and the existence of any associated inflammatory conditions such as pneumonia or spondylitis and it thus appears that the inflammatory response is as a result of the granuloma itself (Mazaki-Tovi et al., 2002).

There are no typical reported biochemical changes in dogs with early disease other than a mildly elevated creatine kinase in 54% of dogs in the Mazaki-Tovi et al. (2002) study. Once neoplastic transformation has occurred, however, increased alkaline phosphatase, creatine kinase, amylase and lactate dehydrogenase have been noted (Ranen et al., 2004). Brodey et al. (1977) reported no blood chemistry or haematological differences between native dogs in Kenya with or without spirocercosis.

Serology

An IFA test using the mid-body region of the male worm as an antigen source that was 100% sensitive and 80% specific for *S. lupi* at a titre of 1:640 has been described (Coskun, 1995). Nothing further has been published in this potentially useful diagnostic field.

Diagnostic imaging

Radiography plays an essential role in the diagnosis of spirocercosis and is often the initial diagnostic modality. Computed tomography (CT) has recently also been shown to be valuable in diagnosing small lesions or for treatment planning (Dvir et al., 2001). In evaluating radiographic or

CT images the changes may be classified as primary or secondary (distant).

In clinically affected patients, the typical oesophageal mass will usually be seen on radiographs. In the majority of patients the mass is found in the caudal oesophagus (Dvir et al., 2001). A moderate amount of air may be present cranial to the mass. The mass is best seen on a ventrodorsal (VD) or dorsoventral (DV) view as a single midline soft tissue opacity superimposing on the caudal cardiac border and diaphragmatic cupula (Fig. 6). The left border of the descending aorta is normally a straight edge converging to the midline in the region of the cranial extent of the diaphragm. In affected dogs this line may become undulant due to aneurysm formation (Fig. 6). These changes are also occasionally seen in the ascending aorta on lateral views.

Dogs presented with a history of vomiting and undergoing abdominal radiography must also have this region evaluated on the cranial periphery of the VD abdominal radiograph. Unless large, the mass is often poorly seen on lateral views where it is located dorsally to the caudal vena cava (Fig. 7). A right lateral recumbent view is preferable as the normal oesophagus is usually not seen on this view, whereas in large breed dogs a normal oesophagus may be seen on left lateral recumbent radiographs which could be mistaken for an oesophageal mass (Avner and Kirberger, 2005). The mass may be up to 165 mm long and 100 mm high and its centre point is likely to be caudal to the eighth thoracic vertebra. The mass may contain mineralised opacities which could be ingested bone debris trapped in the irregular surface of the mass or neoplastic transformation to an osteosarcoma. Mass mineralisation is a radiographic marker for neoplastic transformation. Of the 10 dogs with neoplasia in the study by Dvir et al. (2001), two showed mineralisation of the mass on radiographs.

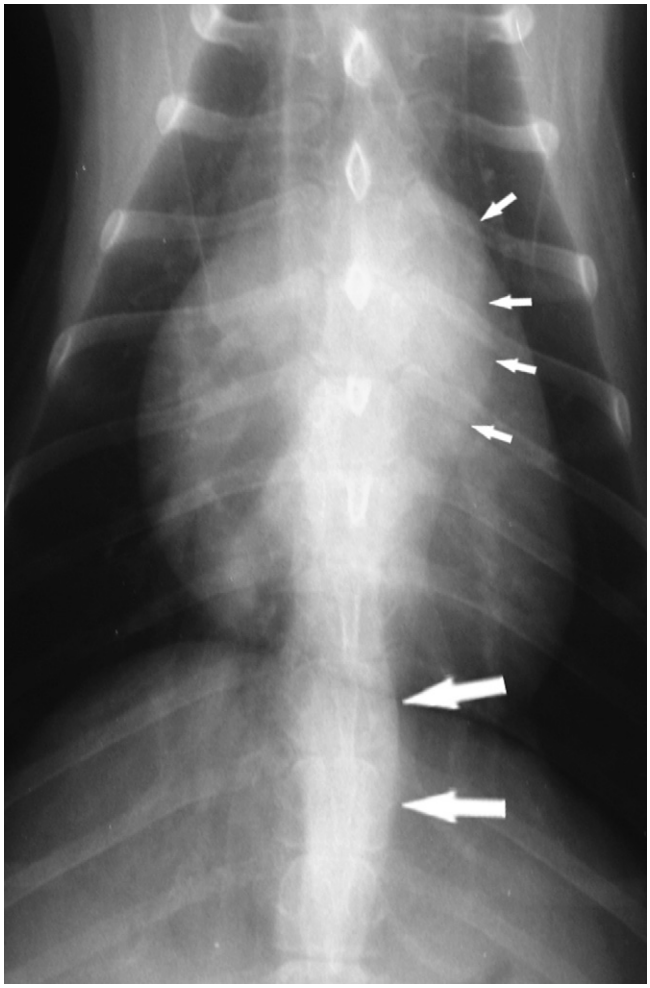

Fig. 6. Dorsoventral thoracic radiograph of a dog. The short arrows indicate the irregular outline of the left lateral border of the initial descending aorta, indicative of multiple aortic aneurysms. The large arrows indicate a typical small caudal oesophageal mass due to *S. lupi*.

On the lateral thoracic radiograph the ventral borders of the caudal thoracic vertebra should be examined for evidence of spondylitis. The ventral vertebral border is usually concave but with presumed aberrant larval migration, a secondary inflammatory reaction can take place on the vertebral body resulting in a lamellar, thick brush-like or solid periosteal reaction filling up the ventral surface of the vertebral body, giving it a rectangular or even bulging appearance (Fig. 8). Spondylitis may be seen in up to 25% of affected dogs and affects one to six vertebrae dorsal to the caudal oesophagus (T5–T12). Occasionally the disc space is bridged giving the appearance of spondylosis. Spondylitis should not be confused with the common radiological finding of spondylosis, which is a non-inflammatory osseous bridging of the intervertebral disc space. Aortic mineralisation secondary to small aneurysms is occasionally seen on the lateral view (Dvir et al., 2001; Mazaki-Tovi et al., 2002). This is seen as one or two 5–10 mm long mineralised streaks in the aortic intima and is thus seen on the dorsal or ventral edge of the thoracic aorta.

Small oesophageal nodules or more cranially located oesophageal pathology (centre point ventral to T6) are difficult to see radiologically due to superimposition of other hilar structures. Cranially located masses are generally about 70% smaller than typical caudal oesophageal masses (Dvir et al., 2001). No radiological masses were observed in 7–14% of cases (Dvir et al., 2001; Mazaki-Tovi et al., 2002). Barium sulphate may be administered and the nodule will usually be seen as a dorsal oesophageal mural filling defect (Fig. 9). An alternative technique is pneumo-oesophagography. Under general anaesthesia an endotracheal tube is placed in the oesophagus, and the latter is inflated and the tube sealed off with a stopper. Lateral, and if required DV/VD, thoracic radiographs are immediately made. This often results in excellent visibility of the nodule(s) due to the contrasting gas in the oesophagus and the surrounding lungs (Fig. 10).

Disease complications (secondary changes) detected on radiographs include tracheal or bronchial displacement or compression (Fig. 9), pleural effusion, pulmonary metastases, alveolar or interstitial lung patterns, mediastinitis,

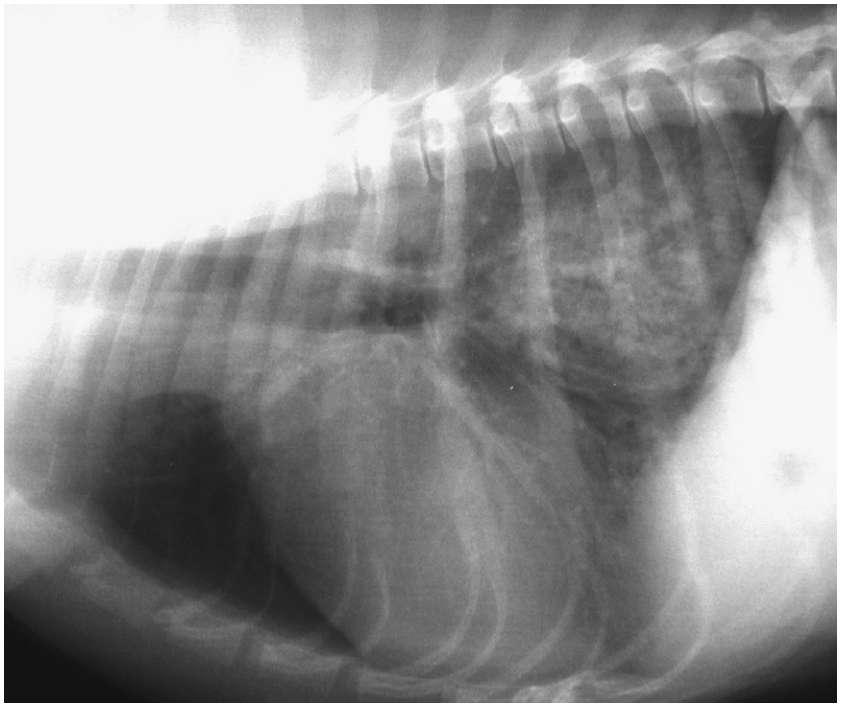

Fig. 7. Right lateral thoracic radiograph of a dog with a large poorly defined soft tissue opacity, an advanced *S. lupi* mass between the caudal vena cava and caudal thoracic aorta. See also Fig. 10.

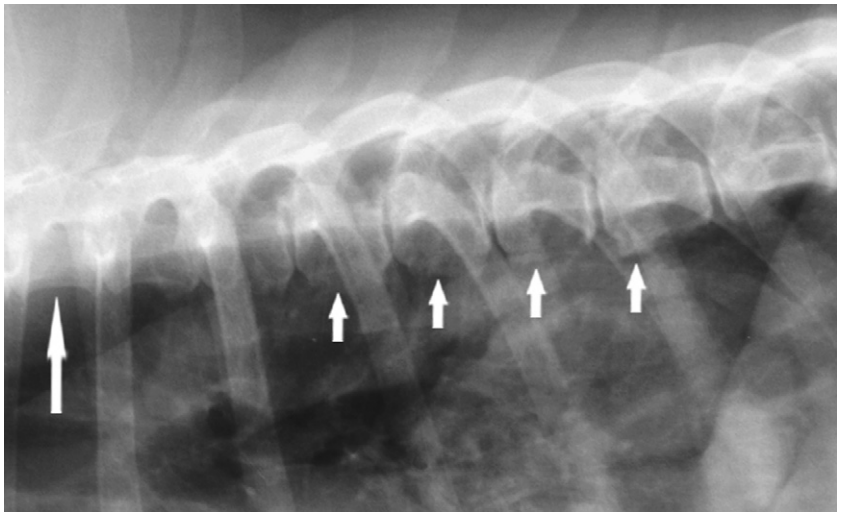

Fig. 8. Close-up lateral view of caudal thoracic vertebrae with short arrows illustrating varying degrees of ventral spondylitis. Compare these to the cranial vertebra (long arrow) with its normal ventrally concave vertebral body.

pneumothorax, mineralisation of the mass, pneumomediastinum and hypertrophic osteopathy (Dvir et al., 2001).

Computed tomography provides cross sectional slices of the thorax and images can also be reformatted into other planes. After image acquisition images can be viewed in soft tissue, bone or air windows allowing different aspects of the disease to be evaluated. In our hospital, CT is used for surgical planning, prognostication and where pleural or mediastinal fluid effaces structures on the radiograph. Adding air to the oesophagus prior to scanning is useful to better delineate the oesophageal mass. Soft tissue windows allow for evaluating the extent of the lesion, identifying pleural, mediastinal and pulmonary pathology, and assessing lesion and aortic mineralisation (Fig. 11). Bone windows allow better evaluation of spondylitis and lung windows allow for detection of pulmonary changes not seen on radiographs such as pulmonary metastases. Intravenous contrast medium administration may assist in delineating pathology in certain cases and is particularly useful for detecting thrombosis associated with thoracic aortic aneurysms. Computed tomography has been shown to be remarkably more accurate than thoracic radiography

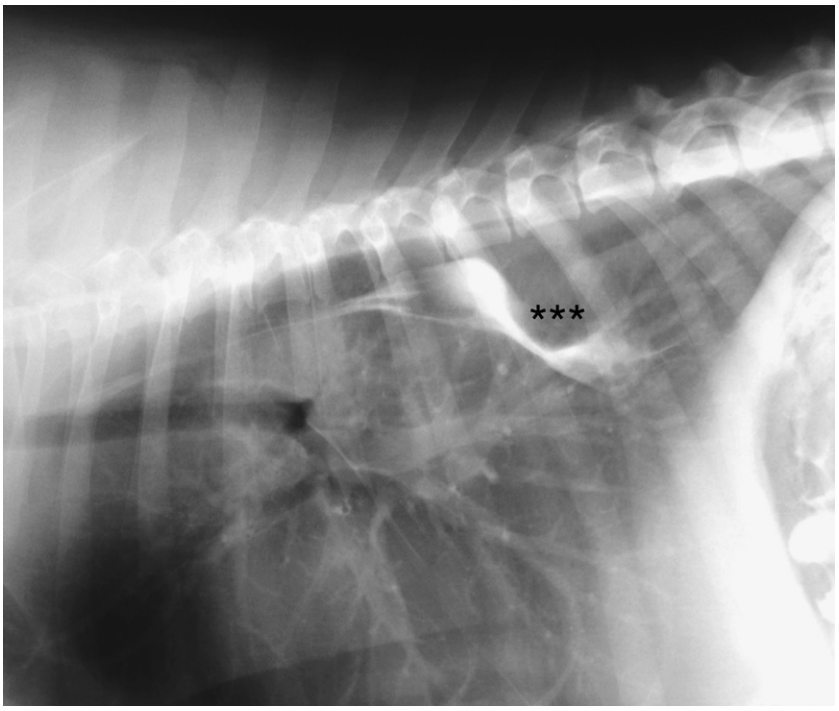

Fig. 9. Positive contrast oesophagogram illustrating a round dorsal mural filling defect (***) due to a *S. lupi* granuloma. The whole oesophagus has been displaced dorsally by a mass in the region of the tracheobronchial lymph nodes, which, on post-mortem, was an abscess secondary to *S. lupi* induced mediastinitis.

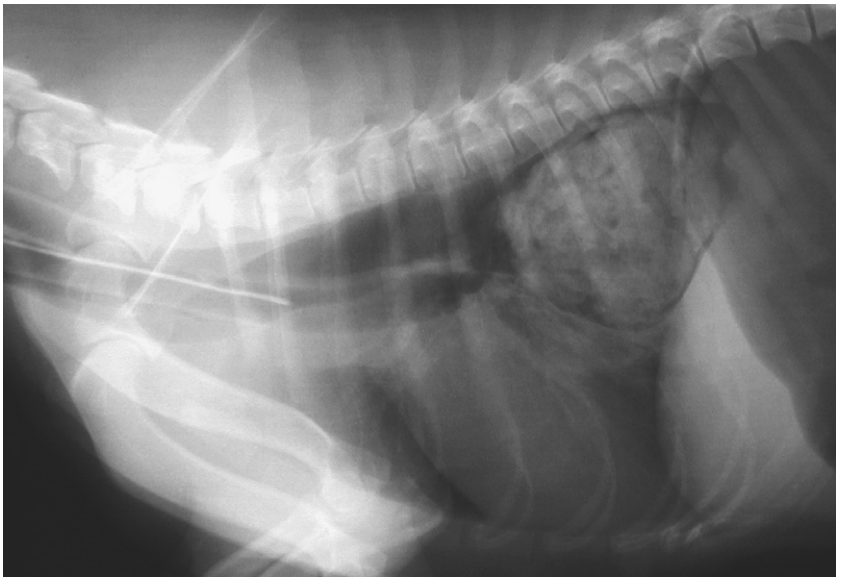

Fig. 10. Right lateral thoracic view with pneumo-oesophagogram of the same dog as in Fig. 7. Note the endotracheal tubes in the trachea and oesophagus. The oesophagus is air filled with a prominent tracheo-oesophageal stripe sign and the caudal oesophageal mass is much better defined than in Fig. 7.

in detecting small pulmonary nodules as well as assessing the total number and location of nodules (Nemanic et al., 2006).

Diagnostic ultrasonography via a trans-hepatic window to avoid the aerated lungs is currently being investigated in our hospital. Oesophageal masses adjacent to the diaphragm can be seen (Fig. 12) and we have taken trans-hepatic ultrasound-guided biopsies of large masses for histopathology.

Oesophagoscopy

Endoscopy is more sensitive than radiography in diagnosing a *S. lupi* infection, which has only progressed to

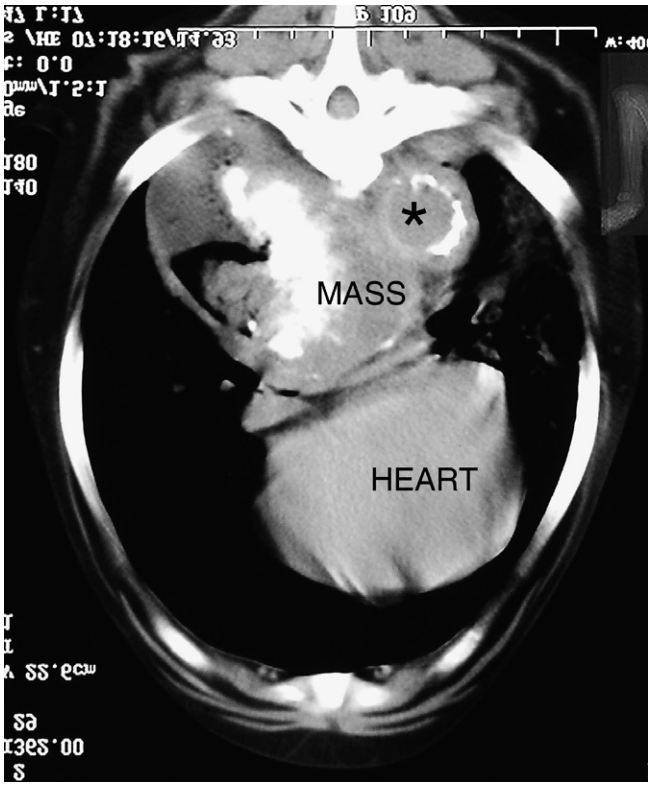

Fig. 11. Transverse thoracic computed tomography image utilising a soft tissue window. The *S. lupi*-associated mass is located dorsal to the heart and shows marked central mineralisation and invasion of the air filled oesophagus. The aorta (*) shows advanced mineralisation of its lateral wall.

small nodule formation within the oesophagus. Mazaki-Tovi et al. (2002) showed a 100% sensitivity of endoscopy compared to a 80% sensitivity of faecal flotation and 53% sensitivity of radiographs in diagnosing an oesophageal mass. The sensitivity of radiographic diagnosis was increased to 86% when the presence of spondylitis, present in 33% of cases, was also considered a positive diagnosis. Endoscopic findings vary depending on the progression of the disease. Early infection typically presents with one or several smooth rounded nodules, which may have a pink nipple-like protuberance through which the female worm may be seen protruding as she lays eggs (Fig. 13). These nodules are typically found caudal to the heart and may extend through the cardia into the stomach (Kumar et al., 1981a). Gastric nodules were found on necropsy in 5% of dogs reported on from Iraq and 3% in Kenya (Brodey et al., 1977). It is important to inflate the oesophagus adequately to avoid mistaking smaller nodules for oesophageal folds.

Over time, nodules may enlarge and become roughened, lobulated, frequently pedunculated, cauliflower-like masses, which obliterate the oesophageal lumen (Fig. 14). These masses are often necrotic and may be ulcerated and friable, bleeding easily if traumatised by the endoscope. It is our experience that once the masses have this macroscopic appearance, that they may have already undergone neoplastic transformation. It is often difficult to determine the extent of the mass, involvement of gastro-oesophageal sphincter and type of attachment to oesophageal wall of these nodules endoscopically as the

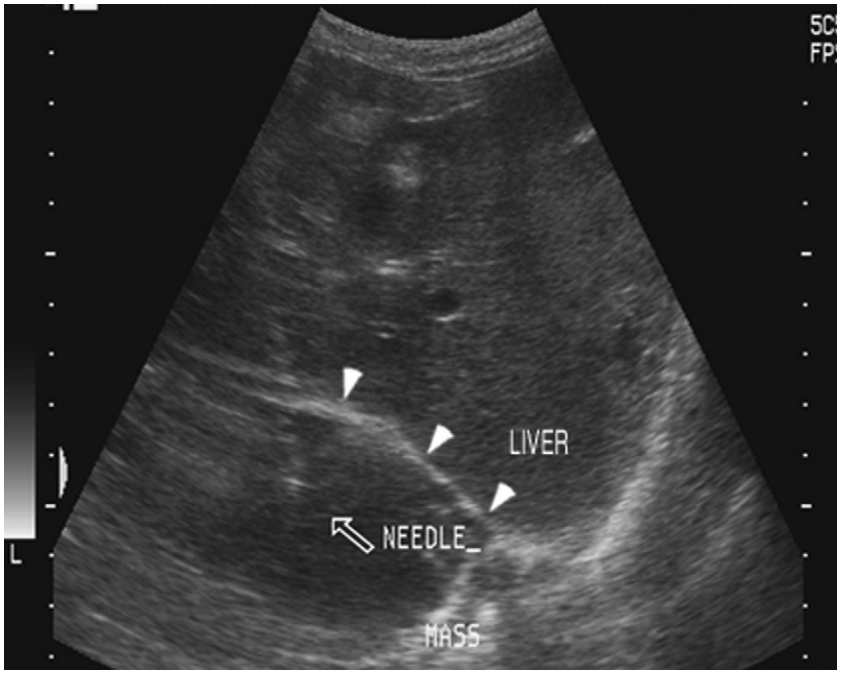

Fig. 12. Transverse trans-hepatic ultrasonographic image of a hypoechoic *S. lupi* mass beyond the hyperechoic diaphragm line (arrows). The open arrow points toward the trans-hepatic echogenic biopsy needle outline.

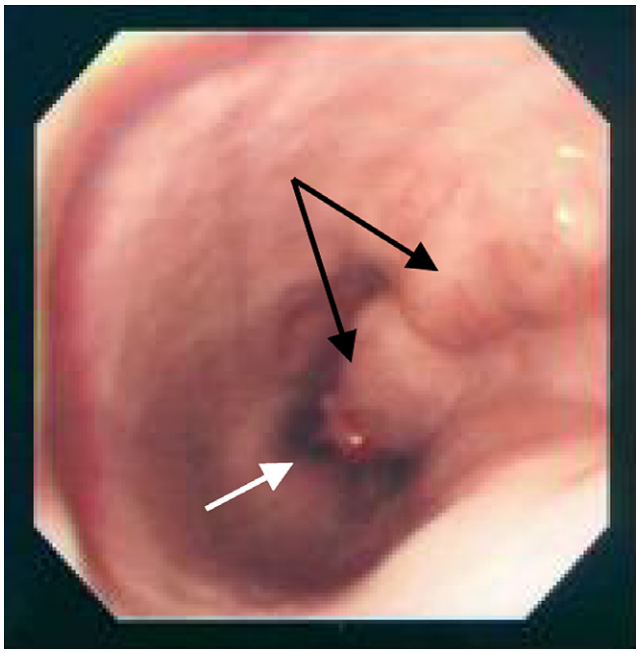

Fig. 13. Oesophageal endoscopy in a dog showing the appearance of the oesophagus in a typical case of spirocercosis. Two coalescing nodules (black arrow) are present. Note the pink tip of the nodule through which the female lays eggs (white arrow). Note also that the oesophagus is distended with air to facilitate visualisation of the nodules.

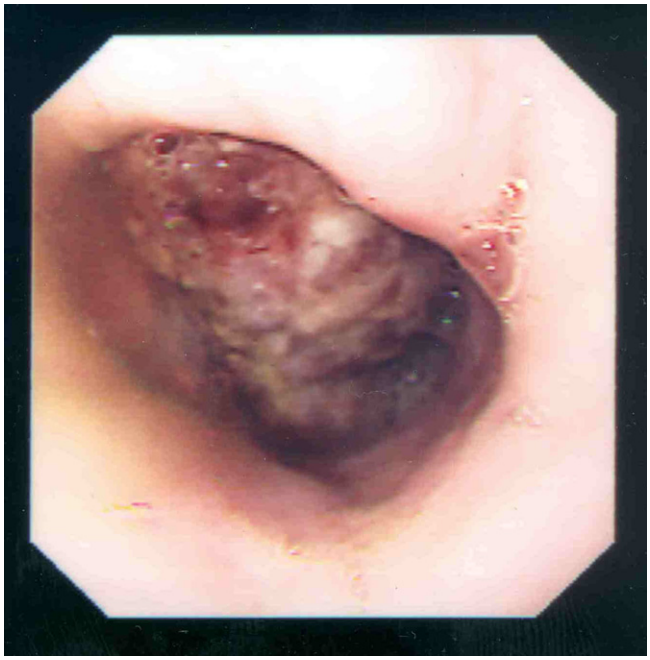

Fig. 14. Oesophageal endoscopy in a dog showing the typical appearance of a *S. lupi*-associated oesophageal sarcoma. Note the roughened surface, necrotic grey–green colour and surface haemorrhages.

mass physically hampers complete visualisation. Some masses are extraluminal (intramural or mediastinal) and the only abnormality visualised is a narrowed oesophagus (Dvir et al., 2001). Additional oesophageal pathology such as oesophagitis may also be diagnosed.

The results of endoscopically performed biopsies are disappointing. In early nodules, the intact stratified squamous epithelium of the oesophageal mucosa resists biopsy efforts. In the larger, more cauliflower-like lesions, where the possibility of neoplastic transformation may alter treatment strategies, the biopsy often does not include diagnostic tissue. Dvir et al. (2001) showed that of 13 endoscopic biopsies taken, eight showed only necrotic tissue on histopathology, whereas on later necropsy evidence two of those proved to be osteosarcomas. Successive biopsies from the same site are recommended to obtain deeper-lying tissue to maximise diagnostic information. The use of alpha agonists as premedication for the above mentioned procedures should be avoided. The alpha-agonist, medetomidine, has been incriminated in a single case as the cause of rupture of the compromised aorta due to the transient increase in peripheral vascular tone it precipitates (Joubert et al., 2005).

Treatment

Medical treatment

Over the years a number of different drugs have been used for treatment and or prophylaxis but to date no one remedy has been effective in killing both adult and larval stages of *S. lupi* while being devoid of host side-effects. Diethylcarbamazine, a piperazine derivative, was the first anthelmintic used for the treatment of spirocercosis and was shown to be effective in ameliorating the typical clinical signs of vomiting and regurgitation in animals with oesophageal nodules and improving the overall health status of the animal (MacGaughey, 1950; Tacal, 1963). While this drug was definitely of clinical benefit, it only suppressed egg shedding but did not affect the adult worm (Seneviratna et al., 1966). Disophenol, a substituted phenol, killed adult worms in nodules at a dose of 7.7 mg/kg. The treatment was repeated after 7 days if poor clinical response was noted (Darne and Webb, 1964). The drug was not, however, effective against juveniles and had a narrow margin of safety and is no longer available (Seneviratna et al., 1966). A combination of nitroxynil (10 mg/kg) and ivermectin (1000 μg/kg) administered subcutaneously was reported to be successful in treating infected dogs in Reunion in 81.6% of cases. Clinical cure was concluded in animals following both endoscopic and faecal flotation evaluation (Reche-Emont et al., 2001).

More recently, the cattle anthelmintic doramectin, a macrocyclic lactone, was shown to have good efficacy under clinical conditions. Dectomax® is 1%, m/v, solution of doramectin in a non-aqueous vehicle of sesame seed oil and ethyl eloate. Its use to treat *S. lupi* is extra-label as it is only licensed for use in cattle, pigs and sheep. Although highly lipophilic, doramectin has a relatively short half-life of 3.09 ± 0.99 and 3.75 ± 0.89 days, following subcutaneous and oral administration, respectively, with a mean tissue residence time of approximately 5 days (Gokbulut et al., 2006).

Safety trials performed by the manufacturers of Dectomax in beagles involved treating dogs per os with the sesame seed solvent formulation of doramectin at 0, 500, 1000 and 2000 μg/kg per day for 91 days. Although the adverse effects were mild, transient, reversible and dose related in doses ⩾500 μg/mL, a no observable effect level (NOEL) of 500 μg/mL was assigned for the study (Conder et al., 2002). This was very similar to the result demonstrated for ivermectin during preclinical safety studies (Pulliam and Preston, 1989), with signs of reversible toxicity occurring at doses of 2500 μg/kg for single administration and 500 μg/kg following 2 weeks of daily dosing.

A specific breed specific toxicity has been reported to occur in collies and other herding dog breeds following the use of both ivermectin and doramectin (Hopper et al., 2002; Yas-Natan et al., 2003). Clinical signs reported included mydriasis, apparent blindness, muscle tremors and disorientation which eventually progresses to stupor and possible coma. In severe cases the clinical signs lasted approximately 22 days for both drugs, which tend to suggest a longer half-life of the macrocyclic lactones is this breed. The clinical signs in the milder toxicities usually resolve over a few days. More recently, it has been demonstrated that toxicity is related to a mutation in the MDR1-1Δ gene and its ability to express the protective P-glycoprotein pump. This deficiency is reported to occur as a homozygous defect in 35% of Collies which corresponds to the species incidence of toxicity of 30% breed susceptibility (Campbell, 1989; Mealey, 2006). In the normal animal the P-glycoprotein pump is protective and is active in excluding certain drugs from the brain, decreasing oral bioavailability and increasing hepatic clearance of certain substances (Buxton, 2005).

Using a different protocol, Berry (2000) demonstrated that 200 μg/kg of doramectin injected SC at 14 day intervals for three subsequent treatments was effective in treating spirocercosis in 5/7 infected animals. Doramectin was again shown to be effective by Lavy et al. (2002) using an alternative dosing regimen of 400 μg/kg, injected SC every 14 days for six treatments, followed by monthly dosing until resolution of the parasitic nodule. Eggs could not be detected in the faeces 3–10 days after the first treatment in four dogs and the second treatment in three dogs. The reduction in egg numbers was however immediate with a 99.3% decrease in egg numbers by the 10th day after first injection, suggesting a marked suppressive effect on egg production or shedding. Radiographic improvement after treatment, defined as resolution of the caudal mediastinal opacity occurred around 203 days after treatment (Lavy et al., 2002). Oesophageal nodules had completely resolved, as visualised endoscopically, between 35 and 544 days after treatment in 6/7 cases. Another study has also shown doramectin to be effective, but at a reduced treatment frequency of 500 μg/kg injected SC and repeated after 7 days. Egg counts performed daily showed no eggs from the fourth day after the second treatment (Kolte et al., 2001).

Most recently, Mylonakis et al. (2004) reported that only two doses of ivermectin at 600 μg/kg, SC, 2 weeks apart, in combination with oral prednisolone (0.5 mg/kg bid for 2 weeks followed by dose tapering) promoted nodular regression in 5/8 animals with natural *S. lupi* infection. Faecal egg shedding was eliminated in all eight animals for up to 2 months following the last treatment. This shortened dosage regimen was believed to result from the combination of two separate pharmacodynamic effects, the prednisolone promoting nodule regression and the ivermectin killing the parasite. However, it is not known if the same would not be true of a shortened dosage regimen in the original study by Lavy et al. (2002). It is our experience in South Africa that these smaller, smooth nodules are very responsive to medical treatment with doramectin utilising a variety of regimens, based on clinician preference.

With the pharmacokinetics of ivermectin and doramectin being described in dogs for both SC and oral administration, certain suppositions may be derived (Gokbulut et al., 2006). With both drugs being shown to have short half-lives of approximately 3 days following either oral or SC administration, this would suggest that dosing every 3–4 days may provide the prolonged exposure necessary to kill the parasite, i.e., instead of fortnightly dosing. From the presented area under the curve a relative oral bioavailability of 67% and 63% for ivermectin and doramectin, respectively was calculated as compared to the parenteral route and tends to suggest that oral dosing would require a 33% increase in dose to achieve the same exposure as parenteral treatment.

Similarities between *Dirofilaria immitis* (heartworm) infection and spirocercosis may suggest that similar treatment protocols could be effective, however, the differences between these two parasitic infections are many. The various dosages of the macrocyclic lactones reported as effective against *S. lupi*, are much higher than those for heartworm (Campbell, 1989; McCall, 2005). Another key difference appears to lie in the stage of life cycle, being treated with the macrocyclic lactones. Since the nodules contain the adult parasite and treatment with the macrocyclic lactones clearly indicates nodule resolution, it is a fair assumption that the drug is effective against the adults. This differs completely to heartworm were the adults are fairly resistant to the effect of the drug as seen with the prolonged time required for the macrocyclic lactones to eliminate adults (McCall, 2005).

With a large amount of the current drug efficacy data being based on a small sample size and extrapolations, it would be of value to determine the inhibitory dose for Spirocerca and use pharmacodynamic/pharmacokinetic modelling to determine the optimum dosage regime to treat this parasite (Sheiner and Steimer, 2000). Until this can be determined, it is dependent on the clinician to optimise treatment in the patient.

Surgical and chemotherapeutic treatment

Non-neoplastically transformed nodules will regress with medical treatment and some have been seen to regress

spontaneously (Bailey, 1972). Surgery is therefore only required in cases where the nodules have undergone neoplastic transformation.

In a report by Ranen et al. (2004), 10/15 patients with oesophageal sarcomas underwent surgery: six had partial oesophagectomies, two had oesophageal resection, one had a gastrostomy and one had a lesion too extensive to resect. The survival times in the six patients with the partial oesophagectomy and medical treatment with doxorubicin and doramectin averaged 267 days. The outcome for the cases with resection was very poor with the dogs surviving only 3 and 4 days, respectively.

Causes for the high complication rates in oesophageal surgery included excessive tension at the suture line, lack of serosa, constant motion of the suture site, passage of undigested food or saliva over the suture site, segmental blood supply and lack of omentum. Resection of >3–5 cm increases the risk of dehiscence. Doxorubicin was prescribed as adjuvant anti-neoplastic therapy in five cases but no conclusions could be reached regarding the efficacy of the therapy. Carboplatin and doxorubicin in combination, or as mono-therapies, have improved survival in dogs with appendicular osteosarcoma after limb amputation, whereas fibrosarcomas are resistant to adjuvant chemotherapy (Straw, 2000). To date, there are, however, no data available on the effectiveness of chemotherapy in the treatment of spirocercosis-associated oesophageal sarcomas.

Prevention

Disease incidence can be reduced by disposal of faeces, preventing dogs from hunting, scavenging and eating uncooked viscera and decreasing egg shedding by infected animals. Control of coprophagous beetles and transport hosts is not a feasible form of control due to the variety and ubiquity of transport hosts in an endemic area.

A study by Lavy et al. (2003) to evaluate the prophylactic effect of doramectin showed that treatment at 400 μg/kg, 30 days prior to exposure to infective larvae delayed the development of parasitic nodules in the oesophagus, resulted in fewer nodules and also subsequently delayed egg shedding by a minimum of 40 days in the treated group. Worm egg production in treated dogs was 97.7% less than the untreated group. The mean EPG in the treated group was 1.8 ± 2.1 and 101.9 ± 102 in the untreated group. This study, however, failed to address the question of ongoing prophylaxis in endemic areas, as the dogs were not treated again during the trial period nor were they further exposed to infective larvae. In reality, dogs from endemic areas would be continuously exposed to infective larvae. It would be of value to determine a minimum serum concentration required to inhibit or kill *S. lupi* adults and larvae and also the maximum treatment interval required to maintain this level. To date, all the macrocyclic lactones used to treat spirocercosis have been administered subcutaneously. The use of these compounds as an easily administered oral or topical preparation needs further investigation.

Preventative treatment should be aimed at maintaining patient health and decreasing environmental contamination. The dosing frequency to maintain optimal patient health would need to be more intense than that to decrease environmental contamination as worm migration in the aorta and larger arteries occurs early in infection and blood vessel rupture and acute death may occur in 2–12% of reported cases (Bailey, 1963).

Conclusions

Spirocercosis is a serious condition in endemic areas. Clinical signs usually develop late in the disease except in those cases presenting with peracute aortic rupture. Clinical signs, which should be regarded as highly suspicious for spirocercosis in endemic areas include vomiting or regurgitation, dyspnoea, persistent coughing and hypertrophic osteopathy. Radiological lesions regarded as diagnostic for spirocercosis in endemic areas are typical oesophageal nodules, aortic aneurysms and mineralisation and caudal thoracic spondylitis. Although endoscopy has a greater sensitivity for diagnosing spirocercosis, the importance of good quality radiographs should not be underestimated. Other secondary thoracic pathologies such as lung metastases, pneumonia, pleural effusion and mediastinitis may be detected radiologically and thus assist in the diagnostic process and the establishment of a prognosis. Thoracic radiographs made for non-spirocercosis related conditions, should be carefully scrutinised for radiological changes associated with spirocercosis to allow for early diagnosis and treatment of non-clinical cases in endemic areas.

Further studies are required to evaluate the efficacy of current macrocyclic lactone containing products. Even though the ideal dosage and dosing interval is not known, the intermittent use of doramectin should be advocated, not only to specifically prevent patient infection but also to decrease environmental contamination by eggs. A serological test to confirm *S. lupi* infection prior to the passage of eggs or the development of nodules could be helpful in endemic areas. Further work is also required on the biological behaviour and chemotherapeutic treatment modalities of the soft tissue sarcomas. Recent Israeli studies resulted in the establishment of a murine xenograft model of spirocerca associated sarcoma, thus establishing a readily available source of tumour cells for experimental purposes. Collaboration between the Universities and individuals studying the disease in the various endemic areas would facilitate more rapid understanding of the disease process.

Acknowledgements

We acknowledge all the clinical staff of the Onderstepoort Veterinary Academic Hospital for allowing the use of their case material.

References

Alvarenga, J., Saliba, A.M., 1971. Iliac embolism in a dog. Modern Veterinary Practice 52, 37–38.

Anataraman, M., Krishna, S., 1966. Experimental spirocercosis in dogs with larvae from a paratenic host, *Calotes versicolor*, the common garden lizard in Madras. Journal of Parasitology 52, 911–912.

Avner, A., Kirberger, R.M., 2005. The effect of the various thoracic radiographic projections on the appearance of selected thoracic viscera. Journal of Small Animal Practice 46, 491–498.

Bailey, W.S., 1963. Parasite and cancer: sarcoma in dogs associated with *Spirocerca lupi*. Annals of the New York Academy of Science 108, 890–923.

Bailey, W.S., 1972. *Spirocerca lupi*: a continuing inquiry. The Journal of Parasitology 58, 3–22.

Bhatia, B.B., Chuahan, P.P.S., Agrawal, R.D., Ahluwalia, S.S., 1979. On helmintic infections of domestic duck and their pathogenic significance. Veterinary Research Bulletin 2, 129–135.

Berry, W., 2000. *Spirocerca lupi* oesophageal granulomas in 7 dogs: resolution after treatment with Doramectin. Journal of Veterinary Internal Medicine 14, 609–612.

Brodey, R.S., Thompson, R.G., Sayer, P.D., Eugster, B., 1977. *Spirocerca lupi* infection in dogs in Kenya. Veterinary Parasitology 3, 49–59.

Buxton, I.L.O., 2005. Pharmacokinetics and pharmacodynamics: the dynamics of drug absorption, distribution, action and elimination. In: Brunton, L., Lazo, J., Parker, K., Buxton, I., Blumenthal, D., Goodman, L.S., Gilman, A. (Eds.), The Pharmacological Basis of Therapeutics. McGraw-Hill, New York, pp. 1–40.

Cabrera, D.J., Bailey, W.S., 1964. A modified Stoll technique for detecting eggs of *Spirocerca lupi*. Journal of the American Veterinary Medical Association 145, 573–575.

Campbell, W.C., 1989. Use of ivermectin in dogs and cats. In: Campbell, W.C. (Ed.), Ivermectin and Abamectin. Springer, New York, pp. 245–259.

Chandrasekharon, K.P., Sastry, G.A., Menon, M.N., 1958. Canine spirocercosis with special reference to the incidence and lesions. The British Veterinary Journal 114, 388–395.

Conder, G.A., Baker, W.J., Genchi, C., 2002. Chemistry pharmacology and safety: doramectin and selamectin. In: Vercruysse, J., Rew, R. (Eds.), Macrocyclic Lactones in Antiparasitic Therapy. CABI, New York, pp. 30–50.

Coskun, S.Z., 1995. Diagnosis of *Spirocerca lupi* by IFAT in naturally infected dogs. Turkiye Parazitoloji Dergisi 19, 541–549.

Darne, A., Webb, J.L., 1964. The treatment of ancylostomiasis and of spirocercosis in dogs by the new compound 2,6-diiodo-4-nitrophenol. The Veterinary Record 76, 171–172.

Dixon, K., McCue, J.F., 1967. Further observations on the epidemiology of *Spirocerca lupi* in the south eastern United States. Journal of Parasitology 53, 1074–1075.

du Plessis, C.J., Keller, N., Millward, I.R., 2007. Journal of Small Animal Practice, in press. doi:10.1111/j1748-5827.2006.00262.x.

Dvir, E., Kirberger, R.M., Malleczek, D., 2001. Radiographic and computed tomographic changes and clinical presentation of spirocercosis in the dog. Veterinary Radiology and Ultrasound 42, 119–129.

Evans, L.B., 1983. Clinical diagnosis of *Spirocerca lupi* infestation in dogs. Journal of the South African Veterinary Association 54, 189–191.

Fox, S.M., Burns, J., Hawkins, J., 1988. Spirocercosis in dogs. Compendium on Continuing Education for the Practicing Veterinarian 10, 807–822.

Gal, A., Kleinbart, S., Aizenberg, I., Baneth, G., 2005. Aortic thromboembolism associated with *Spirocerca lupi* infection. Veterinary Parasitology 130, 331–335.

Garg, U.K., Ghoshal, S.B., Richharia, V.S., Misraulia, K.S., 1989. An unusual occurrence of *Spirocerca lupi* worms in the heart of a dog. Indian Veterinary Journal 66, 1073.

Georgi, M.E., Han, H., Hartrick, D.W., 1980. *Spirocerca lupi* (Rudolphi 1809) nodule in the rectum of a dog. Cornell Veterinarian 70, 43–49.

Gokbulut, C., Karademir, U., Boyacioglu, M., McKellar, Q.A., 2006. Comparative plasma dispositions of ivermectin and doramectin following subcutaneously and oral administration in dogs. Veterinary Parasitology 135, 347–354.

Hamir, A.N., 1984. Perforation of thoracic aorta in a dog associated with *Spirocerca lupi* infection. Australian Veterinary Journal 61, 64.

Hamir, A.N., 1986. Oesophageal perforation and pyothorax associated with *Spirocerca lupi* infestation in a dog. Veterinary Record 119, 276.

Harrus, S., Harmelin, A., Markovics, A., Bark, H., 1996. *Spirocerca lupi* infection in the dog: aberrant migration. Journal of the American Animal Hospital Association 32, 125–130.

Herrera, L.A., Ostrosky-Wegman, P., 2001. Do helminths play a role in carcinogenesis? Trends in Parasitology 17, 172–175.

Hopper, K., Aldrich, J., Haskins, S.C., 2002. Ivermectin toxicity in 17 Collies. Journal of Veterinary Internal Medicine 16, 89–94.

Hu, C.H., Hoeppli, R.J.C., 1936. The migration route of *Spirocerca sanguinolenta* in experimentally infected dogs. Chinese Medical Journal Supplement 1, 293–311.

Johnson, R.C., 1992. Canine spirocercosis and associated esophageal sarcoma. Compendium on Continuing Education for the Practicing Veterinarian 14, 577–580.

Joubert, K.E., McReynolds, M.J., Strydom, F., 2005. Acute aortic rupture in a dog with spirocercosis following administration of medetomidine. Journal of the South African Veterinary Association 76, 159–162.

Kagira, J.M., Kanyari, P.W.N., 2001. Parasitic diseases as causes of mortality in dogs in Kenya: a retrospective study of 351 cases (1984–1998). Israel Journal of Veterinary Medicine 56, 11–99.

Kamara, J.A., 1964. The incidence of canine spirocercosis in the Freetown area of Sierra Leone. Bulletin of Epizoology Diseases of Africa 12, 465–469.

Klainbart, S., Mazaki-Tovi, M., Auerbach, N., Aizenberg, I., Bruchim, Y., Dank, G., Lavy, E., Aroch, I., Harrus, S. Spirocercosis-associated pyothorax in dogs. The Veterinary Journal, in press. doi:10.1016/j.tvjl.2005.08.019.

Kolte, S.W., Maske, D.K., Kurkure, N.V., 2001. Treatment of *Spirocerca lupi* infection in dogs with doramectin. Journal of Veterinary Parasitology 15, 83.

Kumar, N., Vegad, J.L., Kolte, G.N., 1981a. Note on an unusual case of spirocerca granuloma in the stomach of a dog. Indian Journal of Animal Sciences 51, 805–806.

Kumar, N., Vegad, J.L., Kolte, G.N., 1981b. Ossified lesions in canine aortic spirocercosis. Veterinary Record 109, 142–143.

Lavy, E., Aroch, I., Bark, H., Markovics, A., Aizenberg, I., Mazaki-Tovi, M., Hagag, A., Harrus, S., 2002. Evaluation of doramectin for the treatment of experimental canine spirocercosis. Veterinary Parasitology 109, 65–73.

Lavy, E., Harrus, S., Mazaki-Tovi, M., Bark, H., Markovics, A., Hagag, A., Aizenberg, I., Aroch, I., 2003. *Spirocerca lupi* in dogs: prophylactic effect of doramectin. Research in Veterinary Science 75, 217–222.

Lobetti, R., 2000. Survey of the incidence, diagnosis, clinical manifestations and treatment of *Spirocerca lupi* in South Africa. Journal of the South African Veterinary Association 71, 43–46.

Londono, N.Y., Carmona, R.J.U., Giraldo, M.C.E., 2003. Generalised osteosarcoma and secondary megaesophagus caused by *Spirocerca lupi* in a dog. Revista Colombiana de Ciencias Pecuarias 16, 63–69.

Markovics, A., Medinski, B., 1996. Improved diagnosis of low intensity *Spirocerca lupi* infection by the sugar flotation method. Journal of Veterinary Diagnostic Investigation 8, 400–401.

Mazaki-Tovi, M., Baneth, G., Aroch, I., Harrus, S., Kass, P.H., Ben Ari, T., Zur, G., Aizenberg, I., Bark, H., Lavy, E., 2002. Canine spirocercosis: clinical, diagnostic, pathologic and epidemiologic characteristics. Veterinary Parasitology 107, 235–250.

MacGaughey, C.A., 1950. Preliminary note on the treatment of spirocercosis in dogs with a piperazine compound, caricide (Lederle). Veterinary Record 62, 814–815.

Mealey, K.L., 2006. Adverse drug reactions in herding breed dogs: the role of P-glycoprotein. The Compendium of Continuing Education – Small Animal Practice 28, 23–33.

Mense, M.G., Gardiner, C.H., Moeller, R.B., Partridge, H.L., Wilson, S., 1992. Chronic emesis caused by a nematode induced gastric nodule in a cat. Journal of the American Animal Hospital Association 201, 597–598.

McCall, J.W., 2005. The safety-net story about macrocyclic lactone heartworm preventives: a review, an update and recommendation. Veterinary Parasitology 133, 197–206.

Minnaar, W.N., Krecek, R.C., Fourie, L.J., 2002. Helminths of dogs from a peri-urban resource limited community in Free State Province, South Africa. Veterinary Parasitology 107, 343–349.

Murray, M., 1968. Incidence and pathology of *Spirocerca lupi* in Kenya. Journal of Comparative Pathology 78, 401–404.

Mylonakis, M.E., Koutinas, A.F., Liapi, M.V., Saridomichelakis, M.N., Rallis, T.S., 2001. A comparison of the prevalence of *Spirocerca lupi* in three groups of dogs with different life and hunting styles. Journal of Helminthology 75, 359–361.

Mylonakis, M.E., Rallis, T.S., Koutinas, A.F., Ververidis, H.N., Fytianou, A., 2004. A comparison between ethanol-induced chemical ablation and ivermectin plus prednisolone in the treatment of symptomatic oesophageal spirocercosis in the dog: a prospective study on 14 natural cases. Veterinary Parasitology 120, 131–138.

Nemanic, S., London, C.A., Wisner, E.R., 2006. Comparison of thoracic radiographs and single breath-hold helical CT for detection of pulmonary nodules in dogs with metastatic neoplasia. Journal of Veterinary Internal Medicine 20, 508–515.

Oliviera-Sequeira, T.G.C., Amarante, A.F.T., Ferrari, T.B., Nunes, L.C., 2002. Prevalence of intestinal parasites in dogs from Sao Paulo State, Brazil. Veterinary Parasitology 103, 19–27.

Pereira, W.L.A., Guimaraes, F.A.B., Martins, A.K.R., Peixoto, P.C., 1995. Haemopericardium in a dog associated with hyperparasitism by *Spirocerca lupi*. Boletim de Faculdade de Ciencias Agrarias do Para 23, 45–51.

Prunaux, O., Guignard, A., 1991. Helminthoses of dogs on the island of Reunion: results at the department veterinary laboratory 1987–1990. Revue de Medecine Vétérinaire 142, 757–760.

Pulliam, J.D., Preston, J.M., 1989. Safety of ivermectin in target animals. In: Campbell, W.C. (Ed.), Ivermectin and Abamectin. Springer, New York, USA, pp. 149–161.

Rajan, A., Mohiyuddeen, S., 1974. Incidence of spirocercosis in some uncommon sites. Kerala Journal of Veterinary Science 5, 139–142.

Rallis, T.S., Moraitou, K., Vlemmas, J., 1995. Gastroesophageal intussusception in an adult dog. Canine Practice 20, 7–11.

Ramachandran, P.V., Shakir, S.A., Ramakrishnan, R., 1984. Spirocercosis in canines – a necropsy survey. Cheiron Tamil Nadu Journal of Veterinary Science and Animal Husbandry 13, 132–135.

Ranen, E., Lavy, E., Aizenberg, I., Perl, S., Harrus, S., 2004. Spirocercosis-associated esophageal sarcomas in dogs. A retrospective study of 17 cases (1997–2003). Veterinary Parasitology 119, 209–221.

Reche-Emont, M., Beugnet, F., Bourdoiseau, G., 2001. Etude epidemiologique et clinique de la spirocercose canine a I'll de le Reunion a partir de 120 cas. Revue de Medecine Vétérinaire 152, 469–477.

Ridgway, R.L., Suter, P.F., 1979. Clinical and radiographic signs in primary and metastatic oesophageal neoplasms of the dog. Journal of the American Veterinary Medical Association 174, 700–704.

Schroeder, H., Berry, W., 1998. Salivary gland necrosis in dogs: a retrospective study of 19 cases. Journal of Small Animal Practice 39, 121–125.

Seibold, H.R., Bailey, W.S., Hoerlein, B.F., Jordan, E.M., Schwabe, C.W., 1955. Observations of the possible relation of malignant esophageal tumours and *Spirocerca lupi* lesions in the dog. American Journal of Veterinary Research 16, 5–14.

Sen, K., Anataraman, M., 1971. Some observations on the development of *Spirocerca lupi* in its intermediate and definitive hosts. Journal of Helminthology XLV, 123–131.

Seneviratna, P., Fernando, S.T., Dhanapala, S.B., 1966. Disophenol treatment of spirocercosis in dogs. Journal of the American Veterinary Medical Association 148, 269–274.

Sharpilo, V.P., 1983. The reptiles of the USSR considered as intermediate and paratenic hosts of helminths. Parazitologiya 17, 177–184.

Sheiner, L.B., Steimer, J.L., 2000. Pharmacokinetic/Pharmacodynamic modeling in drug development. Annual Reviews in Pharmacology and Toxicology 40, 67–95.

Singh, B., Juyal, P.D., Sobti, V.K., 1999. *Spirocerca lupi* in a subcutaneous nodule in a dog in India. Journal of Veterinary Parasitology 13, 59–60.

Smith, D.A., Knottenbelt, D.C., 1989. *Spirocerca lupi* localisation in the spinal cord of a dog. Zimbabwe Veterinary Journal 18, 19–22.

Soulsby, E.J.L., 1982. Helminths, arthropods, and protozoa of domesticated animals. Lea and Febiger, Philadelphia, USA, pp. 291–294.

Stephens, L.C., Gleiser, C.A., Jardine, J.H., 1983. Primary pulmonary fibrosarcoma associated with *Spirocerca lupi* infection in a dog with hypertrophic pulmonary osteopathy. Journal of the American Veterinary Medical Association 182, 496–498.

Stettner, N., Ranen, E., Dank, D., Lavy, E., Aroch, I., Harrus, S., Brenner, O., Harmelin, A., 2005. Murine xenograft model of *Spirocerca lupi* associated sarcoma. Comparative Medicine 55, 510–514.

Straw, R.C., 2000. Bone and Joint Tumours. In: Ettinger, S.J., Feldman, E.C. (Eds.), Textbook of Veterinary Internal Medicine. Saunders, Philadelphia, USA, pp. 535–540.

Tacal, J.V., 1963. Dithiazanine iodide treatment for canine spirocercosis. Modern Veterinary Practice 44, 70–73.

Thanikachalam, M., Sundararaj, A., Ramakrishnan, R., 1984. Cystitis associated with a nematode in a dog. Cheiron 13, 220–222.

Tudury, E.A., Graca, D.L., Arias, M.V.B., 1995. *Spirocerca lupi* induced acute myelomalacia in the dog. A case report. Brazilian Journal of Veterinary Research and Animal Science 32, 22–26.

Upadhye, S.V., Dhoot, V.M., Kolte, S.W., 2001. *Spirocerca* infection in a tiger. Zoo's Print Journal 16, 450.

Wandera, J.G., 1976. Further observations on canine spirocercosis in Kenya. The Veterinary Record 99, 348–351.

Yas-Natan, E., Shamir, M., Kleinbart, S., Aroch, I., 2003. Doramectin toxicity in a collie. The Veterinary Record 153, 718–720.

RADIOGRAPHIC AND COMPUTED TOMOGRAPHIC CHANGES AND CLINICAL PRESENTATION OF SPIROCERCOSIS IN THE DOG

ERAN DVIR, DVM, ROBERT M. KIRBERGER, BVSC, MMEDVET(RAD), DIETER MALLECZEK, DIPL-TZT

A retrospective study of 39 dogs with spirocercosis is described, emphasizing radiographic and computed tomographic aspects and clinical presentation. Dogs were classified as complicated or uncomplicated, both clinically and radiographically. Besides the expected upper gastrointestinal signs, a high incidence of respiratory (77%) and locomotor (23%) complications were present. All dogs had thoracic radiographs. Esophageal masses were radiographically classified as typical or atypical according to their location. Twenty-seven dogs had a typical caudal esophageal mass. Six dogs had a mass atypically located in the hilar region. These masses were smaller and more difficult to visualize radiographically. The remaining 6 dogs did not have a radiographically detectable esophageal mass. Radiology as an initial diagnostic tool was effective in detecting and localizing the mass and to detect early respiratory abnormalities such as pleuritis, mediastinitis, pneumonia, and bronchial displacement. Endoscopy was the modality of choice to confirm antemortem esophageal masses. In dogs where the mass filled the whole esophageal lumen, endoscopy failed to give essential information necessary for surgical excision of neoplastic masses, such as the extent of esophageal wall attachment. Caudal esophageal sphincter involvement was difficult to determine endoscopically with large caudal esophageal masses. Computed tomography was performed on 3 dogs and did not address the latter problems completely, but was found to be a sensitive tool to detect focal aortic mineralization and early spondylitis, both typical for the disease, and essential in the diagnosis of non- or extramural esophageal abnormalities. *Veterinary Radiology & Ultrasound, Vol. 42, No. 2, 2001, pp 119–129.*

Key words: ***Spirocerca lupi*, spirocercosis, esophagus, sarcoma, granuloma, aortic aneurysm, aortic mineralization, spondylitis, hypertrophic osteopathy, computed tomography, CT, endoscopy, radiography, dog.**

Introduction

SPIROCERCA LUPI, the cause of spirocercosis, is known as the esophageal worm of the dog.[1] It has also been described in wild carnivores and rarely in man, cats, and other domestic animals.[2] The disease occurs worldwide throughout tropical and subtropical areas.[3–11] In endemic areas infestation can occur in up to 100% of dogs.[9–11] Dogs that are allowed to roam appear more likely to become infected.[5] The limiting factor in the disease distribution appears to be that of the intermediate host, the dung beetle.[1]

The life cycle of *Spirocerca lupi* has been described. Eggs shed by the infected dog are ingested by the intermediate host. Here eggs develop to third stage larvae and encyst. The beetle is then ingested, either by the final host (dog), or a transport host, which may be poultry, wild birds, rodents, rabbits, hedgehogs, or lizards.[3,12–14] In the transport host the larvae are released but then re-encyst. The dog ingests encysted third stage larvae via the dung beetle or transport host.[1] The larvae are released in the stomach and migrate through the gastric mucosa to the gastric artery and then to the aorta, which they can reach within 10 days.[1,14] The larvae then migrate cranially and leave the descending aorta and penetrate the esophagus within 3–4 months.[14] Here the worm establishes an opening towards the esophageal lumen, forms a granuloma and completes its development. The adult is a large spiraled pink to red worm, with males reaching a length of 54 mm and females 80 mm.[9] The adult worm can remain in the esophagus for up to two years, and at certain periods the female may produce up to 3 million eggs a day which are deposited into the esophageal lumen.[1,14]

Dogs can develop signs due to spirocercosis from 6 months onwards and there is no breed predisposition.[1] Clinical signs vary depending on the stage of the disease and possible complications. An uncomplicated infection

From the Department of Companion Animal Medicine (Dvir) and Diagnostic Imaging Section, Department of Companion Animal Surgery (Kirberger and Malleczek), Onderstepoort Veterinary Academic Hospital, University of Pretoria, Onderstepoort, 0110, Republic of South Africa.

Address correspondence and reprint requests to Dr. R.M. Kirberger, Department of Companion Animal Surgery, Faculty of Veterinary Science, University of Pretoria, Private Bag X04, Onderstepoort, 0110, Republic of South Africa.

Received February 24, 2000; accepted for publication August 21, 2000.

may either be subclinical, or more commonly, if the esophageal granuloma is big enough, regurgitation, weight loss, and dysphagia will develop.[2,15,16] The granuloma, and possible complications such as neoplastic transformation and its metastases, mediastinitis or pleuritis may all result in dyspnea.[2,15,16] Sudden death can occur due to aortic rupture.[2,6,15] Salivation is a rare clinical presentation due to salivary gland necrosis associated with the esophageal mass.[17] Lameness may develop as a result of secondary hypertrophic osteopathy (HO).[2] Central nervous system involvement due to aberrant migration, including convulsions, paraplegia, and paralysis has been described.[16,18] Anemia may develop as a result of esophageal ulcers.[2,16]

Pathologic changes in spirocercosis result from larval migration. Typical pathognomonic lesions involve the aorta, esophagus, and vertebrae. Aortic purulent panarteritis with thickening of the intima, granuloma of the adventitia, aneurysm, mineralization, stenosis, and scarring are commonly seen, often as incidental findings.[1–3,19] Single or multiple esophageal granulomas up to 40 mm in size may occur.[1,2,11] Spondylitis of the thoracic vertebra is occasionally seen.[2] Spondylitis is a periosteal reaction of the vertebral body which must be distinguished from spondylosis, a non-inflammatory bridging of the intervertebral disc space. Complications that may occur along the normal migration route include aortic rupture resulting in hemothorax, hemopericardium or sudden death,[6] and esophageal perforation with consequent mediastinitis, pneumothorax, and pyothorax.[16,20] Concurrent bacterial infection may lead to discospondylitis,[2] sepsis, and endocarditis.[21] A common and well-described complication is *Spirocerca* granuloma-associated esophageal sarcoma. Fibrosarcoma or osteosarcoma may develop and can metastasize to many other organs, particularly the lungs.[1,3,22,23] In one study, 72% of dogs with sarcomas were older than 6 years with a predisposition to the Hound group.[1] Aberrant migration may also occur, particularly within the thoracic cavity. *Spirocerca* nodules have been reported in the pleura, mediastinum, diaphragm, lung, trachea, bronchi, thymus, heart, lymphatics, subcutaneous tissues,[21,24] stomach,[2,21,23] spinal cord,[18,25] renal capsule,[24] urinary bladder,[2] small intestine, and rectum.[26,27] One of the mechanisms postulated for this aberrant migration is larval migration via a vein rather than an artery.[28]

The typical radiographic sign is a caudal esophageal mass. Spondylitis has been reported in one or more vertebra from T5-12 and may lead to ventral bridging of the disc spaces.[1,2] Vertebral periosteal reaction is often described as lamellar and in one dog was also noted on the ribs.[2] Less common changes include esophageal dilatation[29] and esophageal diverticulum.[2] Radiographic aortic abnormalities are rare but dilatation of the proximal descending aorta[29] and aortic mineralization have been described.[2] Angiography may be used to identify an aneurysm.[1,3,30] Barium per os may help to delineate the boundaries of the esophageal mass.[29]

Initial diagnosis of a suspected *Spirocerca* granuloma is most commonly made radiographically. It can then be confirmed by means of fecal examination and endoscopy. The eggs are small (⅓ of the length of a *Toxocara* egg), thick-shelled, and contain larvae. Finding eggs is difficult, as egg passage is unpredictable. The typical esophageal granuloma is a nodule with a fistulous tract from which the worm tail may protrude.[25] Endoscopically there may be a nodule, protruding into the esophageal lumen, that may have a polyp-like structure or a small opening,[2,15] or may have a cratered center.[2] As the granuloma enlarges it may become malignant, lobulated, ulcerated, and partially necrotic.[2,15] These lesions often do not contain worms and lack a visible opening.[3] The endoscopic appearance of the various stages of the esophageal lesion has not been well described.

Lesions regarded as diagnostic for spirocercosis, even if the worm is not found, are the typical esophageal granuloma, aortic lesions, or thoracic spondylitis.[1–3,21,31]

The life cycle and pathology of spirocercosis has been described extensively but clinical presentation and diagnostic imaging have not been reported in detail, particularly in atypical infections. The diagnosis of atypical infections, which may readily be missed radiographically, and patients with complications can be challenging. In this article we discuss the radiographic and computed tomographic (CT) changes in clinical spirocercosis as well as clinical presentation.

Materials and Methods

This was a retrospective study of 39 patients with a final antemortem or postmortem diagnosis of spirocercosis between 1993 and 1999. Criteria for inclusion were at least 2 orthogonal good quality thoracic radiographs and medical records. In instances of dogs having radiography on multiple occasions, only radiographs at initial presentation were examined. A few dogs that had important follow-up findings are mentioned specifically.

The diagnosis was confirmed by one or more of the following modalities: pathognomonic esophageal granuloma on endoscopy; pathognomonic esophageal or aortic lesion, or atypical lesions containing worms at necropsy; or a caudal esophageal mass together with spondylitis on radiographs.

Age, breed, sex, clinical signs, fecal analysis, necropsy or endoscopic changes, and clinical outcome were all recorded. Fecal flotation had been done on 30 dogs using sodium nitrate solution, whereas zinc sulfate flotation was used in 2 dogs. Direct fecal smears had been examined in 22 dogs.

Endoscopy was performed under general anesthesia on 30 dogs, using a 9.2 mm diameter, 1.3 m long flexible

videoscope.* Biopsies were taken from 13 of these dogs using a 3 mm biopsy forceps.

Radiographs were evaluated individually by 2 of the authors (RMK and DM) and consensus obtained on their findings. The following were evaluated: esophageal mass description (size, location, and mineralization); the presence of moderate or extensive amounts of esophageal air; spondylitis (type of periosteal reaction, severity, and location); tracheal and bronchial displacement; mediastinitis; pneumomediastinum; pulmonary or other metastases; thoracic lymphadenopathy; pleural effusion; pneumothorax; aortic outline or opacity changes; and evidence of HO if limb radiographs had been made. A small amount of esophageal air, commonly seen in normal dogs over the base of the heart, was considered normal, as was spondylosis, which is frequently seen on thoracic radiographs. The radiographic findings were then divided into typical and atypical groups, and each group could have complications. Dogs were considered typical if a caudal mediastinal mass was present, with or without spondylitis and esophageal dilation. Atypical dogs were those with a non-caudal mediastinal mass. Tracheal or main stem bronchus displacement or compression, neoplastic transformation, metastasis, mediastinitis, pleural or pulmonary pathology, non-esophageal mediastinal masses, and HO were considered to be complications.

Computed tomography was performed on 3 dogs.† Two dogs were in sternal and 1 in dorsal recumbency. Transverse images with 5 to 20 mm slice intervals and 3 to 10 mm slice thickness were made. Soft tissue evaluation was performed with a mean window width (WW) of 350 ± 50 Hounsfield units (HU) and a mean window center (WC) of 40 ± 10 HU. Pulmonary evaluation was performed with a WW of 1300–1700 HU and a WC of −300 to −400 HU. To evaluate periosteal reaction on the ventral aspect of the vertebrae a bone window was used with a WW of 3500 ± 500 HU and WC of 350 ± 50 HU. One dog received intravenous contrast medium (600 mg/kg iodine) followed by slightly altered soft tissue windows on selected slices.

Results

The diagnosis was confirmed by endoscopy in 30 dogs, 8 of which had a necropsy, and in 9 dogs by necropsy only.

Clinical Presentation

Age ranged from 7 months to 12 years with no specific age being overpresented. Thirty-three (85%) were large breed dogs. Twelve were German Shepherd dogs (30% compared to 8% in our hospital population). No sex bias was found.

The duration of clinical signs was recorded for 34 dogs. In 33 it ranged from a few days to 10 weeks, and 1 dog had weight loss of 6-months' duration. In 24 of the 34 dogs the duration was between 1 to 4 weeks.

The 4 most common clinical signs were weight loss (77%), vomiting or regurgitation (64%), anorexia (62%), and pyrexia (51%). Twelve dogs had only 1 or a combination of the above clinical signs. The other 27 dogs may have had some of the above signs but additionally had clinical signs that could be related to spirocercosis complications (Table 1).

Respiratory clinical signs were the most common complication and were present in 16 dogs, 8 of these dogs had radiographic or necropsy changes including lung metastases, tracheal or bronchial displacement, mediastinal or pleural effusion, mediastinitis or pleuritis, pneumonia, and abscess rupture into the thoracic cavity. The remaining 8 dogs had no radiographic or necropsy evidence of respiratory involvement. By contrast, 14 dogs without clinical respiratory signs had radiographic or pathologic findings involving the respiratory system, such as bronchial (n = 5) or tracheal displacement (n = 3), pleural effusion (n = 4), lung metastases (n = 2), and pneumothorax, aspiration pneumonia, pleuritis, and mediastinitis in 1 dog each. In total 30 dogs (77%) had some respiratory involvement clinically, radiographically, or at necropsy.

Six dogs had lameness; 4 had HO, and 2 had septic polyarthritis (diagnosed on necropsy). Three additional dogs had HO, 2 with no related signs, and the other with weakness and lethargy. Two dogs died suddenly due to aortic rupture. One of these also had septic complications including valvular endocarditis, which may have contributed to its clinical presentation. Of the 5 dogs with salivation, 1 had salivary gland necrosis diagnosed on cytology.

Fecal flotation with sodium nitrate solution allowed iden-

TABLE 1. Clinical Signs Other Than Weight Loss, Anorexia, Regurgitation/Vomiting, and Pyrexia in Dogs with Spirocercosis

Clinical sign	Number of Dogs (n = 27)
Respiratory signs:	16
dyspnea/increased respiratory effort	11
coughing/retching	7
abnormal respiratory sounds	2
Gastrointestinal signs:	8
salivation/salivary gland enlargement	5
dysphagia	4
melena	1
coprophagia	1
Musculoskeletal signs:	8
lameness	6
weakness/lethargy	3
Peripheral lymph node enlargement	8
Seizures	3
Sudden death	2
Collapsed	1
Muffled heart sounds	1

Dogs may have had more than one sign. Not all signs were necessarily associated with spirocercosis.

*Olympus GIF, type XQ200, Tokyo, Japan.
†Siemens Somaton, Germany.

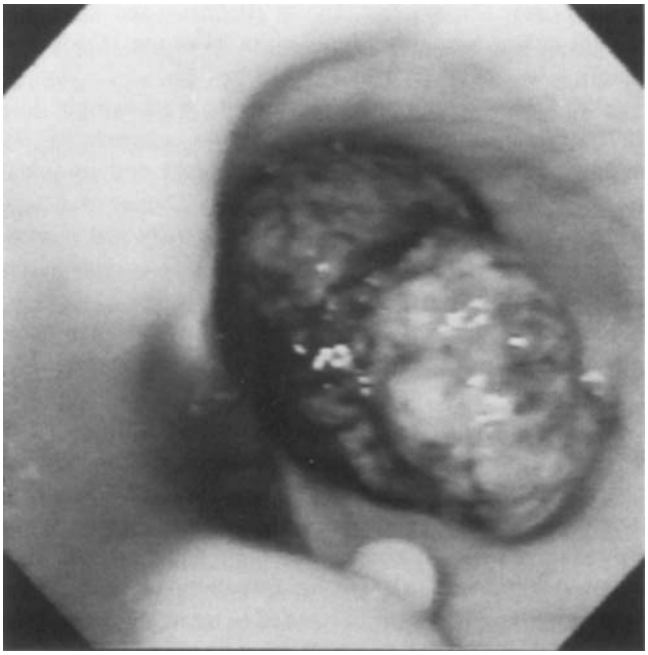

FIG. 1. Endoscopy of caudal esophagus of German Shepherd dog, 4-years-old, with a history of lameness, vomiting, and weight loss of 3 weeks duration. Note the typical *S. lupi* granuloma with a polyp-like structure on top (near field at the bottom of the photo), and a cauliflower-like mass filling the entire esophageal lumen (far field). Histopathologic diagnosis was osteosarcoma.

tification of eggs in only 1 dog. The remaining fecal examinations were negative.

Ten dogs were diagnosed with sarcoma (9 on necropsy or following surgical excision and 1 based on biopsy). Six were osteosarcomas and 4 fibrosarcomas. Two osteosarcomas and 2 fibrosarcomas had undergone metastasis to the thorax; 3 to the lungs and 1 to the ribs. One osteosarcoma also metastasized to the subcutaneous tissues, liver, ileum, and diaphragm, while 1 fibrosarcoma spread to the subcutaneous tissues, liver, spleen, kidney, and heart.

Endoscopy

Endoscopically there were 1–5 typical smooth rounded nodular granulomas, a cauliflower-like, irregular, proliferative esophageal mass, or both (Fig. 1). Worms were not seen but the typical granuloma often had a polyp-like structure on the top of the nodule, or a cratered center, which we believe may indicate the opening from where the worm tail may protrude. The masses were often ulcerated and necrotic. The mass filled the whole esophageal lumen in a few dogs hampering complete endoscopic visualization, thus preventing visualization of the whole mass, its extent of attachment to the esophageal wall, or if the caudal esophageal sphincter was involved. In 1 dog with an extramural esophageal granuloma and abscess, the only endoscopic abnormality was a narrowed esophageal lumen due to external compression. Thirteen masses had endoscopic guided biopsy. In 8 of these masses the diagnosis was necrotic tissue,

TABLE 2. Radiographic Findings of Spirocercosis

Radiographic Change	Typically Located Esophageal Masses (n = 27)	Atypically Located Esophageal Masses (n = 6)	No Visible Masses (n = 6)
Mass center point location	Caudal T8	T6	
Mass size (mm)			
width	20–130	35–90	—
length	35–165	40–110	—
height	20–100	30–70	—
Esophageal air			
moderate amount	8	—	—
large amount	1	1	—
cranial to mass	7	1	—
in mass	4	1	—
caudal to mass	—	1	—
Aorta mineralization	1	1	—
Spondylitis	10	3	2*
Complications	(n = 17)	(n = 4)	(n = 2)
bronchial displacement or compression	6	2	—
hypertrophic osteopathy	3	1	—
pleural effusion	3	2	1
pulmonary metastasis	3	—	—
other lung changes	3	—	1
mediastinitis	2	—	—
pneumothorax	2	—	—
mass mineralization	2	—	—
tracheal displacement or compression	1	2	1
pneumomediastinum	1	—	—
rapid mass enlargement	1	—	—

*One dog had L1–2 spondylitis.

of which 3 had necropsy later. Two of these were found to be sarcoma (2 days and 5 months later). In 5 biopsies there was evidence of neoplastic transformation of which 3 were diagnosed as fibrosarcoma that later proved to be osteosarcoma, after surgical excision in 2 dogs, and necropsy in the other. In 2 dogs there were additional endoscopic changes such as esophagitis and esophageal dilatation.

Radiology

Thirty eight of the 39 dogs had an esophageal mass, of which 33 were radiographically visible (Table 2). The last dog had thoracic aortic rupture.

Typical Dogs

Twenty-seven masses were typical and 17 of these had 1 or more complications. Typical dogs had a single mass located in the caudal mediastinal region with the center point of the mass on average being located at the caudal half of T8 (Fig. 2). The masses extended anywhere from T5–12. Maximum width could be easily measured, length was less well defined and height was difficult to determine, as the masses were often poorly defined on lateral views. Most masses were located between the aorta and caudal vena cava but some extended to the ventral aspect of the vertebral column. A moderate amount of esophageal air, regarded as abnormal, was commonly seen and a large amount of air, similar to megaesophagus was present in 1 dog. Air was most commonly seen cranial to the mass, and occasionally within the mass. No air was seen caudal to any mass. Spondylitis was seen in 10 dogs. The number of vertebrae involved varied from 1–6, ranging from T5–11. Most commonly 3 vertebrae were affected. The periosteal reaction was solid in most dogs and varied from mild, just obliterating the ventral concave vertebral surface, to fairly marked 4–5 mm wide reactions (Fig. 3). Spondylitis was occasionally accompanied by bridging of the disc space while in other dogs only the cranial or caudal half of a vertebra was involved (Fig. 3). This often gave the appearance of spondylosis but tended to extend further to the middle of the vertebra than typically seen in thoracic spondylosis.

Complications were seen radiographically in 63% of typical dogs (Table 2). Mineralization of the mass, believed to be indicative of osteosarcomatous transformation, was only seen in 2 dogs, 1 diagnosed on necropsy as osteosarcoma, and the second as fibrosarcoma based on endoscopic biopsy. Mediastinitis was seen in 2 dogs and pneumomediastinum was present in 1. In 1 dog the caudal mediastinal mass increased in size over 2 days resulting in a diagnosis of a suspected secondary hematoma or abscess and the dog was further evaluated by CT. This dog had an extramural esophageal granuloma and abscess with the worm protruding towards the mediastinum. Pulmonary metastases (Fig. 2) were diagnosed in 3 dogs and were not the dogs with mass mineralization. Other pulmonary changes (alveolar or interstitial patterns) were observed in 3 dogs. No intrathoracic lymphadenopathy was seen. Terminal tracheal and 1 or both main stem bronchial ventral displacement was seen fairly commonly. One main stem bronchus was compressed. Mild to moderate pleural effusion and pneumothorax was occasionally seen. Appendicular HO was seen in 3 dogs. On dorsoventral (DV) views the descending aortic outline was suspected to be irregular in 2 dogs and could have been

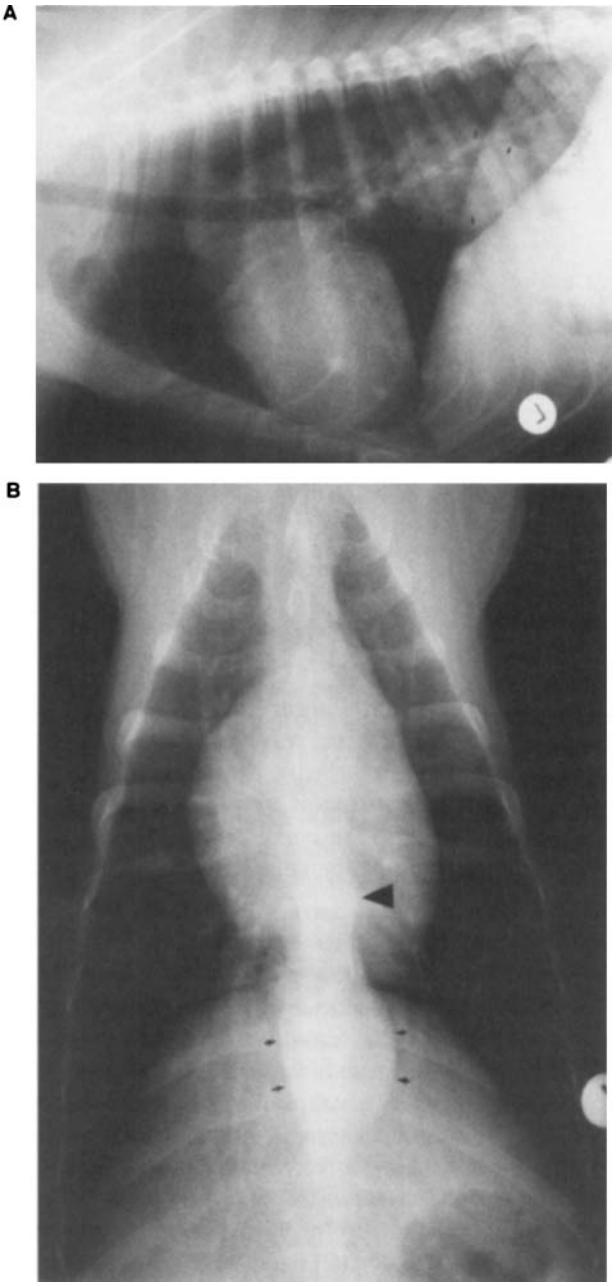

FIG. 2. Same dog as in Fig. 1. (A) Lateral thoracic radiograph. Note the typical caudal esophageal mass (arrows) and pulmonary nodules. The 2 masses seen on endoscopy appear as 1 mass radiographically. (B) DV view with mass (small arrows). Note irregular outline of left aortic margin in caudal heart region (arrow head).

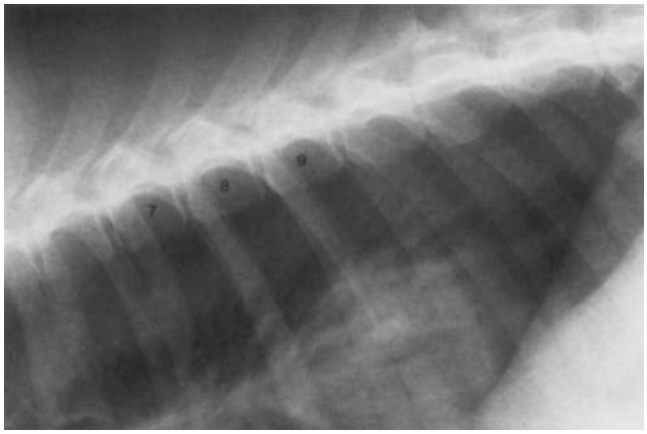

FIG. 3. German Shepherd dog, 8-years-old. Lateral caudodorsal thoracic region radiograph. Note the caudal esophageal mass and different stages of spondylitis. T6 = normal concave ventral vertebral border, T7 = early solid periosteal reaction, T8 & T9 = loss of ventral vertebral border concavity, T10 & 11 = advanced solid periosteal reaction involving mainly the vertebral body, T12 = normal and T12–13 = incidental early spondylosis.

indicative of small aortic aneurysms. A suspected aortic aneurysm, 30 × 20 × 20 mm, was present at the T6–7 level in 1 dog, and was diagnosed as an aortic granuloma on necropsy. Two linear streaks of aortic intima mineralization (1 × 6 mm), located in the initial descending aorta region were visible in 1 dog on the lateral view (Fig. 4).

Atypical Dogs

Six dogs were regarded as atypical of which 4 had complications (Table 2). The mass was located more cranially than expected (Fig. 5) with the center point of the mass located on average at T6. Atypical esophageal masses were about 70% smaller than typical masses. The presence of esophageal air was similar to typical dogs except for 1 dog that had air caudal to the mass. Spondylitis was seen in 3 dogs, all of them solid periosteal reactions and mostly ranging from T7–10. One dog radiographed after endoscopy had an iatrogenically air-distended esophagus, which allowed an esophageal mass to be seen just dorsal to the carina (Fig. 6A). This mass was not visible on routine thoracic survey radiographs (Fig. 6B) although another mass was visible further caudally. The incidence of complications was less than for typical dogs and mainly involved tracheal or bronchial displacement or compression (Table 2).

Comparing the clinical presentation of typical and atypical dogs, typical dogs had a higher incidence of dyspnea and lameness and/or weakness. Atypical dogs had more vomiting and/or regurgitation, coughing, salivation, and peripheral lymph node enlargement. However, the number of atypical dogs was too small to make this comparison conclusive.

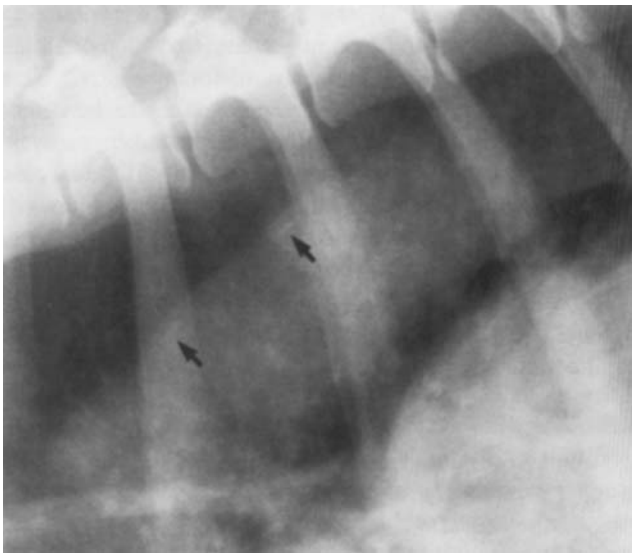

FIG. 4. German Shepherd dog, 4-years-old. Close-up lateral view of aorta. Note 2 linear streaks (arrows) of aortic intimal mineralization of initial descending aorta. Part of a caudal esophageal mass can be seen at bottom right corner.

Non-Visible Masses

Six dogs did not have a radiographically visible esophageal mass (Table 2). Five of these dogs had esophageal masses detected on endoscopy or necropsy. In 1 the diam-

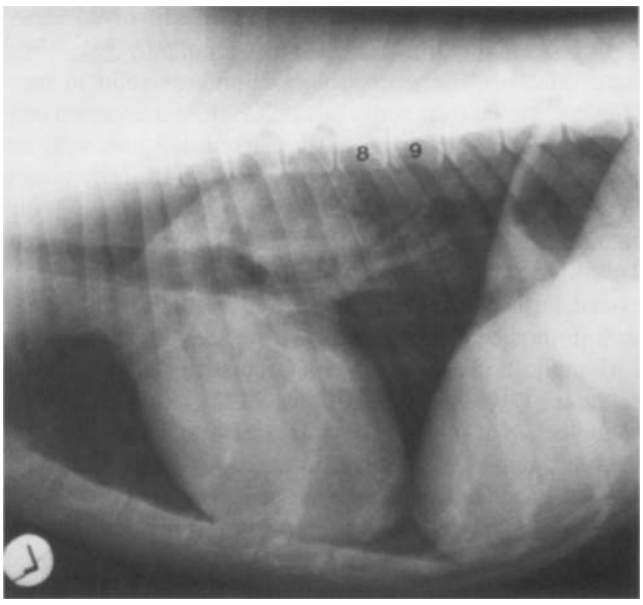

FIG. 5. Dalmation, 7.5-years-old, presented with a history of weight loss and regurgitation of 3 weeks duration. Lateral thoracic radiograph. Note the poorly defined soft tissue opacity in region ventral to aorta and caudodorsal to carina indicative of an atypically located mediastinal mass (center point between T6 and T7). Note loss of ventral vertebral concavity at T7–10 with pseudospondylosis at T9–10 (compare to T12–13 spondylosis in Fig. 3).

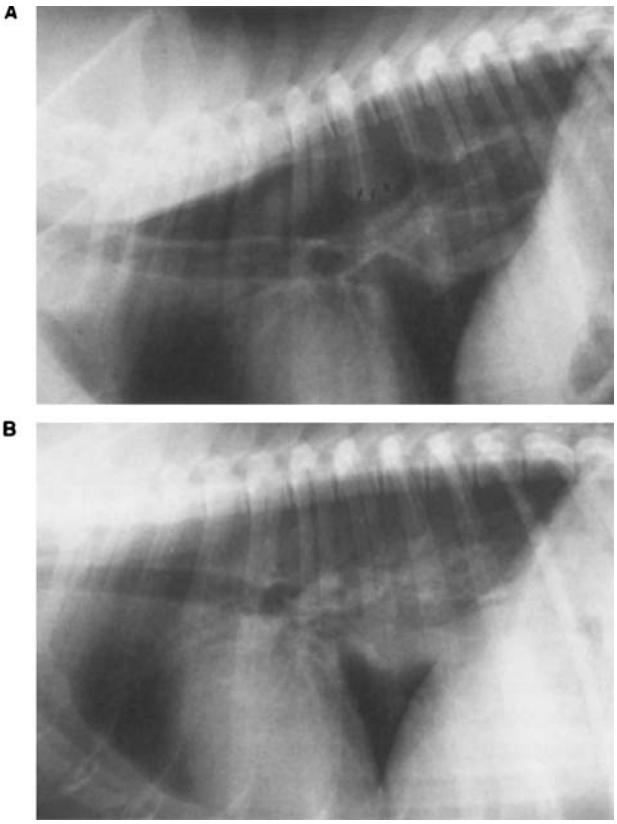

FIG. 6. Dalmation, 2-years-old, presented with anorexia and weight loss. Lateral thoracic radiographs. (A) Iatrogenic air-filled distended esophagus after endoscopy. Note the atypically located (center point T6) esophageal mass (arrows), caudodorsally to the carina. (B) Same dog next day without air in the esophagus. The above mass is not seen but poorly defined increased opacity in caudal mediastinum is visible.

eter was 5 mm and 20 mm in another. Diameter was not measured in the other dogs. Five dogs had other radiographic abnormalities. One of these had a dorsal cranial mediastinal mass extending from C5–T7 (Fig. 7), but this was extraesophageal and at surgery was found to be a craniodorsal mediastinal encapsulated hematoma containing adult worms that had undergone aberrant migration from the aorta. This dog did, however, also have a small granuloma in the caudal esophagus on endoscopy. Another dog had esophageal fluid accumulation with no mass visible. The sixth dog did not have an esophageal mass but had a marked thick brushlike spondylitis of L1–2 with a soft tissue opacity ventral to it. It died from a thoracic aortic rupture a few days after the radiographs had been made. On necropsy this dog had severe focal granulomatous aortitis, a few small aneurysms (1 of which had ruptured), valvular endocarditis and septic polyarthritis.

Computed Tomography

In the first dog, CT was performed 2 days after enlargement of a caudal mediastinal mass was seen radiographically. The dog was in dorsal recumbency. A roundish soft tissue mass was located in the dorsal mid and caudal mediastinum ventral to T7–11. The mass displaced the descending aorta and esophagus moderately to the left with slight compression and ventral displacement of the caudal vena cava (Fig. 8). An esophageal tube resulted in streaking artifacts in all images. The mass was 40 mm high, 36 mm wide, and 60 mm long. These measurements compared well to the radiographic measurements of 40 × 40 × 80 mm, respectively. The mass had a well-demarcated margin with a less opaque homogenous lumen of 18 HU, indicative of fluid. The right caudal lung lobe had moderate consolidation, believed to be pneumonia that was not visible on radiographs. The caudal mediastinum and accessory lung lobe region ventral to the mass appeared fluid-filled. Mild periosteal reaction was present ventrally and ventrolaterally on the vertebral bodies of T6–9. The aorta had several calcified areas in the intima region. The vertebral and aortic changes were not visible radiographically.

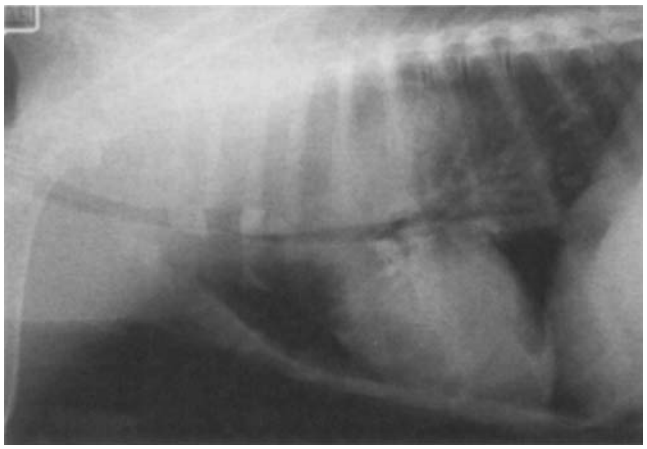

FIG. 7. Weimaraner, 5-years-old, presented with weight loss, dysphagia, and regurgitation of 2 weeks duration. Lateral cranial thoracic radiograph with craniodorsal mediastinal hematoma due to aberrant larval migration. Note large soft tissue opacity extending from C5–T7 depressing the trachea and craniodorsal heart ventrally. Air-filled dilated esophagus is visible on extreme left of the figure. Several bone fragments are trapped in ventrally displaced and compressed esophagus in region of ribs 1–3.

In the second dog, 2 CT examinations were performed at a 6-month interval with surgical removal of the mass after the first examination. The mass was 40 mm high, 30 mm wide and 60 mm long, similar to the radiographic measurements of 40 × 40 × 60 mm, respectively. Several mineralized areas, up to 3 mm diameter, were present in the lumen (debris) and within the esophageal wall. In the dorsal and right aspects of the esophageal lumen small air pockets were visible (Fig. 9). No displacement of surrounding structures was present. Pre- and postsurgically, the esophageal lumen was distended caudal to the mass. On surgery this mass was pedunculated, which was not clearly seen on CT. Ventral vertebral body periosteal reactions were present at T7–10. Similar aortic mineralization to the previous dog was seen.

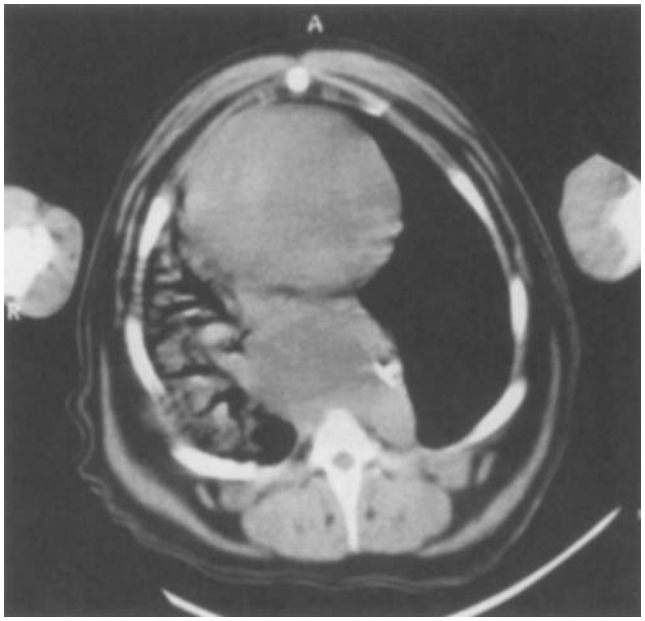

FIG. 8. Jack Russell Terrier, 9-years-old, presented with anorexia, pyrexia, anemia, and dyspnea of 1 week duration. Dorsally recumbent CT image (A is ventral). Transverse 5 mm thick slice at the level of T7 using a soft tissue window (WW 352 and WC 43). Note the roundish mass with a mildly more opaque circular border located between the ventral border of the vertebra and the heart. This mass displaces the esophagus (with tube) and descending aorta to the left. Moderate lung opacification due to bronchopneumonia and lung consolidation are present.

Computed tomography was performed in the third dog after 2 esophageal masses were diagnosed during an endoscopic examination for a suspected stomach ulcer. In radiographs made after this examination there was a mass located just dorsal to the carina in the iatrogenically air

FIG. 9. Same Dalmation as in Fig. 5. Sternal recumbent CT image. Transverse 10 mm thick slice located 30 mm caudal to the carina using a soft tissue window (WW 368 and WC 44). Note irregular mass in the terminal esophagus with gas present dorsally and on the right side. Mass appears to be attached between 4 and 9 o'clock. Early mineralization of the aortic intima is visible between 9 and 11 o'clock. There is no displacement of vascular structures.

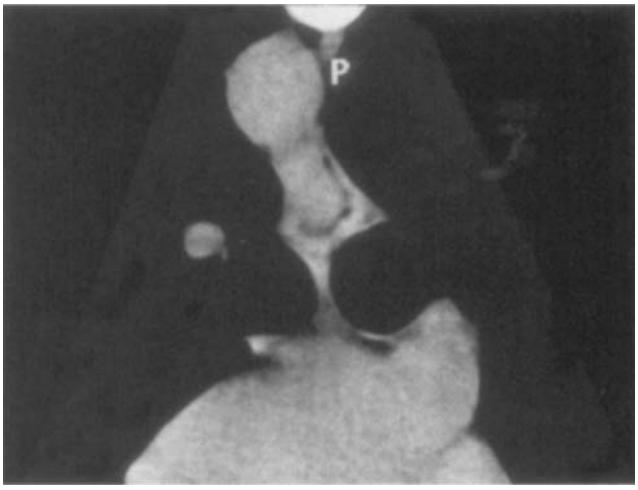

FIG. 10. Same Dalmation as in Fig. 6. Sternal recumbent CT image (P is dorsal). Transverse 5 mm thick slice just caudal to the carina, 2 minutes after intravenous bolus of 600 mg I/kg body weight and using a soft tissue window (WW 186 and WC 79). Intra-esophageal mass visible attached to the wall between 9 and 12 o'clock. Between 12 and 9 o'clock a thin rim of air is seen.

filled esophagus, but the mass was not visible on follow-up radiographs. On CT a 15 mm high, 10 mm wide and 30 mm long mass was present in the esophageal lumen, surrounded by a thin rim of air on the right side (Fig. 10).) A small amount of air was also present cranial to the mass. The second mass was typically located, and in this region, the esophagus widened to 50 mm and contained material iso-opaque, to stomach content. Contrast medium assisted in identifying mediastinal structures. Similar aortic and spondylitic changes to the previous dogs were present.

Outcome

Nineteen of the dogs were treated medically. Seventeen were treated with Doramectin‡ at a dose of 200 μg/kg subcutaneously, for 3 treatments at 14 day intervals or orally at 500 μg/kg day for 6 weeks, a regimen used successfully in our hospital.[32] Two dogs were treated with Ivermectin.§ Fifteen dogs were euthanized at the time of diagnosis. Three underwent successful surgery: 1 for hematoma drainage and 2 for tumor removal of which 1 also received cisplatin chemotherapy and the other doramectin. Two dogs died suddenly due to aortic rupture.

Discussion

Clinical Presentation

German Shepherd dogs were overrepresented in this study, which is in agreement with reports from Kenya[23] and India[33] but not from the United States.[5] This different breed

‡Pfizer, RSA.
§Merial, London, UK.

predilection between countries may indicate an environmental factor. In South Africa dogs are often kept outside as guard dogs, and thus have a greater possibility of becoming infected. The German Shepherd dog is a very common guard dog, and may explain their overrepresentation.

The high incidence of certain clinical signs such as dyspnea and lameness, besides the expected upper gastrointestinal signs, is evidence of the complexity of clinical spirocercosis. Based on our results, in endemic areas spirocercosis should be a consideration in patients with dyspnea, chronic cough and HO.

The use of fecal analysis to confirm spirocercosis has been used extensively in experimental models.[14] In clinical patients it is a problematic diagnostic technique since the worm often does not protrude into the esophagus, or when a tumor has developed, the worm is often not present,[1] or egg laying may be irregular.[2,15] A technical consideration is that the egg is very small and better visualized if the feces are first dissolved in artificial gastric juice,[34] and flotation is performed using a high specific gravity solution such as sugar[35] or zinc sulfate.[36] In this study zinc sulfate was used only twice, both times with negative results, but even considering this, the very poor outcome of 1 positive sodium nitrate flotation out of 30, and no positive fecal smears, indicate the poor sensitivity of routine fecal examinations in clinical circumstances.

Endoscopy

The authors found endoscopy to be the antemortal imaging modality of choice to confirm the diagnosis. However, with large masses filling the whole lumen, commonly seen in this study, endoscopy failed to provide information for surgical decision making such as the extent and type of mural attachment, or whether the caudal esophageal sphincter was involved. In surgery performed on 1 of the dogs the mass was found to be pedunculated and this was not evident on endoscopy or CT. According to the literature, masses are often pedunculated,[3] which would simplify surgical excision, but the mass may also have a broad stalk[23] which emphasizes the need for improved diagnostic procedures for surgical candidates. Although endoscopic biopsy is a useful tool, its sensitivity for detecting neoplastic transformation is limited. Biopsy diagnosis proved to be incorrect after necropsy or surgical excision in 38% of dogs, indicating its limitations in this study. Repeated deeper sampling from the same site may improve its accuracy.

Radiology

In atypical dogs the mass was located more cranially than expected, with the mass center point on average 2.5 vertebrae more cranial than in typical infections. Of the 39 dogs 15% were atypical, similar to previously described 15% of esophageal masses located cranially.[31] The atypical masses were also generally smaller, which together with their location in the hilar region made them more difficult to visualize unless they were surrounded by air. In atypical dogs esophageal air could also be present caudal to the mass. Radiographically 1 mass was usually seen, although endoscopically a few dogs had 2–5 masses (Figs. 1 and 2). A granuloma located in the cardia seen endoscopically was not visualized radiographically.

One would expect that the masses could result in mineralized debris cranial to or at the level of the mass. None was seen, although mineralization of the mass could be confused with this. However, in 1 dog a piece of bone was lodged in the region of the mass and in another, the dog with the cranial mediastinal hematoma, a bone was lodged ventral to the mass due to compression of the esophagus by the hematoma.

Esophageal contrast studies are not routinely performed in our hospital in dogs suspected of having spirocercosis as endoscopy provides more information. However, positive and negative esophageal contrast studies can be useful in the absence of endoscopy to detect small or hilar masses, to distinguish the mass from a foreign body, and to assess its size and the extent or location of mural attachment.[2,15]

Spondylitis was seen in 38% of dogs, thus, confirming the interrelationship between caudal thoracic spondylitis and spirocercosis. Spondylitis tended to be located on average 1 thoracic vertebra more cranially in the atypical dogs. Spondylitis and spondylosis are often confused in the literature. Spondylitis is radiographically visible as a brush-like to solid periosteal reaction ventrally on the vertebral body with minimal involvement of the vertebral end plate. The normal vertebral body typically has a concave appearance and the loss of this concavity is an early sign of spondylitis (Fig. 3). Spondylosis is a non-inflammatory partial or complete bony osteophytic bridging of the intervertebral disc space secondary to degeneration of the annulus fibrosus.[37,38] In the thorax, spondylosis usually originates just from the adjacent vertebral end plate. Some of the dogs in this study had bony bridging of the intervertebral disc spaces, but the bony reaction tended to be more lamellar and extended to the middle of the vertebrae (Fig. 5). As the exact cause of this intervertebral disc bridging reaction is uncertain, the term "pseudospondylosis" may be more appropriate until histologic studies have been performed. The exact etiology of spondylitis caused by spirocercosis is still uncertain. Only the vertebrae directly adjacent to the descending aorta tend to be involved. This supports the theories that aberrant parasite migration[1] or severe periaortic inflammation[39] secondary to aortic migration may be responsible. Two dogs had spondylitis without a radiographically visible esophageal mass. In these dogs endoscopy is always indicated.

A 26% incidence of neoplastic transformation was found, which is higher than the 8.6% and 14.6% in 2 studies described in the southern United States,[1,40] but similar to the

incidence reported in Kenya.[23] In the latter study 21% of the *Spirocerca* positive dogs on autopsy had sarcoma. Seventy-four percent of those that also had typical clinical signs had sarcomas. However, different inclusion criteria in each study make comparison difficult. Our study was biased towards more advanced infections, those presenting with clinical signs. Primary esophageal sarcoma is very rare, while the incidence of *Spirocerca* associated esophageal sarcoma is relatively high.[3,22,31] It thus seems to be justified to regard esophageal sarcoma as a pathognomonic sign for spirocercosis in endemic areas, even if no other lesions and no worms are detected. Ten tumors were diagnosed in this study, but only 2 were diagnosed radiographically based on evidence of mass mineralization. Theoretically, mass mineralization can result from dystrophic calcification of a benign mass, but this was not reported in any of the dogs without tumors on necropsy, or biopsy. Three other dogs had pulmonary metastases indicative of a possible esophageal tumor. Only 50% of tumors were thus diagnosed radiographically. Half of the dogs with osteosarcoma and half of the dogs with fibrosarcoma, had spondylitis, compared to a 38% incidence of spondylitis in the total study. In this study there does not appear to be marked difference in the incidence of spondylitis between dogs with or without neoplasia. These findings are contrary to earlier studies where 7 dogs with *Spirocerca*-associated tumors had spondylitis,[40] and another[22] where 75% of tumors were associated with spondylitis. Our lower figures may be due to earlier diagnosis by means of endoscopy. Computed tomography had a greater sensitivity for detecting early spondylitis, and more CT studies could provide additional information on this as well as detection of early tumor mineralization. Spirocercosis is successfully treated in our hospital with doramectin,[32] but this study emphasizes the need for endoscopy and biopsy to exclude tumors before considering treatment.

Complications were detected radiographically in 23 dogs of which 19 also had clinical or necropsy complications. Another 11 dogs were defined as complicated based on either clinical signs or necropsy. In total 87% of dogs were regarded as complicated. Generally, radiographically detectable complications appeared to be less extensive in the atypically located masses, probably because the masses tended to be smaller. Tracheal and bronchial displacement or compression are two specific complications that appeared to be more common in the atypical masses and this can be ascribed to their closer location to these structures. In atypical infections the higher incidence of clinical complications such as regurgitation, coughing and salivation seem also to be due to the anatomic location of the mass.

Hypertrophic osteopathy may well have been present in more dogs but radiographs were only made of limbs of dogs with a clinical abnormality, and spirocercosis should be considered in endemic areas in dogs with lower limb periosteal reactions.

At necropsy severe aortic lesions may be present and include aneurysms, calcification and irregular aortic borders.[1,31] Minimal aortic changes were seen radiographically. The descending aorta on lateral views is often not well demarcated in normal dogs. In *Spirocerca*-infected dogs it is even less well defined due to the presence of an esophageal mass or inflammation of the aorta and its surrounding tissues. Only the ascending and initial descending aorta are thus likely to have radiographically visible changes. Mineralization of focal areas of intimal necrosis was seen in 2 dogs as short linear mineral opacities in the intima region of the initial descending aorta on lateral views only. One suspect aneurysm was visible in the initial ascending aorta on a lateral view. The left border of the aorta is generally well seen on DV radiographs, but in the current study it sometimes became difficult to differentiate between the aortic and esophageal mass walls. In some dogs there was a suspicion that this aortic wall was irregular secondary to small aneurysms. Aortic angiography has been performed in several studies and is useful to identify aortic aneurysms[1,30] and displacement, but is not used routinely in clinical management of spirocercosis, particularly with the greater availability of CT.

Radiology is thus an essential tool for the diagnosis of spirocercosis. The presence of a caudal mediastinal mass accompanied by spondylitis is considered pathognomonic. Radiology readily detects possible complications, even in the very early stages, allowing better patient management and prognostication. However, atypically located masses and very small masses may be difficult to detect or may not be visible at all. Filling the esophagus with air is an easily performed technique, which may improve mass detection.

Computed Tomography

Computed tomography assists in determining the exact size and shape of the mass, the presence of early mass mineralization indicating neoplastic transformation, as well as changes in the surrounding structures and detecting early pulmonary metastases. Compared to survey and contrast radiographs and endoscopy, CT provides valuable additional information in confirming non-esophageal or extra-esophageal masses to be spirocercosis-related due to earlier detection of aortic mineralization and spondylitis. In dogs with no endoscopic, radiographic vertebral, or fecal evidence of spirocercosis, CT may be the only means of obtaining an antemortem diagnosis. Sternal recumbency is preferable as it allows more normal positioning of the heart and other mediastinal structures. Slice thickness and intervals of 5 mm should be sufficient in large breeds since the area of interest has usually been well defined on the radiographs.

Intravenous contrast medium should be given routinely.

The resultant enhancement of the esophageal mucosa makes the use of a stomach tube superfluous and prevents streaking artifacts which may hamper evaluation of surrounding structures. However, even with contrast medium, it was difficult to determine whether the mass was pedunculated or sessile, and if the caudal esophageal sphincter was involved. Distending the esophagus with air prior to CT may help in these dogs. Despite these limitations, CT should be considered in all dogs undergoing surgical resection of a neoplastic mass.

Thoracic lymphadenopathy is not a feature of spirocercosis, as no evidence of lymphadenopathy was found by any imaging method. Computed tomography would, however, be more sensitive for detection of lymphadenopathy.

REFERENCES

1. Bailey WS. *Spirocerca lupi:* A continuing inquiry. J Parasitol 1972; 58:3–22.
2. Fox MS, Bums J, Hawkins J. Spirocercosis in dogs. Comp Cont Ed 1988;10:807–823.
3. Bailey WS. Parasite and cancer: Sarcoma in dogs associated with *Spirocerca lupi*. Ann NY Acad Sci 1963;108:890–923.
4. Bwangamoi, O. Spirocercosis in Uganda and its association with fibrosarcoma in a dog. J Sm Anim Pract 1967;8:395–398.
5. Dixon KG, McCue JF. Further observations on the epidemiology of *Spirocerca lupi* in the Southeastern United States. J Parasitol 1967;53: 1074–1075.
6. Hamir AN. Perforation of thoracic aorta in a dog associated with *Spirocerca lupi* infection. Aust Vet J 1984;61:64.
7. Hassan JC. Gastrointestinal helminth parasites of dogs in the Western Area—Freetown (Sierra Leone). Beitr trop. Landwirtsch.Veterinärmed. 1982;20:401–407.
8. Le Riche PD, Soe EK, Alemzada Q, Sharifi L. Parasites of dogs in Kabul, Afganistan. Br Vet J 1988;144:370–373.
9. Reinecke RK. Genus Spirocerca. In: Reinecke RK. Veterinary Helmintology. 1st ed. Pretoria: Butterworth, 1983:218–220.
10. Seneviratna P, Fernando ST, Dhanapala SB. Disophenol treatment of spirocercosis in dogs. J Am Vet Med Assoc 1966;148:269–274.
11. Urquhart GM, Armour J, Duncan JL, Dunn AM, Jennings FW. Spirocerca. In: Urquhart GM, Armour J, Duncan JL, Dunn AM, Jennings FW. Veterinary Parasitology. 1st ed. Glasgow: Longman Scientific and Technical, 1991:77–78.
12. Anantaraman M, Krishna S. Experimental spirocercosis in dogs with larvae from a paratenic host, *Calotes versicolor,* the common garden lizard in Madras. J Parasitol 1996;52:911–912.
13. Krahwinkel DJ, McCue JF. Wild birds as transport host of *Spirocerca lupi* in the Southern United States. J Parasitol 1967;53:650–651.
14. Krishna S, Anantaraman M. Some observations on the development of *Spirocerca lupi* in its intermediate and definitive hosts. J Helminthol 1971;XLV:123–131.
15. Evans LB. Clinical diagnosis of *Spirocerca lupi* infestation in dogs. J S Afr Vet Assoc 1983;54:189–191.
16. Ndiritu CG. Pathogenesis & lesions of canine spirocercosis. Mod Vet Pract 1975;57:924–931.
17. Schroeder H, Berry WL. Salivary gland necrosis in dogs: a retrospective study of 19 cases. J Sm Anim Pract 1998;39:121–125.
18. Tudury EA, Graca DL, Arias MVB. *Spirocerca lupi* induced acute myelomalacia in the dog. A case report. Braz J Vet Res Anim Sci 1995; 32:22–26.
19. Kumar N, Vegad JL, Kolte GN. Ossified lesions in canine aortic spirocercosis. Vet Rec 1981;109:142–143.
20. Hamir AN. Oesophageal perforation and pyothorax associated with *Spirocerca lupi* infestation in a dog. Vet Rec 1986;119:276.
21. Harrus S, Harmelin A, Markovics A, Bark H. *Spirocerca lupi* infection in the dog: Aberrant migration. J Am Anim Hosp Assoc 1996;32: 125–130.
22. Thrashler JP, Ichinose H, Pitot HC. Osteogenic sarcoma in the canine esophagus associated with *Spirocerca lupi* infection. Am J Vet Res 1963;24:808–817.
23. Wandera JG. Further observations on canine spirocercosis in Kenya. Vet Rec 1976;99:348–351.
24. Turk RD. *Spirocerca lupi* in unusual locations. J Am Vet Med Assoc 1960;137:721–722.
25. Barker IK, Van Dreumel AA, Palmer N. The Esophagus. In: Jubb KVF, Kennedy PC, Palmer N. Pathology of Domestic Animals. 4th ed. San Diego: Academic Press, Inc., 1993:39–41.
26. Georgi ME, Han H, Hartrick DW. *Spirocerca lupi* (Rudolphi, 1809) nodule in the rectum of a dog from Connecticut. Cornell Vet 1980;70:43–49.
27. Mayaudon HT, Hoepp A. *Spirocerca lupi* (Rudolphi, 1809) description of an atypical localization in the dog. Rev Med Parasitol Mar 1972; 24:57–60.
28. Soulsby EJL. Soirocerca lupi. In: Soulsby EJL. Helminths, Arthropods and Protozoa of Domesticated Animals. 7th ed. London: Baillière Tindall, 1986:291–294.
29. Suter PF. Swallowing problems and esophageal abnormalities. In: Suter PF. Thoracic Radiography. 1st ed. Switzerland: Wettswil, 1984:295–349.
30. Singh J, Bhargava AK, Tyagi RPS. Angiographic findings for the diagnosis of the *Spirocerca* infestations in dogs. Haryana Agr Univ J Res 1974;4:18–21.
31. Head KW. Tumors of the alimentary tract. In: Moulton JE. Tumors in Domestic Animals. Berkeley: University of California Press, 1990:347–435.
32. Berry WL. *Spirocerca lupi* esophageal granuloma: Successful treatment of six dogs with doramectin. Proc 15th ACVIM Forum, Florida, 1997:660.
33. Chandrasekharon KP, Sastry GA, Menon MN. Canine spirocercosis with special reference to the incidence and lesions. Br Vet J 1958;114: 388–395.
34. Cabrera DJ, Bailey WS. A modified stool technique for detecting eggs of *Spirocerca lupi*. J Am Vet Med Assoc 1964;145:573–575.
35. Markovics A, Medinski B. Improved diagnosis of low intensity *Spirocerca lupi* infection by the sugar flotation method. J Vet Diagn Invest 1996;8:400–401.
36. Eckert J, Kutzer E, Rommel M. Untersuchungsmethoden. In: Eckert J, Kutzer E, Rommel K Bürger H-J, Körting W. Veterinärmedizinische Parasitologie. 4th ed. Berlin: Paul Parey, 1992:46–69.
37. Morgan JP, Biery DN. Spondylosis deformans. In: Newton CD, Nunamaker DM. Textbook of Small Animal Orthopedics. 1st ed. Philadelphia: J.B. Lippincott Company, 1985:733–738.
38. Morgan JP, Hansson K, Miyabayashi T. Spondylosis deformans in the female beagle dog: A radiographic study. J Sm Anim Prac 1989;30: 457–460.
39. Chhabra RC. Symptoms and pathogenesis of spirocercosis in dogs. Indian Vet J 1973;50:551–554.
40. Seibold HR, Bailey WS, Hoerlein BF, Jordan EM, Schwabe CW. Observations on the possible relation of malignant esophageal tumors and *Spirocerca lupi* lesions in the dog. Am J Vet Res 1955;16:5–14.

Chapter 2

Optimising visibility of *S. lupi* associated pathology on survey radiographs.

Avner A, **Kirberger RM.** The effect of the various thoracic views on the appearance of selected thoracic viscera. *Journal of Small Animal Practice* 2005;46:491-498.

Kirberger RM, Dvir E, van der Merwe LL. The effect of positioning on the radiographic appearance of caudodorsal mediastinal masses in the dog. *Veterinary Radiology & Ultrasound* 2009;50:630-634.

Kirberger RM, Dvir E, van der Merwe L. Canine pneumoesophagography and the appearance of caudal esophageal masses secondary to spirocercosis. *Journal of the American Veterinary Medical Association* 2012;240:420-426.

Radiography is the mainstay of diagnosing spirocercosis and is often the first clinical procedure performed in a suspected case. In first world countries this is often followed by endoscopy and possibly computed tomography and surgery. However spirocercosis also occurs in many underdeveloped countries and here radiography is often the only sophisticated diagnostic procedure available. Treating patients in these countries is often also a cost-sensitive issue and thus optimising the radiographic techniques to make do with the minimum number of radiographs is essential.

Several papers have been written on the effect that various views have on the visibility of thoracic structures and pathology thereof.[1-4] These have however mainly concentrated on the effect on the cardiac silhouette and the visibility of lung and pleural space pathology. Numerous radiology textbooks have chapters on thoracic organs but the effect of positioning on the structures involved in spirocercosis, namely the oesophagus, aorta and mediastinum, is inadequate.

The first paper in this chapter by Avner and Kirberger described the effect of positioning on selected thoracic viscera in normal dogs, including the oesophagus and aorta. Kirberger and Avner in another article also examined the effect of positioning on selected cranial thoracic structures but these are generally not affected by spirocercosis and were thus not included in this dissertation.[5]

In the second paper the effect of positioning was taken one step further to evaluate what effect a caudodorsal mediastinal mass, in this case spirocercosis associated oesophageal pathology, would have on its visibility in the various thoracic views.

The third paper in this chapter hypothesized that pneumoesophagography, the poor man's endoscope, would improve the clinicians ability to detect and characterise oesophageal pathology.

References

1 Brinkman EL, Biller D, Armbrust L. The clinical usefulness of the ventrodorsal versus dorsoventral thoracic radiograph in the dog. J Am Anim Hosp Ass 2006;42:440-449.

2 Lang JW, Wortman JA, Glickman LT, Biery DN, Rhodes H. Sensitivity of radiographic detection of lung metastasis in the dog. Vet Radiol 1986;27:74-78.

3. Kern DA, Carrig CB, Martin RA. Radiographic evaluation of induced pneumothorax in the dog. Vet Radiol & Ultrasound 1994;35:411-417.

4 Lynch KC, Oliveira CR, Matheson JS, Mitchell MA, O'Brien RT. Detection of pneumothorax and pleural effusion with horizontal beam radiography. Vet Radiol & Ultrasound 2012;1:38-43.

5 Kirberger RM, Avner A. The effect of positioning on the appearance of selected cranial thoracic structures in the dog. Vet Radiol & Ultrasound 2006;47:61-68.

Effect of various thoracic radiographic projections on the appearance of selected thoracic viscera

OBJECTIVES: To assess the effect of different radiographic projections on thoracic width, as well as position and visibility of the trachea, principal bronchi, cardiac silhouette, aorta, caudal vena cava (CVC) and oesophagus.

METHODS: Right lateral recumbency (RLR), left lateral recumbency (LLR), dorsoventral (DV) and ventrodorsal (VD) thoracic radiographs of 42 dogs were reviewed retrospectively.

RESULTS: In 78 per cent of cases the thoracic width was significantly larger on the VD projection than on the DV projection. The angle of divergence formed by the principal bronchi was significantly larger on the VD projection than on the DV projection in 80 per cent of dogs. A cardiac silhouette bulge at 1 to 2 o'clock was apparent on the VD projection in 22 per cent of dogs but was never seen on DV projections. The descending aorta was more visible at the 4 to 5 o'clock cardiac silhouette level on the DV projection and laterally at the T8 level on LLR projections. The CVC was better seen on VD and LLR projections. The oesophagus was visible as a soft tissue opacity in LLR in large dogs with normal thoracic conformation in 35 per cent of cases.

CLINICAL SIGNIFICANCE: The DV projection appears to be more reliable for assessing the cardiac silhouette, the descending aorta and the angle of divergence of the principal bronchi. The VD projection should be considered for evaluating the CVC. LLR should be used for assessing the descending aorta and CVC.

A. AVNER AND R. M. KIRBERGER

Journal of Small Animal Practice (2005) **46**, 491-498

Diagnostic Imaging Section, Department of Companion Animal Clinical Studies, Faculty of Veterinary Science, University of Pretoria, Private Bag X04, Onderstepoort 0110, Republic of South Africa

A. Avner's current address is The Queen's Veterinary School Hospital, Department of Clinical Veterinary Medicine, University of Cambridge, Madingley Road, Cambridge CB3 0ES

INTRODUCTION

Routine thoracic radiographic examination consists of one lateral (right or left) projection and its orthogonal dorsoventral (DV) or ventrodorsal (VD) counterpart. In order to choose the most informative projections, the investigator must have an understanding of the effect of positioning on the radiographic appearance of thoracic structures. In most cases right lateral recumbency (RLR) is standard since it provides the most accurate information for evaluating the cardiac silhouette (Spencer and others 1981). In RLR the cranioventral cardiac border and apex have more sternal contact compared with left lateral recumbency (LLR), in which the elevated cardiac apex may be mistaken for pathology (Berry and others 2002). The DV projection provides for greater consistency of the cardiac position. The cardiac silhouette tends to be in contact with the diaphragm and the apex points towards the left because of the cranial excursion of the dependent diaphragmatic cupula (Berry and others 2002). Ruehl and Thrall (1981) reported that on VD projection the cardiac silhouette appeared more elongated, there was little cardiac-diaphragmatic contact and the heart base was located closer to the dorsal limit of the thoracic cavity, suggesting movement of the thoracic viscera in response to gravitational forces.

Changes in the position of the diaphragmatic components on the various projections have been well described (Grandage 1974, Pechman 1987, Dennis and others 2001, Berry and others 2002). On VD projections the more dependent right and left diaphragmatic crura have a convex appearance and are superimposed over the more central cupula, often resulting in three bulges. On DV projections the cupula is clearly seen as a single dome with no sign of the crura as the abdominal contents, now located ventrally, push only the cupula forwards. The more dependent crus is always forced to move cranially due to the pressure exerted by the more dependent abdominal contents, and this is seen on lateral radiographs.

The effect of positioning on the visibility of pulmonary blood vessels and pathology is well known. The caudal lobar pulmonary vessels are best seen on DV projections because they are magnified, surrounded by well aerated lung and are more perpendicular to the primary x-ray beam (Ruehl and Thrall 1981). However, on VD projections the accessory lung lobe has less superimposition of the heart and diaphragm, which allows more accurate assessment of caudal mediastinal

or accessory lobe pathology (Berry and others 2002). One very important effect of lateral recumbency is the difference in conspicuousness of a lung lesion, depending on whether the lesion is in the dependent or non-dependent lung. Pechman (1987) reported that in lateral recumbency the subsequent increased radiopacity of the dependent lung lobe masks lung pathology. However, the uppermost lung will tend towards slight compensatory overinflation, resulting in excellent contrast of any possible pathology. Ahlberge and others (1985) suggested that fine detail and small lung lesions may go undetected in the partially collapsed dorsal lung region when evaluating VD projections.

The fact that a pulmonary artery bulge may be seen in normal dogs is well recognised (Suter 1984, Dennis and others 2001). Possible causes are rotation of the chest, radiographs taken at the end of ventricular systole, particularly in deep-chested dogs, and radiographs taken in dorsal (VD projection) or sternal (DV projection) recumbency. This might easily be confused with a bulge caused by pulmonic stenosis (Finland and others 1986, Owens and Biery 1999, Berry and others 2002). The authors have occasionally seen a 1 to 2 o'clock bulge only on VD projections in normal dogs and suspect that positioning may make a significant contribution to the visibility of this bulge. Additionally, variation in the thoracic conformations of different breeds accounts for large differences in apparent cardiac size (Lamb and others 2001, Berry and others 2002). Berry and others (2002) thus advocate the subjective assessment of cardiac size on DV or VD projections in addition to vertebral heart scale measurements (Buchanan and Bucheler 1995). Changes in thoracic conformation and size on DV and VD projections that may alter the subjective perception of cardiac size have not been investigated to date.

Similarly, the effect of positioning on the location of the trachea and principal bronchi has not yet been evaluated, to the best of the authors' knowledge. On DV/VD projections the trachea is normally located slightly to the right of the midline, while on lateral projections there is slight divergence of the trachea from the thoracic spine. Deviation of the intrathoracic trachea may be due to a mediastinal mass or might be an artefact resulting from the neck being bent to the right on DV/VD projections and dorsally on lateral projections (Suter 1984, Berry and others 2002). Also, a rotated, oblique lateral radiograph may present a false impression of dorsal tracheal displacement (Biery 1974). In order to avoid potential misdiagnoses it is important to assess whether the position of the trachea changes on the various projections. Similarly, in the authors' experience, positioning may affect the angle of divergence of the principal bronchi, which could be confused with an enlarged left atrium or regional lymph node.

The normal oesophagus is usually not seen on survey radiographs. However, it is observed sometimes as a faint soft tissue opacity in the caudal thorax on lateral projections (Suter 1984, Kealy and McAllister 2000). The effect of LLR versus RLR on its appearance has not been investigated.

The aims of the present retrospective study were to assess positional variations and visibility of these viscera on the various thoracic projections.

MATERIALS AND METHODS

The radiographic archives of the Onderstepoort Veterinary Academic Hospital were searched for skeletally mature dogs that had been radiographed using four standard thoracic projections as a routine screening for pulmonary metastasis. These dogs had not been routinely sedated. Rotated, oblique and expiratory radiographs were excluded. Radiological records and histories from accompanying request forms were reviewed. All cases with possible clinical thoracic pathology as well as radiological pathology were excluded except those cases with a maximum of three metastatic nodules (of up to 2 cm diameter), provided they did not interfere with the visibility of the structures under investigation.

The dogs were divided into three groups: group 1 (large dogs weighing more than 30 kg); group 2 (medium-sized dogs weighing from 10 to 30 kg); and group 3 (small dogs weighing less than 10 kg).

A method was devised to estimate obesity. On the VD projection the sixth rib width was measured at its most lateral curvature using a calliper. The thicknesses of the adjacent subcutaneous tissues were determined as multiples of this width. Each rib width of tissues was graded as one unit of obesity. Gradings of 1 to 3 were included in the study and gradings greater than 3 were excluded as being too obese.

Thoracic conformation was determined from the thoracic depth:width ratio, as described by Buchanan and Bucheler (1995). Depth was measured in RLR whereas width was measured on DV radiographs. Dogs with depth:width ratios of greater than 1·25 were considered to have a deep thorax. Those with ratios of less than 0·75 were considered to have a broad thorax. The rest were regarded as having a normal thoracic conformation.

Radiographic measurements and observations

The following were measured in millimetres on DV and VD projections and compared.

- Thoracic width was measured as the distance between the medial borders of the eighth ribs at their most lateral curvatures.
- The distance of the lateral tracheal border from the middle of the vertebral body was measured at the third intercostal space.
- The angle formed by the principal bronchi was measured from a point at the centre of the bifurcation and two central points located caudally in the principal bronchi at 10, 15 and 20 mm in small, medium and large breeds, respectively.

The following were evaluated subjectively on DV and VD projections and compared.

- Relative conformation of the principal bronchi.
- Focal bulges of the cardiac silhouette, in particular at the 1 to 2 o'clock region. The potential effect of obesity resulting in a widened cranioventral mediastinum affecting the visibility of this region was also assessed.
- Visibility of the left lateral border of the aorta at the levels of 2 to 3 o'clock and 4 to 5 o'clock of the cardiac silhouette.
- Visibility of the caudal vena cava (CVC) at the regions superimposed on the cardiac silhouette and lung.

The perpendicular distance from the terminal dorsal tracheal wall to a line connecting the ventral borders of the associated vertebral bodies was also measured in millimetres in RLR and LLR and compared.

Visibility of the aorta in the region ventral to T8, visibility of the CVC between the heart and the diaphragm, and visibility of the terminal oesophagus were also evaluated subjectively in RLR and LLR and compared.

Visibility of structures was graded as 1, not seen; 2, vaguely seen; 3, seen with ill-defined borders; and 4, seen with well-defined borders. All radiographs were evaluated by the senior author and all radiographs of each dog and each group were evaluated at the same time to ensure consistency.

Statistical analysis

Results were expressed as mean (sd). Significant results were found between the two samples using paired *t* tests. Statistical analysis of the data was performed using a SPSS statistical package. The significance level for all tests was $P<0{\cdot}05$.

RESULTS

Forty-two sets of radiographs from dogs ranging in age from two to 12 years were selected (Table 1). There were 17 large-breed dogs (group 1), 15 medium-breed dogs (group 2) and 10 small-breed dogs (group 3).

Table 1. Signalment and body condition of the 42 dogs

Group	Breed	Age in months	Sex	Obesity grading
Group 1	GSD	108	M	1
	GSD	84	M	1
	Rottweiler	84	F	2
	Rottweiler	30	M	2
	Pointer	36	F	2
	GSD	78	F	2
	GSD	42	M	2
	GSD cross	Mature	NA	3
	GSD	Mature	NA	2
	Dalmatian	48	M	1
	Dobermann	144	M	3
	Dobermann	132	M	2
	Labrador cross	132	F	3
	Rottweiler	60	M	2
	Labrador	96	F	3
	Crossbreed	168	M	3
	Bullmastiff	Mature	NA	2
Group 2	Crossbreed	72	M	2
	SBT	96	M	3
	SBT	144	F	3
	SBT	84	M	2
	SBT	72	M	2
	Bull terrier	Mature	NA	2
	Crossbreed	144	F	3
	SBT	84	F	3
	SBT	48	F	2
	Bull terrier	Mature	NA	3
	SBT	96	M	3
	SBT	72	M	2
	Spaniel	96	F	3
	Pit bull terrier	Mature	M	3
	Beagle	Mature	NA	3
Group 3	Maltese	Mature	F	1
	Boston terrier	48	M	3
	Maltese	Mature	NA	3
	Maltese	Mature	F	3
	Maltese	Mature	F	2
	Maltese	144	F	3
	Scottish terrier	132	F	3
	Fox terrier	108	M	3
	Maltese	119	F	3
	Maltese	144	F	3

M Male, F Female, SBT Staffordshire bull terrier, GSD German shepherd dog, NA Information not available, Mature Radiographically skeletally mature

All group 1 dogs had a normal thoracic conformation. In group 2, 10 dogs had a normal thoracic conformation, four dogs had a broad conformation and one dog had a deep conformation (Fig 1). In group 3, eight dogs had a normal thoracic conformation and two had a broad thoracic conformation. Certain breeds dominated the groups: German shepherd dogs (GSDs, 35 per cent) in group 1, bull terrier-like dogs (75 per cent) in group 2 and Maltese (70 per cent) in group 3 (Table 1).

The majority of cases (78·6 per cent) had a VD width measurement larger than the DV measurement (Fig 2). The difference was statistically significant (t=–3·549, degrees of freedom (df)=37, $P<0{\cdot}001$).

The distance from the terminal trachea to the ventral border of the vertebral bodies was larger in RLR in 68·75 per cent of group 1 dogs (Fig 3). In groups 2 and 3,

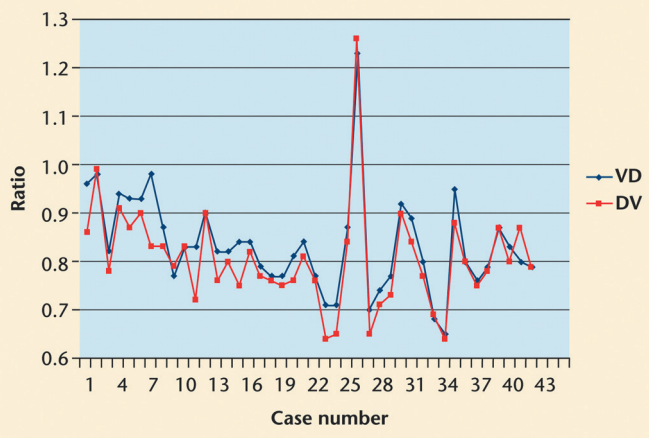

FIG 1. Graph comparing the thoracic conformation ratio calculated on dorsoventral (DV) and ventrodorsal (VD) projections. Note the fairly consistent greater thoracic conformation ratio on the VD projections

the distance was greater in LLR in 66·6 and 70 per cent of dogs, respectively. The difference was only significant in group 3 dogs (t=2·714, df=9, P=0·024). When combining all the groups together, the differences between LLR and RLR of each individual were not significant (P=0·932).

On DV projections, the distance of the lateral tracheal border from the middle of the vertebral bodies was significantly larger than on VD projections in 81 per cent of all dogs (t=–3·575, df=37, P<0·001) (Fig 4). However, in the individual groups a significant difference was only found in group 2 (t=–4·702, df=13, P<0·001) and group 3 (t=–2·605, df=9, P=0·029).

The angle formed by the principal bronchi was larger on the VD projection in 80 per cent of the cases; 11 per cent had equal angles, while in 9 per cent of the cases the angle was larger on the DV projection (Figs 5 and 6). The angle difference was statistically significant in all dogs (t=–6·159, df=36, P<0·001) and was most marked in group 1 (t=4·665, df=11, P<0·001), compared with groups 2 and 3. Subjective assessment suggested that the increased divergence of the principal bronchi on the VD projection was largely attributable to greater lateral divergence of the left principal bronchus. Group 2 dogs

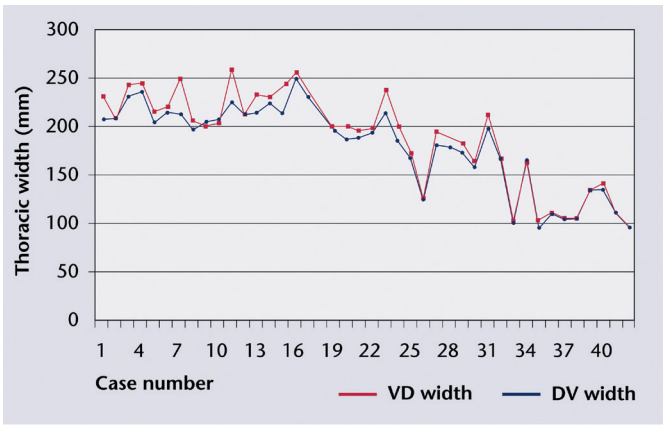

FIG 2. Graph comparing the thoracic width on DV and VD projections in large-breed (cases 1 to 17), medium-breed (cases 18 to 32) and small-breed (cases 33 to 42) dogs

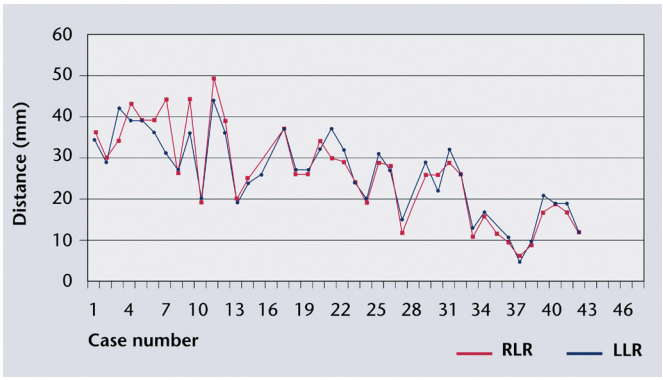

FIG 3. Graph comparing the perpendicular distance between the terminal dorsal tracheal wall and the ventral border of the vertebral bodies on left lateral recumbency (LLR) and right lateral recumbency (RLR) projections

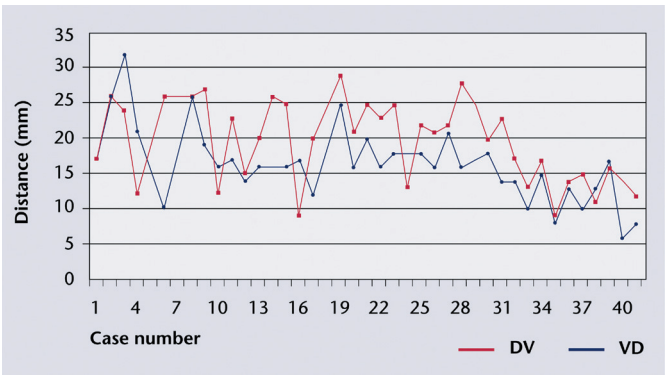

FIG 4. Graph comparing the distance between the lateral tracheal border and the thoracic midline on VD and DV projections. The DV projection generally has the trachea lying further away from the midline

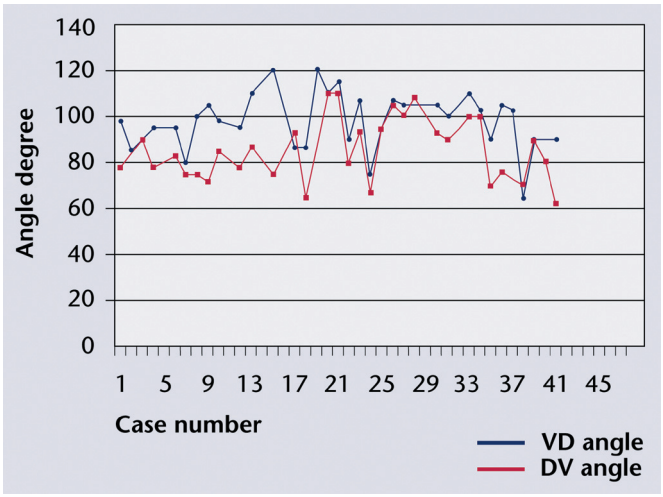

FIG 5. Graph comparing the angle formed by the principal bronchi on VD and DV projections

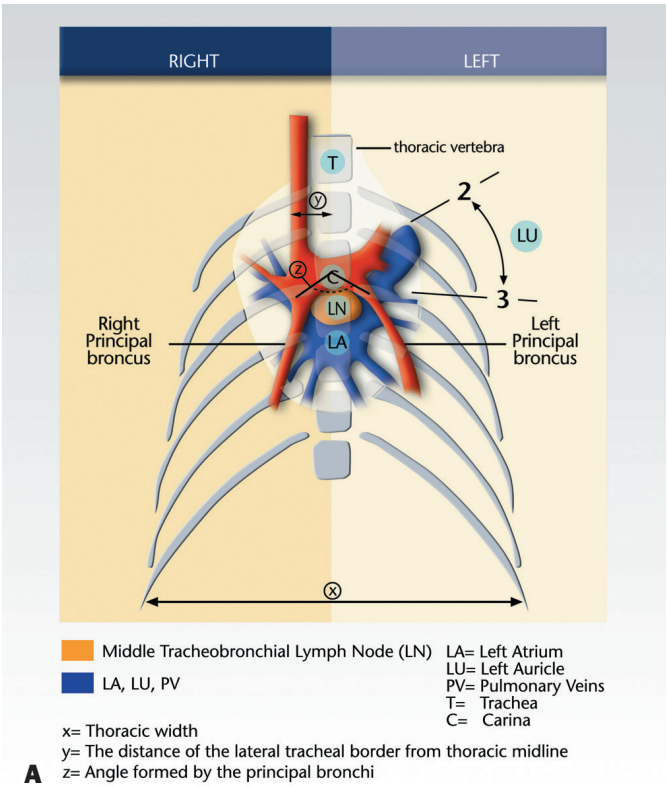

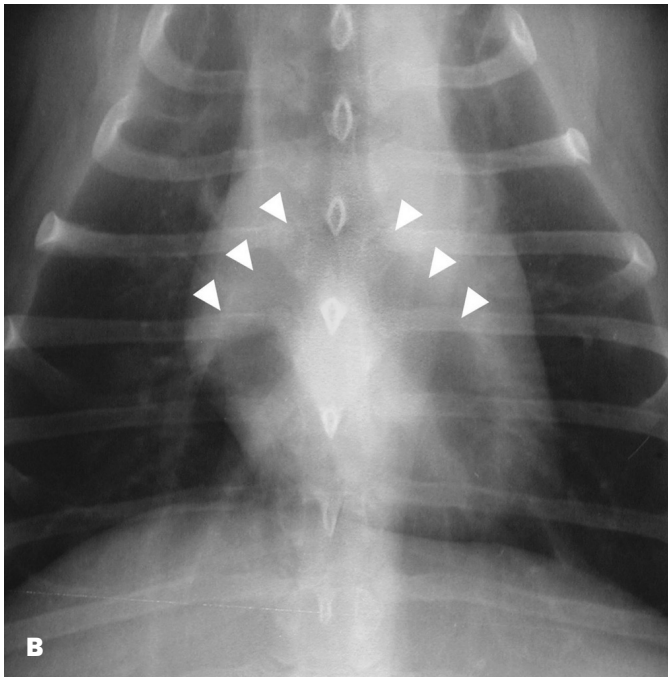

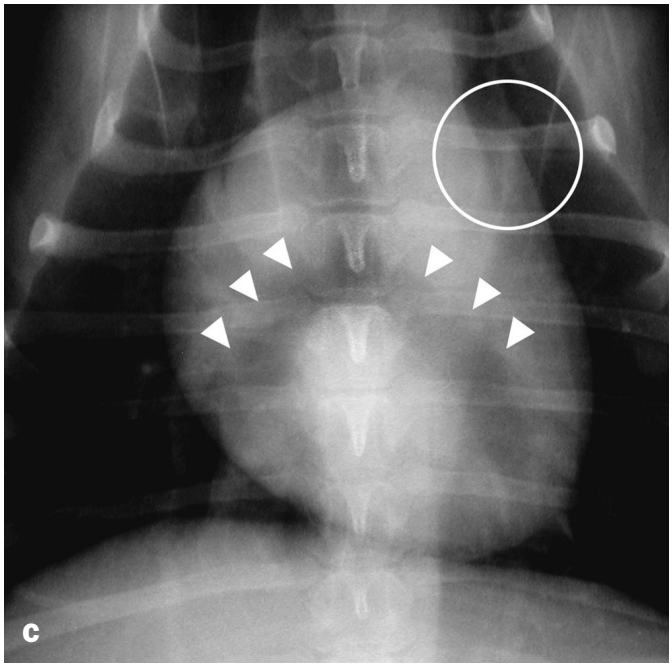

FIG 6. (A) Sketch of the appearance of the principal bronchi and their location with respect to the left atrium (LA) and middle tracheobronchial lymph node (LN). Enlargement of the LA will displace the principal bronchi laterally. The same pattern may be seen on VD projection as the heart base gravitates to the dependent side. (B) DV and (C) VD radiographs of the S4 principal bronchi of a small-breed dog with a normal thoracic conformation (ratio 0·8). On the VD projection there is marked splaying of the principal bronchi (arrowheads), mostly attributed to lateral divergence of the left principal bronchus. Note the triangular fatty opacity (cranioventral mediastinum) superimposed on the cardiac silhouette at 2 o'clock (circle)

had a more curved conformation of the main stem bronchi on both projections when subjectively compared with the other groups.

A cardiac silhouette bulge at 1 to 2 o'clock, correlating with the location of the pulmonary trunk, was seen in 22 per cent of VD projections (three from each group). In dogs with a normal to broad thorax and higher obesity score, the caudal border of the cranioventral mediastinum was visible on VD projections as a fatty, opaque triangular structure that merged with the cardiac silhouette at 1 to 2 o'clock, mimicking a cardiac bulge (Fig 6C). None of the cases had a detectable cardiac silhouette bulge on the DV projection (Fig 7).

There was no difference seen in the visibility of the descending aorta's left border on DV and VD projections at the 2 to 3 o'clock level but at 4 to 5 o'clock it was better seen on the DV projection (Fig 8). At the T8 level the aorta was more clearly seen in LLR (Fig 8).

On VD projections, the CVC (Fig 9) was better identified both in the pulmonary region and where it was superimposed over the cardiac silhouette. On lateral projections, the CVC was slightly more visible in LLR.

The oesophagus was visible in LLR in 35 per cent of group 1 dogs and 13·3 per cent of group 2 dogs (Fig 10). All these dogs had a normal thoracic conformation, except one that showed a broad thorax. In one group 2 dog the oesophagus was seen in RLR. The

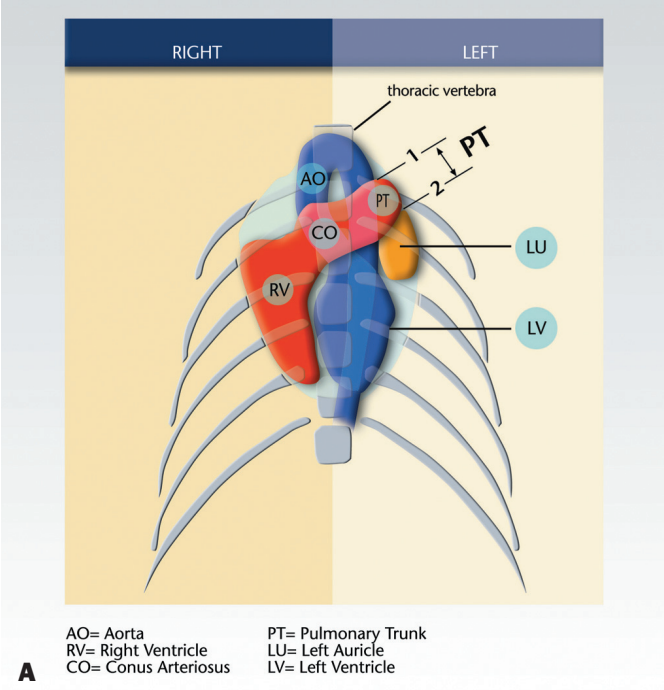

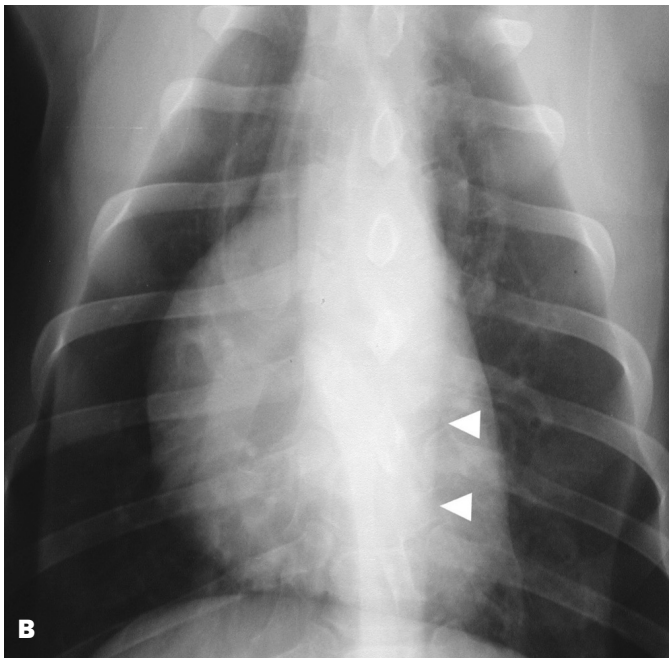

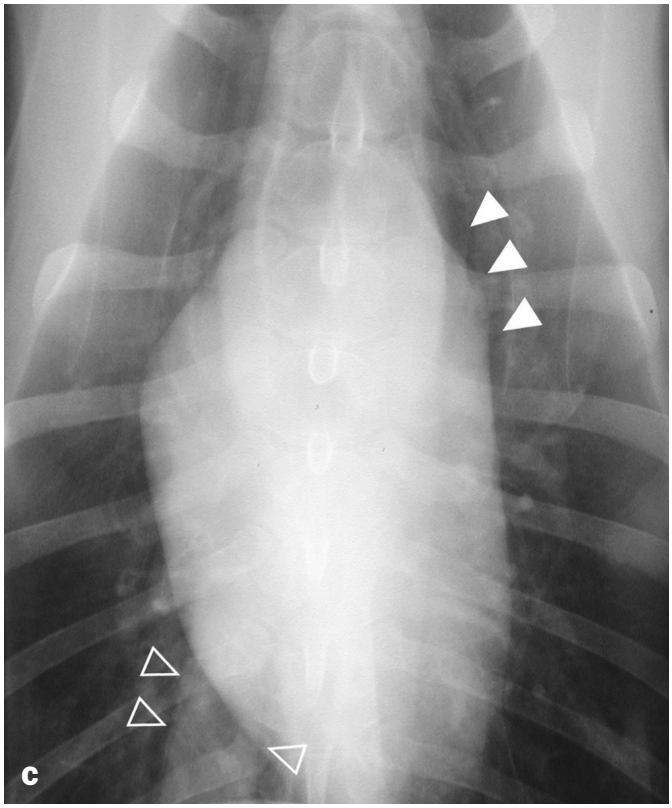

FIG 7. (A) Sketch of the appearance of the heart on the VD projection. The craniocaudal axis of the heart appears longer and the apex closer to the midline. The heart is nearly parallel to the spine. This projection skylines the main pulmonary artery trunk (PT) and may simulate a 1 to 2 o'clock bulge. (B) DV and (C) VD radiographs at the level of L9 at 1 to 2 o'clock in a large-breed dog of normal thoracic conformation (ratio 0·78). On the DV projection, the heart appears wider and the left cardiac border is fairly straight whereas on the VD projection the heart appears longer, more parallel to the midline and there is a subtle bulge at 1 to 2 o'clock (arrows). Note that the aorta is better seen at the level of 4 to 5 o'clock on the DV radiograph (arrows) and the caudal vena cava is better seen on the VD radiograph (empty arrows)

visibility grading was mostly 2 or 3. The oesophagus was not seen in group 3 dogs and obesity did not appear to influence its visibility.

DISCUSSION

When investigating the canine thorax, two orthogonal projections for pulmonary pathology screening or two opposing lateral projections are routinely used (Lang and others 1986, Berry and others 2002). It is essential for clinicians to be aware of the effect that various projections have on the radiographic visibility and location of thoracic viscera. If on initial survey films or based on clinical suspicion alternative projections can be considered to highlight suspect pathology, or limitations of specific views are known, diagnostic accuracy is increased.

In this study it was clear that the thorax was often wider on the VD projection (Fig 2). The reason for this is uncertain at this stage but could include greater inspiratory effort in an unnatural position or less impedance of rib movement. The more cranial position of the front limbs on the VD projection could contribute to less impedance of rib movement. This altered width could also result in body conformation differences when calculated from the VD instead of the DV projection (Fig 1). This finding may explain Ruehl and Thrall's (1981) subjective impression that the heart appeared narrower on VD projections despite only subtle variations in measured cardiac width (VD versus DV).

The distance between the terminal trachea and the vertebrae was significantly larger on LLR projections (versus RLR) only in the group of small-breed dogs. The smaller dogs had a higher obesity grading and subsequently more abdominal, mediastinal and sternal fat as well as a more globoid cardiac silhouette. The authors postulate that in LLR these factors somehow facilitate greater movement of the cardiac apex away from the sternum to the left side. This in turn displaces the carina and

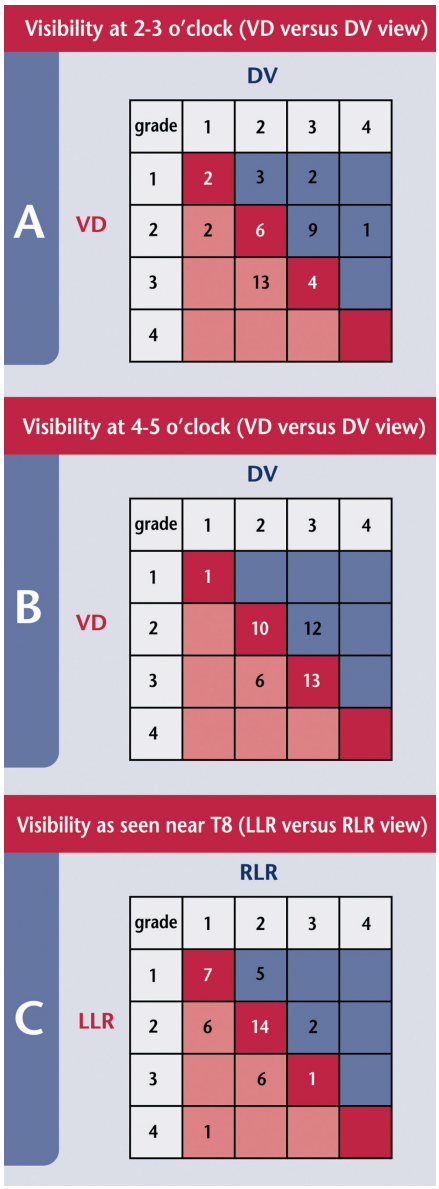

FIG 8. Aorta visibility. The number of cases allocated a particular combination of grading is indicated in the boxes. Red boxes = Grading the same for the two projections, Blue boxes = Number of cases in which visibility is better in the DV or RLR projection, Pink boxes = Number of cases in which visibility is better in the VD or LLR projection

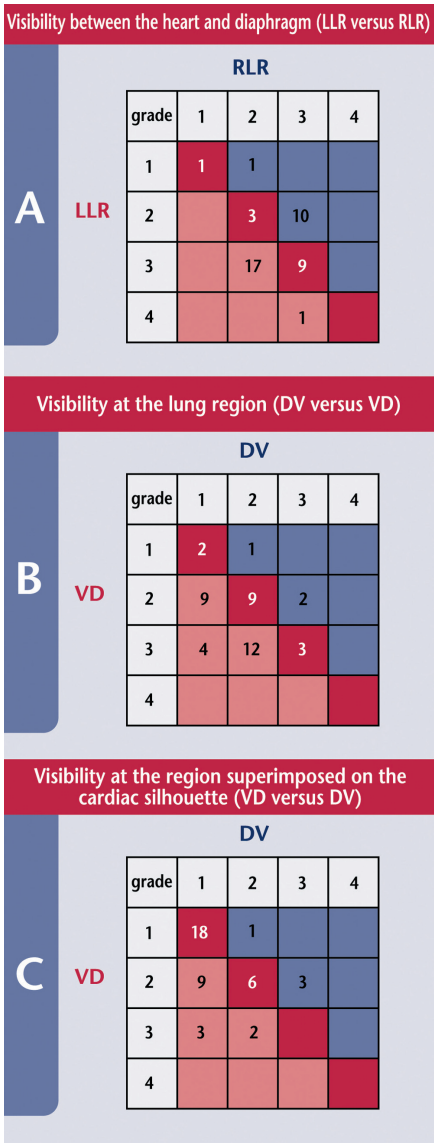

FIG 9. Caudal vena cava visibility. The number of cases allocated a particular combination of grading is indicated in the boxes. Box details as given in Fig 8

associated trachea and mediastinal structures ventrally. The distance of the trachea from the middle of vertebral bodies on DV projections was significantly greater than on VD projections and could be misdiagnosed as a mediastinal mass effect. It is believed that on DV views the heart is displaced forwards by the adjacent diaphragmatic cupula and sternal pressure. As the carina is intimately associated with the cardiac base it can be assumed that it will also move cranially, resulting in the trachea bending and moving away from the midline. This may be exaggerated in cases of intra-abdominal distension. Additional studies are required to validate this theory.

The angle formed by the principal bronchi is routinely assessed on DV or VD projections because lateral divergence of the principal bronchi in conjunction with other radiological signs may indicate enlargement of the middle tracheobronchial lymph nodes or the left atrium (Suter 1984, Thrall 2002). In the present study it was shown that the angle of divergence was significantly larger on VD projections and may falsely simulate pathology (Fig 6C). In dorsal recumbency the heart and adjacent viscera become displaced towards the spine due to gravity (Ruehl and Thrall 1981). This in turn pushes the heart base in this region (mainly the left atrium) against and in between the principal bronchi, thus increasing the angle of divergence. The left principal bronchus is the one more likely to be displaced because the left atrium is more associated with the left side of the heart, thus causing the increased angle of divergence. However, this subjective observation is yet to be confirmed by thoracic measurement. The predominant breed type in group 2 was the bull terrier, which suggests that the curved appearance of the principal bronchi angle may be a breed variant.

The authors postulate that the more elongated and centrally aligned heart on the VD projection is more likely to skyline the pulmonary trunk, simulating a 1 to 2 o'clock cardiac bulge (Fig 7C). This should not be mistaken for pulmonic artery poststenotic dilation or overcirculation, and if these conditions are suspected a DV projection must be used. An additional complicating factor on VD projections (compared with DV projections) in small-breed dogs with a high obesity grading is the cranioventral mediastinal fat. In these dogs it may be visible as a triangular opacity in the 1 to 2 o'clock region, therefore hampering evaluation.

The results of this study confirm that the CVC is better seen on VD projections, as has been reported previously (Ruehl and Thrall 1981). This also applies to the accessory lung lobe region. The poorer visibility of this area on DV projections is due to superimposition of pulmonary blood vessels and greater contact between the cardiac silhouette and adjacent diaphragmatic cupula, which is displaced cranially by the abdominal contents located ventrally (Berry and others 2002).

No significant difference in aorta visibility was found at the 2 to 3 o'clock level between VD and DV projections. However, it seems that visibility is better on DV projections more caudally. This may be

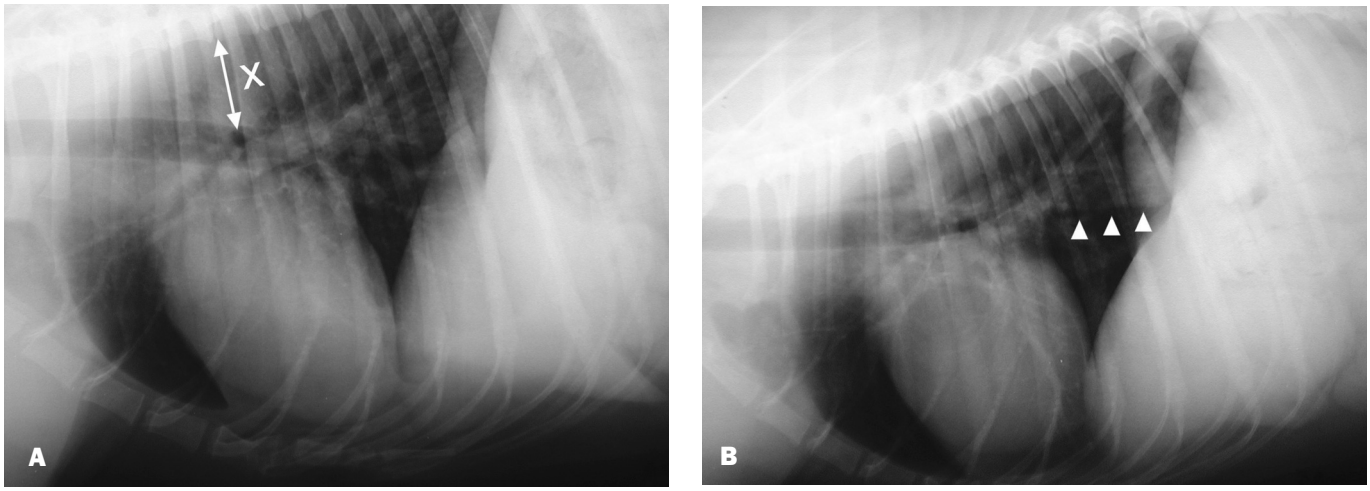

FIG 10. Radiographs of a Labrador with a normal thoracic conformation (ratio 0·82) positioned in right lateral (A) and left lateral (B) recumbency. (A) X denotes the perpendicular distance from the ventral border of the thoracic spine to the terminal dorsal tracheal wall. (B) The aorta and caudal vena cava are better seen. The oesophagus is seen as a horizontal band adjacent to the diaphragm midway between the aorta and the caudal vena cava (arrows). Note that the cardiac apex falls away from the midline giving it a more spherical appearance and less sternal contact

attributed to the fact that there is improved contrast due to more surrounding aerated lung tissue and less perihilar soft tissues (ventral movement of the heart and this part of the aorta further away from the hilus). There is also an improved aortic visibility in LLR and this may simply be due to the aorta lying closer to the cassette and there being less magnification distortion. The crisper aorta edges are thus more readily visible. These positions for optimal aortic visibility should be utilised when looking for aortic aneurysms or intimal mineralisation, as found during *Spirocerca lupi* larval migration (Dvir and others 2001).

It is important to know that a poorly defined caudal oesophageal soft tissue opacity may be seen in LLR in larger breeds that are not sedated. This must not be misdiagnosed as pulmonary or oesophageal pathology. The reason for its visibility in LLR is uncertain, but gastric reflux is a possibility.

Conclusions

The results of this study provide interesting information not previously described regarding the position and visibility of selected thoracic viscera in the dog. Specifically, the DV projection is more reliable for assessing the cardiac silhouette, the descending aorta and angle of divergence of the principal bronchi. The VD projection should be considered for evaluating the CVC. LLR should be used to assess the descending aorta and CVC.

The authors are aware that some of the statistically significant differences between positions may be of minor significance in a clinical scenario. Yet, an understanding of those changes and their possible causes can greatly improve the clinician's comprehension of thoracic radiography. However, it should be noted that a radiographic diagnosis is not made in isolation and that several complementary radiographic signs on various projections ought to be identified to make a definitive diagnosis.

The relatively low number of dogs and limited breed diversity in this study may have influenced findings and the accuracy of the study may be improved in future studies by using a larger number of dogs from a greater variety of breeds.

Acknowledgements

The authors would like to thank Michael Herrtage and Lizza Baines for their advice on the manuscript. Special thanks to Dr Orna Chishinski for the statistical analysis and Neta Lasarowich for the graphical presentation.

References

AHLBERGE, N. E., HOPE, F., KELTER, U. & SVENSSON, L. (1985) A computed tomographic study of volume and x-ray attenuation of the lungs of beagles in various body positions. *Veterinary Radiology* **26**, 43-47

BERRY, C. R., LOVE, N. E. & THRALL, D. E. (2002) Interpretation paradigms for the small animal thorax. In: Textbook of Veterinary Diagnostic Radiology. 4th edn. Ed D. E. Thrall. W. B. Saunders, Philadelphia. pp 307-322

BIERY, D. (1974) Differentiation of lung diseases of inflammatory or neoplastic origin from lung disease in heart failure. *Veterinary Clinics of North America: Small Animal Practice* **4**, 711-721

BUCHANAN, J. W. & BUCHELER, J. (1995) Vertebral scale system to measure canine heart size in radiographs. *Journal of the American Veterinary Medical Association* **206**, 194-199

DENNIS, R., KIRBERGER, R. M., WRIGLEY R. H. & BARR, F. J. (2001) Small Animal Radiological Diagnosis. W. B. Saunders, London. p 160

DVIR, E., KIRBERGER, R. M. & MALLECZEK, D. (2001) Radiographic and computed tomographic changes and clinical presentation of spirocercosis in the dog. *Veterinary Radiology and Ultrasound* **42**, 119-129

FINLAND, R. B., BONAGURA, J. D. & MYER, C. W. (1986) Pulmonic stenosis in the dog: 29 cases (1975-1984). *Journal of the American Veterinary Medical Association* **189**, 218-226

GRANDAGE, J. (1974) The radiology of the dog's diaphragm. *Journal of Small Animal Practice* **15**, 1-17

KEALY, J. K. & MCALLISTER, H. (2000) The abdomen. In: Diagnostic Radiology and Ultrasonography of the Dog and Cat. 3rd edn. W. B. Saunders, Philadelphia. pp 47-51

LAMB, C. R., BOSWOOD, A., VOLKMAN, A. & CONNOLLY, D. (2001) Assessment of survey radiography as a method for diagnosis of congenital cardiac diseases in dogs. *Journal of Small Animal Practice* **42**, 541-545

LANG, J., WORTMAN, J. A., GLICKMAN, L. T., BIERY, D. N. & RHODES, H. (1986) Sensitivity of radiographic detection of lung metastases in the dog. *Veterinary Radiology* **27**, 74-78

OWENS, J. M. & BIERY, D. N. (1999) Heart. In: Radiographic Interpretation for the Small Animal Clinician. 2nd edn. Lippincott Williams & Wilkins, Philadelphia. pp 185-216

PECHMAN, R. D. (1987) Effect of dependency versus non-dependency on lung lesion visualization. *Veterinary Radiology* **28**, 185-190

RUEHL, W. W. & THRALL, D. E. (1981) The effect of dorsal versus ventral recumbency on the radiographic appearance of the canine thorax. *Veterinary Radiology* **22**, 10-16

SPENCER, C. P., ACKERMAN, N. & BURT, J. K. (1981) The canine lateral thoracic radiograph. *Veterinary Radiology* **22**, 262-266

SUTER, P. F. (1984) Normal radiographic anatomy and radiographic examination. In: Thoracic Radiography, Atlas of Thoracic Diseases of the Dog and Cat. Ed P. F. Suter. Wettswil, Switzerland. pp 1-461

THRALL, D. E. (2002) The mediastinum. In: Textbook of Veterinary Diagnostic Radiology. 4th edn. Ed D. E. Thrall. W. B. Saunders, Philadelphia. pp 313-320

THE EFFECT OF POSITIONING ON THE RADIOGRAPHIC APPEARANCE OF CAUDODORSAL MEDIASTINAL MASSES IN THE DOG

ROBERT M. KIRBERGER, ERAN DVIR, LIESEL L. VAN DER MERWE

In this prospective study, the effect of thoracic positioning on the visibility and size of caudal esophageal masses caused by spirocercosis was investigated. Dorsoventral (DV), ventrodorsal (VD) as well as left lateral recumbent (LLR) and right lateral recumbent (RLR) thoracic radiographs of 28 dogs, diagnosed endoscopically with spirocercosis, were evaluated. The radiographic findings were compared with those of esophageal endoscopy. Masses were seen equally well in left vs. right recumbency as well as in DV vs. VD positions but in DV/VD views 86% of masses were detected whereas in lateral views only 50% of masses were identified. In spirocercosis-endemic areas DV and RLR views are advised as they also allow for better visualization of descending aorta aneurysms and to avoid interpreting the potentially normally visible esophagus in LLR in large dogs as a mass.
Veterinary Radiology & Ultrasound, Vol. 50, No. 6, 2009, pp 630–634.

Key words: dog, esophagus, mediastinum, positioning, radiology, spirocercosis, *Spirocerca lupi*, thorax.

Introduction

ROUTINE RADIOGRAPHIC EXAMINATION of the thorax consists of a lateral view, left (LLR) or right lateral recumbent (RLR) and its orthogonal dorsoventral (DV) or ventrodorsal (VD) counterpart. In order to select the most informative views, the investigator must understand the effect positioning has on the radiographic appearance of the normal thorax as well as that of thoracic disease. The effect of various radiographic views on the visibility or position of normal thoracic structures has been described.[1,2] Various views have also been used to better define thoracic disease.[3–5] Mediastinal lesions are generally better delineated on a DV or VD.[3,6,7] However, standard texts do not discuss the effect of positioning on the caudodorsal mediastinum or ignore caudodorsal mediastinal masses completely,[6] with only some texts commenting that a VD is better for caudoventral mediastinal disease[3,6] or that a VD is better for mediastinal disease in general.[3,8]

Anatomic structures in the caudodorsal mediastinum are the dorsal intercostal arteries and veins, esophagus, thoracic duct, right and left sympathetic trunks and vagal nerves, descending aorta, bronchoesophageal arteries and veins, and the azygos vein.[6] In normal dogs the esophagus is not visible except occasionally in large breed dogs just cranial to the diaphragm in LLR radiographs.[2] The descending mid-mediastinal aorta is seen reasonably well at the level of the heart and is seen better on DV and LLR radiographs,[2] however, the caudal mediastinal aorta becomes less well defined on the lateral view as well as on the DV/VD views as its left edge joins the vertebral column border. The remaining caudodorsal mediastinal structures are not visible in the normal dog.

Caudodorsal mediastinal disease, and in particular that causing a mass effect, primarily involves the esophagus. Abnormalities include foreign body, in endemic areas *Spirocerca lupi* nodules and neoplastic transformation thereof, food or fluid filled megaesophagus, hiatal hernia, gastroesophageal intussusception, primary and metastatic neoplasia, and esophageal diverticula.[6,8–11] Caudodorsal mediastinal mass effect may also be due to paraesophageal hernia, diaphragmatic rupture, hernia, abscess or hematoma, neoplasia of neural or vertebral body origin, migrating foreign bodies, and mediastinitis secondary to esophageal perforation.[6,8,10,11] Vascular causes of a caudodorsal mediastinal mass include aortic aneurysms, usually secondary to *S. lupi* larval migration and markedly distended azygos vein secondary to absent prehepatic caudal vena cava or a portoazygous shunt.[10,12]

This prospective study was undertaken to determine the effect of positioning on the visibility and size of the caudodorsal mediastinum, and particularly in dogs with endoscopically confirmed intraluminal *S. lupi* nodules in the caudal esophagus.

Materials and Methods

We selected 28 dogs from a larger prospective spirocercosis trial in which caudal esophageal nodules were diagnosed by means of endoscopy within 5 days of the radiographic examination. Dogs had a mean age of 52.5 ± 29.6 months (range 9–125) and weight of 19.4 ± 12.4 kg (range 3.6–41.5). Breeds were six Jack Russell Terriers, three German

From the Department of Companion Animal Clinical Studies, Faculty of Veterinary Science, University of Pretoria, Private Bag X04, Onderstepoort 0110, Pretoria, South Africa.

Address correspondence and reprint requests to Robert M. Kirberger, at the above address. E-mail: robert.kirberger@up.ac.za

Received April 4, 2009; accepted for publication May 11, 2009.
doi: 10.1111/j.1740-8261.2009.01594.x

Shepherd dogs, three Boerboels, three Bull Terriers, and the remaining 13 were mixed or single representatives of a purebreed. All dogs were evaluated over a 1-year period (2007/2008). Each dog had four standard radiographic thoracic views made (DV, VD, RLR, and LLR). All images were digital radiographs retrieved from the Onderstepoort Veterinary Academic Hospital picture archiving system. All radiographs were evaluated by a single board certified radiologist (R.M.K.) and contrast, brightness, and magnification adjusted to optimize pathology. All four views were examined independently from each other to avoid interpretation bias due to known mass on another view.

On each of the four views the visibility of a mass was evaluated as definitely not present, possibly present, likely to be present, and definitely present. Additionally, the length and height of the mass was measured in millimeters on lateral views and the length and width on DV and VD views.

Confirmation of a suspect caudodorsal mediastinal mass was made in all patients by means of esophageal and gastric endoscopy.* Patients were premedicated with a variety of drugs depending on clinician preference, but all were induced with propofol† and maintained on isoflurane‡. The dogs were in LLR and esophageal and gastric endoscopy, particularly of the cardia, was performed. The *S. lupi*-associated nodules were assessed according to number, characteristics (smooth or cauliflower like) and individual length as well as confluent length of esophageal involvement. The length of each nodule was determined by measuring its distance from the canine tooth and subtracting the most caudal measurement from the more cranial. Where several nodules were present the total length of esophagus involved was taken to be the distance from the cranial edge of the first nodule to the caudal edge of the last nodule or cardia, if the nodule involved the cardia. This was then compared with the radiographs where only one mass was visible. The diameter of the nodules could not be ascertained endoscopically.

Data were captured and analyzed statistically in Excel software. Results were expressed as mean ± standard deviation and range. Visibility of the masses between the four views was compared using the χ^2-test. To measure the sensitivity of each view for mass detection, definitely not present and possibly present were combined and classified as not detected, and likely to be present and definitely present were combined and classified as detected. Length measurements on the different views were tested for a linear association with endoscopic measurements. The difference in the nodule mean length was compared between the better lateral view, based on the above mentioned analyses, and the better VD/DV view using paired Student's *t*-test. The significance level for all tests was $P<0.05$.

*Olympus GIF video endoscope, type XQ200, Tokyo, Japan.
†Fresenius Kabi Pty Ltd., Halfway House, South Africa.
‡Safeline pharmaceuticals Pty Ltd., Florida, South Africa.

TABLE 1. Total Length of Esophageal Involvement in Endoscopically Seen Nodules and Radiographically Identified Masses

View	Range (mm)	Mean ± SD
RLR	19–118	56.29 ± 30.93
LLR	23–135	54.44 ± 29.94
DV	20–145	66.25 ± 37.36
VD	24–151	67.79 ± 30.21
Mean of four views	26–137.2	58.45 ± 28.41
Endoscopy	10–150	62.22 ± 43.18

RLR, right lateral recumbent; LLR, left lateral recumbent; DV, dorsoventral; VD, ventrodorsal thoracic views.

Results

One to nine nodules (mean 2.4, median 1) were identified endoscopically per dog and 14 dogs had more than one nodule. The total length of esophageal involvement in endoscopically seen nodules and radiologically identified masses are given in Table 1.

Masses were seen equally well in left vs. right recumbency as well as in DV vs. VD positions (Table 2). However, in the latter 24/28 (86%) masses were identified, whereas in lateral views only 14/28 (50%) masses were identified and this difference was statistically significant ($P<0.01$) (Fig. 1). In 10 dogs masses were seen only on DV and VD radiographs. While DV or VD views were superior for detection, the right lateral recumbent view was superior for measurement, being characterized by the strongest association with endoscopic measurement ($r^2=0.83$ (Fig. 2) compared with $r^2=0.44$ for the DV). The mean length measurements of the lateral view having the best correlation to endoscopy, namely RLR, and the best view in terms of detectability, namely DV, were compared and were significantly different ($P<0.001$) with shorter length measured on lateral recumbency compared with DV. There was no significant difference between the endoscopic measurement and lateral recumbent view measurement. Endoscopic details, such as proliferation and necrotic craters could not be detected radiologically.

Height and width of masses could not be compared with endoscopic data as these measurements cannot readily be made endoscopically. The correlation between the average of mean DV and VD width was 1.15 times bigger (data not

TABLE 2. Visibility of Masses on Different Views

	Not Visible		Visible	
View	Definite No	Possibly	Likely	Definite Yes
RLR	8	6	6	8
LLR	4	10	4	10
DV	2	2	5	19
VD	4	0	7	17

RLR, right lateral recumbent; LLR, left lateral recumbent; DV, dorsoventral; VD, ventrodorsal thoracic views.

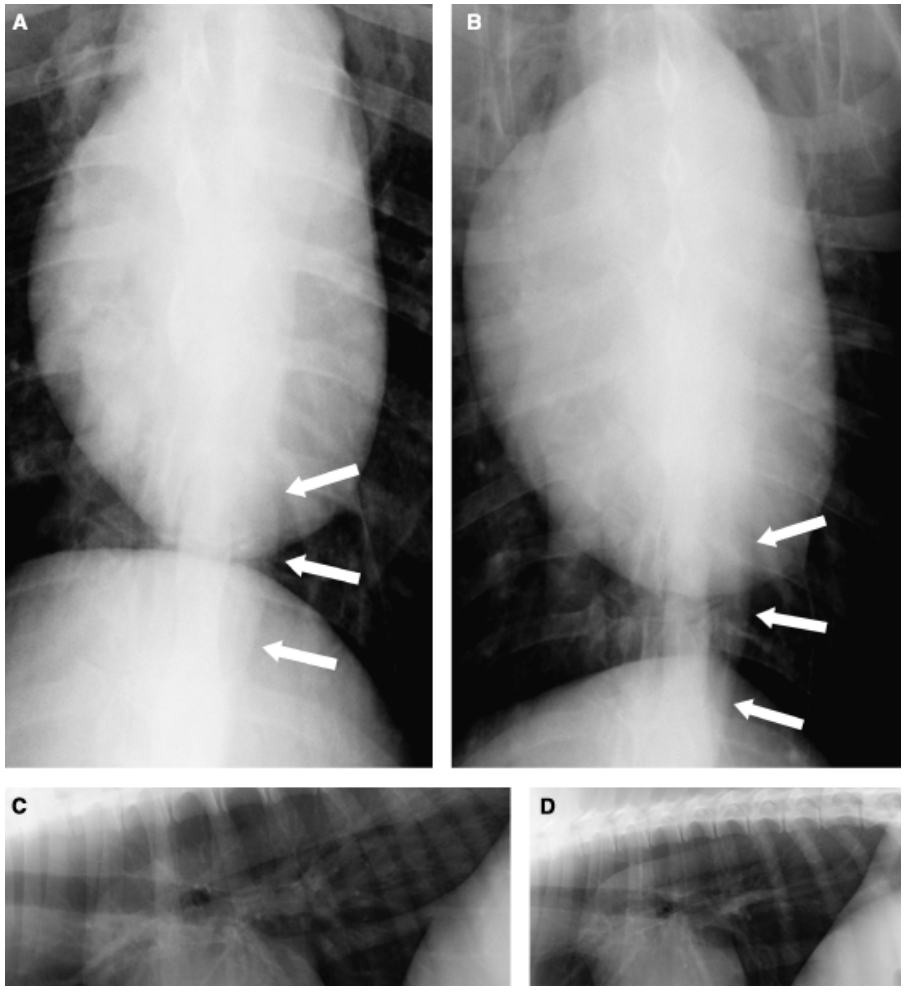

FIG. 1. Mid caudal and caudodorsal thoracic radiographs of a 6-year-old Great Dane with spirocercosis. (A) Dorsoventral view with obvious lesion superimposed on caudal cardiac and diaphragmatic silhouettes. (B) Ventrodorsal view with similar lesion. (C) Right lateral recumbent and (D) left lateral recumbent views with no caudodorsal mediastinal mass visible.

shown) compared with the average of the mean RLR and LLR heights, indicating the *S. lupi*-induced masses had a discoid shape radiographically.

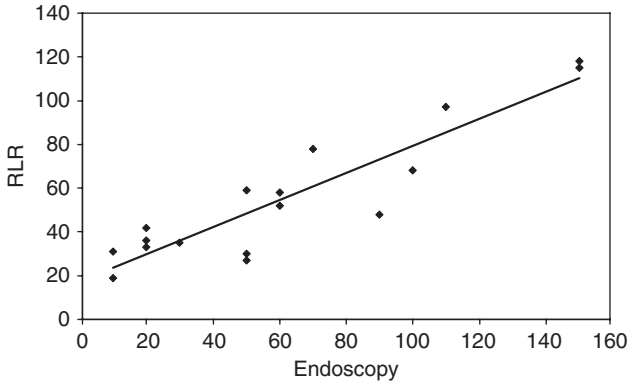

FIG. 2. Radiographic measurement (mm) in right lateral view as a function of endoscopic measurement (mm). The line is the best fitting linear regression line. $R^2 = 0.83$.

The smaller radiologically detected masses consistently measured slightly larger on the radiographic vs. the endoscopic measurements, whereas the larger radiographic masses were smaller than the endoscopic measurements (Fig. 3).

Discussion

When radiographing the canine thorax, it is essential for the clinician to be aware of the effect that a radiographic projection can have on the radiographic conspicuity and location of normal thoracic structures as well as abnormalities.

The effect of positioning on a variety of thoracic lesions has been described[3–5] but to date the accuracy of various views to diagnose caudodorsal mediastinal disease, and in particular esophageal disease, has not been described.

Subtle or early disease of the mediastinum is often difficult to assess and a thorough knowledge of the factors that influence its size and visibility are imperative.

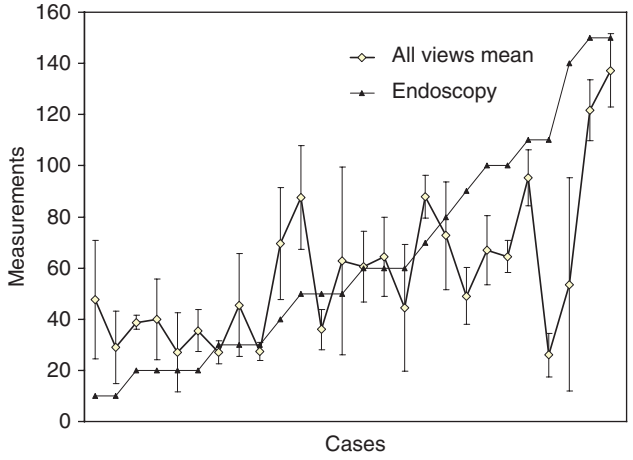

FIG. 3. Mean nodule size in mm (scale bar = SD) as seen on radiographs compared with endoscopic size. Note that smaller nodules are larger radiographically than endoscopically and vice versa for larger nodules.

Based on our results, DV/VD radiographs are more reliable for detection of a caudodorsal mediastinal mass than are lateral radiographs. There were no significant differences in the visibility indices between VD and DV. As there is no significant difference in mass detectability between VD and DV views, other factors should be taken into consideration when deciding which view to make. In spirocercosis-endemic areas the left lateral border of the descending aorta is evaluated for evidence of aneurysms and as the aorta is better defined on the DV view, this view should take preference.[10,13]

Although not proven to have a beneficial effect in this study, factors that should result in improved visibility should be considered. On the DV view the surrounding lung is more air filled, which should result in greater contrast between it and the soft tissue opacity of the esophagus as well as having slight magnification of the dorsal mediastinal structures.[3,14] Making a choice between RLR and LLR is also possible. Although the aorta is seen better on an LLR view spirocercosis aneurysms are rarely seen on lateral views. A normal esophagus may be seen in large breed dogs in LLR radiographs[2] and this could be confused with disease and a RLR should thus be made to avoid this pitfall. The RLR view also resulted in the most accurate quantification of the dimensions of the mass. Under no circumstances should only lateral views be made as lesions may be missed. There were two dogs with 10 mm nodules, one of which was seen on two views and the other on three views, whereas one dog had a 20 mm nodule that was not seen on any view. Many nodules were seen on all views but some nodules endoscopically <150 mm long were only seen on some views. The two dogs with the largest nodules of 150 mm were seen on all views. The above emphasizes the fact that a negative radiographic study does not necessarily rule out a caudal esophageal mass or foreign body and if clinical signs persist, endoscopy, a contrast study or computed tomography (CT) examination with the esophagus inflated[13] should be performed.

The fact that smaller masses detected radiographically were larger than that measured endoscopically (Fig. 3) can be explained by the fact that the esophagus will taper on either side of the mass to a normal empty diameter resulting in increased length. Larger endoscopic nodules were seen as smaller masses radiographically, which is likely due to the fact that the larger nodules measured on endoscopy were often the result of several nodules added together to give the total length of the mass. In these instances of multiple nodules, some nodules were very small and could have been on the extremities of the length measured and would not have distended the esophagus sufficiently to create a radiographic mass effect.

Possible limitations were that all dogs were known to be positive and specificity and predictive values of various views compared with known normal dogs could not be determined. However, the objective was to determine which views were most appropriate to detect masses in dogs with known disease and it can be concluded that RLR and DV views should be made to evaluate caudodorsal mediastinal abnormalities, particularly in spirocercosis endemic areas. Using endoscopy as the standard for mass detection is also not ideal. Endoscopy is good for nodule detection,[10] but only detects the intraluminal esophageal part of the nodule and therefore, the measurement might not be that accurate. CT is a better three-dimensional tool to assess nodule size and future radiographic studies should be compared with CT as the gold standard.

REFERENCES

1. Kirberger RM, Avner A. The effect of positioning on the appearance of selected cranial thoracic structures in the dog. Vet Radiol Ultrasound 2006;47:61–68.

2. Avner A, Kirberger RM. Effect of various thoracic radiographic projections on the appearance of selected thoracic viscera. J Small Anim Pract 2005;46:491–498.

3. Brinkman EL, Biller D, Armbrust L. The clinical usefulness of the ventrodorsal versus dorsoventral thoracic radiograph in the dog. J Am Anim Hosp Assoc 2006;42:440–449.

4. Thrall DE. The pleural space. In: Thrall DE (ed): Textbook of veterinary diagnostic radiology, 5th ed. Philadelphia: WB Saunders, 2007; 555–567.

5. Lang JW, Wortman JA, Glickman LT, Biery DN, Rhodes H. Sensitivity of radiographic detection of lung metastases in the dog. Vet Radiol 1986;27:74–78.

6. Thrall DE. The mediastinum. In: Thrall DE (ed): Textbook of veterinary diagnostic radiology, 5th ed. Philadelphia: WB Saunders, 2007; 541–554.

7. Baines E. The mediastinum. In: Schwarz T, Johnson V (eds): BSAVA manual of canine and feline thoracic imaging. Quedgeley: BSAVA, 2008;177–199.

8. Watrous BJ. Esophagus. In: Thrall DE (ed): Textbook of veterinary diagnostic radiology, 5th ed. Philadelphia: WB Saunders, 2007;495–509.

9. Ridgway R, Suter P. Clinical and radiographic signs in primary and metastatic esophageal neoplasms of the dog. J Am Vet Med Assoc 1974;174: 700–774.

10. Dvir E, Kirberger RM, Malleczek D. Radiographic and computed tomographic changes and clinical presentation of spirocercosis in the dog. Vet Radiol Ultrasound 2001;42:119–129.

11. Dennis R, Kirberger RM, Wrigley RH, Barr FJ. Small animal radiological differential diagnosis. London: WB Saunders, 2001;143–153.

12. Fischetti AJ, Kovak J. Imaging diagnosis: azygous continuation of the caudal vena cava with and without portocaval shunting. Vet Radiol Ultrasound 2008;49:573–576.

13. van der Merwe LL, Kirberger RM, Clift S, Williams M, Keller N, Naidoo V. *Spirocerca lupi* infection in the dog: a review. Vet J 2008;176: 294–309.

14. Berry CR, Graham JP, Thrall DE. Interpretation paradigms for the small animal thorax. In: Thrall DE (ed): Textbook of veterinary diagnostic radiology, 5th ed. Philadelphia: WB Saunders, 2007;462–485.

Pneumoesophagography and the appearance of masses in the caudal portion of the esophagus in dogs with spirocercosis

Robert M. Kirberger, BVSc, MMedVet; Liesel L. van der Merwe, BVSc, MMedVet; Eran Dvir, DVM, MMedVet

Objective—To determine the usefulness of pneumoesophagography, compared with that of survey radiography, for characterization of esophageal pathological changes in dogs with endoscopically confirmed intraluminal *Spirocerca lupi* nodules in the caudal portion of the esophagus.

Design—Diagnostic test evaluation.

Animals—30 dogs with endoscopically confirmed spirocercosis.

Procedures—Dorsoventral (DV) and right lateral recumbent (RLR) thoracic survey radiographs were obtained for each dog. Endoscopy was subsequently performed, the esophagus was inflated with air, and left lateral recumbent, RLR, DV, and ventrodorsal thoracic radiographs were obtained. The amount of esophageal and gastric distention was recorded. Visibility, location, and surface characteristics of lesions and total length of esophageal involvement were recorded independently for each radiograph and modality and compared with each other.

Results—Survey DV radiographs were more reliable than survey RLR radiographs for detecting caudal esophageal pathological changes. Lateral pneumoesophagograms showed more esophageal air and had more visible nodules than did their orthogonal counterparts. Right lateral recumbent pneumoesophagograms allowed for evaluation of the air-filled stomach, particularly the cardiac portion, for additional pathological changes. Pneumoesophagography allowed the mural position (47% located dorsally) and surface characteristics of *Spirocerca* nodules to be determined. Six of 9 dogs with confirmed malignant disease had an irregular nodule surface suggestive of neoplastic transformation.

Conclusions and Clinical Relevance—Pneumoesophagography was easily performed in dogs with spirocercosis and showed promise as a cost-effective and safe initial diagnostic procedure for further evaluation and characterization of suspected caudal esophageal lesions. (*J Am Vet Med Assoc* 2012;240:420–426)

Routine radiographic examination of the thorax in dogs consists of an LLR or RLR view and its orthogonal DV or VD counterpart. The effect of various radiographic views on the visibility or position of thoracic structures in healthy dogs has been described.[1,2] Various views have also been used to better define thoracic pathological changes,[3–5] and the effect of positioning on the appearance of caudodorsal mediastinal masses has been reported.[6] Mediastinal lesions are generally better delineated on a DV or VD radiograph than on LLR or RLR views.[3,7,8]

Anatomic structures in the caudodorsal mediastinum include the dorsal intercostal arteries and veins, esophagus, thoracic duct, right and left paravertebral ganglia and associated nerves, vagal nerves, descending aorta, bronchoesophageal arteries and veins, and the azygos vein.[7] In clinically normal dogs, the esophagus is not visible, except occasionally in large-breed dogs, in which the esophagus may be detected just cranial to the diaphragm on an LLR radiograph.[2] The descending mid mediastinal aorta is seen reasonably well at the level of the heart and is seen better on DV and LLR projections[2]; however, the caudal mediastinal aorta becomes less well-defined on the lateral view as well as on DV and VD views because its left edge joins the vertebral column border. The remaining caudodorsal mediastinal structures are not visible in clinically normal dogs.

Caudodorsal mediastinal disease, in particular disease that causes a mass effect (ie, pathological process that displaces adjacent organs or structures), primarily involves pathological changes in the esophagus. Causes in dogs include foreign bodies, *Spirocerca lupi* nodules (in geographic regions in which the parasite is endemic) and neoplastic transformation thereof, food- or fluid-filled megaesophagus, hiatal hernia, gastroesophageal intussusception, primary and metastatic neoplasia, and esophageal diverticula.[7,9–12] A

Abbreviations

DV	Dorsoventral
LLR	Left lateral recumbent
RLR	Right lateral recumbent
VD	Ventrodorsal

From the Department of Companion Animal Clinical Studies, Faculty of Veterinary Science, University of Pretoria, Onderstepoort 0110, Republic of South Africa.

Presented in abstract form at the European Association of Veterinary Diagnostic Imaging Congress, Giessen, Germany, July 2010.

Address correspondence to Prof. Kirberger (robert.kirberger@up.ac.za).

caudodorsal mediastinal mass effect may also be attributable to paraesophageal hernia; diaphragmatic rupture, hernia, abscess, or hematoma; neoplasia of neural or vertebral body origin; migrating foreign bodies; and mediastinitis secondary to esophageal perforation.[7,9,11,12] Vascular causes of caudodorsal mediastinal lesions include aortic aneurysms, usually secondary to *S lupi* larval migration, and a markedly distended azygos vein secondary to absent prehepatic caudal vena cava or a portoazygous shunt.[11,13]

Positive contrast esophagography is routinely performed in dogs to elucidate pathological esophageal changes[9] but may lead to pulmonary aspiration of barium or obscure the visibility of small nodules. Pneumoesophagography as a contrast radiographic procedure was alluded to in a literature review[14] on *S lupi* infection in dogs but is not mentioned in a recent standard radiology textbook[9] as a possible diagnostic tool. Safety and cost-effectiveness are major advantages of the technique.

The purpose of the study reported here was to determine the usefulness of pneumoesophagography, compared with that of survey radiographs, for determining the visibility and size of esophageal masses in dogs with endoscopically confirmed intraluminal *S lupi* nodules in the terminal portion of the esophagus. Although computed tomography and endoscopy are sensitive techniques for detecting esophageal disease, they involve the use of expensive equipment that is not always readily available in routine small animal practice. Pneumoesophagography may be a less expensive yet effective option by which to diagnose various causes of esophageal lesions ranging from foreign bodies to mural neoplasia.

Materials and Methods

Animals—Thirty dogs from a larger prospective spirocercosis study[15–17] in which terminal esophageal nodules were diagnosed by means of endoscopy were selected. All dogs were evaluated over a 1-year period (2007 to 2008). This study was approved by the University of Pretoria Animal Use and Care Committee as well as the Research Committee.

Survey radiography—Four standard radiographic thoracic views (DV, VD, RLR, and LLR) were obtained from each dog. However, because DV and RLR thoracic views are better than VD and LLR views for identifying caudodorsal mediastinal masses,[6] only DV and RLR radiographs were used for study purposes.

Endoscopic measurements—Twenty-four to 48 hours after radiography, dogs underwent esophageal and gastric endoscopy.[a] For this procedure, dogs were premedicated with various drugs on the basis of clinician preference. Anesthesia was then induced with propofol[b] and maintained with isoflurane.[c] Each dog was positioned in LLR, and a complete esophageal and gastric endoscopic examination, including the cardia, was performed. The *S lupi*–associated nodules and masses were counted and assessed for appearance (smooth or cauliflower-like), individual length, and confluent length of esophageal involvement. Nodule length was determined by measuring its distance from the canine tooth and subtracting the most caudal measurement from the more cranial one. When several nodules were present, the total length of esophagus involved was measured as the distance from the cranial edge of the first nodule to the caudal edge of the last nodule or, when the nodule involved the cardia, to the cardia. These findings were then compared with the survey radiographs when only 1 mass was visible and with pneumoesophagograms when multiple nodules were suspected. The width of the nodules could not be ascertained endoscopically, and the circumferential location of the nodules was not recorded. Dogs were classified as positive for *S lupi* infection on the basis of typical endoscopic and radiographic signs or identification of characteristic eggs during fecal testing.[14]

Pneumoesophagographic technique—Immediately after endoscopy, each anesthetized dog was transferred to the radiography room. An additional endotracheal tube was placed in the esophagus with the tip located in the distal cervical region of the esophagus, and a resuscitator was attached. Adult and infant silicone resuscitators[d] were used in dogs > 10 kg (22 lb) and < 10 kg, respectively. The esophagus was initially inflated with room air by use of 3 to 4 resuscitator compressions. Routine RLR and LLR thoracic radiography was subsequently performed. The esophagus was then reinflated, and DV and VD radiographs were obtained.

Image evaluation—All radiographs obtained were stored in digital format and subsequently retrieved from the Onderstepoort Veterinary Academic Hospital picture archiving system for interpretation. All were evaluated by 1 board-certified radiologist (RMK), who subjectively adjusted the image contrast, brightness, and magnification to optimize visibility of pathological changes. All radiographs were examined independently from each other to avoid interpretation attributable to a mass having been identified on another view.

Each of the 2 survey radiographs and 4 pneumoesophagograms was assessed for the visibility of a nodule or mass (seen or not seen), and the total length of affected esophagus was recorded. The potential effect of radiographic magnification was ignored. On the 4 pneumoesophagograms, the degree of esophageal and gastric distention with air was graded by use of a 5-point scale (0 = no air evident; 4 = marked distention evident). Mass margins were classified as smooth or irregular. The point of esophageal attachment was recorded by use of a clock face analogy, with dorsal, left side, ventral, and right side defined as 12, 3, 6, and 9 o'clock, respectively.

Nodules were characterized as sessile or pedunculated. When > 1 mass was identified, the total number was counted and the 2 largest masses were evaluated. The total length of affected esophagus was measured. Whether a nodule or mass was identified in the air-filled stomach was also noted. In addition, factors that might have influenced image interpretation such as poor dog positioning or the presence of lung lesions were also recorded.

Statistical analysis—Data were recorded and statistically analyzed by use of a spreadsheet program[e] and statistical software.[f] Results were expressed as median and range. Visibility of the *S lupi* masses (seen or not

seen) on the various views was compared by use of the χ^2 test. Affected esophageal length was compared among the pneumoesophagographic, survey radiographic, and endoscopic measurements by use of a paired *t* test. Descriptive statistics were used to summarize the total number of nodules identified, nodule surface outline, mural attachment location, cardia visibility, and degree of gastric distention (distention score). The esophageal distention score was compared among views by use of the Mann-Whitney test. For all tests, values of $P \leq 0.05$ were considered significant.

Results

Animals—Dogs had a median age of 49 months (range, 9 to 125 months) and median body weight of 21 kg (46.2 lb; range, 3.6 to 41.4 kg [7.9 to 91.1 lb]). Purebreds included 5 Jack Russell Terriers, 3 German Shepherd Dogs, 3 Boerboels, 2 Bull Terriers, 2 Rottweilers, and 2 Labrador Retrievers; the remaining 13 were mixed breeds or single representatives of various other breeds.

Esophageal distention scores—The degree of esophageal distention with air evident on pneumoesophagograms ranged from 2 to 4 for lateral views (**Figure 1**) and 0 to 4 for the DV and VD views, with a median of 3 for all views. When distention scores were compared among the 4 views, the lateral views (LLR and RLR) showed significantly ($P = 0.020$) more distention than did orthogonal views (DV and VD). There was no significant difference in distention scores between the 2 lateral ($P = 1.00$) and 2 orthogonal ($P = 0.87$) views. Most dogs had concomitant gastric distention, which improved visibility of the cardiac region. Cardiac region gas distention was most commonly seen in RLR views (29/30 [97%] dogs); it was only evident in 12 (40%) dogs when DV and VD views were used and in 8 (27%) dogs when LLR views were used.

Nodule detection—The ability of the different imaging techniques to show caudal esophageal nodules varied (**Table 1**). Survey radiography allowed most nodules to be seen on DV views (**Figure 2**), whereas with pneumoesophagography, most nodules were visible on lateral views (**Figure 3**).

The combined 2 survey radiographic views (RLR and DV) had a sensitivity of 93% for detecting esophageal masses (Table 1). The combined 4 pneumoesophagographic views (DV, VD, RLR, and LRL) had a sensitivity of 90%, and a combination of all views had a sensitivity of 97%. Right lateral recumbent pneumoesophagograms were significantly ($P = 0.030$) more sensitive than DV pneumoesophagograms for caudal esophageal mass de-

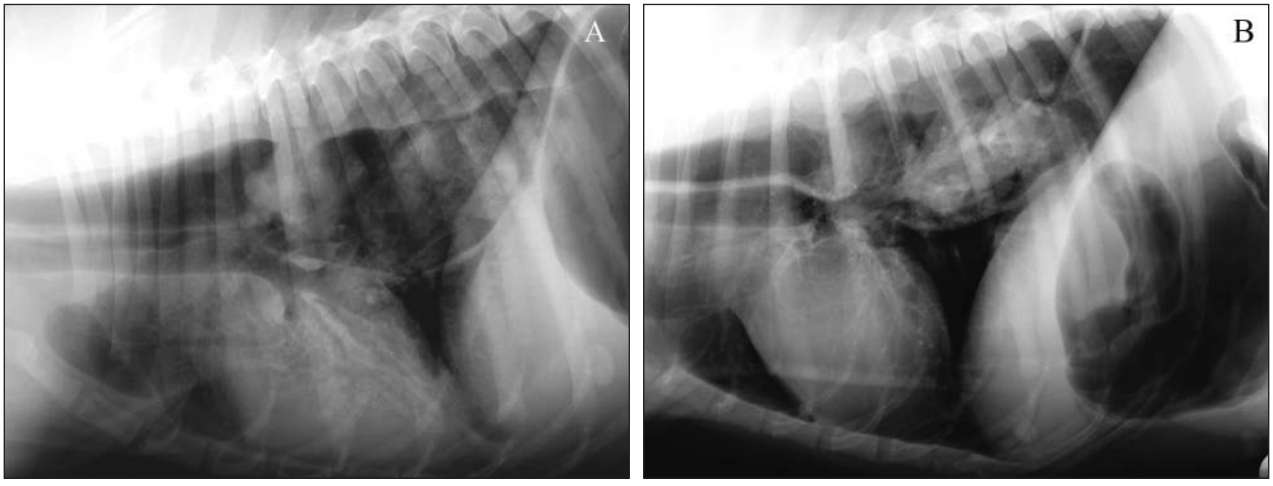

Figure 1—Lateral recumbent pneumoesophagographic views of a 7-year-old Labrador Retriever with several caudal esophageal nodules caused by *Spirocerca lupi* infection. A—The RLR view shows gas in the corpus and cardiac regions of the stomach. The degree of esophageal distention was graded as 4 (marked distention). B—The LLR view reveals gas in the pylorus and duodenum. Esophageal distention was graded as 3 (moderate distention).

Table 1—Findings of survey radiography and pneumoesophagography in 30 dogs with endoscopically confirmed spirocercosis.

	Survey radiography*			Pneumoesophagography					Both methods
Variable	RLR	DV	Either view	RLR	LLR	DV	VD	Any view	Any view
No. of dogs with nodules	14	25	27	24	25	16	16	27	29
Sensitivity for nodule detection (%)	48	86	93	80	83	53	53	90	97

*One dog had megaesophagus and the esophagus was not filled with air; therefore, the dog could not be evaluated.
For sensitivity calculations, endoscopy was considered the reference standard.

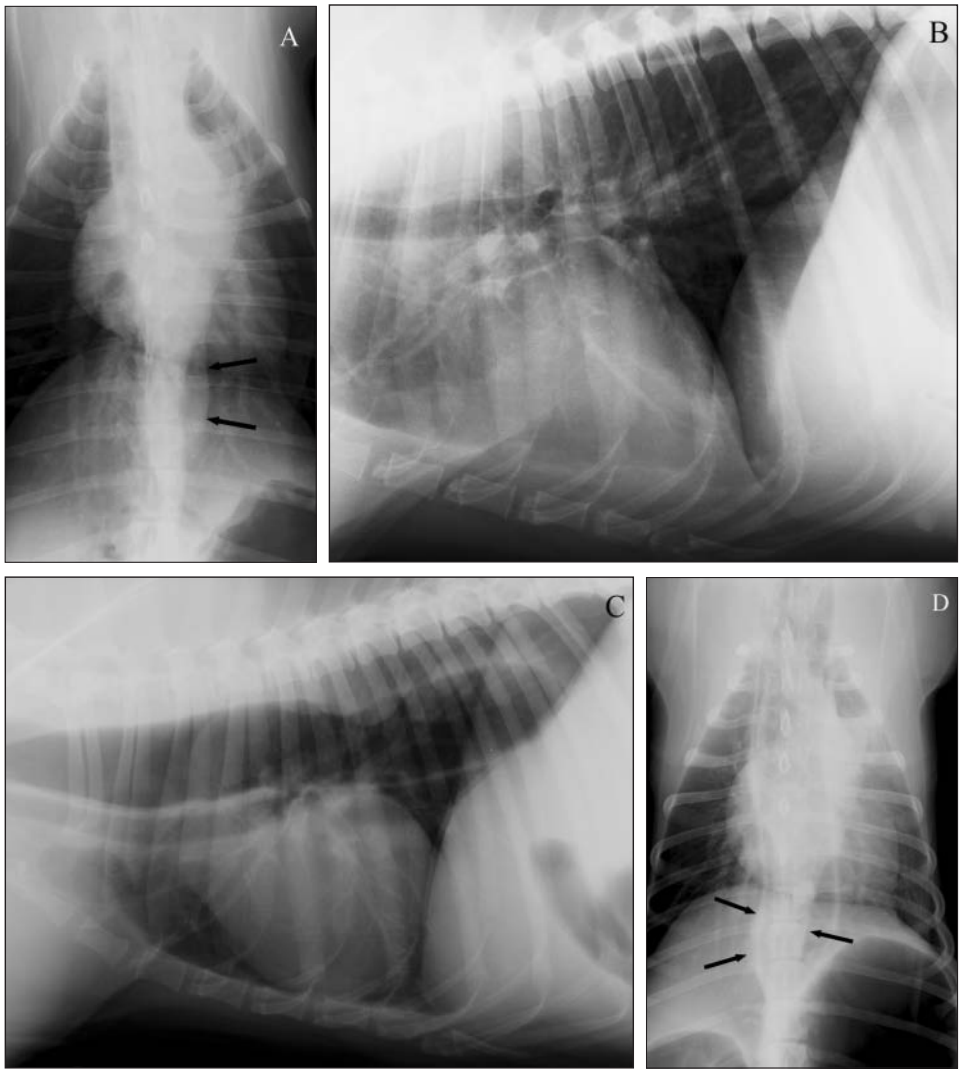

Figure 2—Thoracic radiographic views of a 2-year-old Rottweiler with *S lupi* infection. A—The DV survey radiograph shows a small caudal esophageal mass (arrows). B—The RLR survey radiograph shows no obvious esophageal mass. C—The RLR pneumoesophagogram shows a dorsal esophageal mass. D—The DV pneumoesophagogram shows a midline mass (arrows).

tection, whereas DV survey radiographs were significantly (P = 0.003) more sensitive than lateral survey radiographs. The sensitivity of LLR pneumoesophagograms was similar to that of RLR pneumoesophagograms, and the sensitivity of VD pneumoesophagograms was similar to that of DV pneumoesophagograms. Findings from 1 dog were not included in the statistical analysis of survey radiographic findings because it had megaesophagus.

Nodules—Although the survey DV views allowed detection of more nodules than the DV and VD pneumoesophagograms, pneumoesophagography aided in detecting the origin of the nodules on the lateral esophageal wall (11 on DV views and 9 on VD views). In 2 dogs that did not have a nodule visible on the survey radiographs, 1 had nodules detected on the pneumoesophagograms. In 1 dog, no nodules or masses could be detected in any of the 6 radiographic views. In 2 dogs in which survey radiographs revealed a mass, the mass could not be seen on pneumoesophagograms. Two dogs had no radiographic lesions evident, and endoscopy revealed nodules 10 mm long in one and 20 mm long in the other. However, there were 8 dogs in which 10- to 20-mm nodules were visible via endoscopy as well as via pneumoesophagography.

Location of nodules—No gastric nodules or masses were seen by means of radiography or endoscopy. When a nodule was dorsally or ventrally attached to the esophagus, it usually only had a luminal appearance on the DV and VD views with no attachment seen, particularly for smaller nodules. Similarly, lateral nodules often appeared luminal on RLR and LLR views (**Figure 4**). Mural location was readily seen with pneumoesophagography but could not be compared with the endoscopic images because the location was not recorded. Fourteen (47%) dogs had dorsal, 10 (33%) had ventral (Figure 3), and 4 (13%) had lateral wall attachment of nodules. Twelve of the dorsally and 4 of the ventrally attached nodules also had lateral wall involvement.

Number of nodules—Esophageal endoscopy identified between 1 and 9 nodules/dog (median, 2 nodules/dog), which ranged in size from 5 to 100 mm. Pneumoesophagography allowed detection of multiple nodules on a single view in 4 dogs, whereas 15 dogs had multiple nodules on endoscopic images. The total length of esophageal involvement in endoscopically seen nodules, survey radiographs, and pneumoesophagograms did not differ significantly among the views and modalities (**Table 2**).

Mass characteristics—Nine dogs had esophageal nodules or masses that were confirmed to be malignant on the basis of results of histologic examination or no response to treatment. Endoscopy revealed surface roughening, tissue proliferation, and necrotic craters on the esophageal mucosal surface. Pneumoesophagography allowed correct identification of an irregular nodule surface in 6 of the 9 dogs on at least 1 view and an irregular surface in 1 dog in which lesions appeared benign and smooth with endoscopy. Only 3 dogs were assessed as having a pedunculated mass on pneumoesophagograms, of which 2 had confirmed malignant lesions.

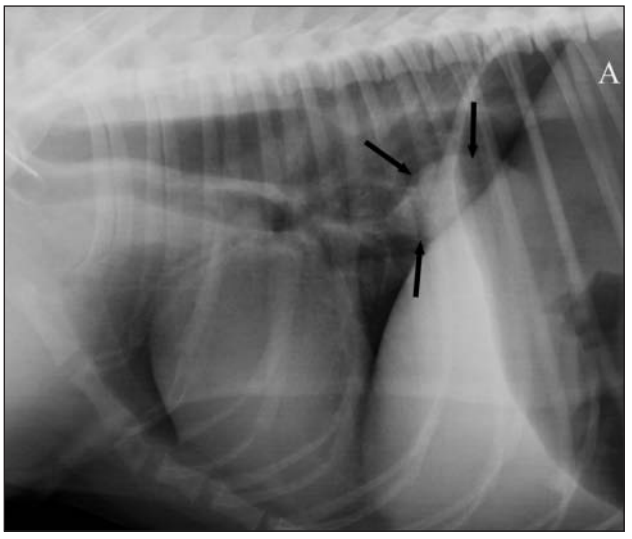

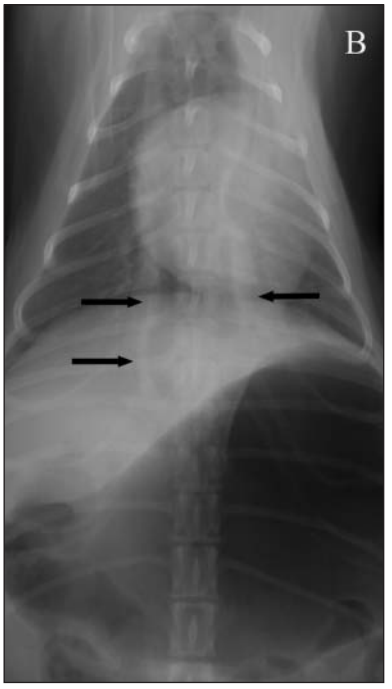

Figure 3—Pneumoesophagographic views of a 5-year-old Miniature Pinscher with a large caudoventral esophageal mass caused by *S lupi* infection. A—The RLR view shows a luminal and mural sessile smooth-surfaced mass adjacent to the diaphragm (arrows). This mass appeared 31 mm long on radiographs and 30 mm long on endoscopy. B—The DV view shows the esophageal wall with a difficult-to-discern mass (arrows).

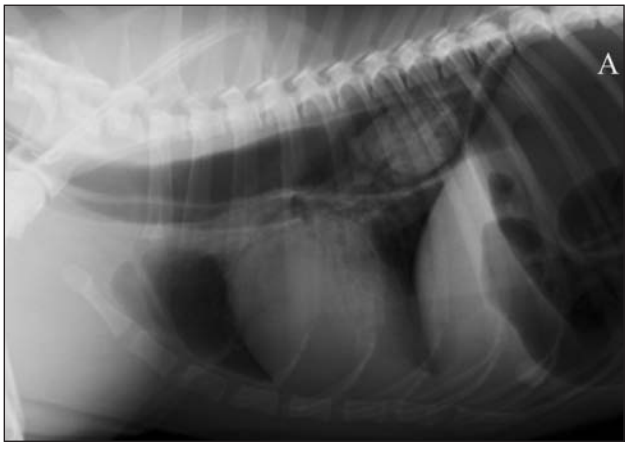

Figure 4—Pneumoesophagographic views of a 6-year-old Boxer with a large, sessile esophageal mass caused by *S lupi* infection. A—The RLR view shows a luminal mass with a smooth surface. B—The DV view shows a mass (arrows) attached to the left esophageal wall.

Table 2—Mean ± SD length of apparent esophageal involvement of lesions identified via survey radiography, pneumoesophagography, and endoscopy in 30 dogs with *Spirocerca lupi* infection.

View	Length (mm)	*P* value*
RLR pneumoesophagography	68.0 ± 41.1	0.53
LLR pneumoesophagography	67.6 ± 37.8	0.73
DV pneumoesophagography	68.0 ± 37.8	0.22
VD pneumoesophagography	79.3 ± 31.1	0.19
RLR radiography†	59.7 ± 29.1	0.08
DV radiography†	69.4 ± 39.2	0.85
Endoscopy	64.5 ± 41.7	—

— = Not applicable.
*Represents comparison of indicated view measurements with endoscopic findings. †One dog had megaesophagus and the esophagus was not filled with air; therefore, the dog could not be evaluated.

Several dogs had various degrees of left lung lobe consolidation secondary to having been positioned in LLR for an extended period for endoscopy. This consolidation did not appear to affect evaluation of lateral pneumoesophagograms but did hamper interpretation of the DV and VD views by effacing the esophageal wall to some extent.

Discussion

When dogs are screened for pulmonary disease, 2 orthogonal radiographs or 2 opposing lateral views are routinely obtained.[5,7] Veterinary clinicians need to be aware of the effect a chosen view can have on the radiographic visibility and location of healthy thoracic structures as well as thoracic lesions. We previously showed that DV and RLR survey thoracic views are best to define caudodorsal mediastinal masses and, in particular, those caused by spirocercosis.[6] However, small nodules or nodules located in the hilar region may be difficult to see on survey radiographs, and in these situations, pneumoesophagography is useful to detect pathological changes or to better define obvious caudal esophageal lesions.

Use of the silicone resuscitator inflation technique resulted in good distention of the esophagus, particularly on lateral views, which provided the contrast required to detect nodules, length of esophageal involvement, location, and surface characteristics. The technique also allowed an estimation of nodule size and number. In addition, gastric distention took place, allowing for evaluation of potential gastric pathological changes, including aberrant *S lupi* nodules. Such evaluation was important because up to 5% of *S lupi* nodules involve the cardia.[18] Right lateral recumbent pneumoesophagographic views allowed air to accumulate in the corpus and fundus of the stomach and away from the

pylorus, through which air would escape in LLR views, in which the pylorus would be uppermost. The RLR pneumoesophagograms therefore optimized visibility of the cardiac sphincter region, allowing greater accuracy in determining nodule location. The degree of gastric distention may still have been a result of the endoscopic procedure used in our study. However, after the study, when we performed pneumoesophagography in dogs without concurrent endoscopy, gastric filling with air usually still took place. In the absence of a resuscitator, the esophagus can be inflated by other means and the opening closed with a stopper.

Survey radiographs allowed most nodules to be seen on DV views as previously described,[6] whereas lateral views were better for nodule detection when pneumoesophagography was used. On lateral survey radiographs, minor esophageal pathological changes are masked by the overlying lung tissue, whereas on DV views, the bulge in the caudodorsal mediastinum is clearly outlined by the adjacent lungs, even in the presence of the vertebral column and sternum.[6] On lateral pneumoesophagograms, the walls of the air-filled esophagus were contrasted by the air within the esophagus and the surrounding pulmonary tissue, clearly outlining intraluminal, mural, and even extramural nodules. On DV and VD pneumoesophagograms, mass visibility was reduced because dorsal (47%) or ventral (33%) mass location was superimposed on the vertebral column and sternum, making masses poorly visible unless markedly enlarged. On survey radiographs, the esophageal wall was added to this soft tissue opacity, thus widening the apparent size of the mass, whereas in the pneumoesophagograms, the esophageal wall was displaced away from the mass by the introduced air. The decreased luminal filling seen on DV and VD pneumoesophagograms also contributed to less intraluminal contrast, and the superimposition of less aerated, atelectic lungs contributed to this as well. On the lateral views, any possible atelectic lung changes caused minimal interference.

The DV and VD pneumoesophagograms in the present study were useful for seeing the origins of nodules on the lateral esophageal wall, which in turn often had a luminal appearance on the RLR and LLR views (Figure 1). The high prevalence of dorsally located nodules was expected because *S lupi* larvae migrate from the aorta to the adjacent ventrally located esophagus. Most nodules appeared sessile. Dorsally or ventrally attached nodules, particularly smaller nodules, typically had only a luminal appearance on the DV and VD pneumoesophagograms. This information can aid surgeons in planning their surgical approach to the caudal portion of the esophagus, even though a left-sided thoracotomy is usually performed. In disease processes other than *S lupi* infection in which lesions may be more laterally located, DV and VD pneumoesophagographic views may be more useful than lateral views.

Pneumoesophagography allowed detection of multiple nodules on a single view in 4 dogs, but endoscopy revealed multiple nodules in 15 dogs. We did not attempt to determine whether nodule location was similar among the various pneumoesophagographic views, and multiple nodules were only counted when seen on a single view. Thus, a single nodule seen on each of several pneumoesophagograms could have represented multiple individual nodules. Such an explanation could account for the poor sensitivity of pneumoesophagography for multiple nodule detection.

Performance of pneumoesophagography in dogs with spirocercosis would be highly useful for practitioners in endemic areas. Early nodule diagnosis can allow intervention before neoplastic transformation.[14,17,19] This imaging technique improves the ability to characterize nodules. In spirocercosis, all of the smaller, early, benign nodules are sessile and appear as a mound on the esophageal luminal wall. As neoplastic transformation occurs, the nodules proliferate into a more vegetative structure, which may have a broad-based attachment to the esophageal wall.[14,17,19] Lesions in 9 dogs in our study were confirmed to be malignant on the basis of results of histologic examination or absence of response to treatment. At least 1 pneumoesophagographic view revealed an irregular proliferative surface in 6 and a pedunculated mass in 2 of these 9 dogs. Many of the larger masses may have been pedunculated, but because they were lying closely adjacent to the wall because of the restricted esophageal space, they may have been mischaracterized. Sessile tumors necessitate greater resection of the esophageal wall, which has a negative effect on healing.[19] Knowledge that a mass is pedunculated is therefore useful in determining a surgical prognosis.

Several dogs in the present study had various degrees of consolidation in the left lung lobe that was secondary to the fact that dogs were in LLR for an extended period for the endoscopy. This consolidation did not appear to affect lateral pneumoesophagographic interpretation but did hinder interpretation of the DV and VD views to some extent. The order of procedures in the study was dictated in part by their order in the larger spirocercosis study[15-17] and could not be adapted. However, in a clinical situation, pneumoesophagography will be performed when endoscopy is not available. Dogs in that situation should consequently be positioned in sternal recumbency for anesthesia and only be placed in lateral recumbency immediately prior to imaging to avoid the impact of atelectasis on results. Theoretically, postendoscopic reflux could have affected the pneumoesophagographic findings in the study dogs, but because food had been withheld from them prior to imaging, the effect of this reflux would have been minimal and was not believed to affect interpretation.

The present study had several limitations. Performance of endoscopy immediately prior to pneumoesophagography resulted in pulmonary atelectasis in some dogs and prefilling of the stomach with gas. In addition, all dogs were known to have spirocercosis and no clinically normal dogs were included; as such, the specificity and predictive values of various imaging views could not be determined. However, the objective was to determine which views were most appropriate to detect masses in dogs with known disease, particularly during pneumoesophagography. Endoscopy is excellent for nodule detection and characterization[14] but only identifies the intraluminal esophageal portion of the nodule; therefore, the nodule size measurement might not be highly accurate. Computed tomography is a supe-

rior cross-sectional imaging technique for assessment of nodule characteristics, and future studies of the diagnostic accuracy of various radiographic techniques should involve computed tomography as the reference standard. However, pneumoesophagography allowed nodule characteristics, location, and mural and extramural nodule formation to be readily determined. Additionally, pneumoesophagography appears to be an easy, cost-effective, and safe additional initial diagnostic procedure for elucidating esophageal pathological changes, including pathological changes other than spirocercosis nodules. Given that there was no significant difference in pneumoesophagographic findings between LLR and RLR or DV and VD views, 1 lateral and 1 orthogonal view should be sufficient for diagnosing and characterizing pathological changes in the esophagus. However, additional views can be obtained to further define any identified lesions.

a. Olympus GIF video endoscope, type XQ200, Tokyo, Japan.
b. Fresenius Kabi Pty Ltd, Halfway House, Midrand, Gauteng, South Africa.
c. Safeline Pharmaceuticals Pty Ltd, Roodepoort, Johannesburg, South Africa.
d. AmbuSilicone Resuscitator, SSEM, Johannesburg, South Africa.
e. Excel, Microsoft Corp, Redmond, Wash.
f. SPSS, version 17, SPSS Inc, Chicago, Ill.

References

1. Kirberger RM, Avner A. The effect of positioning on the appearance of selected cranial thoracic structures in the dog. *Vet Radiol Ultrasound* 2006;47:61–68.
2. Avner A, Kirberger RM. Effect of various thoracic radiographic projections on the appearance of selected thoracic viscera. *J Small Anim Pract* 2005;46:491–498.
3. Brinkman EL, Biller D, Armbrust L. The clinical usefulness of the ventrodorsal versus dorsoventral thoracic radiograph in dogs. *J Am Anim Hosp Assoc* 2006;42:440–449.
4. Thrall DE. The pleural space. In: Thrall DE, ed. *Textbook of veterinary diagnostic radiology*. 5th ed. Philadelphia: WB Saunders Co, 2007;555–567.
5. Lang JW, Wortman JA, Glickman LT, et al. Sensitivity of radiographic detection of lung metastases in the dog. *Vet Radiol* 1986;27:74–78.
6. Kirberger RM, Dvir E, van der Merwe LL. The effect of positioning on the radiographic appearance of caudodorsal mediastinal masses in the dog. *Vet Radiol Ultrasound* 2009;50:630–634.
7. Thrall DE. The mediastinum. In: Thrall DE, ed. *Textbook of veterinary diagnostic radiology*. 5th ed. Philadelphia: WB Saunders Co, 2007;541–554.
8. Baines E. The mediastinum. In: Schwarz T, Johnson V, eds. *BSAVA manual of canine and feline thoracic imaging*. Quedgeley, Gloucester, England: British Small Animal Veterinary Association, 2008;177–199.
9. Watrous BJ. Esophagus. In: Thrall DE, ed. *Textbook of veterinary diagnostic radiology*. 5th ed. Philadelphia: WB Saunders Co, 2007;495–509.
10. Ridgway RL, Suter PF. Clinical and radiographic signs in primary and metastatic esophageal neoplasms of the dog. *J Am Vet Med Assoc* 1979;174:700–704.
11. Dvir E, Kirberger RM, Malleczek D. Radiographic and computed tomographic changes and clinical presentation of spirocercosis in the dog. *Vet Radiol Ultrasound* 2001;42:119–129.
12. Dennis R, Kirberger RM, Barr FJ, et al. *Handbook of small animal radiology and ultrasound: techniques and differential diagnoses*. 2nd ed. London: Elsevier, 2010;210–219.
13. Fischetti AJ, Kovak J. Imaging diagnosis: azygous continuation of the caudal vena cava with and without portocaval shunting. *Vet Radiol Ultrasound* 2008;49:573–576.
14. van der Merwe LL, Kirberger RM, Clift S, et al. *Spirocerca lupi* infection in the dog: a review. *Vet J* 2008;176:294–309.
15. Dvir E, Clift SJ. Evaluation of selected growth factor expression in canine spirocercosis (*Spirocerca lupi*)-associated non-neoplastic nodules and sarcomas. *Vet Parasitol* 2010;174:257–266.
16. Dvir E, Clift SJ, Williams MC. Proposed histological progression of the *Spirocerca lupi*-induced oesophageal lesion in dogs. *Vet Parasitol* 2010;168:71–77.
17. Dvir E, Kirberger RM, Mukorera V, et al. Clinical differentiation between dogs with benign and malignant spirocercosis. *Vet Parasitol*. 2008;155:80–88.
18. Brodey RS, Thompson RG, Sayer PD, et al. *Spirocerca lupi* infection in dogs in Kenya. *Vet Parasitol* 1997;3:49–59.
19. Ranen E, Lavy E, Aizenberg I, et al. Spirocercosis-associated esophageal sarcomas in dogs. A retrospective study of 17 cases (1997–2003). *Vet Parasitol* 2004;119:209–221.

Chapter 3

The use of computed tomography and alternative imaging techniques in *Spirocerca lupi* associated disorders

Kirberger RM, Zambelli A. Aortic thromboembolism associated with spirocercosis in a dog. *Veterinary Radiology & Ultrasound* 2007;48:418-420.

Kirberger RM, Stander N, Cassel NN, Carstens A, Mukorera V, Christie J, Pazzi P, Dvir E. Computed tomographic and radiographic characteristics of aortic lesions in 42 dogs with spirocercosis. *Veterinary Radiology & Ultrasound* 2013;54:212-222.

Petite A, **Kirberger R.** Mediastinum. In: Schwarz T, Saunders J (eds): Veterinary computed tomography (chapter 25). Oxford: Wiley-Blackwell, 2011;249-260.

Radiography has been the mainstay of diagnosing spirocercosis over the years. However, alternative imaging techniques do have a role to play. As most of spirocerca pathology is in the thorax, diagnostic ultrasound has limited use. However we have described ultrasound-guided transhepatic caudal oesophageal mass biopsies[1] and currently we routinely examine the caudal oesophagus trans-abdominally in suspect spirocerca cases. Cranial abdominal aortic aneurysm formation has also been described[2] and abdominal examination of any spirocerca case should include the abdominal aorta. Diagnostic ultrasound may also be used investigate the secondary effects of the thoracic pathology and in the first paper we used this modality to diagnose terminal aortic thromboembolism secondary to a caudal thoracic spirocerca-induced aortic thrombus. For the latter we were the first to use CT to illustrate thoracic aortic thrombus formation using CT angiography. The second paper investigated in detail the spirocercosis-induced radiographic and CT changes seen in the aorta and emphasizes the greater sensitivity of CT to detect aortic mineralization and aneurysm formation over radiographs. Additionally CT found unsuspected thoracic aortic thrombi in two cases in this study. In our book chapter on mediastinal CT we elaborated further on the vallue of thoracic CT to detect and define the primary oesophageal pathology and the secondary changes in the thorax and elsewhere. We also postulated on the CT characteristics of the oesophageal mass and possible indicators of malignancy. This is currently under investigation by our spirocercosis study group.

Finallly, magnetic resonance imaging also has a role to play in imaging spirocercosis pathology and at this stage is mainly used for determining aberant migration of larvae to the vertebral canal with secondary extradural cord compresion[3] or intramedullary migration.[4,5] The lack of magnetic resonance imaging at our institution has hampered this investigator to further evaluate this imaging modality.

References

1 van der Merwe LL, Kirberger RM, Clift S, Williams M, Keller N, Naidoo V. *Spirocerca lupi* infection in the dog: A review. Vet J 2008;176:303-304.

2 Gal A, Kleinbart S, Aizenberg Z, Baneth, G. Aortic thromboembolism associated with *Spirocerca lupi* infection. Vet Parasitol 2005;130:331-335.

3 du Plessis CJ, Keller N, Millward IR. Aberrant extradural spinal migration of *Spirocerca lupi*: four dogs. J Small Anim Pract 2007;48:275-278.

4 Chai O, Shelef I, Brenner O, Dogadkin O, Aroch I, Shamir MH. Magnetic resonance imaging findings of spinal intramedullary spirocercosis. Vet Radiol Ultrasound 2008;49:456-459.

5. Dvir E, Perl S, Loeb E, Hirsch SS, Chai O, Mazaki-Tovi M, Aroch I, Shamir HM. Spinal intramedullary aberrant *Spirocerca lupi* migration in 3 dogs. J Vet Intern Med 2007;21:860-864.

IMAGING DIAGNOSIS—AORTIC THROMBOEMBOLISM ASSOCIATED WITH SPIROCERCOSIS IN A DOG

ROBERT M. KIRBERGER, ANTHONY ZAMBELLI

An 8-year-old neutered female Rhodesian Ridgeback developed acute, nonneurological right pelvic limb lameness. Femoral pulsation was poor, and oscillometric blood pressure measurements between the two pelvic limbs differed markedly. A caudal aortic right external iliac embolus was detected sonographically. Radiographically, there was a caudal esophageal mass and thoracic vertebral spondylitis typical of spirocercosis. Using CT-angiography, a caudal thoracic aortic aneurysm with a mural thrombus was detected. The dog recovered following heparin and aspirin therapy but signs recurred 7 months later. Subsequently, the patient improved on treatment and remains asymptomatic. This report illustrates the value of CT-angiography in detecting aortic thrombosis in dogs with spirocercosis. *Veterinary Radiology & Ultrasound, Vol. 48, No. 5, 2007, pp 418–420.*

Key words: aortic aneurysm, aortic thromboembolism, CT-angiography, dog, *Spirocerca lupi*, ultrasound.

History and Physical Findings

AN 8-YEAR-OLD 45 kg neutered female Rhodesian Ridgeback developed acute right pelvic limb lameness. On examination, the right femoral pulse was absent, the limb was cool to the touch, and a nail cut to the quick bled poorly. Patellar reflexes and extensor strength were decreased on the right pelvic limb. Blood pressure was measured across the dorsal metatarsal artery using an oscillometric blood pressure monitor.* Five readings were taken from each limb and averaged. Diastolic and systolic pressure averaged 40 and 76 mmHg, respectively, in the right pelvic limb and 90 and 132 mmHg, respectively, in the left pelvic limb.

Laboratory Data

Fecal flotation with a modified sugar solution[1] was negative for *Spirocerca* eggs. There was a mild thrombocytopenia (179×10^9/l, normal range $200–500 \times 10^9$/l). Results from routine serum chemistry testing, urinalysis, and coagulation profile evaluation were normal.

Imaging

Sonographically, the caudal aorta contained a 3-cm-long, mildly echogenic mass, which extended 6 cm into the right external iliac artery. The mass also appeared to extend into the median sacral artery. Color flow Doppler confirmed the absence of flow in this region. There was no sonographic evidence of altered cardiac chamber size or function, valvular growths, or free or intramural masses. On thoracic radiographs a 4-cm-diameter soft tissue opacity was present in the region of the caudal esophagus (Fig. 1). The 11th thoracic vertebra was characterized by mild ventral spondylitis. The aortic outline appeared smooth. These changes were consistent with spirocercosis.[2]

A CT examination† of the region between C7 and L1 was performed with the patient in sternal recumbency and under general anesthesia. Pre- and postcontrast images were reviewed in soft tissue (WL 32, WW 349) and lung (WL −400, WW 1600) windows. Sagittal and dorsal 2-mm-thick reconstructions were made as required.

The esophageal mass was clearly delineated as it arose from the left ventrolateral aspect of the esophagus just caudal to the heart, extending caudodorsally to terminate just cranial to the gastroesophageal junction. The mass was 10 cm long and 5 cm in diameter at its widest point. There was no evidence of mineralization of the mass and it had moderate vascularization (Fig. 2). Specks of dorsal aortic intimal mineralization were seen at the level of T12. The aorta at the level of T12–13 had a 4-cm-long mural filling defect on its right ventrolateral aspect. The mass involved about 35% of the circumferential luminal wall and protruded 10 mm into the lumen (Figs. 2 and 3). The cranial portion of this filling defect appeared to arise from a slightly widened aorta, indicative of an aneurysmal dilatation. These changes were compatible to an aortic thrombus, secondary to aorta intimal damage caused by migrating *Spirocerca lupi* larvae. There was no evidence of pulmonary metastasis.

*Cardell Cardiometer, Sharn Veterinary Inc., Tampa, FL.

From the Department of Companion Animal Clinical Studies, Faculty of Veterinary Science, University of Pretoria, Private Bag X04, Onderstepoort 0110, Republic of South Africa.

Address correspondence and reprint requests to Robert M. Kirberger, at the above address. E-mail: Robert.kirberger@up.ac.za

Received January 3, 2007; accepted for publication February 28, 2007.
doi: 10.1111/j.1740-8261.2007.00270.x

†Aquilon 16 slice helical CT, Toshiba Corporation Medical Systems Company, Tochigi-ken, Japan.

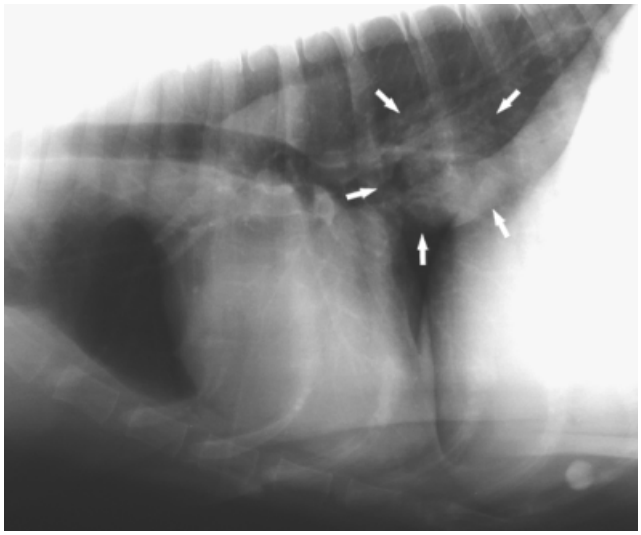

FIG. 1. Right lateral recumbent thoracic radiograph. Note the caudal esophageal mass (white arrows).

Doramectin injections at 0.5 mg/kg subcutaneously every 2 weeks for 12 weeks were planned to treat the *S. lupi* infection.[3,4] Owing to poor client compliance, the second injection was given 3.5 weeks after the first, after which compliance improved. In addition, aspirin (6 mg/kg orally per day for 2 weeks) and low molecular weight heparin (50 IU/kg subcutaneously twice daily for 72 h) were used to prevent ongoing thrombogenesis.

The clinical signs related to the iliac thrombosis resolved after 4 days and the dog continued to improve for 7 months before developing a mild relapse. The dog was clinically healthy otherwise and alert but had bilateral

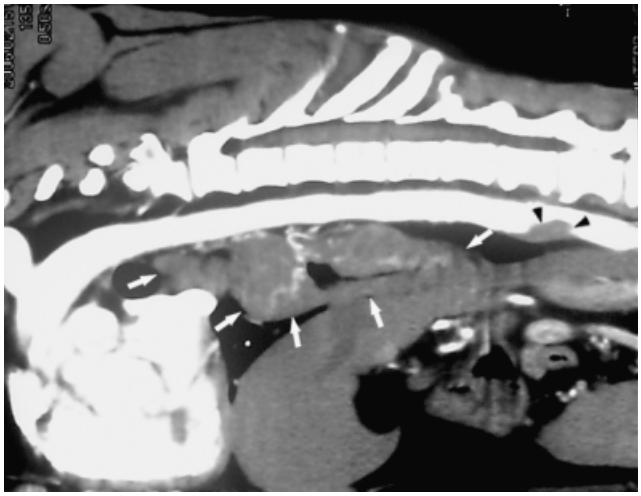

FIG. 2. CT-angiogram (WL 32, WW 349) sagittal reconstruction. Note the multilobulated irregular esophageal mass (white arrows) with conspicuous vessels, likely to be enlarged esophageal branches of the bronchoesophageal artery. There is mild aneurysmal dilation of the aorta at the origin of the ventrally located thrombus (black arrow heads).

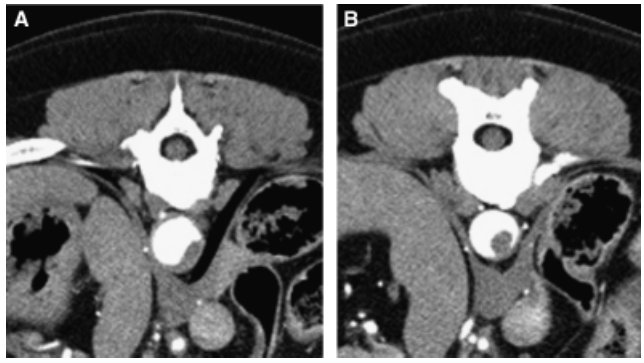

FIG. 3. Transverse CT-angiogram images of the aorta. (A) At level of caudal T12. (B) At level of caudal T13 illustrating aorta filling defect due to mural thrombus formation at 3–6 o' clock.

weak femoral pulses. Sonographically, the aorto-iliac thrombus was more extensive extending 3 cm more cranially with no evidence of blood flow past the site of embolization. Radiographically, the esophageal mass had resolved. Treatment with doramectin and aspirin at the same dosages and intervals was repeated and the patient was reportedly normal within 2 weeks. The patient continued to do well 3 months later.

Discussion

Canine aortic thromboembolism is rare. Reported causes are cardiac disease, neoplasia, glomerulonephropathy, atherosclerosis associated with hypothyroidism and hyperadrenocorticism, septicemic states, vegetative endocarditis, and corticosteroid therapy. These various etiologies result in a hypercoagulable state.[5,6] Thromboembolism is more common in the cat where it is usually associated with dilated or restrictive cardiomyopathy.[7]

S. lupi typically results in a caudal esophageal granuloma, which may undergo neoplastic transformation. Associated intrathoracic abnormalities include spondylitis, aortic aneurysm, and intimal mineralization.[2] Aorto-iliac thromboembolism associated with spirocercosis has been diagnosed previously in two dogs at necropsy. One was a Cavalier King Charles Spaniel[8] and the other a Boxer,[9] both of which died following unsuccessful treatment.

Caudal aortic thromboembolism in cats is often associated with cardiomyopathy, and leads to acute hindquarter paresis with pain, rhabdomyolysis, signs of peripheral vascular occlusion, and more serious systemic illness.[7] Although some of the latter signs arise from cardiomyopathy, the release of intracellular substances from ischemic muscles (such as calcium, serum inorganic phosphate, and potassium) contributes to the general clinical picture.[7] The concomitant release of platelet-derived thromboxanes and other chemical factors, as well as collateral blood supply, determine the different courses of hindquarter ischemic

disease when compared with dogs in which this syndrome often causes chronic intermittent pelvic limb paresis.[7,10,11]

To the best of our knowledge, this is only the third reported aorto-iliac embolism secondary to spirocercosis-induced aortic thrombus and the first to image the primary thrombus in the thoracic aorta. Previously, a cranial abdominal aortic thrombus was observed with diagnostic ultrasound.[8] Parasitic migration in the aorta can cause extensive intimal damage and it is surprising that more instances of iliac thromboembolism are not encountered in endemic areas. There may well be a higher incidence of aortic thrombi but the lack of sophisticated imaging to date may be the reason why they have gone undiagnosed. Aortic aneurysm formation in the cranial abdominal aorta occurs rarely but abdominal ultrasound examinations in known spirocercosis patients should include evaluation of the abdominal aorta. CT is performed on *S. lupi* patients in our institution to determine possible malignancy as indicated by early mass mineralization[2] or pulmonary metastasis and for surgical planning before mass removal. Based on the findings of this patient, imaging should include a CT-angiogram to evaluate subclinical or clinically evident aortic thromboembolism when there is suggestion thereof based on prior radiographic, clinical, or ultrasonographic findings. The aortic intima (in the thoracic portion) should be carefully examined for evidence of dilatation, stenosis, obstruction, or calcification. The diagnosis of early thrombotic disease may allow for better treatment with antithrombotic medications. On survey, thoracic radiographs' evidence of aortic aneurysm include aortic intimal calcification and an irregular outline of the aorta, particularly the descending aorta on VD or DV radiographs.[2] The latter is commonly seen in patients in our hospital and these patients should be put on prophylactic antithrombotic therapy for at least 2 weeks. No evidence-based guidelines exist for canine patients suffering from thrombogenic diseases, but based on human experience with atherosclerosis of other causes, aspirin, heparins (particularly dexaparin), warfarin, or other medications may have a place.[12,13] Given the length of the embolus, the blood flow velocity in the aorta, and the concurrent inflammation (thoracic intimal aortitis and within the thoracic granuloma), it is not surprising that the patient suffered such a dramatic clinical episode. Treatment of the primary pathogenic agent with doramectin is undoubtedly of some value in these patients.

Recanalization of the embolus may begin within hours of the initial event and may be more important in the normalization of regional blood flow than the development of new collateral vessels.[14,15] It is difficult to determine if in this patient the initial thrombus did not canalize over time or got canalized and then reoccluded.

Spirocercosis is an unusual cause of aortic thromboembolism and should be considered in dogs with acute or intermittent pelvic limb paresis in endemic areas. CT-angiography proved to be a useful diagnostic modality to determine the primary thrombus location as well as its size and other coexisting spirocercosis-associated pathology.

REFERENCES

1. Markovics A, Medinski B. Improved diagnostics of low intensity *Spirocerca lupi* infection by the sugar flotation method. J Vet Diag Invest 2002;8:400–401.

2. Dvir E, Kirberger RM, Malleczek D. Radiographic and computed tomographic changes and clinical presentation of spirocercosis in the dog. Vet Radiol Ultrasound 2001;42:119–129.

3. Lavy E, Aroch I, Bark H, et al. Evaluation of doramectin for the treatment of experimental canine spirocercosis. Vet Parasitol 2002;109: 65–73.

4. Berry WL. *Spirocerca lupi* oesophageal granulomas in 7 dogs: resolution after treatment with doramectin. J Vet Intern Med 2000;14: 609–612.

5. Dufort RM, Matros L. Acquired coagulopathies. In: Ettinger SJ, Feldman EC (eds): Textbook of veterinary internal medicine (chapter 273). St. Louis: Elsevier Saunders, 2005;1929–1933.

6. Fox PR, Petrie JP, Hohenhaus AE. Peripheral vascular disease. In: Ettinger SJ, Feldman EC (eds): Textbook of veterinary internal medicine (chapter 208). St. Louis: Elsevier Saunders, 2005;1145–1165.

7. Schoeman JP. Feline distal aortic thromboembolism: a review of 44 cases (1990–1998). J Feline Med Surg 1999;1:221–231.

8. Gal A, Kleinbart S, Aizenberg Z, Baneth G. Aortic thromboembolism associated with *Spirocerca lupi* infection. Vet Parasitol 2005;130:331–335.

9. Alvarenga J, Saliba AM. Iliac embolism in a dog. Mod Vet Pract 1971;52:37–38.

10. Brofman PJ, Thrall DE. Magnetic resonance imaging findings in a dog with caudal aortic thromboembolism and ischemic myopathy. Vet Radiol Ultrasound 2006;47:334–338.

11. Boswood A, Lamb CR, White RN. Aortic and iliac thrombosis in six dogs. J Small Anim Pract 2000;41:109–114.

12. Goodnight SH, Coull BM, McAnulty JH, Taylor LM. Antiplatelet therapy—Part II. West J Med 1993;158:506–514.

13. Goodnight SH, Coull BM, McAnulty JH, Taylor LM. Antiplatelet therapy—Part I. West J Med 1993;158:385–392.

14. Bick RL, Kaplan H. Syndromes of thrombosis and hypercoagulability. Congenital and acquired causes of thrombosis. Med Clin North Am 1998;82:409–415.

15. Bick D, Fugger EF, Pool SH, Hazelrigg WB, Yadvish KN, Spence WC. Disseminated intravascular coagulation: pathophysiological mechanisms and manifestations. Semin Thromb Hemost 1998;24:3–18.

COMPUTED TOMOGRAPHIC AND RADIOGRAPHIC CHARACTERISTICS OF AORTIC LESIONS IN 42 DOGS WITH SPIROCERCOSIS

ROBERT M. KIRBERGER, NERISSA STANDER, NICKY CASSEL, PAOLO PAZZI, VARAIDZO MUKORERA, JEVAN CHRISTIE, ANN CARSTENS, ERAN DVIR

Spirocerca lupi **is a common cause of vomiting, regurgitation, and sudden death in dogs that live in tropical or subtropical regions. Sudden death due to aortic rupture may occur with no preceding clinical signs. The purpose of this prospective study was to compare radiographic and computed tomographic (CT) characteristics of aortic lesions in a cohort of 42 dogs with endoscopically confirmed spirocercosis. Dorsoventral and right lateral recumbent thoracic radiographic findings were compared with pre- and postcontrast thoracic CT findings. Aortic mineralization was detected using CT in 18/42 dogs (43%). Three dogs had faint diffuse aortic wall mineralization. Using CT as the reference standard, radiographs had a sensitivity and specificity of 6% and 96%, respectively, for detecting aortic mineralization. A total of 20 aortic aneurysms were detected using CT in 15/42 dogs (36%). Using CT as the reference standard, radiographs had a sensitivity and specificity of 86% and 56%, respectively, for detecting aortic aneurysms. Respiratory motion, aortic displacement by esophageal masses and** ***Spirocerca*** **nodules adjacent to the aorta mimicked aneurysm formation on radiographs. Aortic thrombi were seen in two dogs in postcontrast CT images. Findings from this study indicated that aortic mineralization and aneurysm formation are common in dogs with spirocercosis. Findings also supported the use of pre- and postcontrast CT as effective methods for detecting and characterizing these lesions.** © 2013 *Veterinary Radiology & Ultrasound.*

Key words: Aneurysm, aorta, CT, dog, mineralization, radiography, ***Spirocerca lupi*****, thrombus.**

Introduction

SPIROCERCA LUPI *(S. lupi)* is a nematode with worldwide distribution and is most commonly found in tropical and subtropical areas. In South Africa, prevalence of this disease in dogs may reach up to 80%.[1] Dogs are definitive hosts and become infected by ingesting the intermediate host (coprophagous beetles) or paratenic host (lizards, wild and domestic birds, etc.).[2,3] After ingestion, the larvae migrate from the stomach via the celiac artery to the abdominal aorta and then migrate intramurally to the caudal thoracic aorta. They remain in this location for up to 3 months while maturing to young adults.[2] The young adults then penetrate the adjacent esophagus where they mature and form fibroblastic nodules. These nodules may undergo malignant transformation and progress to an esophageal sarcoma.[4] Aortic lesions in affected dogs typically occur within the intima, connective tissues and elastic fibers of the aortic wall. In locations where large numbers of larvae congregate, these may protrude into the aortic lumen.[2] Tissue destruction may be quite extensive with thrombosis and aneurysm formation occurring 4 months after infection. By 6 months postinfection, extensive scar formation may also be present.[2] Dystrophic mineralization and osseous metaplasia of the aortic muscular layer often occur secondary to tissue destruction.[5]

Clinical diagnosis of spirocercosis can be challenging because regurgitation and vomiting are present in only 60% of cases.[5] The diagnosis may be confirmed by finding *Spirocerca* eggs in the feces, however the sensitivity of this test is only 67%.[6] Gastroesophageal endoscopy is the current reference standard for a definitive diagnosis, however this test is invasive and expensive.[3] For dogs in endemic areas, computed tomography (CT) may be an effective reference standard if a combination of pathognomonic lesions could be identified. Such lesions include aortic aneurysms, aortic mineralization, spondylitis of the thoracic vertebra, and a caudodorsal mediastinal mass.[3,5] Computed tomographic

From the Department of Companion Animal Clinical Studies, Faculty of Veterinary Science, University of Pretoria, Private Bag X04, Onderstepoort 0110, Republic of South Africa (Kirberger, Stander, Cassel, Pazzi, Mukorera, Christie, Carstens, Dvir).

Dr Christie's current address is Perth Veterinary Specialists, 305 Selby Street, Osborne Park, Western Australia, 6017.

Portions of this study were presented at the IVRA congress in Bursa Turkey 2012.

The senior author received funding from the South African National Research Foundation for this project.

Address correspondence and reprint requests to Robert M. Kirberger, at the above address. E-mail: robert.kirberger@up.ac.za

Received September 6, 2012; accepted for publication January 5, 2013.

doi: 10.1111/vru.12021

detection of *S. lupi* induced aortic lesions may also be beneficial because these lesions occur early in the disease, exist in virtually all dogs that are infected, and are a cause of sudden death. In most cases, these lesions are subclinical and diagnosed at necropsy.

Imaging characteristics of aortic lesions for dogs with spirocercosis have been previously described. In one report, aortic mineralization was seen in 2/39 dogs in lateral thoracic radiographs and 2/3 dogs using CT.[5] Initially nonspirocercosis related aortic aneurysms were described in radiographs using aortic angiography.[7] In 2001, the authors first described the diagnosis of aortic aneurysms on survey radiographs. Radiographic lesions were detected on the left border of the descending aorta in dorsoventral radiographs and in a single lateral view in the initial ascending aorta in 3/37 dogs.[5] Aortoiliac thromboembolism due to spirocercosis has been reported in two dogs. For both dogs, lesions were confirmed at necropsy and, for one of the dogs, the inciting cranial abdominal aorta aneurysm was diagnosed ultrasonographically.[8,9] In a separate case report, CT imaging characteristics of a spirocercosis-associated caudal thoracic aortic thrombus and aortoiliac thromboembolism were described.[10] In that case, CT diagnosis aided in successful management of the case. While aortic thrombus formation has been described at necropsy, the incidence of aortic thrombus formation secondary to spirocercosis in clinical patients with esophageal pathology is unknown.

One objective of this prospective study was to describe the prevalence, location, extent, and size of thoracic aortic lesions (mineralization, aneurysm, and thrombus formation) using CT and radiography in a cohort of dogs with spirocercosis. Additional objectives were to compare CT and radiographic diagnostic sensitivities for detection of aortic lesions, and to compare the imaging characteristics of aortic lesions in neoplastic and non-neoplastic esophageal nodules. It was hypothesized that CT would be more sensitive than radiographs for detecting aortic lesions that occur in dogs with spirocercosis.

Materials and Methods

All procedures were approved by and conducted in accordance with institutional animal care requirements. Forty-two dogs were prospectively recruited. All included dogs had caudal esophageal nodules that were diagnosed by means of endoscopy within 5 days of radiographic and computed tomographic examinations. Dogs were classified into neoplastic or non-neoplastic nodule groups based on tissue biopsy, postmortem histology, or response to treatment. All dogs were evaluated over a 2-year period (2009–2010).

Each dog had dorsoventral and right lateral recumbent thoracic radiographs made using a digital computed radiography system (Fuji—AXIM, Midrand South Africa). The radiographs for each dog were retrieved from the Onderstepoort Veterinary Academic Hospital picture archiving system and interpreted without knowledge of clinical or CT findings by a single board certified radiologist (N.S.). The contrast, brightness, and magnification were adjusted to optimize lesion visualization and images were inverted as required to enhance detection of mineralization.

Thoracic CT was performed with dogs positioned in sternal recumbency. A dual slice CT scanner (Siemens Emotion Duo, Erlangen, Germany) was used for all dogs and technique settings included 3 mm slices, a pitch of 1.95 and 1.5-mm-thick slice reconstructions. All dogs were under general anesthesia with forced maintenance of an inspiratory phase using positive pressure ventilation techniques. An additional endotracheal tube was placed in the esophagus and inflated with air prior to CT examination in order to optimize visibility of esophageal nodules. Precontrast and postcontrast arterial phase scans were acquired for each dog after pressure injector administration of 2 ml/kg of iohexol 300 mg I/ml at 3 ml/s. Thoracic CT examinations were reloaded onto the CT computer and interpreted by a single board certified radiologist (R.K.) who was unaware of clinical or radiographic findings. Images were viewed in bone and mediastinal windows. Window levels, window widths, and magnification were adjusted as needed in order to optimize visualization of lesions in reconstructed multiplanar display formats.

For both radiographic and CT studies, presence and characteristics of aortic lesions were recorded by examining the thoracic and, where visible, the cranial abdominal aorta and celiac artery. A localized dilatation of the aorta was defined as an aneurysm for this study. A localized area of hyperattenuation in the aortic wall was defined as aortic mineralization. On lateral radiographs, the dorsal or ventral location of each aortic mineralization lesion was defined as 12 and 6 o'clock, respectively. On dorsoventral radiographs, the left or right location of each aortic mineralization lesion was defined as 3 and 9 o'clock, respectively. On CT transverse images, the location of each aortic mineralization lesion was defined as anywhere from 1 to 12 o'clock. Other characteristics recorded for aortic mineralization lesions included number, location relative to the thoracic vertebra, size (mm), and association with esophageal mass or aortic aneurysm lesions. Aortic aneurysms were characterized in a similar fashion. These data were recorded for the three largest mineralization and aneurysm lesions if there were more than three lesions. Additionally, postcontrast CT images were used to record presence and characteristics of aortic thrombus lesions. Aortic thrombus lesions were defined as regions lacking contrast within the lumen of the aorta. Regions of the aortic wall that appeared widened and lacked contrast enhancement were recorded as pseudoaneurysm formation.

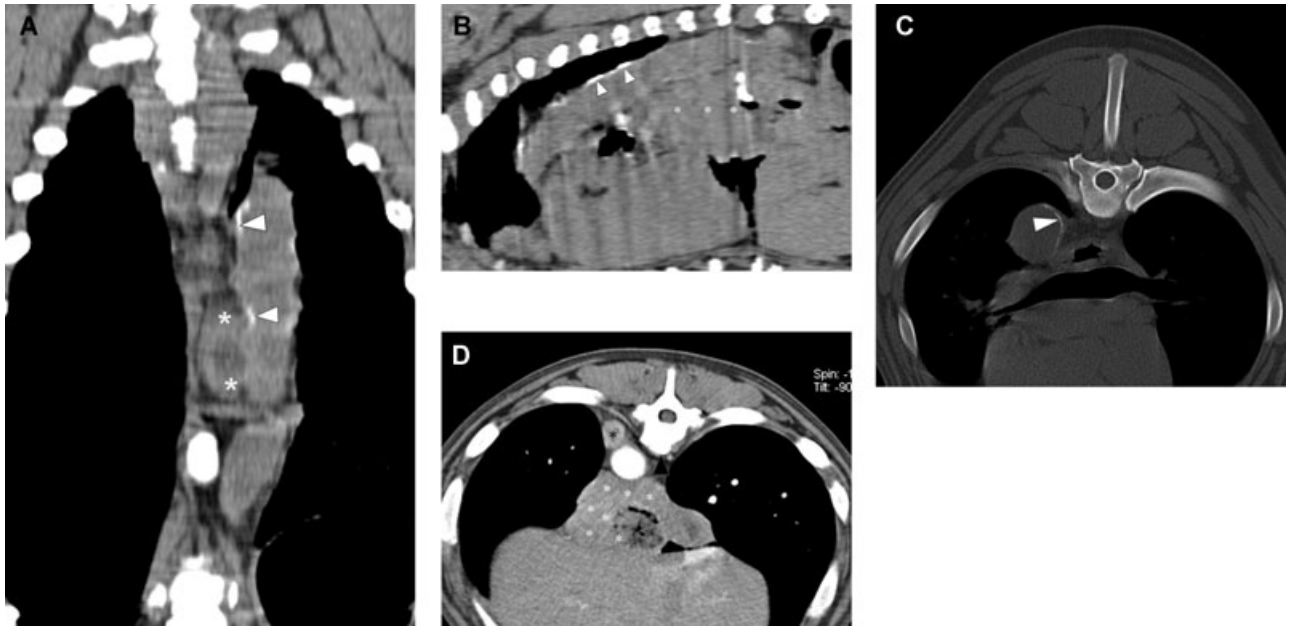

FIG. 1. Boerboel 6.5 years old with a neoplastic esophageal mass (white**). CT images. (A) Dorsal and (B) sagittal images through thoracic descending aorta in a mediastinal window. WW 400, WL40. Note irregular outline of the initial descending aorta with streaky mural mineralization (white arrowheads). (C) Transverse image in a bone window. WW 1500, WL 450. Note mineralized wall of aorta medially. Patient's left is always on the left of the image on transverse images. (D) Transverse image postcontrast in a mediastinal window. WW 400, WL40. Note additional nodule (black*) dorsolaterally to the aorta, which on radiographs could mimic an aneurysm. Adjacent spondylitis (black arrowhead) and an esophageal mass are present ventral to the aorta.

Confirmation of a *S. lupi* esophageal nodule or mass was made in all patients by means of esophageal and gastric endoscopy (Olympus GIF video endoscope, type XQ200, Tokyo, Japan). Patients were premedicated with a variety of drugs depending on clinician preference, but all were induced with propofol (Fresenius Kabi Pty Ltd, Halfway House, SA) and maintained on isoflurane (Safeline Pharmaceuticals Pty Ltd, Florida, SA). Each dog was placed in left lateral recumbency and a complete gastroesophageal endoscopy, with particular attention to the cardia, was performed. Biopsies were taken of suspect neoplastic lesions.

Statistical tests were selected and performed by one of the co-authors (E.D.), using commercially available statistical analysis software (Excel 97–2003®, Microsoft Corporation, Redmont, WA). For radiographic diagnostic sensitivity calculations, CT findings were used as the reference standard. The prevalence of aortic lesions (mineralization, aneurysm, thrombus) was compared for groups of dogs with neoplastic vs. non-neoplastic nodules using the Chi-square test. Results of comparisons were expressed as mean ± standard deviation, median, and range. The significance level for all tests was set at $P < 0.05$.

Results

Dogs

Dogs had a mean age of 65 ± 39 months and a median age of 60 months (range 10–160). There were six Jack Russell terriers; five each of German Shepherd dogs (GSDs) and Boerboels; and two each of Rhodesian ridgebacks, Boxers, Staffordshire terriers, Scottish terriers, Pit Bull terriers, and Labrador retrievers. The remaining 14 dogs were breeds with one dog each or cross breed dogs. There were 16 intact and seven sterilized females, and 14 intact and five sterilized males. Twenty-five dogs had non-neoplastic nodules and 17 dogs had neoplastic nodules.

Aortic Mineralizations

Aortic mineralization lesions were detected radiographically in 2/42 dogs (5%), one GSD and one Boerboel. Lesions were best seen following manipulation of the brightness and contrast settings on digital image displays. In the GSD, no aortic mineralization was identified using CT. On reevaluation of radiographs for this dog, the focal area of hyperattenuation was present in the ventral aortic wall at the level of T10 and interpreted to be due to a summation of the edge of the aorta and a superimposing pulmonary blood vessel. In the Boerboel, two moderately mineralized lesions were detected in radiographs. The larger was on the lateral margin of the aorta on the dorsoventral view, measuring 97 mm long and 2 mm wide at the level of T9–11, and with associated spondylitis. The second mineralization was on the dorsal margin of the aorta at the level of T4 and measured 15 mm long and 1 mm wide. In the CT images for this dog, three mineralized areas were seen. These were located dorsally and laterally but did not appear to be as

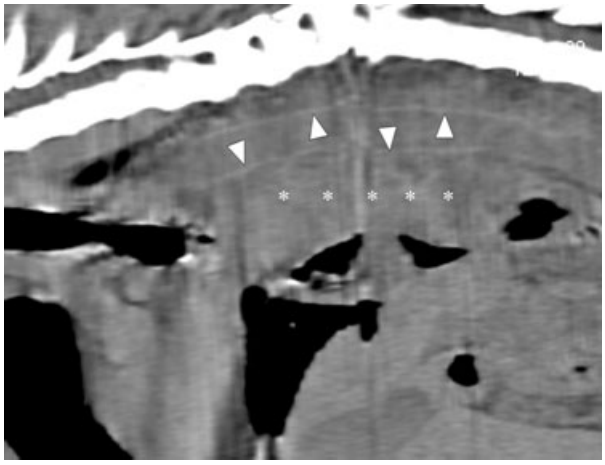

FIG. 2. Dobermann 4 years old with a neoplastic esophageal mass (white**). Sagittal CT image in a mediastinal window. WW 400, WL40. Note faintly mineralized wall of the whole thoracic aorta (white arrowheads) and esophageal mass ventral to the aorta.

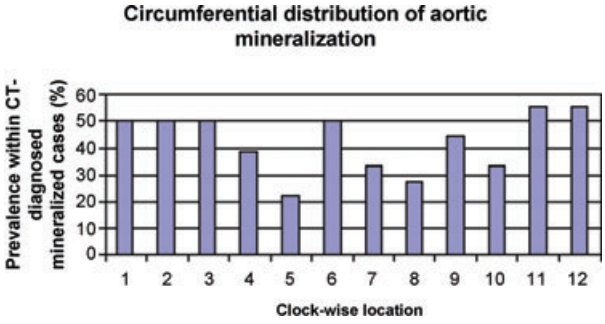

FIG. 3. Bar graph illustrating the CT determined circumferential distribution of the thoracic aortic mineralizations.

extensive as those seen on radiographs. Lesions were at the level of T4–7 and T11 (Fig. 1A–D).

Eighteen/Forty-two (45%) of dogs had aortic mineralization visible in CT images, with a total of 30 mineralized lesions and up to four differing lesion locations in two dogs. Aortic wall mineralization lesions measured 1–3 mm thick and 3–69 mm long and appeared streaky or solid. In one dog, lesions were circumferential. In 66% of dogs, mineralization lesions were adjacent to esophageal pathology. In 20% of dogs, aortic aneurysms had adjacent aortic mineralization lesions. Three dogs had atypical, extensive, faint mineralization of the entire aortic wall in CT images (Fig. 2). One of these three dogs had additional patchy mineralization and another had a neoplastic esophageal mass.

Circumferential locations of aortic mineralization lesions were highly variable, with no discernible pattern of predilection (Fig. 3). Eleven/Eighteen dogs had aortic mineralization lesions at one vertebral level and these extended around the aorta from 8% to 42% of the total circumference. Seven/Eighteen dogs had aortic mineralization lesions at more than one vertebral level and these had circumferential involvement ranging from 42% to 100%. For 47% of all aortic mineralization lesions detected using CT, mineralization was present adjacent to the esophageal mass.

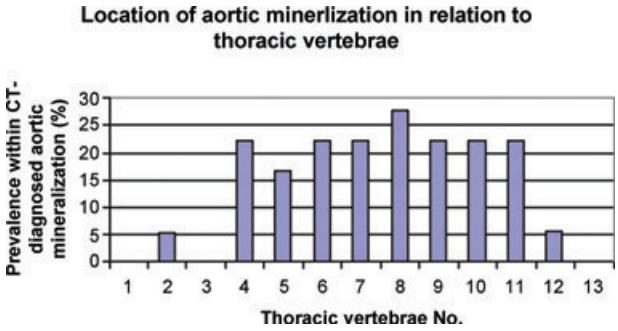

FIG. 4. Bar graph illustrating the CT determined level of aortic involvement containing the largest mineralized area relative to the thoracic vertebrae.

Aortic locations with the greatest number of mineralized lesions commonly extended from the level of T4 to T11 (Fig. 4), with one each found at T2 and T12. Aortic lesions for one dog involved four vertebral lengths and lesions for four dogs involved three vertebral lengths. The second and third largest aortic mineralizations involved only one vertebral length and had circumferential involvement between 17% and 34%.

The sensitivity of radiographs was 6% and specificity 96% for detecting aortic mineralization compared to CT. Neoplastic transformation of at least one spirocercosis nodule was identified in 12/18 (67%) of the dogs with aortic mineralization detected using CT. The remaining six dogs (33%) with aortic mineralization had non-neoplastic nodules. Neoplastic transformation of at least one spirocercosis nodule was identified in 5/24 (21%) of the dogs with no aortic mineralization. The difference in prevalence of aortic mineralization for neoplastic versus non-neoplastic nodule groups was significant ($P = 0.002$).

Aortic Aneurysms

Thirty-three aortic aneurysms were seen in 25/42 (60%) dogs in radiographs, whereas 20 aneurysms were seen in 15/42 (36%) of dogs using CT. No abdominal arterial lesions were detected in the 42 cases. In 13/15 of the CT aneurysm positive dogs, aneurysms were also seen in the radiographs (Fig. 5A–E). Based on the CT reference standard, the sensitivity of radiographs for detecting aortic aneurysms was 86%. However, a large number of false-positive aneurysms (12/25) in radiographs resulted in a low specificity value (56%) for this modality. One or more aneurysms were detected on the lateral margin of the aorta in dorsoventral radiographic views and on the dorsal and ventral aortic margins in lateral radiographic views. The location of aortic involvement relative to the thoracic vertebrae for the largest aneurysm area detected in radiographs was at T3 to T10 with the latter location only occurring

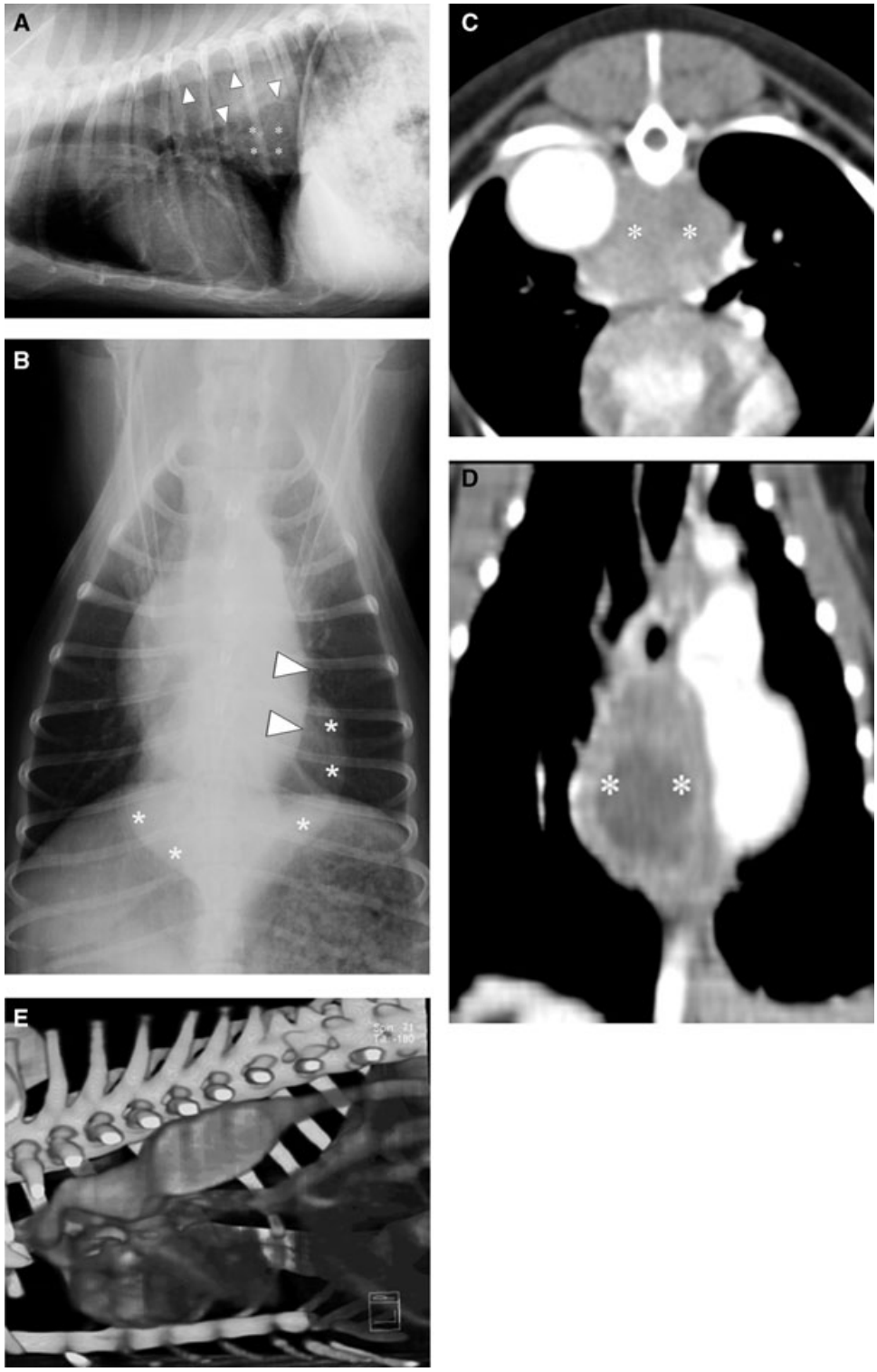

FIG. 5. Maltese 10 years old with a non-neoplastic esophageal mass (white**) and a large aortic aneurysm dorsolateral to it. (A) Lateral and (B) DV thoracic radiographs (white arrowheads delineate edge of aneurysm, which ventrally superimposes on mass). (C) Transverse, (D) dorsal, and (E) volume rendered postcontrast CT images in a mediastinal window. WW 400, WL40.

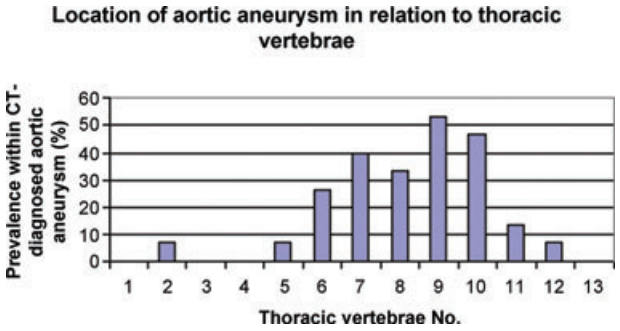

FIG. 6. Bar graph illustrating the CT determined level of aortic involvement relative to the thoracic vertebrae for the largest aneurysm.

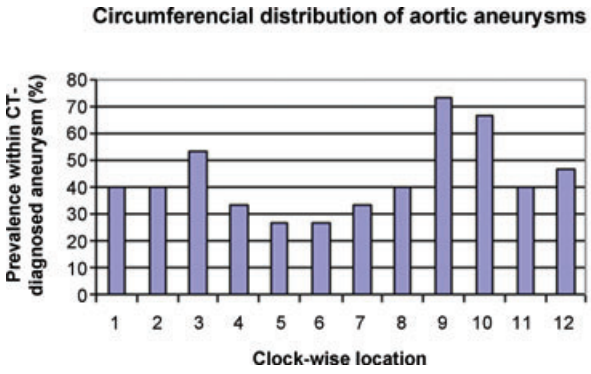

FIG. 7. Bar graph illustrating the CT determined circumferential distribution of aortic aneurysms

once with T4–7 making up 72% (31/43) of aortic involvement. One aneurysm involved five vertebral lengths, five aneurysms involved three lengths, three aneurysms involved two vertebral lengths, and the remainder involved one vertebral length or less.

On CT, the location of aortic involvement relative to the thoracic vertebrae for the largest aneurysm area was at T2, and T5–T12 with the T2, T5, and T12 location only occurring once and T6–T10 making up 76% (26/36) of aortic involvement (Fig. 6). One aneurysm each involved seven, six, five, and four vertebral lengths. Two aneurysms involved two vertebral lengths. The remaining aneurysms involved one vertebral length or less. On CT all circumferential locations of the aorta were involved, with the entire circumference being affected in two dogs (Fig. 7). In 2/25 of the dogs with aneurysms, the aneurysm formation extended into the associated intercostal arteries (Fig. 8A–C). The height of aneurysm protrusion beyond the borders of the aorta varied from 3 to 24 mm. In 3/25 dogs, the lesions were fairly rounded whereas in the rest of the cases the aneurysms were elongated. In the dog with the longest aneurysm (123 mm long and 12 mm high), the aneurysm did not enhance with contrast (Fig. 9A–E). In another dog, a nonenhancing thickening of the aortic wall was detected peripheral to the contrast filled lumen. On CT, 11 aneurysms were located adjacent to the esophageal mass.

In one dog, the esophageal mass displaced the adjacent aorta and resulted in an apparent aneurysm on survey CT images. In the postcontrast CT images for this dog, the aorta was normal (Fig. 10A–D). In another dog, two nodules were seen adjacent to the aorta at the level of T10 and were believed to be due to aberrant larval migration (Fig. 1D). This dog was negative on CT for aneurysm formation but positive on radiographs, albeit not at the exact same location.

In 4/15 (27%) of the dogs with aortic aneurysms on CT, neoplastic transformation of the esophageal nodule was identified. In 11/15 (73%) of the dogs with aortic aneurysms, non-neoplastic nodules were identified. The difference in prevalence of aortic aneurysms for neoplastic and non-neoplastic groups was not significant ($P = 0.17$).

Aortic Thrombi

Intraluminal thrombi were seen in postcontrast CT images in two dogs. One dog was a Labrador crossbreed, a 12 × 10 × 11 mm sessile thrombus was identified in the ventral aortic lumen at the level of T8 and another smaller thrombus was identified in the ventral aortic lumen at the level of T7. This dog also had a small aortic aneurysm and neoplastic esophageal lesion in this region. The second dog with intraluminal aortic thrombi was a Dalmatian. This dog had a large sessile thrombus (19 × 19 × 13 mm) in the ascending aorta at the level of T2 and this thrombus was adjacent to a large aortic aneurysm (Fig. 11). An additional, pedunculated, 36-mm-long, 4-mm-wide thrombus was present in the intrahepatic caudal vena cava. A suspect thrombus was present in the left ventricle, attached to a papillary muscle. This dog had a non-neoplastic esophageal nodule.

Discussion

A relatively high prevalence (43%) of aortic mineralization was identified using CT in the spirocercosis affected dogs of our study. The sensitivity of radiographs for detecting this change was poor. Additionally, 36% of the dogs in this study had aortic aneurysms on CT, with radiographs having poor sensitivity (56%). Asymptomatic intraluminal aortic thrombi were found in two dogs. No dogs had intraluminal thrombi involving other arteries. A poor correlation was found between radiographs and CT regarding the location of aortic mineralization and aneurysm formation. This was likely due to different patient positions used for imaging, forced inspiration during CT vs. normal inspiratory radiographs or esophageal inflation during CT versus no esophageal inflation during radiography.

Aortic wall mineralization is a rare finding in dogs in nonendemic spirocercosis regions. Aortic valve, aortic bulb, ascending aortic, and initial descending aortic mineralizations have been reported as rare incidental findings in older

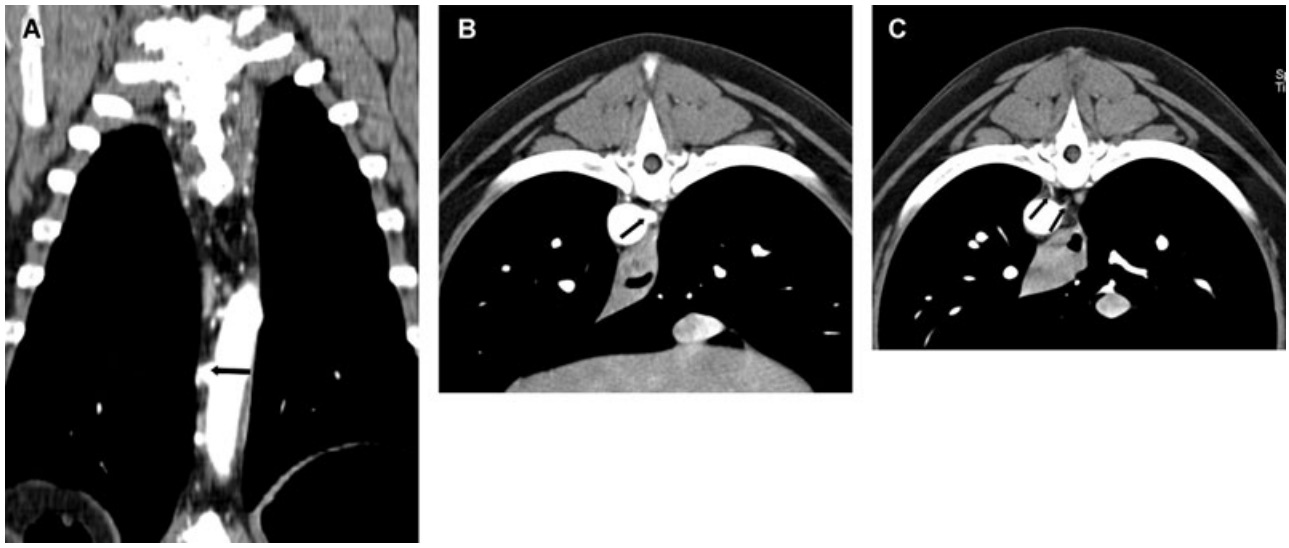

FIG. 8. Boerboel 6 years old with a non-neoplastic esophageal mass. Postcontrast CT images in a mediastinal window. WW 400, WL 40. Note the extension of the aortic aneurysm into the intercostal arteries in the (A) dorsal and (B) transverse images. (C) Transverse image of normal intercostal arteries. Arrows indicate intercostal arteries.

large breed dogs, often associated with coronary artery mineralization.[11,12] Mineralization of the caudal aorta has been associated with an arteriosclerotic lesion,[13] chronic renal insufficiency,[14] hypervitaminosis D, and idiopathic causes in dogs.[15] Ascending aortic mineralization has also been associated with chronic septic necrotizing endarteritis with secondary perforation and hemopericardium in a dog.[16] In the cat, aortic mineralization has been associated with chronic renal failure and hypertension with arteriosclerosis.[17,18] In dogs with spirocercosis, aortic wall mineralizations have been found to be caused by dystrophic mineralization and metaplastic ossification of the aortic wall after larval migration induced purulent panarteritis.[2] The mineralizations can be extensive and may be associated with aortic aneurysm formation or an esophageal mass. This association distinguishes spirocercosis-induced aortic mineralizations from other causes of aortic mineralization. Spirocercosis-induced thoracic lesions are usually located in the caudal thorax; however our finding of involvement of the ascending aorta (T4 region) demonstrates how far cranially the larvae can migrate in the aorta.

The extensive, faintly mineralized, entire aortic wall seen on CT in three of our dogs was an unexpected finding, as it is unlikely to be dystrophic in origin and has not been previously described in dogs with spirocercosis. The lesion was confined to the thoracic aorta, except in one dog for which the cranial abdominal aorta was also involved. Since these locations can be part of the larval migration route, it is reasonable to assume the mineralization was associated with spirocercosis. In retrospective review of medical record entries, two of these three dogs had elevated serum inorganic phosphate. This finding, together with high normal total serum calcium, suggests that the aortic mineralization could have been caused by metastatic calcification. The elevated serum inorganic phosphate may have been from extensive tissue damage and necrosis, however the concurrent increase in serum calcium may warrant further investigation. Interestingly, these three dogs also had enlarged salivary glands and this finding has been previously associated with spirocercosis.[3] At this stage, possible relationships between these findings remain unknown. Histopathologic examination would have been required to characterize the atypical mineralization of the aortic wall in these cases. We will endeavor to do this for future cases that go to necropsy.

Based on the current study findings, aortic aneurysms were overdiagnosed on radiographs. Part of the reason may be that imaging clinicians in our hospital are sensitized to look for incidental spirocercosis-related pathology on all thoracic radiographs. Based on CT image comparisons, the aorta may be displaced by an esophageal mass or aberrantly located *S. lupi* nodule adjacent to the aorta and this may mimic aneurysms in radiographs. Most aneurysms were seen on the left margin of the descending aorta on the dorsoventral radiographs and only larger aneurysms were seen on the lateral views, more so in the aortic arch and initial descending aorta. In the caudal thoracic region, the aorta and esophageal mass margins may have been difficult to distinguish from each other on dorsoventral views, even when trying to trace the left lateral margin of the aorta cranial to the mass. Although CT images were the reference standard for this study, it is possible that motion may have resulted in incorrect diagnosis of an aneurysm. The similar attenuation of the aorta and adjacent esophagus in

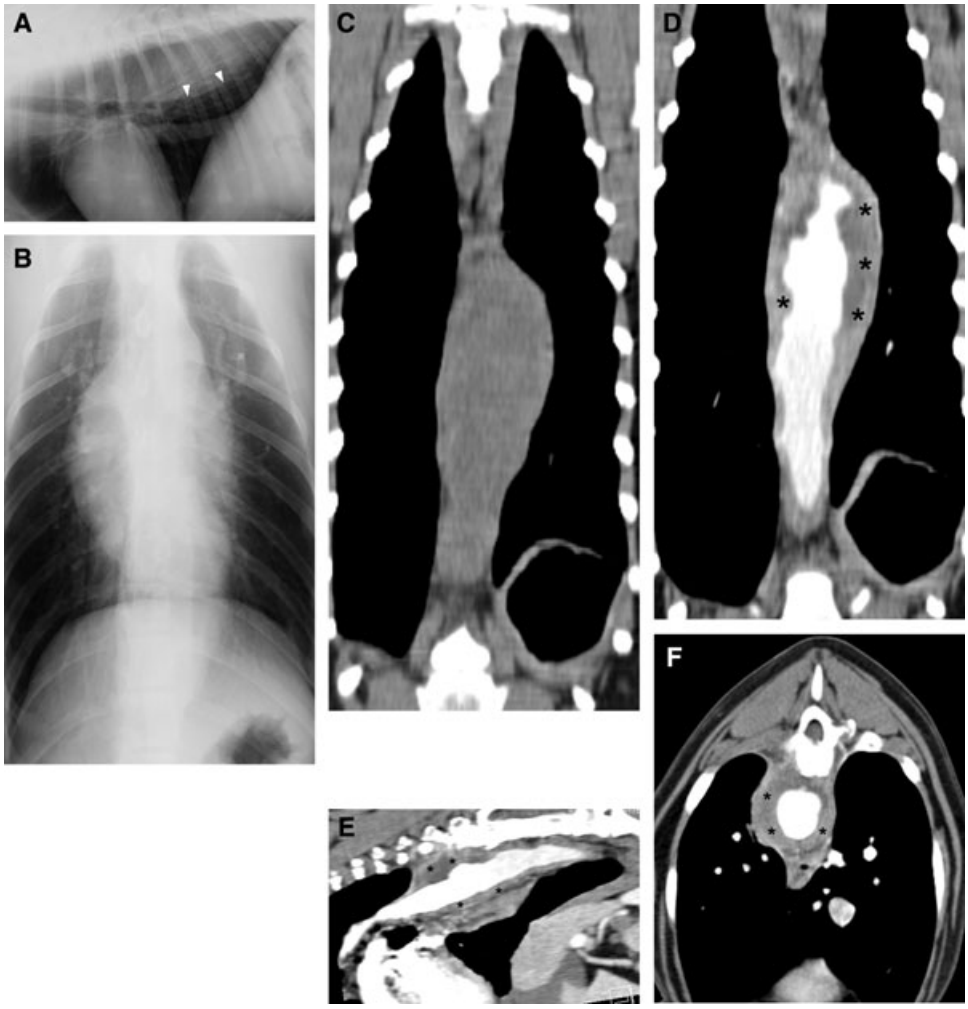

FIG. 9. Rhodesian ridgeback 7 months old. (A) Lateral (white arrowheads demarcate ventral edge of aorta) and (B) DV thoracic radiographs. (C) Dorsal precontrast and (D) dorsal (E) sagittal and (F) transverse postcontrast CT images in mediastinal window. WW 400, WL 40. Note the massively enlarged aorta, which on postcontrast images shows several smaller aneurysms with surrounding hypoattenuating old hemorrhage (black**) (HU 15–20).

precontrast CT images may also have resulted in incorrect aneurysm diagnosis. The use of postcontrast, arterial phase CT, as was done in this study, was essential for minimizing the latter misinterpretation.

Besides aortic changes associated with congenital cardiac disease, aortic enlargement is quite rare in dogs, except in endemic spirocercosis areas as illustrated in this report. Aortic dilatation of the ascending aorta is most commonly caused by aortic stenosis or volume overload secondary to a patent ductus arteriosus in dogs.[19] Dilatation may also be due to coarctation of the aorta, a rare congenital constriction in the region of the ductus or ligamentum arteriosus or just cranial to it.[20] Caudal to the constriction, a poststenotic dilatation occurs with concomitant intercostal artery enlargement and secondary changes on the adjacent ribs. Familial fusiform aortic aneurysm of the ascending aorta has been described in Leonberg dogs, and proposed to be due to cystic medial necrosis from familial connective tissue disorders.[21] A canine case of caudal abdominal aortic aneurysm has been associated with systemic fungal disease.[22]

Our study did not attempt to distinguish the various forms of aortic aneurysms and focused on detection of focal enlargements of the aorta. In man, an aortic aneurysm is defined as a permanent localized dilatation of the aorta with a 50% increase in diameter with increases <50 classified as aortic ectasia.[23] A pseudoaneurysm contains blood in the periarterial connective tissues secondary to total disruption of the arterial wall and usually do not take up contrast.[23] Intramural hematoma occurs as a consequence of a penetrating ulcer and will also not take up contrast. In animals an aneurysm is defined as a circumscribed dilation of an arterial wall or a blood containing swelling connecting directly with the arterial lumen.[24] The same authors define a pseudoaneurysm in dogs the same as in man.

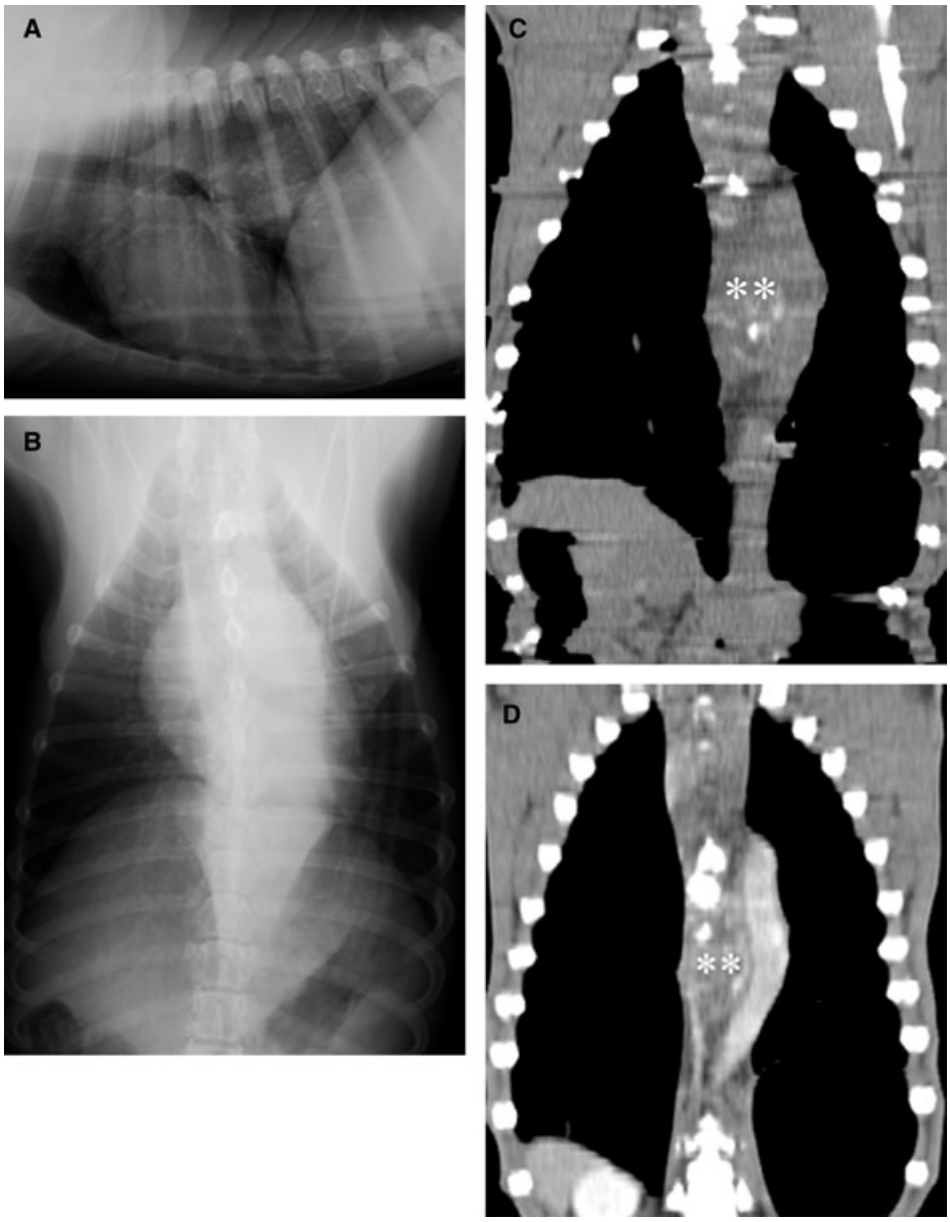

FIG. 10. Pit bull 8 years old with a neoplastic esophageal mass (white**). (A) Lateral and (B) DV thoracic radiographs. (C and D) Dorsal pre- and postcontrast CT images in a mediastinal window. WW 400, WL40. Note the esophageal mass displacing the aorta mimicking an aneurysm, which can only be excluded after delineating the aorta with contrast medium.

In two dogs of our study the aorta appeared focally dilated but did not take up contrast in the enlarged areas. This could have been due to pseudoaneurysms or intramural hematomas. The extra-aortic areas were hypoattenuating (<20 HU) and thus believed to be old hematomas.[25] If a 50% enlargement of aortic diameter was to be used as the criterion for aortic aneurysm formation the incidence would have been much lower and many cases would have been classified as ectasia.

No cranial abdominal aortic changes were seen in the dogs of this study. However subsequent to our study, we have seen cranial abdominal aortic aneurysms in two spirocercosis affected dogs that also involved the celiac artery. A cranial abdominal aortic aneurysm with thrombus formation and secondary aortoiliac thromboembolism also has been previously described.[9] The aneurysm was diagnosed by means of diagnostic ultrasound and this was found to be a useful imaging modality for detecting abdominal aortic pathology. We believe it is essential to include the cranial abdomen when investigating spirocercosis by means of CT and to ensure that the celiac artery and associated aorta are not affected. Lesions in this location should be

FIG. 11. Dalmatian 2.5 years old with a non-neoplastic esophageal mass. Postcontrast CT transverse image in a mediastinal window. WW 400, WL40. Note the filling defect (white*) in the ascending aortic aneurysm caused by a thrombus.

distinguished from a previously described celiac artery pseudoaneurysm secondary to a migrating grass awn.[26]

Computed tomographic angiography would be expected to have greater sensitivity for detecting aortic thrombi because it is a cross-sectional imaging modality. While not statistically tested, this expectation was supported in the current study. Two dogs with radiographically unsuspected aortic thrombi had lesions detected in CT angiographic images. One of the dogs had a thrombus at the expected caudal thoracic aorta and this was assumed to have been instigated by intimal damage. The other dog had an aortic thrombus in the ascending aorta that was associated with a large aneurysm. While this thrombus could also have been due to intimal damage, this dog also had thrombi in the left ventricle and caudal vena cava where intimal damage caused by spirocercosis would be highly unlikely. Aortic thrombosis is a relatively rare disease in dogs and may arise following the disturbance of one or more of four factors: blood flow, endothelial integrity, coagulation, and fibrinolysis.[24] Canine aortic thromboembolism usually occurs as result of a hypercoagulable state.[24,27] Common etiologies for the latter are cardiac disease, neoplasia, glomerulonephropathy, atherosclerosis, septicemia, vegetative endocarditis, and corticosteroid therapy.[24,27] Our research group has recently completed a study investigating the hemostatic and inflammatory alterations present in spirocercosis and found that 97% of infected dogs were hypercoagulable as determined by thromboelastography (Pazzi P, Goddard A, Kristensen AT, Dvir E. Evaluation of haemostatic abnormalities in canine spirocercosis and its association with systemic inflammation. 22nd ECVIM-CA Congress Proceedings, Maastricht, 6–8 September 2012, p. 219). The severity of hypercoagulability increased as the *S. lupi* nodules progressed from non-neoplastic to neoplastic. The degree of hypercoagulability had a strong positive correlation to the acute inflammatory indicators, fibrinogen, and C-reactive protein. This close correlation supports the hypothesis that an inflammatory state exists in all forms of spirocercosis, which in turn leads to the hypercoagulable state, which is exacerbated in the neoplastic stage. The initial vascular injury due to larval migration, although unlikely to be an active site of inflammation once mature esophageal nodules are present, may contribute to the thrombus formation. Embolic aortic obstruction may also be secondary to cardiac disease such as vegetative endocarditis, mitral valve endocardiosis, and left atrial thrombus formation as well as neoplastic emboli from primary tumors anywhere in the body.[28] Primary aortic intimal damage with secondary thrombus formation is rare in animals. Atherosclerosis, usually secondary to hypothyroidism, results in aortic and iliac artery intima disruption.[7,24,28] The endothelium plays an important role in anticoagulation and larval-induced endothelial injury may promote thrombosis as occurs in hypothyroid dogs.[24] Spirocercosis should be included in the differential diagnosis of thrombus formation in the dog, especially in endemic areas.

Most cases of *S. lupi* associated thrombi are only diagnosed after presenting with clinical signs of aortic thromboembolism but the true incidence of pre-embolic primary aortic thrombus formation cannot be assessed clinically. Ultrasonography can detect abdominal aortic thrombus formation but the thoracic aorta is inaccessible to ultrasonographic investigation unless transesophageal ultrasonography is performed.

One limitation of this study was that all cases were known to be positive and specificity and predictive values of the various findings compared to known normal dogs could not be determined. We chose this study design because our primary objective was to determine prevalence of aortic lesions in affected dogs and to compare imaging characteristics for radiography vs. CT. Another limitation was that we did not have histopathologic confirmation of aortic lesions in this study. Future studies are needed in which aortic wall histopathologic findings are compared with CT findings for dogs scheduled to be euthanized in spirocercosis-endemic areas.

In conclusion, findings from our study indicated that aortic mineralizations and aortic aneurysms are common in dogs with spirocercosis. Detection of these lesions in thoracic CT images therefore warrants a presumptive diagnosis of spirocercosis for dogs living in endemic areas, even if dogs do not have other clinical signs of spirocercosis.

Additionally, if a concurrent esophageal mass is identified, aortic mineralization may be associated with neoplastic transformation. This combination of CT findings justifies a poorer prognosis and additional investigation by endoscopy, biopsy, and histopathology. Arterial-phase, postcontrast CT examination of the thoracic and cranial abdominal aorta is recommended for dogs in spirocercosis-endemic areas to screen for aortic thrombi.

REFERENCES

1. Kok DJ, Williams EJ, Schenker R, Archer NJ, Horak IG. The use of milbemycin oxime in a prophylactic anthelmintic programme to protect puppies, raised in an endemic area, against infection with *Spirocerca lupi*. Vet Parasitol 2010;174:277–284.
2. Bailey WS. *Spirocerca lupi*: a continuing inquiry. J Parasitol 1972;58:3–22.
3. van der Merwe LL, Kirberger RM, Clift S, Williams M, Keller N, Naidoo V. *Spirocerca lupi* infection in the dog: a review. Vet J 2008;176:294–309.
4. Dvir E, Clift SJ, Williams MC. Proposed histological progression of the *Spirocerca lupi*-induced oesophageal lesion in dogs. Vet Parasitol 2010;168:71–77.
5. Dvir E, Kirberger RM, Malleczek D. Radiographic and computed tomographic changes and clinical presentation of spirocercosis in the dog. Vet Radiol Ultrasound 2001;42:119–129.
6. Christie J, Schwan EV, Bodenstein LL, Sommerville JEM, van der Merwe LL. The sensitivity of direct faecal examination, direct faecal flotation, modified centrifugal faecal flotation and centrifugal sedimentation/flotation in the diagnosis of canine spirocercosis. J S Afr Vet Assoc 2011;82:71–75.
7. Boswood A, Lamb CR, White RN. Aortic and iliac thrombosis in six dogs. J Small Anim Pract 2000;41:109–114.
8. Alvarenga J, Saliba AM. Iliac embolism in a dog. Mod Vet Pract 1971;52:37–38.
9. Gal A, Kleinbart S, Aizenberg Z, Baneth, G. Aortic thromboembolism associated with *Spirocerca lupi* infection. Vet Parasitol 2005;130:331–335.
10. Kirberger RM, Zambelli A. Imaging diagnosis—aortic thromboembolism associated with spirocercosis in a dog. Vet Radiol Ultrasound 2007;48:418–420.
11. Schwarz T, Sullivan M, Störk CK, Willis R, Harley R, Mellor DJ. Aortic and cardiac mineralization in the dog. Vet Radiol Ultrasound 2002;43:419–427.
12. Douglas JP, Berry CR, Thrall DE, Malarkey DE, Spaulding KA. Radiographic features of aortic bulb/valve mineralization in 20 dogs. Vet Radiol Ultrasound 2003;44:20–27.
13. Drost WMT, Bahr RJ, Henry GA, Campbell GA. Aortoiliac thrombus secondary to a mineralized arteriosclerotic lesion. Vet Radiol Ultrasound 1999;40:262–266.
14. Barber DL, Rowland GN. Radiographically detectable soft tissue calcification in chronic renal failure. J Am Vet Rad Soc 1979;20:117–123.
15. Lamb CR, Kleine LJ, McMillan MC. Diagnosis of calcification on abdominal radiographs. Vet Radiol 1991;32:211–220.
16. Peterson PB, Miller MW, Hansen EK, Henry GA. Septic pericarditis, aortic endarteritis and osteomyelitis in a dog. J Am Anim Hosp Assoc 2003;39:528–532.
17. Keppie N, Nelson N, Rosenstein D. Imaging diagnosis: mineralization of the aorta, celiac and cranial mesenteric arteries in a cat with chronic renal failure. Vet Radiol Ultrasound 2006;47:69–71.
18. Lefbaum BK, Adams WH, Weddle DL. Mineralized arteriosclerosis in a cat. Vet Radiol Ultrasound 1996;47:420–423.
19. Dennis R, Kirberger RM, Barr FJ, Wrigley RH. Handbook of small animal radiology and ultrasound. Techniques and differential diagnosis, 2nd ed. London: WB Saunders, 2010;183.
20. Herrtage ME, Gorman NT, Jefferies AR. Coarctation of the aorta in a dog. Vet Radiol Ultrasound 1992;33:25–30.
21. Chetboul V, Tessier D, Borenstein N, et al. Familial aortic aneurysm in Leonberg dogs. J Am Vet Med Assoc 2003;223:1159–1162.
22. Gershenson RT, Melidone R, Sutherland-Smith J, Rogers CL. Abdominal aortic aneurysm associated with systemic fungal infection in a dog. J Am Anim Hosp Assoc 2011;47:45–49.
23. Hiratzka LF, Bakris GL, Beckman JA, et al. 2010 ACCF/AHA/AATS/ACR/ASA/SCA/SCAI/SIR/STS/SVM guidelines for the diagnosis and management of patients with thoracic aortic disease: executive summary: a report of the American College of Cardiology Foundation/American Heart Association Task Force on Practice Guidelines, American Association for Thoracic Surgery, American College of Radiology, American Stroke Association, Society of Cardiovascular Anesthesiologists, Society for Cardiovascular Angiography and Interventions, Society of Interventional Radiology, Society of Thoracic Surgeons, and Society for Vascular Medicine (developed in collaboration with the American College of Emergency Physicians). J Am Coll Cardiol 2010;55:1509–1544.
24. Fox PR, Petrie JP, Hohenhaus AE. Peripheral vascular disease. In: Ettinger SJ, Feldman EC (eds): Textbook of veterinary internal medicine, 6th ed. St Louis: Elsevier Saunders, 2005;1145–1165.
25. Hecht S. Brain. In: Schartz T, Saunders J (eds): Veterinary computed tomography. Ames, Iowa: John Wiley & Sons, 2011;189.
26. Llabrés-Díaz F, Brissot H, Ibarrola P. Imaging diagnosis—celiac artery pseudoaneurysm associated with a migrating grass awn. Vet Radiol Ultrasound 2010;51:508–511.
27. Dufort RM, Matros L. Acquired coagulopathies. In: Ettinger SJ, Feldman EC (eds): Textbook of veterinary internal medicine. 6th ed. St. Louis: Elsevier Saunders, 2005;1929–1933.
28. van Winklle TJ, Hackner SG. Clinical and pathological features of aortic thromboembolism in 36 dogs. J Vet Emerg Crit Care 1993;3:13–21.

CHAPTER TWENTY-FIVE

MEDIASTINUM

Audrey Petite and Robert Kirberger

IMAGING PROTOCOL (TABLE 25.1)

Images are also viewed in lung and bone windows allowing different aspects of a disease to be evaluated.

CT: ANATOMY AND NORMAL VARIANTS

The mediastinum is the thoracic midline space comprised between the left and right pleural cavities. The mediastinum is continuous with the soft tissues of the neck cranially through the thoracic inlet. It is continuous caudally with the retroperitoneum through the aortic hiatus. In dogs and cats, the mediastinum contains the thoracic trachea (*see* Chapter 24) and the esophagus, lymph nodes, the thymus, the thoracic duct, several important nerves, the heart and the great vessels (*see* Chapter 23). The mediastinum also contains a variable amount of fat deposits. Although in cats the width of the cranial mediastinum is fairly consistent (Box 25.1), brachycephalic and/or obese dogs accumulate a large amount of mediastinal fat, which is responsible for widening of the mediastinum (Figure 25.1). On CT, the fat present in the cranial mediastinum provides a natural contrast with the other mediastinal structures and may help their visualization.

The mediastinum has three anatomic reflections: cranioventral, caudoventral and the plica venae cavae (Figure 25.2A). For interpretation purposes, it is classically divided into three sections: cranial, middle and caudal (Figure 25.2B and Table 25.2).

Although the mediastinum represents the midline space of the thoracic cavity, it runs obliquely craniocaudally from right to left. The ventral cranial mediastinum lies slightly to the right due to the extension of the cranial left lung lobe across the midline. Caudally, the accessory lobe extends to the left across the midline, locating the caudal mediastinum to the left.

Mediastinal shift is an important radiographic interpretative concept that can be applied to CT imaging. It refers to a displacement of the mediastinum from its original location. It is usually due to a pathologic process inducing a change in volume of one hemithorax. An increased hemithoracic volume displaces the mediastinum away from the process, while a decreased volume displaces the mediastinum towards the process. Causes of mediastinal shift are numerous (Box 25.2).

Esophagus

The esophagus is a tubular structure that connects the oropharynx to the stomach at the level of the cardia. It is composed of four soft tissue layers: fibrous, muscular, submucous and mucous, which are not distinguishable on CT. The esophagus is divided into three portions: cervical, thoracic and abdominal. In its cervical portion, it runs dorsally and to the left of the trachea to finish laterally and to its left at the level of the thoracic inlet. In its thoracic portion, the esophagus crosses dorsally over the tracheal bifurcation with the aortic arch on its left. It then lies more or less midline, to the right of the descending aorta until it reaches the esophageal hiatus of the diaphragm. The abdominal portion is very short and wedge-shaped, merging with the cardia of the stomach.

In CT, the esophagus can be followed along its entire length. It adopts a rounded to ovoid shape of soft tissue density in the neck, cranial and middle mediastinum. In the caudal mediastinum, it often adopts a more triangular shape (Figure 25.2A). Its lumen may be highlighted by a variable amount of air, particularly

Veterinary Computed Tomography, First Edition. Edited by Tobias Schwarz, Jimmy Saunders.

Table 25.1
CT imaging protocol (intravenous contrast study: standard protocol; *see* Chapter 5).

Series	Pre- and post-contrast: mediastinal window
Decubitus	Ventral or dorsal
Special positioning	Placement of orogastric tube or air insufflation of the esophagus when necessary
Scan margins	Thoracic inlet ⟷ Insertion of the diaphragm on L3
Voltage (kVp)	120
Current (mAs)	60–150
Tube rotation time (s)	1
Slice width (mm)	3–5
Kernel frequency	Medium smooth
Collimator pitch	1.75
Helical image reconstruction interval	0.5 × slice width
Motion control	Induced respiratory pause with manual hyperventilation
Window level (HU)	+40
Window width (HU)	400

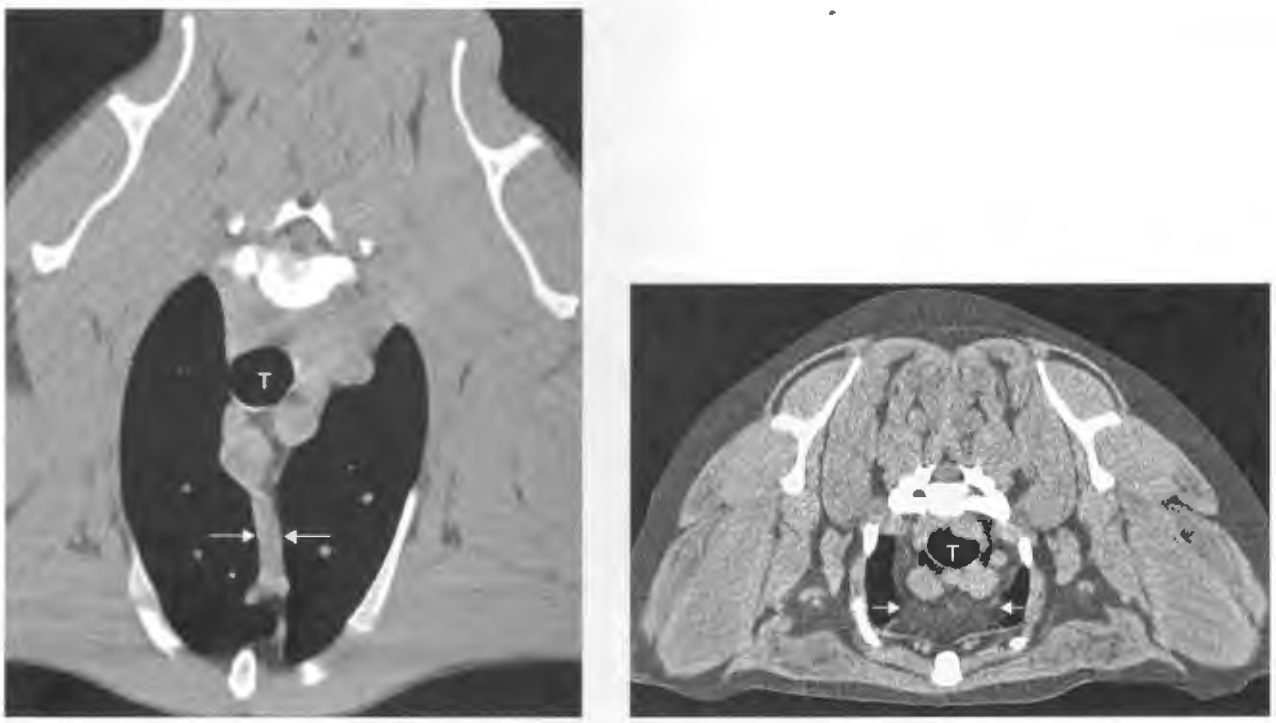

A B

Figure 25.1 Post-contrast transverse CT image of the cranial mediastinum in (A) a greyhound and (B) an English bulldog. Both images are set with the same window (level 40 HU, width 400 HU). In addition to the difference in cranial mediastinal width (between arrows), note the better contrast provided by the mediastinal fat in the bulldog. *T* = trachea.

Box 25.1 Cranial mediastinal width
Dog: should be less than twice the width of the vertebral column
Cat: should have a similar width to the vertebral column

when animals are anesthetized. Occasionally, the caudal esophagus contains some fluid due to regurgitation, and a distinct horizontal fluid line can be seen. When visualization of the esophagus is hindered by surrounding structures or lesions, an orogastric tube can be placed. If an esophageal condition is suspected,

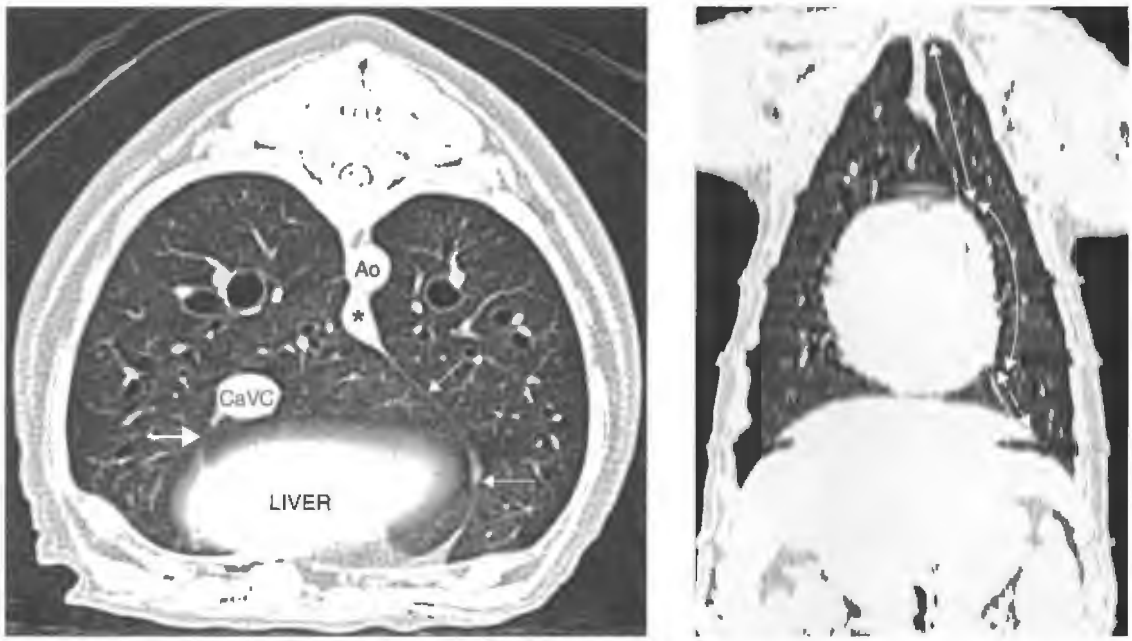

Figure 25.2 CT anatomy of the mediastinum. (A) Transverse CT image: caudoventral (small arrows) and plica venae cavae (large arrow). (B) Dorsally reconstructed CT image: cranial (continuous straight arrow), middle (curved arrow) and caudal (dashed arrow) mediastinum. Ao = aorta; CaVC = caudal vena cava; * = esophagus.

Table 25.2
The three mediastinal sections and their content.

Mediastinal area	Main structures present
Cranial	Trachea, esophagus, thymus, thoracic arteries, veins and lymphatics, brachiocephalic trunk and cranial vena cava
Middle	Heart, aortic arch, ascending aorta, esophagus, carina and bronchial lymph nodes
Caudal	Esophagus, caudal vena cava, descending aorta, azygos vein, thoracic duct and vagal nerves

Box 25.2 Common causes and direction of mediastinal shift

Away from the process
Unilateral pneumothorax
Unilateral pleural effusion
Unilateral lobar overinflation
Large pulmonary mass(es)
Unilateral diaphragmatic hernia or rupture

Towards the process
Unilateral lung collapse (Figure 25.3)
Pleural adhesions secondary to pleural disease

an additional endotracheal tube is passed into the esophagus to inflate the esophagus just prior to the scan. The distended air-filled esophagus allows better delineation of the intraluminal component of any mural mass. If the esophagus and stomach are distended with air, virtual endoscopy allows generation of images similar to a direct endoscopic examination (Figure 25.4). It is important to distend the esophagus adequately to avoid mistaking smaller nodules for esophageal folds. In cases where the mass totally occludes the esophagus precluding the passage of the endoscope, virtual endoscopy allows visualization of structures beyond the mass and/or retrograde viewing of the mass.

Lymph nodes

In the mediastinum, three groups of lymph nodes are present: the sternal, the mediastinal and the bronchial lymph nodes.

The sternal lymph nodes, also known as retrosternal or presternal, are located at the level of the second

Figure 25.3 Transverse CT image of an adult cat with complete right lung lobe collapse and a mediastinal shift (arrow) towards the lesion (completely deviated to the right). The midline double arrow line represents the normal location of the mediastinum. E = esophagus; T = trachea.

sternebra. Although they are usually paired, a large individual variation exists, the left one being more consistently present than the right. They drain the lymphatics from the thoracic wall and the abdominal cavity. Therefore, their enlargement should raise a suspicion of abdominal disease.

The mediastinal lymph nodes consist of a chain of nodes along the large vessels of the heart in the cranial mediastinum. Their number and size vary.

The bronchial lymph nodes are divided into two groups, the pulmonary and the tracheobronchial lymph nodes. The pulmonary ones are most frequently absent, but when present are distributed along the main bronchi. Three tracheobronchial lymph nodes are normally present and are located at the level of the carina. The right and left tracheobronchial lymph nodes are ovoid structures found on their respective side of the base of the main bronchi. The middle or bifurcational tracheobronchial lymph node is more V-shaped and lies caudal to the angle created by the bifurcation of the trachea. It is the largest of the three nodes.

With CT, the normal lymph nodes are barely visible but a moderate enlargement can be demonstrated. CT assessment of mediastinal lymphadenopathy repre-

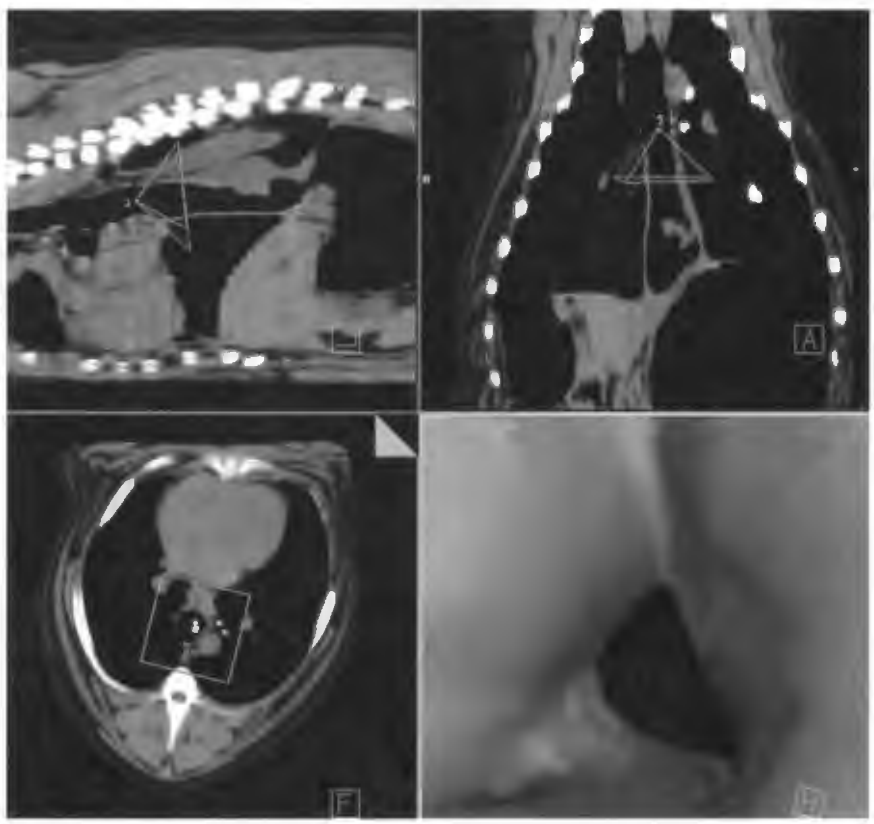

Figure 25.4 Screenshot from a virtual endoscopy of an air-insufflated esophagus generated from CT images of a dog with a caudal esophageal mass. The prism-shaped viewfinder is looking down the esophagus with the virtual endoscopic picture seen on the bottom right of the image. Small nodules can be seen on the left ventrolateral surface of the esophagus. The viewfinder can be moved backwards and forwards to give a real-time endoscopic appearance.

Table 25.3

CT features associated with mediastinal lymphadenopathy.

Group of lymph nodes	CT features associated to lymphadenopathy
Sternal	One or two soft tissue densities dorsal to second sternebra
Mediastinal	Soft tissue density associated with a widening of the cranial mediastinum, elevation of the thoracic trachea, if gross enlargement
Tracheobronchial	Soft tissue density in their respective location Right and left: caudal and ventral displacement of the ipsilateral main bronchus, associated to a variable degree of compression Middle: widening of the angle created by the mainstem bronchi, which can be slightly deviated ventrally

sents an important part of the routine oncologic staging and pre-surgical planning. Enlarged lymph nodes can be identified as rounded homogeneous soft tissue densities in their respective location. They are associated with a mass effect, which displaces or compresses the adjacent structures (Table 25.3).

Thymus

The thymus is mainly a lymphoid structure located in the cranial mediastinum, which has a role in the T-lymphocyte maturation. Its size varies with the animal's age. Already relatively large at birth, it grows until sexual maturity; thereafter it progressively involutes during the rest of the animal's life, the lymphoid tissue being replaced by fatty tissue.

Thoracic duct

The thoracic duct is formed by a single or multiple lymphatic ducts that coalesce in the cranial part of the thorax. It originates from the cisterna chyli, which is located ventrally to L4 and drains the pelvic and abdominal viscera as well as the pelvic limbs. It enters the thoracic cavity through the aortic hiatus and runs dorsally to the aorta and ventrally to the azygos vein. It crosses to the left of the aorta more or less at the level of T6. It may join any major cranial vein, including the left external jugular vein, the left subclavian vein, the left brachiocephalic vein, the azygos vein or the cranial vena cava. On a plain CT, the lymphatic ducts are usually not visible in the thorax and merge with the rest of the surrounding soft tissue structures. In the cranial abdomen the cisterna chyli can sometimes be seen as a hat-shaped structure draping dorsally over the aorta. The lymphatic visualization is not improved with intravenous contrast administration unless there is increased alternative lymphatic uptake in case of reduced renal clearance of vascular contrast medium. CT lymphangiography allows a better detection of the number and topography of the lymphatic ducts than radiography.

Nerves

In normal circumstances, the nerves crossing the mediastinum are not visible with CT.

Disease Features

Congenital

Esophageal diverticulum

Esophageal diverticulum refers to a sacculation of the esophageal wall, which can be congenital or acquired. Ingesta accumulate in the diverticulum and can cause significant esophagitis.

CT features

- Focal dilatation of the esophagus in the cranial mediastinum.
- Presence of mixed attenuating content corresponding to filling with ingesta.
- Possible signs of aspiration pneumonia.

Megaesophagus

Strictly speaking, a megaesophagus refers to the dilatation of a part of or the entire esophagus. It can be congenital or, more commonly, acquired secondary to neuromuscular or other diseases, esophageal obstruction or intoxication. General anesthesia induces in most dogs and cats a moderate esophageal distention, which is incidental.

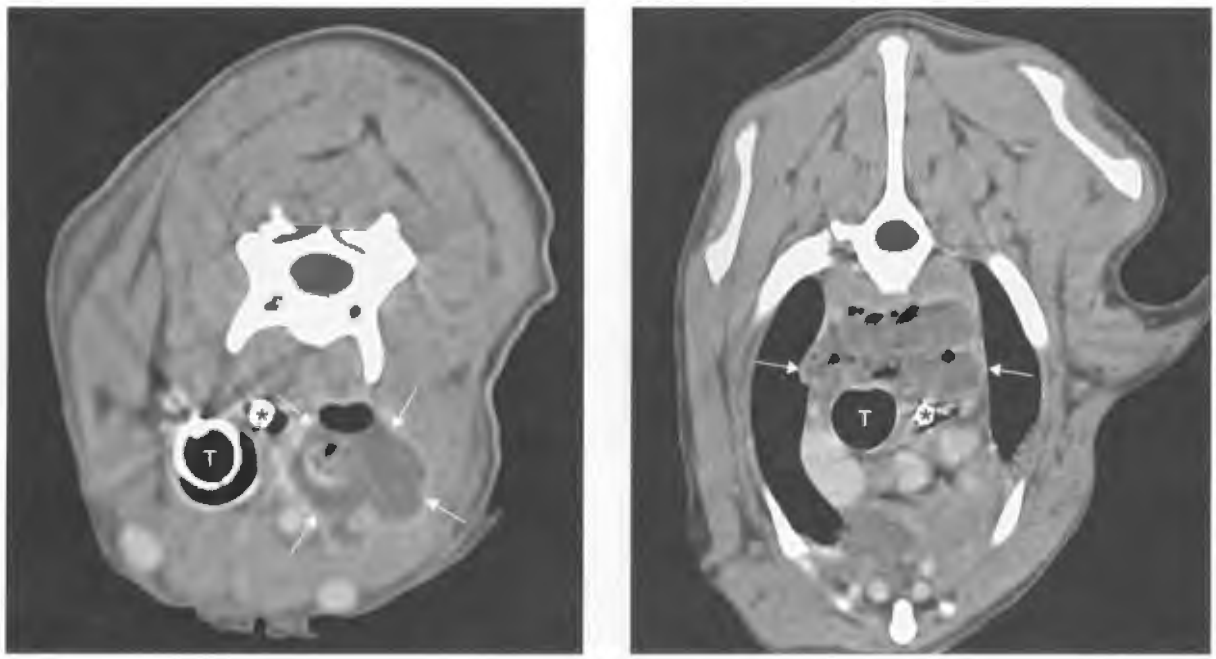

Figure 25.5 Transverse CT images of a dog with a perforating cervical esophageal foreign body leading to (A) paraesophageal abscess delineated with a contrast enhancing thin wall (arrows) and (B) moderate pneumomediastinum and mediastinitis (arrows). * = esophagus; T = trachea.

CT features

- Visualization of the esophageal walls over a variable length.
- Presence of non-attenuating gas within the esophageal lumen.
- Possible signs of aspiration pneumonia.

Trauma

Pneumomediastinum

Pneumomediastinum corresponds to the presence of free gas, usually air, in the mediastinum. It is most commonly the result of a traumatic event affecting any cervical or thoracic structure in direct contact with air (thoracic, tracheal, esophageal or cervical injury). Spontaneous pneumomediastinum can occur following severe respiratory disease. If all identifiable causes have been ruled out, idiopathic pneumomediastinum is diagnosed. Although a pneumomediastinum can lead to a pneumothorax, a pneumothorax is never the cause of pneumomediastinum. CT is particularly useful to investigate the cause of pneumomediastinum. Both the neck and the chest should be scanned, starting from the oropharynx. If esophageal or tracheal perforation is suspected, 5–10 ml of non-ionic water-soluble iodinated contrast medium can be administered into the organ of concern. The CT scan should be repeated after enough time to allow contrast extravasation (5–10 min).

CT features (Figure 25.5)

- Presence of non-attenuating gas tracking along the mediastinal structures, resulting in enhancement of their visualization.
- The full thickness of the trachea and esophagus are visible.
- Visualization of individual vessels is enhanced.
- Non-attenuating gas is often simultaneously found along the fascial planes of the neck, subcutaneously and in the retroperitoneum.
- If a perforating foreign body is present, a focal area of hypo- or hyperattenuation, depending on the attenuation properties of the foreign body, may be seen in the periphery of the perforated organ.
- Extravasation of contrast medium may be seen in the fascial planes surrounding the perforation site.

Esophageal stricture

Esophageal stricture usually develops as a consequence of a traumatic or inflammatory lesion of the esophageal mucosa. The clinical signs vary greatly with the degree of stenosis.

CT features

- Under normal circumstances, the stricture is not visible.
- Moderate esophageal gas distention proximal to the stenotic portion.
- Insufflation of gas in the esophagus may enhance visualization of the stricture.

Esophageal foreign body

Retained esophageal foreign bodies are common in dogs. They are most frequently found at the thoracic inlet, the heart base or the esophageal hiatus. Occasionally, perforation can occur and cause mediastinitis.

CT features

- Direct visualization of the foreign body depends on its density.
- Moderate esophageal gas distention proximal to the foreign body.
- Enhanced visualization achieved with gas insufflation in the esophagus.

Infection/Inflammation

Esophagitis

Inflammation or ulceration of the mucosal surface of the esophagus is usually secondary to gastroesophageal reflux, chronic vomiting or direct trauma to the mucosa. In extreme cases, perforation can cause mediastinitis.

CT features (Figure 25.6)

- No abnormalities are usually detected with CT.
- Occasionally, moderate focal esophageal dilatation ± presence of fluid/ingesta.

Mediastinitis

Mediastinitis is an inflammatory or infectious process affecting the mediastinum. A large number of etiologies may be responsible for mediastinitis (Box 25.3). Mediastinitis can be generalized or focal, depending on the cause.

CT features (Figure 25.5)

- Moderate widening of the affected part of the mediastinum, due to thickening of the mediastinal pleura and variable amount of effusion.
- Irregular outline of the mediastinum.

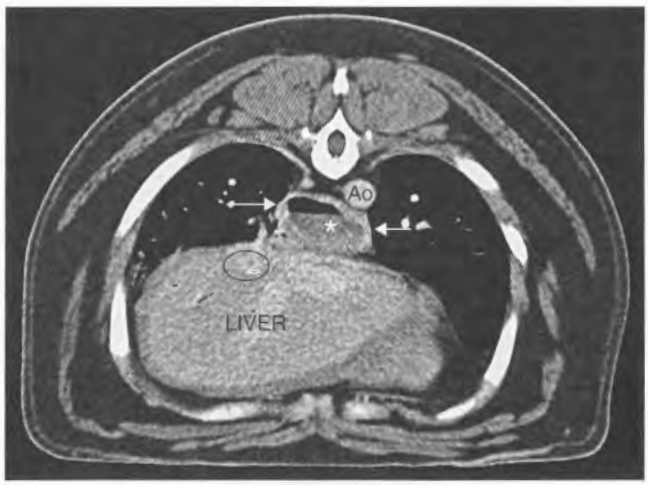

Figure 25.6 Post-contrast transverse CT image of an English bulldog with chronic vomiting and esophagitis. The thoracic esophagus (arrows) is moderately distended and partially fluid-filled (asterisk) due to esophageal reflux. Ao = aorta; black oval = caudal vena cava.

Box 25.3 Causes of mediastinitis

Primary
Fungal: *Histoplasma, Cryptococcus*
Bacterial: *Actinomyces, Nocardia*
Parasitic: *Spirocerca lupi*
Cats: mediastinal Feline Infectious Peritonitis

Secondary
Esophageal perforation
Tracheal perforation
Extension from pleural, pulmonary, pericardial or cervical disease

- Increased attenuation of the mediastinal content due to accumulation of exudate, chyle.
- Mediastinal lymph node enlargement may be present depending on the cause.
- In case of mediastinits secondary to tracheal or esophageal perforation, mediastinal air (pneumomediastinum) may be present.
- Mild contrast uptake may be seen in areas of active inflammation and in the thickened mediastinal pleura.

Spirocercosis

Spirocerca lupi is a nematode that is a common cause of mediastinal pathology in endemic areas. Following penetration of the gastric wall, the larvae migrate to

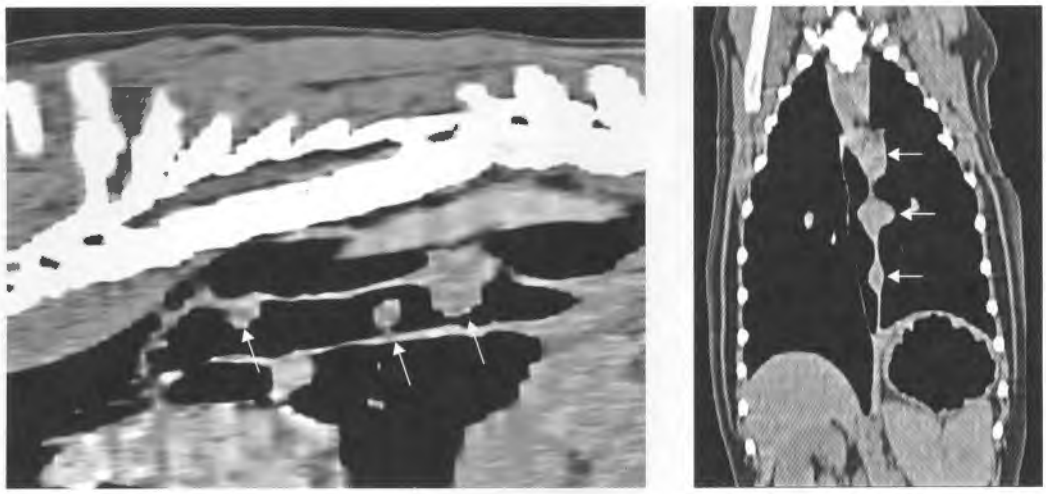

A B

Figure 25.7 (A) Sagittally and (B) dorsally reconstructed CT images of a dog with three spirocercosis nodules (arrows) in an air-insufflated esophagus, two cranial luminal and a caudal mural nodule.

the aorta through the arteries, then to the esophageal wall. There, they transform into their adult form. The typical imaging appearance is that of a caudodorsal mediastinal mass as a result of a terminal esophageal mural nodule or nodules, which bulge into the esophageal lumen (Figure 25.7). Depending on the mass size, it may be readily seen on routine thoracic radiographs, particularly dorsoventral/ventrodorsal (DV/VD) projections. Nodules may also occur in the hilar region, where they are more difficult to detect radiographically. CT is the modality of choice to evaluate masses that are located on the esophageal serosal surface which cannot be fully evaluated endoscopically or when pleural or mediastinal fluid effaces structures on the radiograph. With time, the nodules may undergo neoplastic transformation or may lead to other complications. The latter and possible pathology from the primary migration route or aberrant migration are given in Table 25.4. CT is used for surgical planning and prognostication in spirocercosis patients. In endemic areas, all the potential pathological processes must be assessed on a thoracic CT, even if the dog has been presented for a different problem, because of the sensitivity of CT in detecting even small, clinically insignificant masses. An additional endotracheal tube is passed into the esophagus to inflate the esophagus just prior to the scan. The routine scan is usually followed by a CT angiogram to assess mass perfusion and to detect aortic aneurysms and thrombi (Figure 25.8). Images are viewed in mediastinal, bone and lung windows, allowing evaluation of different aspects of the disease.

CT features

Benign masses often have a more hypodense central region indicative of a fluid or necrotic component with a soft tissue density periphery that will enhance with the CT angiogram. Benign nodules that have undergone neoplastic transformation to osteosarcoma or fibrosarcoma have a more homogeneous soft tissue density with patchy enhancement after CT angiography.

Neoplasia

Mediastinal neoplasia can have numerous origins, but all result in the presence of a mediastinal mass. The location of the mass is the key point in the differential diagnosis and for interpretation purposes. The mediastinum can be divided into five areas: cranioventral, craniodorsal, perihilar, caudoventral and caudodorsal. Also, mediastinal masses can have a non-neoplastic etiology. Table 25.5 summarizes the differential diagnosis of mediastinal masses according to their location and the CT features potentially associated with the mass effect.

The internal CT features of mediastinal neoplasia largely depend on the origin of the tumor. Most commonly, the tumor has a homogeneous soft tissue density with a variable contrast enhancement according to its degree of perfusion. Hypoattenuating areas may be present in the core of the lesion corresponding to a necrotizing center.

Table 25.4
Pathology that may be seen on a thoracic CT examination in cases with spirocercosis. Pathology is given in order of most to least likely.

Possible forms and complications associated with spirocercosis	
Primary pathology	Caudal esophageal mass or masses (Figure 25.7) Large masses compress main stem bronchi and trachea depending on location Neoplastic masses tend to be large, occur in older dogs (6.4 ± 1.91 vs 4.93 ± 2.87 years in benign cases) and may show pulmonary metastasis or mass mineralization Hilar esophageal mass or masses Gastric mass in cardia region
Pathology secondary to normal or aberrant migration	Spondylitis (Figure 25.9) Aortic dystrophic mineralization (Figure 25.10) Aortic aneurysm Abnormally located mass Aortic rupture with periaortic streak-like hemorrhage or marked hemorrhage resulting in hemomediastinum or more commonly acute death due to hemothorax Focal thoracic hematoma, often associated with a blood vessel Thoracolumbar extradural cord compression Thoracolumbar intramedullary spinal cord swelling Aortic thrombus formation (Figure 25.8)
Complications	Hypertrophic osteopathy, primarily in malignant cases Esophageal perforation with mediastinitis and/or pyothorax Pleuritis Pneumomediastinum Aspiration pneumonia Pneumothorax Gastro-esophageal intussusception

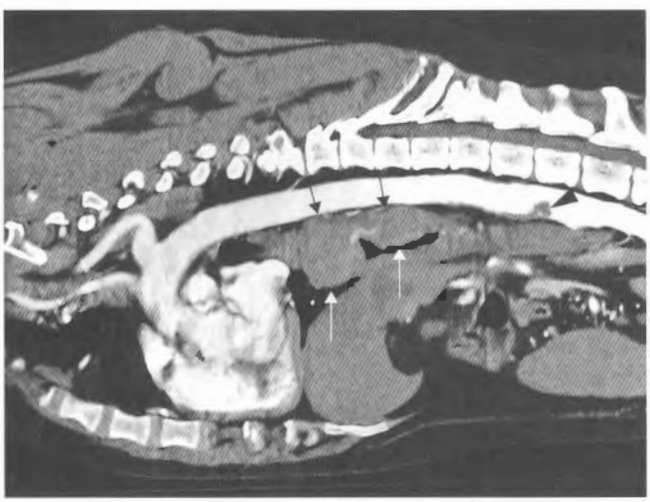

Figure 25.8 Sagittally reconstructed CT-angiogram of a dog with spirocercosis. There is a multilobulated irregular caudal esophageal mass (arrows) with mild aneurysmal dilatation of the aorta at the origin of a ventrally located aortic thrombus (arrowhead). The dog presented with iliac thromboembolism.

Figure 25.9 Transverse CT image in a dog with spondylitis secondary to aberrant *S. lupi* larval migration. Small nodules are visible in the ventral esophagus (arrows). Ao = aorta.

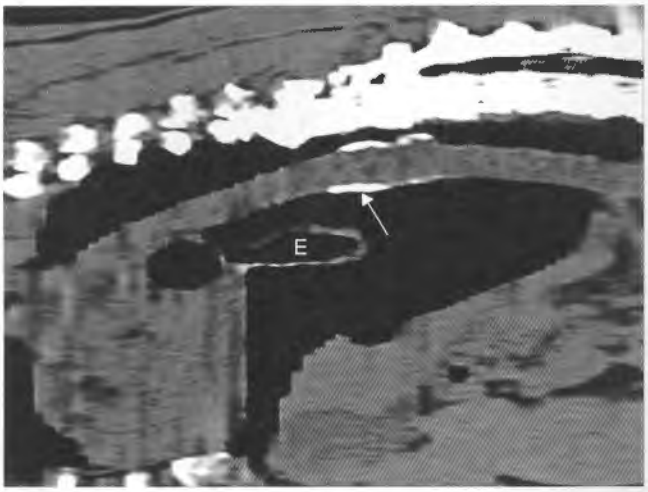

Figure 25.10 Sagittally reconstructed CT image of a dog with spirocercosis. There is dystrophic aortic calcification of the dorsal and ventral intima (arrow). E = air-filled esophagus.

Other masses

Cysts

Mediastinal cysts are usually benign, incidental findings that occur in both dogs and cats. They can go unnoticed until their size leads to compressive effects. Occasionally they rupture and can cause mediastinitis. They can have a pleural, branchial, thymic, lymphatic, bronchogenic or neoplastic origin. They are most commonly found in the cranioventral mediastinum, but can occasionally be located in the caudal mediastinum.

CT features (Figure 25.13)

Rounded mass lesion with variable mass effect on surrounding structures (cf. Table 25.5).

- Thin wall of soft tissue density.
- Fluid density filling the lesion.
- Mild contrast enhancement of the wall.

Granuloma/Abscess

An abscess or a granuloma can develop in the mediastinum secondary to an infectious or a traumatic process.

CT features (Figure 25.11)

- Rounded mass lesion with variable mass effect on surrounding structures (cf. Table 25.5).
- Thick, irregular wall of soft tissue density.
- Mixed soft tissue/fluid/gas density filling the lesion.
- Mild contrast enhancement of the wall.

Further Reading

Ballegeer EA, Adams WM, Dubielzig RR, Paoloni MC, Klauer JM and Keuler NS (2010) Computed tomography characteristics of canine tracheobronchial lymph node metastasis. *Vet Radiol Ultrasound* **51**: 397–403.

Dvir E, Kirberger RM and Malleczek D (2001) Radiographic and computed tomographic changes and clinical presentation of spirocercosis in the dog. *Vet Radiol Ultrasound* **42**: 119–29.

Esterline ML, Radlinsky MAG, Biller DS, Mason DE, Roush JK and Cash WC (2005) Comparison of radiographic and computed tomography lymphangiography for identification of the canine thoracic duct. *Vet Radiol Ultrasound* **46**: 391–5.

Paoloni MC, Adams WM, Dubielzig RR, Kurzman I, Vail DM and Hardie RJ (2006) Comparison of results of computed tomography and radiography with histopathologic findings in tracheobronchial lymph nodes in dogs with primary lung tumors: 14 cases (1999–2002). *J Am Vet Med Assoc* **228**: 1718–22.

Van der Merwe LL, Kirberger RM, Clift S, Williams M, Keller N and Naidoo V (2008) *Spirocerca lupi* infection in the dog: a review. *Vet J* **176**: 294–309.

Yoon J, Feeney DA, Cronk DE, Anderson KL and Ziegler LE (2004) Computed tomographic evaluation of the canine and feline mediastinal masses in 14 patients. *Vet Radiol Ultrasound* **45**: 542–6.

Table 25.5
Differential diagnosis of mediastinal masses according to their location and associated CT features.

Mediastinal area	Differential diagnosis	CT features
Cranioventral (Figure 25.11)	Lymphoma Thymic diseases (thymoma, lymphosarcoma, cysts, hematoma, hyperplasia, amyloidosis)	• Soft tissue/mixed density mass • Widening of the cranioventral mediastinum • Elevation ± compression of the trachea • Caudal displacement of the heart and carina • Caudal displacement of the cranial lung lobes ± pulmonary atelectasis • Pooling of contrast in the veins of the neck and thoracic limbs
Craniodorsal (Figure 25.12)	Esophageal diseases Neural or neuroendocrine tumors Vertebral or paravertebral tumors (Aortic aneurysm, chemodectoma or thymoma reported)	• Soft tissue/mixed density mass, dorsal to the thoracic trachea • Ventral depression ± compression of the trachea • Ventral or lateral displacement of the esophagus if extra- or intra-mural esophageal mass • Variable amount of esophageal dilatation proximal to the lesion
Perihilar	Perihilar lymphadenopathy Heart-based tumors Esophageal diseases Bronchogenic cyst Vascular or cardiac enlargement	• Soft tissue/mixed density mass • Displacement ± compression/obstruction of the corresponding mainstem bronchus • If mass is caudal to the carina, widening of the angle created by the tracheal bifurcation ± possible compression of the carina
Caudoventral	Diaphragmatic lesions Peritoneo-pericardial hernia	• Soft tissue/mixed density mass • Widening of the caudoventral mediastinum or plica venae cavae • Displacement of the caudal vena cava • Displacement ± atelectasis of the accessory lung lobe
Caudodorsal (Figure 25.13)	Esophageal diseases Neural tumors Hiatal hernia Diaphragmatic mass	• Soft tissue/mixed density mass • Widening of the caudodorsal mediastinum • Ventral or lateral displacement of the esophagus if extra- or intra-mural esophageal mass • Variable amount of esophageal dilation proximal to the lesion
Any location	Primary mediastinal tumors (hemangiosarcoma, lipoma/sarcoma, histiocytic sarcoma) Abscess/granuloma Hematoma	• According to the location (cf. above)

Chapter 4

Malignancy and metastasis

Dvir E, **Kirberger RM**, Mukorera V, van der Merwe LL, Clift SJ. Clinical differentiation between dogs with benign and malignant spirocercosis. *Veterinary Parasitology* 2008;155:80-88.

Lindsay NL, **Kirberger RM,** Williams M. Spirocercosis associated spinal cord chondrosarcoma. *Veterinary Radiology & Ultrasound* 2010;51:614-616.

Pazzi P, Thompkins S, **Kirberger RM.** Canine spirocercosis-associated extraskeletal osteosarcoma with central nervous system metastasis. *Journal of the South African Veterinary Association* 2013. 84:Art. #71, 4 pages. http.//dx.doi.org/10.4102/jsava.v84i1.71.

The malignant transformation of spirocercosis-associated oesophageal lesions has been recognised since 1955 and is well described.[1,2] Malignant transformation of the spirocercosis associate oesophageal nodule has grave implications for the patient, usually resulting in expensive surgery and possible chemo- or radiation therapy, or alternatively, euthanasia. In the first article by Dvir, Kirberger and others we looked at clinical parameters, including diagnostic imaging findings, which could help in distinguishing benign from malignant cases. This study is ongoing in our Department with publications involving clinical pathological and histological parameters already published[3-5] and others, including looking at perfusion parameters of the oesophageal pathology on computed tomography, are in progress.

Metastasis of the spirocercosis-induced oesophageal sarcoma, usually osteosarcoma or fibrosarcoma, is well recognised. Metastatic sites reported include the lungs, tracheobronchial lymph nodes, liver, heart, pleura and kidney most commonly[2] with less frequent spread to the omentum, peritoneum, pancreas, diaphragm, spleen, mediastinum and subcutis.[6] We describe two new metastatic locations. In the publication by Lindsay, Kirberger and Williams the first case of *S. lupi*-associated oesophageal chondrosarcoma and its spread to the spinal cord is recorded and in the paper by Pazzi, Thompkins and Kirberger metastatic spread of a spirocercosis associated oesophageal osteosarcoma to the brain as well as the spinal cord is described.

References

1 Seibold HR, Bailey WS, Hoerlein BF, Jordan EM, Schwabe CW. Observations on the possible relation of malignant esophageal tumours and *Spirocerca lupi* lesions in the dog. Am J Vet Res 1955;16:5-14.

2 Bailey WS. Parasites and cancer: sarcoma associated with *Spirocerca lupi*. Ann NY Acad Sci 1963;108:890-923.

3 Dvir E, Clift SJ. Evaluation of selected growth factor expression in canine spirocercosis *(Spirocerca lupi)*-associated non-neoplastic nodules and sarcomas Vet Parasitol 2010; 174:257–266.

4 Mukorera V, Dvir E, van der Merwe LL, Goddard, A. Serum c-reactive protein concentration in benign and malignant canine spirocercosis. J Vet Int Med 2011;25:963-966.

5 Mukorera V, van der Merwe LL, Lavy E, Aroch I, Dvir E. Serum alkaline phosphatase activity is not a marker for neoplastic transformatiom of esophageal nodules in canine spirocercosis. Vet Clin Path 2011;40:389-392.

6 Bailey WS. 1972. *Spirocerca lupi:* A continuing enquiry. Vet Parasitol 1972;58:3-22.

Available online at www.sciencedirect.com
ScienceDirect
Veterinary Parasitology 155 (2008) 80–88
veterinary parasitology
www.elsevier.com/locate/vetpar

Clinical differentiation between dogs with benign and malignant spirocercosis

Eran Dvir [a,*], Robert M. Kirberger [a], Varaidzo Mukorera [a], Liesel L. van der Merwe [a], Sarah J. Clift [b]

[a] *Department of Companion Animal Clinical Studies, Faculty of Veterinary Science, University of Pretoria, Private Bag X04, Onderstepoort 0110, South Africa*
[b] *Department of Paraclinical Sciences, Faculty of Veterinary Science, University of Pretoria, Private Bag X04, Onderstepoort 0110, South Africa*

Received 17 February 2008; accepted 10 April 2008

Abstract

Spirocerca lupi is a nematode infesting the canine oesophagus, where it induces the formation of a nodule that may transform into a malignant sarcoma. The current, retrospective study compared the clinical presentation, haematology, serum albumin and globulin and radiology of benign cases ($n = 31$) and malignant cases ($n = 31$) of spirocercosis.

Dogs with spirocercosis-induced sarcoma were significantly older (6.4 ± 1.91 years) than benign cases (4.93 ± 2.87). In the malignant cases there were significantly ($p = 0.03$) more sterilized females (10/31) and fewer intact males (4/31) compared to 2/31 and 13/31, respectively, in the benign cases. Hypertrophic osteopathy was observed in 38.7% of malignant cases and in none of the benign cases ($p = 0.0002$). Common clinical signs included weight loss, regurgitation, anorexia, pyrexia ($T \geq 39.5^{\circ}$), respiratory complications and salivation but did not differ in prevalence between groups. On haematology, the malignant group had significantly ($p < 0.05$) lower haematocrit (0.34 ± 0.08 vs. 0.41 ± 0.07) and higher white cell count (31.6 ± 27.83 vs. $17.71 \pm 13.18 \times 10^3\ \mu l^{-1}$), mature neutrophil count (26.06 ± 26.08 vs. $12.23 \pm 9.96 \times 10^3\ \mu l^{-1}$) and thrombocyte count (493.15 ± 151.61 vs. $313.27 \pm 128.54 \times 10^9\ \mu l^{-1}$). There were no differences in the mean corpuscular volume and immature neutrophil count. On radiology, the mass length was not significantly different, but the height and the width of the malignant masses were significantly larger (62.59 ± 15.15 mm and 73.93 ± 20.94 mm) compared to the benign group (46.43 ± 23.62 and 49.29 ± 25.56, respectively). Spondylitis was more prevalent in the malignant group (67.86% vs. 38.46%, $p = 0.03$). Examining secondary pulmonary changes revealed significantly higher prevalence of bronchial displacement in the malignant group (52% vs. 17%, $p = 0.008$).

Hypertrophic osteopathy appeared to be a very specific but relatively rare (poor sensitivity) marker of malignancy. Female gender, anaemia, leukocytosis, thrombocytosis, spondylitis and bronchial displacement are significantly more common in malignant cases, but appear in benign cases as well. However, if found together in a specific case, they should increase the index of suspicion for malignancy in a diagnosed spirocercosis case.

Keywords: Spirocercosis; Dog; Sarcoma; Oesophageal nodule; Hypertrophic osteopathy

* Corresponding author. Tel.: +27 12 529 8366; fax: +27 12 529 8308.
E-mail addresses: eran.dvir@up.ac.za, edvir2000@yahoo.com (E. Dvir).

0304-4017/$ – see front matter © 2008 Elsevier B.V. All rights reserved.
doi:10.1016/j.vetpar.2008.04.006

1. Introduction

Spirocerca lupi (*S. lupi*) is a nematode of worldwide distribution, but it is most commonly found in tropical and subtropical areas (Bailey, 1972). Dogs are the definitive hosts and become infested by ingesting the coprophagous beetle intermediate hosts (Bailey, 1972). After ingestion the larvae are liberated in the gastric lumen, and migrate via the gastric mucosa, gastric arteries, aorta and eventually through the thoracic aortic wall to the caudal oesophagus. Typically, the worms settle within the oesophageal wall, mature to adults and promote formation of a nodule (Bailey, 1963, 1972; van der Merwe et al., 2008). The nodules are often referred to as granulomatous (Bailey, 1963, 1972), but histologically this is inappropriate as the mature nodule is composed mostly of actively dividing immature fibroblasts with relatively pronounced vascularisation (van der Merwe et al., 2008). The host inflammatory reaction is commonly mild to moderate and is not characterized by a predominance of macrophages, as would be expected in granulomatous inflammation (Bailey, 1963; van der Merwe et al., 2008). Spirocercosis induces a few pathognomonic lesions including: aortic scarring with aneurysm formation, thoracic vertebral spondylitis and caudal oesophageal nodule formation. The typical clinical signs associated with spirocercosis are related to the presence of oesophageal nodules and include regurgitation, vomiting, dysphagia and weight loss, together with non-specific signs like pyrexia (Dvir et al., 2001; Mazaki-Tovi et al., 2002). The clinical diagnosis of spirocercosis is largely dependant upon thoracic radiography, which demonstrates the caudal oesophageal soft tissue masses, caudal thoracic vertebral spondylitis and aortic undulation due to aneurysm formation. Faecal flotation tests are also used to detect the typical embryonated eggs. Oesophagoscopy typically demonstrates one or more nodules with a nipple-like protuberance.

The oesophageal nodule may undergo malignant neoplastic transformation (Bailey, 1963; Seibold et al., 1955). The association between *S. lupi* infection with oesophageal sarcoma was first described in 1955 (Seibold et al., 1955). This association was based on the finding of *S. lupi* worms and related oesophageal nodules close to the malignant neoplasm or the pathognomonic findings of spondylitis or aortic aneurysm in conjunction with the malignant neoplasm. Macroscopically, an increased size, and progression to cauliflower-like shape and area of necrosis in the malignant nodule compared to the smooth appearance of the benign nodule may be indicative of neoplastic transformation (Ranen et al., 2004). Histologically the malignant neoplasms are classified as fibrosarcoma, osteosarcoma or anaplastic sarcoma (Ranen et al., 2004, 2007). The histopathological characteristics of the *S. lupi*-induced fibrosarcoma include interwoven bundles of tapered to plump spindle shaped cells, variable amounts of intercellular collagenous matrix and a high mitotic index (Bailey et al., 1963). Histological characteristics of the *S. lupi*-induced osteosarcoma include foci of polygonal osteoblasts, and variable numbers of osteoclasts and/or interwoven bundles of spindle cells, variable amount of osteoid matrix with or without foci of chondroid differentiation. Sometimes obvious spicules or trabeculae of bone are identified amidst solid foci of neoplastic spindle or polygonal cells (Bailey, 1963). In areas where spirocercosis does not exist, malignant neoplasms of the oesophagus are extremely rare (Ridgway and Suter, 1979), making spirocercosis the major cause of malignant oesophageal neoplasms in the dog. Spirocercosis-induced sarcoma metastasizes commonly to the lung but also to a variety of abdominal organs (Bailey, 1963; Dvir et al., 2001).

Benign spirocercosis is treated successfully with avermectins {doramectin (Dectomax, Pfizer, France) 400 μg/kg SC at 2-week intervals} (Lavy et al., 2002). However, malignant neoplasms can only be treated by surgical excision with or without chemotherapy and the success rate is lower (Ranen et al., 2004). This difference in prognosis emphasizes the need to improve diagnostic and prognostic markers for the ante-mortem diagnosis of the oesophageal nodule and the need for a better understanding of the malignant transformation that may improve treatment for the malignant cases.

While spirocercosis has a few pathognomonic lesions, the ante-mortem differentiation of malignant neoplasm-bearing cases and benign cases has not been studied. The objectives of the present study were to identify clinical ante-mortem differences between malignant and benign spirocercosis cases to assist in diagnosis, treatment and prognostication.

2. Material and methods

Medical records of 297 dogs diagnosed with spirocercosis at the Onderstepoort Veterinary Academic Hospital, University of Pretoria, South Africa, during 1995–2006, were retrospectively reviewed. From these records two groups of cases were selected: confirmed benign cases and confirmed malignant oesophageal nodule cases.

The inclusion criteria for the benign group were: An endoscopic diagnosis of spirocercosis with an obvious

response to treatment within at least 6 weeks or a histological diagnosis of a benign nodule after surgical resection of the whole nodule or diagnosis of benign spirocercosis at necropsy, including histological appraisal of the entire nodule. A diagnosis of benign nodule based only on endoscopic guided biopsy was judged to be unsatisfactory as it has been shown to be highly insensitive in a few studies (Dvir et al., 2001; Mazaki-Tovi et al., 2002; Ranen et al., 2004). The inclusion criteria for the malignant group were: histological diagnosis of malignancy of an oesophageal nodule obtained either by endoscopic-guided biopsy, surgical resection or necropsy. Cases with radiographic diagnosis of caudal oesophageal nodules, spondylitis and thoracic metastases, with no other obvious primary neoplasm elsewhere in the body and without histological analysis of the oesophageal nodule or the metastasis were also included in the malignant group.

The following clinical parameters were compared: age, breed, gender, body weight, duration of illness and the prevalence of weight loss, vomiting regurgitation, anorexia, pyrexia ($\geq$39.5 °C), lameness, hypertrophic osteopathy (HO), respiratory signs and salivary gland enlargement. The clinicopathological parameters that were compared included: haematocrit (Ht), mean corpuscular volume (MCV), white blood cell count (WBC), mature and immature neutrophil, monocyte and eosinophil counts and serum albumin and globulin concentrations.

Thoracic radiographic evaluation and measurements were done by one board-certified radiologist (RK) on cases having at least dorsoventral and right lateral thoracic films. The following radiological parameters were compared: mass location (relative to thoracic vertebrae) and mass size (length, width, height). The presence of the following radiological findings were recorded and their prevalence was compared between the two groups: mass mineralization, oesophageal gravel sign (ingested mineralized debris) and air (indicating partial obstruction), spondylitis, pulmonary parenchymal changes, fissure lines/pleural effusion, thoracic lymph node visualization, tracheal displacement, bronchial displacement/compression and aortic changes.

Differences in the above stated categorical parameters (age, breed, gender and prevalence of clinical signs and clinicopathological and radiological abnormalities) were then compared between the two groups using the chi-square (χ^2) test. Continuous parameters (body weight, duration of illness, clinicopathological values and radiological measurements) are presented as mean $\pm$ standard deviation and were compared between the two groups using the *t*-test. The level of significance for both tests was determined as $p < 0.05$.

3. Results

Sixty-two dogs had adequate data to fulfil the inclusion criteria. Thirty-one were included in the benign group; 19 were based on endoscopic diagnosis and response to treatment, 12 were based on histology of the entire oesophageal nodule, 10 of which were necropsy cases, and two were surgical resection cases. Thirty-one dogs were included in the malignant group; 27 were diagnosed histologically and four cases were selected according to the combination of a caudal oesophageal mass, spondylitis and thoracic metastasis.

3.1. Signalment

There was a significant difference in the gender distribution between the groups ($p = 0.03$) with more females, especially sterilised ones, in the malignant group and more males, especially intact ones, in the benign group (Table 1). The age of the dogs differed significantly between the two groups ($p = 0.02$) being 4.93 ± 2.87 years in the benign group and 6.40 ± 1.91 years in the malignant group. There were no significant differences between the average body weight of the two groups (23.61 ± 9.90 kg vs. 26.27 ± 11.10 kg in the benign and malignant group, respectively).

3.2. Clinical presentation

HO was the only clinical sign with a significantly different prevalence between the two groups (Fig. 1), as it presented only in the malignant group (38.7% prevalence $p = 0.0001$). The prevalence of the remaining clinical signs: weight loss, vomiting/ regurgitation, anorexia, pyrexia, lameness, respiratory signs and salivary gland enlargement, did not differ significantly between groups (Table 2). There were also no significant group differences on average body temperature (39.13 ± 0.73 °C vs. 39.19 ± 0.69 °C) and average

Table 1
Gender differences between benign and malignant groups ($p = 0.03$, χ^2-test)

Gender	Benign group, $n = 31$ (%)	Malignant group, $n = 31$ (%)
Intact female	38.7	41.9
Sterilized female	9.7	32.3
Intact male	41.9	12.9
Sterilized male	9.7	12.9

duration of illness (7.89 ± 7.92 weeks vs. 8.83 ± 20.58 weeks) between the benign and malignant groups, respectively.

3.3. Haematology

Complete blood counts were available for 27 dogs in each group (Table 3). Although the haematocrit was significantly lower in the malignant group ($p = 0.002$), there was a substantial overlap in the range of both groups. Anaemia, defined as a haematocrit <37%, was diagnosed with significantly higher prevalence in the malignant group ($p = 0.003$) and was normocytic in most cases (50% vs. 64.71% in the benign and malignant groups, respectively). The prevalence of leukocytosis was significantly higher in the malignant group ($p = 0.03$), but there was a substantial overlap in the range of the counts. The increase in cells consisted of mature neutrophils and monocytes. Eosinophil counts were significantly higher in the benign group ($p = 0.04$), however, the overlap in the range between the two groups was marked. The thrombocyte count and prevalence of thrombocytosis was significantly higher in the malignant group ($p < 0.001$ and $p = 0.002$, respectively).

3.4. Serum proteins

Serum protein concentrations were available for 19 cases in each group. Serum albumin was higher in the benign group compared to the malignant group (2.87 ± 0.77 mg/dl vs. 2.5 ± 0.53 mg/dl, normal range 2.7–3.5 mg/dl), but there was a marked overlap in the range and the difference between the groups was not significant ($p = 0.09$). Serum globulin was significantly higher in the benign group (5.09 ± 1.60 mg/dl vs. 4.11 ± 0.91 mg/dl in the benign and malignant group, respectively, $p = 0.03$, normal range 2–3.7 mg/dl) but again, the overlap was substantial.

3.5. Radiology

Thoracic radiographs were available for 25 dogs from the benign group and for 28 dogs in the malignant group (Table 4).

In the benign group, 24 dogs had a confirmed oesophageal mass diagnosed on endoscopy or necropsy, but the mass was only radiologically visible in 21 dogs. In the malignant group 27/28 masses were visible radiologically (Fig. 2). In both groups the masses were located between T5 and T12. Comparing the length, height and width of the oesophageal masses between the groups revealed significant differences in the height and width only (higher values In the malignant group, $p = 0.006$ and 0.0006, respectively) with substantial overlap. Mass mineralization was a relatively rare sign, more likely to be seen with malignant transformation. Bronchial displacement was significantly more common in the malignant group ($p = 0.008$), as was spondylitis ($p = 0.03$).

4. Discussion

Previous studies that discussed spirocercosis-associated malignancy hypothesized that genetic and environmental factors may play a role in carcinogenesis (Bailey, 1972). In the current study, the number of sterilised females with malignant transformation was significantly higher compared to those with benign disease. Intact males were more prevalent in the benign group. This higher prevalence of malignant transformation in sterilised females has also been described in a previous study evaluating only malignant *S. lupi* cases (Ranen et al., 2004, 2007). This might indicate a predisposition of sterilised female dogs with spirocercosis to undergo malignant transformation of the oesophageal nodule and a possible resistance in intact males. This may indicate protective effect of sex steroids, especially androgens.

Table 2
Prevalence differences of clinical signs between the benign and malignant groups

Sign	Prevalence (%)	
	Benign group, $n = 31$ (%)	Malignant group, $n = 31$ (%)
Weight loss	58.06	77.42
Vomiting/regurgitation	67.74	67.74
Anorexia	45.16	48.39
Pyrexia	32.26	41.94
Lameness	12.9	19.35
Respiratory signs	33.26	35.48
Hypertrophic osteopathy*	0	38.71
Salivary glands enlargement	22.58	25.81

* $p = 0.0001$ (χ^2-test).

The mean age of the group with malignant transformation is similar to the mean age previously described in *S. lupi*-induced sarcoma cases (Ranen et al., 2004). The difference in age between the two groups, observed in the current study, may be partially explained by the time taken for the malignant neoplasm to develop and be diagnosed, but may also indicate an increased predisposition to malignant transformation with advanced age.

A comparison of the clinical presentation of the two groups revealed only one clinical sign which appeared to be highly specific for malignant cases, namely HO. HO is often reported in conjunction with *S. lupi*-induced sarcomas (Bailey, 1963; Brodey et al., 1977). It is characterised by irregular thickening of the parosteal tissue and exostotic proliferation of bone and cartilage in the distal limbs (phalanges, metatarsal and metacarpal) and vascularisation (Brodey, 1979; Seibold et al., 1955). Radiologically, HO is described as periosteal new bone formation (Brodey, 1971). HO has been linked to intrathoracic, especially pulmonary, masses (Brodey, 1971). Pulmonary neoplasia is the most common cause of HO. However, before 1944 the most common aetiology was tuberculosis, indicating that inflammatory-induced masses can also cause HO (Brodey, 1971). It is not clear from the literature if only spirocercosis-induced malignant neoplasms can induce HO or if benign nodules can also induce it (Brodey, 1971). In the current study, with its limited case numbers, only malignant spirocercosis-induced nodules were associated with HO. We therefore, encourage clinicians to look for signs of HO on those parts of the thoracic limb seen on thoracic radiographs as a possible clue for malignancy and to perform distal limb radiographs in any suspected swollen limbs.

Four theories have been proposed for the pathogenesis of HO: vagal nerve stimulation, pulmonary arteriovenous shunting, the production of a humeral substance by neoplastic cells and factors secreted by megakaryocytes or platelet clumps lodged in blood vessels of distal limbs (Dunn et al., 2007). Vagotomy caused dramatic reversal of HO (Brodey, 1979). This finding formed the basis of the theory that vagal stimulation is responsible for the development of HO. Bailey observed involvement of the vagus nerve within some of the malignant *S. lupi*-induced neoplasms (Bailey, 1963), and mass infiltration within the oesophageal vagus has

Fig. 1. Mediolateral view of the tibia of a 6-year-old Staffordshire bull terrier in the malignant group with hyopertrophic osteopathy. Note the thick brush like periosteal reaction on the tibia, distal femur and caudal aspect of calcaneus. This reaction was present extensively on all the limbs.

Table 3
Haematology differences between the benign and malignant groups

Parameter	Benign group, $n = 27$	Malignant group, $n = 27$	Normal range
Haematocrit (%)*	0.41 ± 0.07	0.34 ± 0.08	0.37–0.55
Prevalence of anaemia*	22.22%	62.96%	
Mean corpuscular volume (fl)	63.67 ± 6.01	61.11 ± 7.62	60–77
Prevalence of microcytosis within the anaemic cases	50%	35.29%	
White blood cell count* ($\times 10^3\ \mu l^{-1}$)	18.03 ± 12.71	31.60 ± 27.84	6–15
Prevalence of leukocytosis*	44.44%	81.48%	
Mature neutrophil count* ($\times 10^3\ \mu l^{-1}$)	12.16 ± 9.81	26.06 ± 26.08	3–11.5
Prevalence of mature neutrophilia*	33.33%	70.37%	
Immature neutrophil count ($\times 10^3\ \mu l^{-1}$)	1.35 ± 3.04	1.06 ± 2.46	0–0.5
Prevalence of immature neutrophilia	29.63%	33.33%	
Monocyte count ($\times 10^3\ \mu l^{-1}$)	1.49 ± 1.47	2.20 ± 1.35	0.15–1.35
Prevalence of monocytosis*	33.33%	66.67%	
Eosinophil count* ($\times 10^3\ \mu l^{-1}$)	0.86 ± 0.79	0.49 ± 0.50	0.1–1.25
Prevalence of eosinophilia	25.93%	11.11%	
Prevalence of eosinopaenia	14.81%	29.63%	
Thrombocyte count* ($\times 10^9\ \mu l^{-1}$)	313.27 ± 128.54	493.15 ± 151.61	200–500
Prevalence of thrombocytosis*	7.41%	37.04%	

* $p < 0.05$ (t-test for absolute values and χ^2-test for prevalence).

been postulated as the major cause of HO in spirocercosis. Increased limb blood flow was proposed as a major contributor to the development of HO. It might be induced by the vagal stimulation and can be reduced by resection of the affected lung lobe and vagotomy (Brodey, 1971). Experimentally created right-to-left shunts can cause HO (Brodey, 1979). It was proposed that shunting allows humoral substances that are normally inactivated by the lungs to escape and reach the distal limbs (Martinez-Lavin, 1992). Later it was shown that platelet clumps are commonly lodged in the blood vessels of the extremities in HO cases, and it was hypothesized that megakaryocytes that escape the pulmonary capillary beds via the shunts facilitate the production of the platelet clumps that induce HO (Atkinson and Fox, 2004). The same might happen in diseases that release platelet aggregates from the left side of the heart, as happens in mitral or aortic vegetative endocarditis (Dunn et al., 2007). In the early form of HO in humans, also called digital clubbing, increased platelet derived growth factor and vascular endothelial growth factor expression was observed in tissue samples from digits stained immunohistochemically (Atkinson and Fox, 2004). These growth factors

Table 4
Radiological differences between the benign and malignant groups

Thoracic radiological findings	Benign group, $n = 25$	Malignant group, $n = 28$
Oesophageal mass length (mm)	81.90 ± 41.79	91.67 ± 28.86
Oesophageal mass height (mm)*	46.43 ± 23.62	62.59 ± 15.15
Oesophageal mass width (mm)*	49.29 ± 25.56	73.93 ± 20.94
Prevalence of oesophageal mass mineralization	4.76%	22.22%
Prevalence of oesophageal gravel sign	0%	11.11%
Prevalence of oesophageal air	52.38%	48.15
Prevalence of pulmonary parenchyma changes	16.00%	14.29%
Prevalence of fissure lines/pleural effusion	12.00%	21.43%
Prevalence of lymph nodes visualization	8.00%	0%
Prevalence of tracheal displacement	8.00%	17.86%
Prevalence of bronchial displacement*	16.00%	53.57%
Prevalence of aortic changes	48.00%	42.86%
Spinal radiological findings	$n = 26$	$n = 28$
Prevalence of spondylitis*	38.46%	67.86%
Number of spondylitis vertebrae	3.40 ± 1.78	3.55 ± 1.83

* $p < 0.05$ (t-test for absolute values and χ^2-test for prevalence).

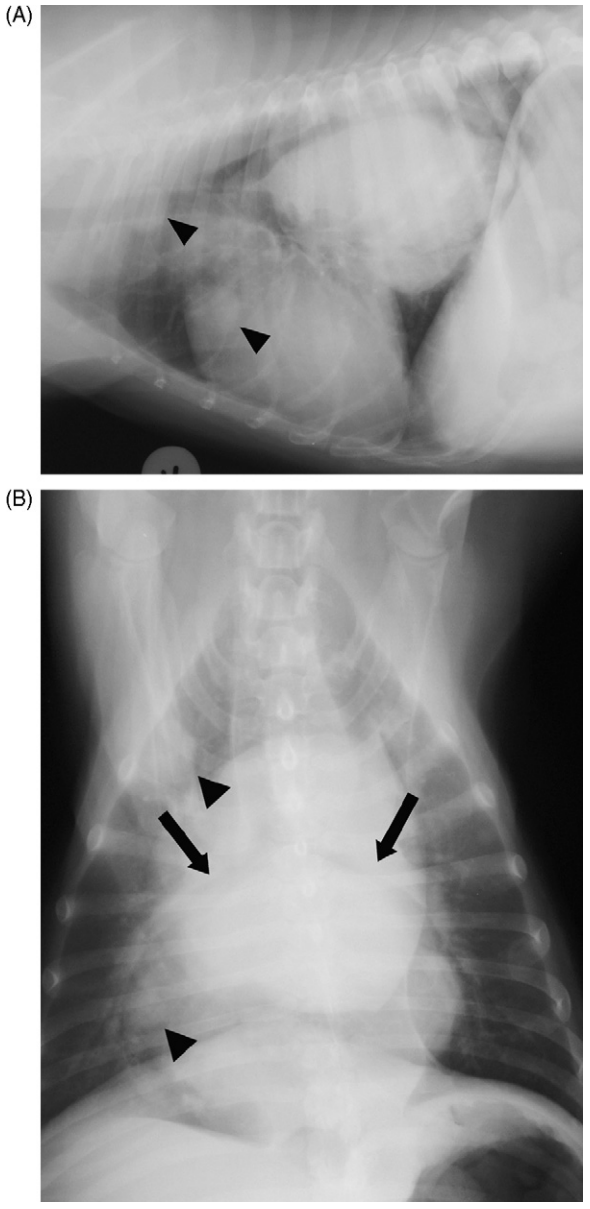

Fig. 2. Lateral (A) and ventro-dorsal (B) thoracic radiographs of the same dog as in Fig. 1. Note the large soft tissue mass superimposing on the caudal cardiac silhouette and cranial diaphragm. The mass displaces and compresses the main stem bronchi (arrows). Poorly defined metastatic nodules are visible (arrow heads).

were postulated to be released from the platelet clumps, inducing the tissue proliferation, increased vascularity and capillary permeability seen in HO (Atkinson and Fox, 2004). In a unifying theory for the pathogenesis of HO, platelet derived growth factor was proposed as the humeral substance inducing HO (Martinez-Lavin, 1992). Vagal stimulation was suggested to be only a contributing factor, which presumably causes increased blood flow in distal limbs and therefore, facilitate platelets lodging and increased circulation of the humeral agent, which would explain the improvement in some patients following vagotomy. The concept of a humeral factor causing HO in spirocercosis seems very attractive. Spirocercosis appears to induce connective tissue proliferation throughout the course of the disease (spondylitis, oesophageal nodule, sarcoma and HO). It may be postulated that a circulating oncogenic or growth factor induced by the worm infection, which induces connective tissue proliferation, might provide a unifying pathogenesis for the development of the different forms of connective tissue proliferation in spirocercosis.

A few reports have claimed that spondylitis is more common in malignant cases (Brodey et al., 1977; Ranen et al., 2004), as shown in the current study. However, the prevalence of spondylitis in the benign cases was 38.26%, indicating that spondylitis starts early in the disease process and is progressive. The finding of larvae in the muscles between the aorta and the spine led to the theory that aberrant migration may be responsible for the spondylitis (Bailey, 1972). This explanation is under investigation in our institute and it appears to be at best only partially true, because often the malignancy appears to progress long after the worms have disappeared and they therefore, can no longer play a role in the development of more overt spondylitis. It can be postulated that the worm may induce the spondylitis by stimulating changes that later become independent of its presence or further changes could be induced by the malignant tumour.

Other than HO, no other presenting clinical signs or complications, or period of illness before presentation occurred significantly more frequently in either group. In a recent publication describing only spirocercosis associated oesophageal sarcoma cases (Ranen et al., 2004), the prevalence of vomiting and/or regurgitation (94%) was higher than what we observed in any of the groups and was reported in prior spirocercosis studies that investigated malignant and benign cases together (Dvir et al., 2001; Mazaki-Tovi et al., 2002). Thus, an increased prevalence of vomiting or regurgitation might be more frequent in malignant cases but we cannot support it comparing the two groups.

Anaemia related to spirocercosis has been described in benign (Brodey et al., 1977) as well as malignant cases (Ranen et al., 2004). In the current study, anaemia was proved to be more severe and more prevalent in malignant cases, but the overlapping range was quite broad. Comparing our results with those of the other study of *S. lupi*-induced sarcoma (Ranen et al., 2004), the current study showed fewer microcytic anaemia

cases (35% vs. 63% in Ranen's study) and the current study also revealed no statistical difference from the benign group. Comparing the mean MCV in both studies reveals similar results, making the differences between the studies negligible. The most common explanation for microcytic anaemia is chronic blood loss, which can easily be explained by the predisposition of the *S. lupi* nodule to ulcerate. However, considering the high prevalence of dogs with normocytic anaemia, there are probably other factors that play a role in *S. lupi*-associated anaemia, such as anaemia of chronic disease or possibly a paraneoplastic effect.

In the current study, leukocytosis was significantly more severe and prevalent in the malignant cases, as has been reported in another study (Ranen et al., 2004). Leukocytosis and eosinopenia has also been reported in malignant fspirocercosis cases in an earlier study based only on three dogs (Brodey et al., 1977). In the current study, we confirmed these observations using a larger number of cases and by comparing values between malignant and benign cases. In the current study, thrombocytosis was also more common in the malignant group. This set of abnormalities, anaemia, leukocytosis and thrombocytosis, could be caused by continuous oesophageal irritation and blood loss from the malignant neoplasm. However, these haematological abnormalities may have a paraneoplastic origin and may provide a hint about the role that thrombocytes and leukocytes may play in the malignant transformation of the oesophageal nodule. Further research is required to explore this issue.

The search for radiological parameters to differentiate malignant from benign cases revealed substantial overlap in most measurements excluding HO. It may seem surprising that the mass length was similar for benign and malignant nodules, but this is probably due to the number of nodules, which can range from 1 to 8 and may coalesce longitudinally on radiographs. The height and width of the nodules are more reliable parameters, reflecting the larger size of malignant nodules. Bronchial displacement was also more common in the malignant group, and is probably secondary to the mass size.

Mass mineralization was assumed to be a relatively rare but specific marker for malignant transformation; however, we did detect one benign case with mineralization on radiographic examination and two additional benign cases with foci of osseous metaplasia within a nodule (seen histologically), which could provide a pathophysiological mechanism for the presence of mineralization in benign nodules. The presence of ingested mineralized debris should not be mistaken for mineralization of the nodule. The presence of osseous metaplasia may be another indication of the slow progression from benign to malignant nodules in spirocercosis. The gradual transition to sarcoma and the evidence of large numbers of embryonic fibroblasts in early benign nodules (Bailey, 1972), may be at least partially responsible for the big overlap or lack of significant differences in most of the parameters compared between benign and malignant groups. Computed tomography with its greater sensitivity to detect mineralization and to assess nodule perfusion after contrast medium administration may provide more clues in future about nodule

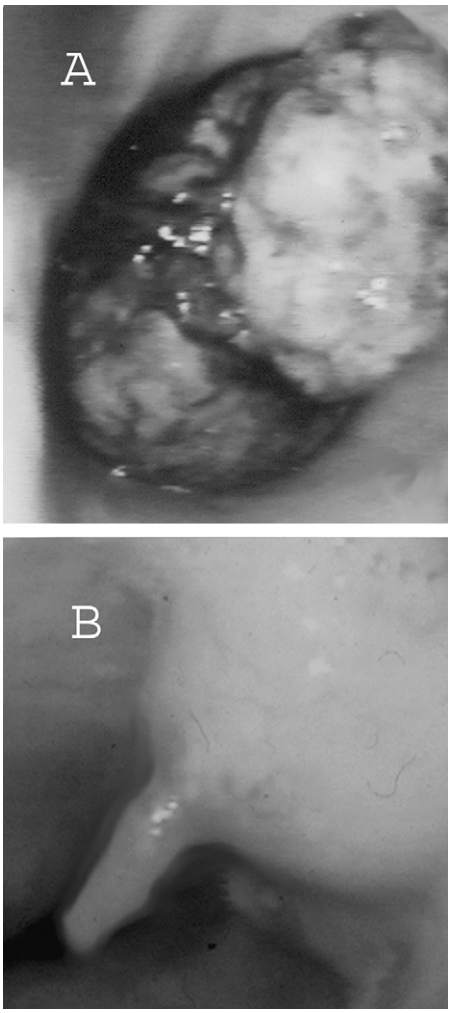

Fig. 3. Oesophageal endoscopic pictures of neoplastic nodule (A) and benign nodule (B). In the neoplastic nodule, note the lobulated proliferation, area of black colouration indicating ulceration and necrosis and the size of the nodule occupying most of the lumen. In the benign nodule, note the smooth, round appearance with typical protuberance, the healthy mucosa surrounding it and the small size in relation to the oesophageal lumen.

characteristics and is currently being investigated by our institution.

Endoscopy was reported to be the most sensitive tool for spirocercosis diagnosis (Dvir et al., 2001; Mazaki-Tovi et al., 2002) and Ranen et al. (2004) reported that they were able to make a tentative diagnosis of *S. lupi*-induced sarcoma on all the 15 cases they have scoped. We did not perform a detailed retrospective evaluation of our endoscopic and gross pathology changes as no consistent descriptions were used. However, in going through the available material various descriptions of irregularity, proliferation, necrosis and ulceration were common in the malignant cases (Fig. 3A), but two cases were described as smooth, which was an unexpected finding in malignant nodules. Benign nodules were very often described as typical (with a nipple-like protuberance), small and smooth (Fig. 3B); however, in a few cases, inflammation, ulceration and necrosis were reported, which could raise the index of suspicion for malignant transformation. These lesions could be secondary to mechanical irritation of the partially obstructed oesophagus. Currently we are prospectively investigating the predictability of endoscopy to determine malignancy. Endoscopy guided biopsy can only help if it is positive for malignancy as it is specific but not sensitive (Dvir et al., 2001). Therefore, although we find endoscopy a reliable tool, equivocal cases need to be monitored carefully for their response to treatment. In case of uncertainty following biopsy and a short treatment course, resection is indicated for both treatment and diagnosis of malignant vs. benign nodule.

The search for ante-mortem indicators of malignant transformation of the oesophageal nodules did not yield any highly sensitive and specific marker. Hypertropic osteopathy was highly specific for malignancy but it is a relatively rare finding (38.7%). Female gender, anaemia, leukocytosis, thrombocytosis, spondylitis and bronchial displacement are more sensitive and less specific parameters that should be evaluated as a constellation of parameters, and, if found together in a specific case, should increase the index of suspicion for malignancy in a diagnosed spirocercosis case. They may also provide clues about the pathogenesis of the malignant transformation, which requires further investigation.

References

Atkinson, S., Fox, S.B., 2004. Vascular endothelial growth factor (VEGF)-A and platelet-derived growth factor (PDGF) play a central role in the pathogenesis of digital clubbing. J. Pathol. 203, 721–728.

Bailey, W.S., 1963. Parasites and cancer: sarcoma in dogs associated with *Spirocerca lupi*. Ann. NY Acad. Sci. 108, 890–923.

Bailey, W.S., 1972. *Spirocerca lupi*: a continuing inquiry. J. Parasitol. 58, 3–22.

Bailey, W.S., Cabrera, D.J., Diamond, D.L., 1963. Beetles of the family Scarabaeidae as intermediate hosts for *Spirocerca lupi*. J. Parasitol. 49, 485–488.

Brodey, R.S., 1971. Hypertrophic osteoarthropathy in the dog: a clinicopathologic survey of 60 cases. J. Am. Vet. Med. Assoc. 159, 1242–1256.

Brodey, R.S., 1979. Hypertrophic osteoarthropathy. In: Andrews, E.J., Ward, B.C., Altman, N.H. (Eds.), Spontaneous Animal Models of Human Disease. Academic Press, New York, USA, pp. 241–246.

Brodey, R.S., Thomson, R.G., Sayer, P.D., Eugster, B., 1977. *Spirocerca lupi* infection in dogs in Kenya. Vet. Parasitol. 3, 49–59.

Dunn, M.E., Blond, L., Letard, D., DiFruscia, R., 2007. Hypertrophic osteopathy associated with infective endocarditis in an adult boxer dog. J. Small Anim. Pract. 48, 99–103.

Dvir, E., Kirberger, R.M., Malleczek, D., 2001. Radiographic and computed tomographic changes and clinical presentation of spirocercosis in the dog. Vet. Radiol. Ultrasound 42, 119–129.

Lavy, E., Aroch, I., Bark, H., Markovics, A., Aizenberg, I., Mazaki-Tovi, M., Hagag, A., Harrus, S., 2002. Evaluation of doramectin for the treatment of experimental canine spirocercosis. Vet. Parasitol. 109, 65–73.

Martinez-Lavin, M., 1992. Pathogenesis of hypertrophic osteoarthropathy. Clin. Exp. Rheumatol. 10 (Suppl. 7), 49–50.

Mazaki-Tovi, M., Baneth, G., Aroch, I., Harrus, S., Kass, P.H., Ben-Ari, T., Zur, G., Aizenberg, I., Bark, H., Lavy, E., 2002. Canine spirocercosis: clinical, diagnostic, pathologic, and epidemiologic characteristics. Vet. Parasitol. 107, 235–250.

Ranen, E., Lavy, E., Aizenberg, I., Perl, S., Harrus, S., 2004. Spirocercosis-associated esophageal sarcomas in dogs. A retrospective study of 17 cases (1997–2003). Vet. Parasitol. 119, 209–221.

Ranen, E., Dank, G., Lavy, E., Perl, S., Lahav, D., Orgad, U. 2007. Oesophageal sarcomas in dogs: histological and clinical evaluation. Vet. J. (Epup ahead of print, doi:10.1016/j.tjvl.2007.06.024).

Ridgway, R.L., Suter, P.F., 1979. Clinical and radiographic signs in primary and metastatic esophageal neoplasms of the dog. J. Am. Vet. Med. Assoc. 174, 700–704.

Seibold, H.R., Bailey, W.S., Hoerlein, B.F., Jordan, E.M., Schwabe, C.W., 1955. Observations on the possible relation of malignant esophageal tumors and *Spirocerca lupi* lesions in the dog. Am. J. Vet. Res. 16, 5–14.

van der Merwe, L.L., Kirberger, R.M., Clift, S., Williams, M., Keller, N., Naidoo, V., 2008. *Spirocerca lupi* infection in the dog: a review. Vet. J. 176, 294–309.

IMAGING DIAGNOSIS—SPINAL CORD CHONDROSARCOMA ASSOCIATED WITH SPIROCERCOSIS IN A DOG

NICOLETTE LINDSAY, ROBERT KIRBERGER, MARK WILLIAMS

A 7-year-old neutered female Boerboel cross was examined for progressive left pelvic limb lameness. There was no left patellar reflex but the remaining pelvic limb reflexes were hyperreflexic. Radiographically, there was a poorly mineralized opacity occupying the intervertebral foramen at L4–L5. On computed tomography images there was a hyperattenuating intramedullary lesion at L4–L5 that continued caudally, lateralized to the left and became extramedullary, terminating at L5–L6. In addition, well marginated, hyperattenuating lesions were noted at two muscular sites. The dog underwent euthanasia and a caudal esophageal mass was found at post mortem examination. The tumors in the spinal cord, the esophagus, and the skeletal muscles were diagnosed histologically as low-grade chondrosarcoma undergoing endochondral ossification. Spirocerca lupi-induced esophageal chondrosarcoma was believed to be the primary site from which the other, presumably metastatic, lesions originated. © 2010 *Veterinary Radiology & Ultrasound, Vol. 51, No. 6, 2010, pp 614–616.*

Key words: chondrosarcoma, computed tomography, spinal cord, *Spirocerca lupi*.

History and Clinical Findings

A 7-YEAR-OLD NEUTERED female Boerboel cross was examined for progressive left pelvic limb lameness that developed over a period of 6 weeks. There was marked muscle atrophy of the affected limb and mild hyperaesthesia during extension of the lumbosacral region. There was marked pelvic limb ataxia. The left pelvic limb had decreased extensor strength, delayed proprioception, decreased visual and tactile placing and an absent patellar reflex. The remainder of the pelvic limb reflexes were hyperreflexic bilaterally. Deep pain perception was present in the pelvic limbs. A nerve sheath or nerve root tumor was suspected.

Imaging

Radiographically, there was a poorly marginated mineralized opacity occupying approximately 70% of the intervertebral foramina at L4–L5 (Fig. 1). Computed tomography (CT) images of the region were acquired.* Beginning just cranial to the caudal end plate of L4 there was a small irregular, 0.5×0.4 cm hyperattenuating, central, tubular, intramedullary lesion (Fig. 2A). The lesion coursed caudally and at L4–L5 it widened slightly and became more heterogenous. Extending further caudally, the lesion assumed a bilobed appearance with a thin hypoattenuating rim and lateralized further to become extramedullary with a heterogeneous appearance (Fig. 2B). At the level of the cranial third of L5, the lesion tapered suddenly to form a round, well marginated, homogeneously hyperattenuating 0.3 cm structure that coursed caudally to the left L5–L6 intervertebral foramen where it terminated (Fig. 2C). The Hounsfield units (HU) of the lesion varied from 428 to 767. Considerations included chordoma, teratoma, and mineralizing nerve sheath tumor.[1,2]

Presumed foci of dystrophic mineralization were noted in the distal right semitendinous muscle, where there was a well marginated, small oval mass with a hyperattenuating rim, and a moderately hypoattenuating central region, and in the caudal aspect of the ventral abdominal muscles where there was a similar oval hyperattenuating structure.

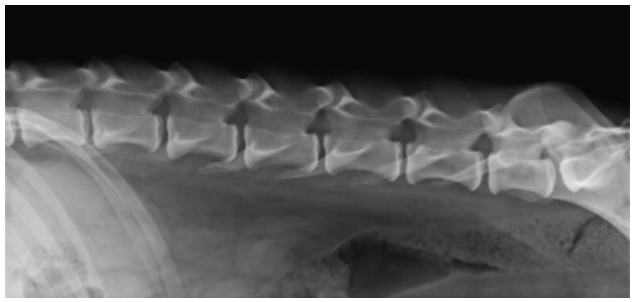

FIG. 1. Lateral radiograph of the lumbar spine. Note the poorly marginated mineralized opacity occupying most of the intervertebral foramen at L4–L5.

*Somatom Emotion dual slice, Siemens, Forchheim, Germany.

From the Department of Companion Animal Clinical Studies (Lindsay, Kirberger), and Department of Paraclinical Sciences, (Williams), Faculty of Veterinary Science, University of Pretoria, Private bag x04, Onderstepoort, Pretoria, South Africa 0110.

Address correspondence and reprint requests to Dr. Nicolette Lindsay, at the above address. E-mail: nicky.lindsay@up.ac.za

Received February 11, 2010; accepted for publication May 5, 2010.
doi: 10.1111/j.1740-8261.2010.01718.x

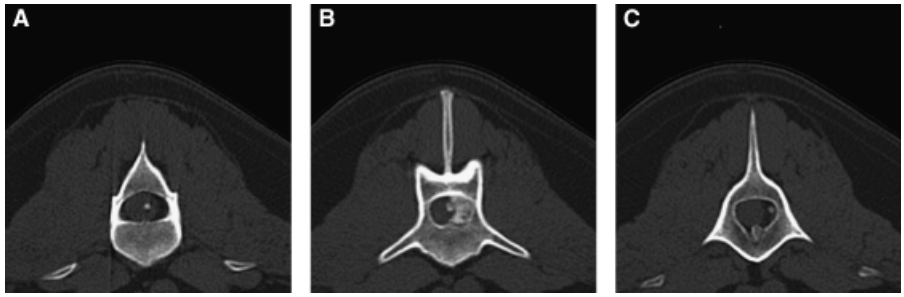

FIG. 2. Transverse computed tomography images of the lumbar spine. (A) At the level of the caudal third of L4. (B) At the level of the cranial third of L5. (C) At the level of the L5–L6 intervertebral foramen. Note the hyperattenuating intramedullary lesion that becomes lateralized and extramedullary caudally (left is to the right of the image).

Diagnosis

Based on the poor prognosis, the patient underwent euthanasia. Grossly, the spinal cord lesion and both muscular lesions were hard and smoothly marginated. Unexpectedly, a caudal esophageal mass measuring approximately $3 \times 2 \times 2$ cm, was found. This was diagnosed macroscopically as a *Spirocerca lupi* nodule.

Microscopically, the lesions in the esophagus, muscle and spinal cord were similar and were classified as low-grade chondrosarcomas. The final diagnosis was esophageal chondrosarcoma, secondary to *S lupi* infection, with metastasis to the spinal cord and two muscular sites.

Discussion

'Chondrosarcomas commonly affect the flat bones but approximately 1% of chondrosarcomas develop in extraskeletal locations such as the spleen, kidney, liver, mammary gland, intestine, omentum, lung, mitral leaflet, atrium, aorta, pulmonary artery, urethra, and eye.[3–12] Extraskeletal chondrosarcomas can arise from areas where cartilage is not normally found, and are suspected to originate from cartilaginous differentiation of primitive mesenchymal cells.[7–9,13]

Approximately 17–20% of chondrosarcomas metastasize.[4] The most common site for metastasis is the lung but other sites have been reported.[3,4,12] In the dog, extraskeletal chondrosarcoma occurs more commonly in males, with patients commonly being middle to old aged.[11]

Esophageal tumors are rare in dogs. In *S. lupi* endemic areas, the incidence of esophageal osteosarcoma and fibrosarcoma increases,[14] with osteosarcoma occurring more commonly than fibrosarcoma.[15,16] Chondrosarcoma as a consequence of *S. lupi* has not been found previously. There is a noted predisposition for neutered female dogs to undergo neoplastic esophageal transformation with resistance in males, suggesting a protective effect of androgens.[14]

Clinical signs of spirocercosis vary greatly depending on the stage of disease, the presence of aberrant migration and complications.[16] Dogs may have a large esophageal mass and still be asymptomatic.[16] Reported sites of metastasis from *S. lupi* induced esophageal sarcomas include lung, kidney, regional lymph nodes, stomach, spleen, pancreas, adrenal gland, heart, and tongue.[14,16,17] In several patients the primary tumor did not match the metastases tumor type histopathologically.[17] The pathogenesis of *S. lupi* induced esophageal neoplasia is unknown but may be related to the intense inflammatory reaction leading to uncontrolled fibroblast proliferation and malignant transformation.[16] Similarly, feline vaccine associated sarcomas arise from a secondary inflammatory reaction but are less aggressive biologically than spirocercosis-induced sarcoma.[18]

S. lupi can cause neurologic signs similar to thoracolumbar disc syndrome due to aberrant migration of larvae to the spinal cord.[19–21] To date, however, spinal metastasis, due to an *S. lupi* induced sarcoma has not been described. There is one report of a spirocerca-induced esophageal fibrochondrosarcoma,[22] which is a term not used in any modern classification of tumors.

In areas where *S. lupi* is endemic, aberrant migration of the nematode and metastasis from *S. lupi* induced sarcomas should be considered as a differential diagnosis for patients with neurologic signs.[19,20]

REFERENCES

1. Gruber A, Kneissl S, Vidoni B, Url A. Cervical spinal chordoma with chondromatous component in a dog. Vet Pathol 2008;45:650–653.

2. Wong MA, Mariani CL, Powe JR, Clemmons RM. Teratoma in the cervical spinal cord of a dog. J Am Anim Hosp Assoc 2007;43:292–297.

3. Miller JM, Walshaw R, Bourque AC. Primary splenic mesenchymal chondrosarcoma in a dog. Can Vet J 2005;46:163–165.

4. Waltman SS, Seguin B, Cooper BJ, Kent M. Clinical outcome of non-nasal chondrosarcoma in dogs: thirty-one cases (1986–2003). Vet Surg 2007;36:266–271.

5. Davis GJ, Holt D. Two chondrosarcomas in the urethra of a German shepherd dog. J Small Anim Pract 2003;44:169–171.

6. Munday JS, Prahl A. Retroperitoneal extraskeletal mesenchymal chondrosarcoma in a dog. J Vet Diagn Invest 2002;14:498–500.

7. Chikata S, Nakamura S, Katayama R, et al. Primary chondrosarcoma in the liver of a dog. Vet Pathol 2006;43:1033–1036.

8. Dupuy-Mateos A, Wotton PR, Blunden AS, White RN. Primary cardiac chondrosarcoma in a paced dog. Vet Rec 2008;163:272–273.

9. LaRock RG, Ginn PE, Burrows CF, Newell SM, Henson KL. Primary mesenchymal chondrosarcoma in the pericardium of a dog. J Vet Diagn Invest 1997;9:410–413.

10. Mellanby RJ, Holloway A, Woodger N, Baines E, Ristic J, Herrtage ME. Primary chondrosarcoma in the pulmonary artery of a dog. Vet Radiol Ultrasound 2003;44:315–321.

11. Rhind SM, Welsh E. Mesenchymal chondrosarcoma in a young German shepherd dog. J Small Anim Pract 1999;40:443–445.

12. Rodrigues EF Jr., Ribeiro AP, Perlmann E, Brooks DE, Laus JL. Metastatic intraocular chondrosarcoma in a dog. Vet Ophthalmol 2009;12:254–258.

13. Kim H, Nakaichi M, Itamoto K, Taura Y. Primary chondrosarcoma in the skull of a dog. J Vet Sci 2007;8:99–101.

14. Dvir E, Kirberger RM, Mukorera V, van der Merwe LL, Clift SJ. Clinical differentiation between dogs with benign and malignant spirocercosis. Vet Parasitol 2008;155:80–88.

15. van der Merwe LL, Kirberger RM, Clift S, Williams M, Keller N, Naidoo V. *Spirocerca lupi* infection in the dog: a review. Vet J 2008;176:294–309.

16. Ranen E, Lavy E, Aizenberg I, Perl S, Harrus S. Spirocercosis-associated esophageal sarcomas in dogs. A retrospective study of 17 cases (1997–2003). Vet Parasitol 2004;119:209–221.

17. Ranen E, Dank G, Lavy E, Perl S, Lahav D, Orgad U. Oesophageal sarcomas in dogs: histological and clinical evaluation. Vet J 2008;178:78–84.

18. Dvir E, Clift S, Williams M. Proposed histological progression of the *Spirocerca lupi*-induced oesophageal lesion in dogs. Vet Parasitol 2010;168:71–77.

19. Du Plessis CJ, Keller N, Millward IR. Aberrant extradural spinal migration of *Spirocerca lupi*: four dogs. J Small Anim Pract 2007;48:275–278.

20. Dvir E, Perl S, Loeb E, et al. Spinal intramedullary aberrant *Spirocerca lupi* migration in 3 dogs. J Vet Intern Med 2007;21:860–864.

21. Chai O, Shelef I, Brenner O, Dogadkin O, Aroch I, Shamir MH. Magnetic resonance imaging findings of spinal intramedullary spirocercosis. Vet Radiol Ultrasound 2008;49:456–459.

22. Sivadas CG, Nair MK, Rajan A. Neoplastic changes associated with oesophageal spirocerca tumour in a dog. Indian Vet J 1966;43:195–200.

Canine spirocercosis-associated extraskeletal osteosarcoma with central nervous system metastasis

Authors:
Paolo Pazzi[1]
Samantha Tompkins[2]
Robert M. Kirberger[1]

Affiliations:
[1]Department of Companion Animal Clinical Studies, University of Pretoria, South Africa

[2]Department of Paraclinical studies, University of Pretoria, South Africa

Correspondence to:
Paolo Pazzi

Email:
paolo.pazzi@up.ac.za

Postal address:
Private Bag X04, Onderstepoort 0110, South Africa

Dates:
Received: 19 Apr. 2012
Accepted: 26 Nov. 2012
Published: 24 Apr. 2013

How to cite this article:
Pazzi P., Tompkins S. & Kirberger R.M., 2013, 'Canine spirocercosis-associated extraskeletal osteosarcoma with central nervous system metastasis', *Journal of the South African Veterinary Association* 84(1), Art. #71, 4 pages. http://dx.doi.org/10.4102/jsava.v84i1.71

A five-year-old male Boerboel presented for examination, collapsed for an unknown period of time. On clinical examination, multifocal subcutaneous masses and enlarged prescapular lymph nodes as well as neurological deficits that suggested a multifocal neurological syndrome were found. Fine needle aspirates of the prescapular lymph nodes revealed cells suggestive of osteosarcoma. Radiographs showed foci of mineralisation within the soft tissue masses as well as diffuse pulmonary metastasis and a caudodorsal mediastinal mass believed to be a *Spirocerca lupi* nodule. Computed tomography imaging, necropsy and histopathology confirmed *S. lupi* oesophageal neoplastic transformation (extraskeletal osteosarcoma), believed to be the primary lesion, and the majority of secondary metastasis to the brain, spine, heart, multiple muscular groups and abdominal organs. This is the first known report of extraskeletal osteosarcoma metastasis to the brain and spinal cord in a dog.

Introduction

Spirocerca lupi is a nematode that occurs in tropical, subtropical and temperate climates, with dogs as the final host. After ingestion, the larvae penetrate the dog's gastric mucosa, migrate within the walls of the gastroepiploic arteries to the cranial abdominal aorta and continue cranially to the caudal thoracic aorta. Here maturation occurs within approximately three months, before the worms finally migrate through the mediastinum to the submucosa or muscular layer of the oesophageal wall. A fibrous nodule forms around the worms (Dvir, Clift & Williams 2010) and is visible three to nine months after larval ingestion (Bailey, Cabrera & Diamond 1963). Pathognomonic radiographic findings for spirocercosis includes, amongst others, caudal thoracic spondylitis together with a caudodorsal mediastinal soft tissue mass (Dvir, Kirberger & Malleczek 2001; Mazaki-Tovi *et al.* 2002).

Malignant oesophageal neoplasia in non-endemic spirocercosis areas is very rare (< 0.5% of all neoplasia cases) and does not typically include sarcoma (Ridgway & Suter 1979). Neoplastic transformation of the oesophageal nodule induced by *S. lupi* is a relatively common finding, with up to 26% of clinical cases becoming neoplastic (Dvir *et al.* 2001). Although extraskeletal osteosarcoma (ESO) is rare in dogs, oesophageal ESO is the most common type of neoplasia associated with spirocercosis; however, fibrosarcoma, undifferentiated sarcoma and chondrosarcoma also occur (Bailey *et al.* 1963; Lindsay, Kirberger & Williams 2010; Ranen *et al.* 2004; Wandera 1976). Sarcomas induced by *S. lupi* have been reported to metastasise to pulmonary, renal, gastric, adrenal and cardiac sites, as well as to the tongue and lymph nodes (Bailey 1972; Ranen *et al*. 2004).

Osteosarcomas are classified as skeletal or extraskeletal, with skeletal osteosarcoma metastasis to the central nervous system reported rarely in humans and dogs (Marina *et al.* 1993; McNeill *et al.* 2007; Spodnick *et al.* 1992; Stefanowicz *et al.* 2011). Primary sites of ESO in dogs, other than the oesophagus, include mammary tissue, subcutaneous tissue, the spleen, intestine, the liver, kidneys, testicles, the vagina, eyes, synovia, the omentum, adrenal glands and meninges (JiHyun *et al.* 2007; Kuntz *et al.* 1998; Misdorp *et al.* 1971; Patnaik 1990; Patnaik, Liu & Johnson 1976; Ringenberg, Neitzel & Zachary 2000; Salm & Mayes 1969; Schena *et al.* 1989; Turnwald, Smallwood & Helman 1979) but not the central nervous system to date. The most common sites of metastasis of ESO include the liver, lungs, local lymph nodes and the omentum, and occasionally the kidneys and heart (Kuntz *et al*. 1998; Patnaik 1990). In humans, metastasis of ESO to the brain has been reported only twice (Bindal *et al.* 1994; Salm 1959).

To our knowledge, this is the first report describing ESO metastasis to the brain and spinal cord in canines and only the third reported in any species. This case also involved extensive metastasis to the heart, subcutaneous tissue, musculature, lungs, lymph nodes and multiple abdominal organs.

Case history

A five-year-old intact male Boerboel presented in a state of collapse, the duration of which was unclear. Clinical examination revealed normal vital parameters, multifocal thoracic subcutaneous masses, severely enlarged prescapular lymph nodes and firm, swollen left semimembranous and semitendinous muscles. Findings on neurological examination included tetraparesis, head tilt to the right, bilateral rotary nystagmus, mydriatic pupils, bilateral decreased facial sensation and hyporeflexia of all limbs except for the left patellar reflex, which was hyperreflexic. No deep pain sensation was present in the right limbs and only superficial pain was present in the left limbs. A multifocal neurological syndrome was suspected.

Haematology showed a mild normocytic, hypochromic and slightly regenerative anaemia (haematocrit = 0.26 L/L, reference range 0.37 L/L – 0.55 L/L; mean corpuscular haemoglobin content = 31 g/dL, reference range 32 g/dL – 36 g/dL), moderate left-shift neutrophilia (mature neutrophils = 30.7 × 10^9/L, reference range 3.0 × 10^9/L – 11.5 × 10^9/L; immature neutrophils = 2.8 × 10^9/L, reference range 0.0 × 10^9/L – 0.5 × 10^9/L) and mild thrombocytosis (532 × 10^9/L, reference range 200 × 10^9/L – 500 × 10^9/L). Biochemistry revealed mild hypoalbuminaemia (19 g/L, reference range 27 g/L – 35 g/L). Fine needle aspirates of both prescapular lymph nodes indicated cells consistent with osteocytes and osteoblasts, suggestive of osteosarcoma.

Thoracic radiographs (right and left lateral and ventrodorsal views) were taken whilst the patient was conscious. Radiological abnormalities included spondylitis of five caudal thoracic vertebrae and an extensive nodular lung pattern, with nodules ranging from 3 mm to 40 mm in diameter, as well as a 60 mm diameter caudodorsal mediastinal soft tissue mass. Subcutaneous soft tissue opacities containing amorphous bone bilaterally without visible underlying rib involvement were present on dorsoventral skyline views of the left and right ribs centred at the level of the fifth intercostal space. Shoulder radiographs allowed visualisation of bilaterally enlarged centrally mineralised prescapular lymph nodes and additional soft tissue opacities medial to the right scapula and caudolateral to the left mid-humerus, with the latter showing central mineralisation. A mediolateral left femoral view revealed severe soft tissue swelling involving the entire caudal and proximal–cranial aspect of the left femur and contained poorly and inhomogeneously marginated to well-marginated central amorphous new bone. The caudal mid-femoral diaphysis had a 60 mm long thick, brush-like periosteal reaction.

Owing to the poor prognosis the patient was euthanased. This was followed by a whole-body helical computed tomography (CT) scan (Siemens Emotion Duo, Siemens, Germany), primarily for academic purposes. The subcutaneous and thoracic nodules found clinically and on the radiographs were all identified on the CT scan, as well as some additional nodules (e.g. a left temporal subcutaneous nodule of 3 cm diameter [Figure 1]). Most of these nodules had varying degrees of central mineralisation. In the superficial area of the left temporal lobe there was a well-marginated, round, mildly hyperattenuating (Hounsfield units 56) nodule of 20 mm diameter (Figure 1). Additional thoracic and abdominal changes seen by CT included extensive thoracic and abdominal aortic mineralisation (Figure 2 and Figure 3), two mineralised nodules (6 mm and 12 mm in diameter, respectively) in the interventricular septum, mineralised 20 mm

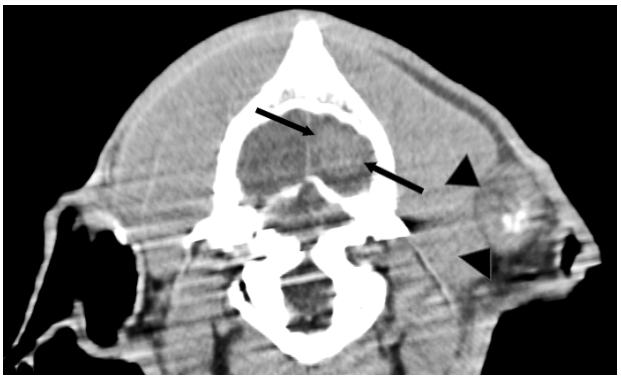

Source: Authors' own work
Black arrows, A slightly hyperattenuating left temporal lobe neoplasm; Black arrowheads, Centrally mineralising subcutaneous metastatic nodule displacing the adjacent temporal muscle medially.
Window width, 268; Window length, 67.

FIGURE 1: Transverse computed tomography image over the temporal region of the head using a soft tissue brain window.

Source: Authors' own work
White arrowheads, Mineralised wall of the ascending aorta; Long black arrow, Mineralised mass in the region of the ventral right rib; Black arrowheads, Soft-tissue-attenuating nodules in the lung and a large, poorly defined and slightly mineralised mass medial to the proximal right scapula.
Window width, 334; Window length, 60.

FIGURE 2: Transverse thoracic computed tomography image at the level of T4, using a soft tissue window.

diameter nodules associated with the pylorus (Figure 3), and an 8 mm mineralised nodule in the caudal pole of the left kidney. A caudal oesophageal soft tissue nodule was extensively mineralised (Figure 3).

A complete necropsy was performed and showed a cauliflower-like neoplastic caudal oesophageal *S. lupi* nodule, which was believed to be the primary site of neoplasia, and a smaller, smooth and slightly more caudal nodule that contained live *S. lupi* worms. A well-circumscribed expansile mass that was almost indistinguishable from the compressed cortical tissue was seen macroscopically within the brain. Suspected sites of central nervous system metastasis, in addition to those seen on the CT scan, included four firm, well-circumscribed nodules (3 mm – 10 mm in diameter) in the spinal cord. Sites of suspected metastasis outside the central nervous system correlated with those seen on the CT scan and included the lungs, bilateral ribs, the myocardium, the gastrointestinal tract, kidneys, the pancreas, the left and right triceps and femoral muscles, peripheral lymph nodes and multiple subcutaneous sites.

Histopathology of all the nodules confirmed diffuse multifocal metastatic osteosarcomas, with the primary lesion believed to have originated from the oesophageal *S. lupi* nodule. Within the temporal lobe, several small foci of malacic brain tissue were all that remained of the neural tissue in the area. The origin of the tumour appeared to be associated with blood vessels. It subsequently grew within the brain parenchyma and was characterised by loosely associated yet densely packed spindle-shaped osteoblasts, together with multi-nucleated osteoclasts. Osteoid was a prominent feature, with several small spicules of mineralised osteoid forming bone. Histopathology of a representative sample of a spinal nodule at the junction of the grey and white matter showed a well-circumscribed metastatic focus, characterised by typical large, spindle-shaped osteoblasts, with round to oval vesicular nuclei and prominent single nucleoli. Homogenous eosinophilic osteoid was prominent between the cells.

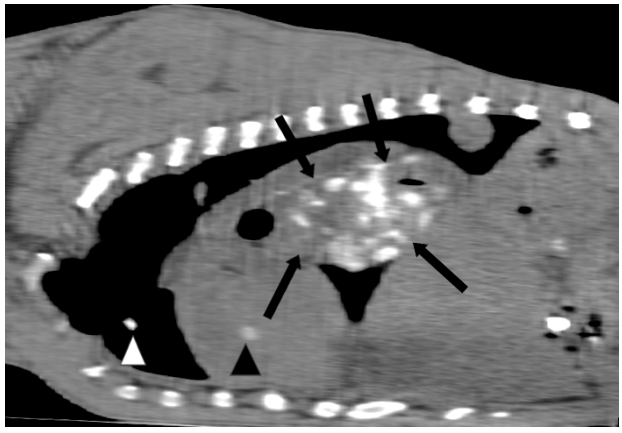

Source: Authors' own work
Long black arrows, Neoplastically transformed *Spirocerca lupi* oesophageal nodule and caudodorsal soft-tissue-attenuating lung nodules; White arrowhead, A smaller, cranioventrally mineralised lung nodule; Black arrowhead, A poorly mineralised intracardiac nodule.
Window width, 356; Window length, 54.

FIGURE 3: Sagittal thorax computed tomography image using a soft tissue window.

Discussion

The pathognomonic radiographic findings of a caudodorsal mediastinal soft tissue mass, caudal thoracic vertebral spondylitis in conjunction with multifocal soft tissues opacities within the lung parenchyma and extrapulmonary mineralised masses (diffuse osteosarcomas based on cytology) led to the clinical diagnosis of metastatic osteosarcoma secondary to spirocercosis. Other differentials considered included pulmonary abscessation and granulomatous or fungal disease, but these seemed unlikely. The CT and necropsy findings explained the clinical status of the dog, confirmed the diagnosis and supported the multifocal neurological syndrome described. Essential to clinical diagnosis were the thoracic radiographs and cytology of the prescapular lymph nodes.

The frequency of oesophageal neoplastic transformation induced by *S. lupi*, together with confirmation of the *S. lupi* nodule as an osteosarcoma, supports but does not confirm the suspicion of the *S. lupi* nodule as the primary neoplastic site. In this case, some degree of mineralisation was visualised radiographically in a number of metastatic soft tissue nodules, but the absence of radiographically visible mineralisation does not exclude the possibility of osteosarcoma (Kuntz *et al*. 1998). Extraskeletal osteosarcomas are generally more aggressive than skeletal osteosarcomas and may explain the widespread metastasis.

Extraskeletal osteosarcomas are rare in humans and animals, but in areas where spirocercosis is endemic neoplastic transformation of *S. lupi* nodules to an osteosarcoma is found frequently (Dvir *et al.* 2008; Van der Merwe *et al.* 2008). The pathogenesis of *S. lupi* neoplastic transformation is unclear, but two leading hypotheses to explain the infection-associated neoplastic transformations exist. These include (1) uncontrolled local inflammation leading to genetic instabilities and malignant transformations (Vennervald & Polman 2009) and (2) that the transformations are caused by the parasite itself, most likely in conjunction with the inflammatory response it produces (Kaewpitoon *et al.* 2008; Mulvenna *et al.* 2010; Smout *et al.* 2009). The most common site of ESO metastasis induced by *S. lupi* is the lungs (Ranen *et al*. 2004), whilst uncommonly reported sites of metastasis include the kidneys, regional lymph nodes, the stomach, the spleen, the pancreas, adrenal glands, the heart and the tongue (Dvir *et al*. 2008; Ranen *et al*. 2004; Ranen *et al.* 2008).

Neurological signs previously associated with aberrant migration of *S. lupi* larvae or metastatic neoplastic transformation include paraparesis, seizures, unilateral hindlimb lameness and hindlimb paralysis mimicking intervertebral disk disease (Du Plessis, Keller & Millward 2007; Dvir *et al.* 2001; Lindsay *et al.* 2010; Mazaki-Tovi *et al.* 2002). Metastasis to the spinal cord from *S. lupi* neoplastic

transformation has been reported only as a result of a low-grade chondrosarcoma (Lindsay *et al*. 2010). The neurological findings presented here indicate that in endemic areas spirocercosis should be on the list of differential diagnoses in dogs displaying focal or multifocal neurological syndrome.

Conclusion

This is the first report of an extraskeletal osteosarcoma associated with *S. lupi,* with severe diffuse metastasis to soft tissues, including the brain. Other than two cases described in humans (Bindal *et al*. 1994; Salm 1959), metastasis to the brain has now been described for the first time in another species.

Acknowledgements

Competing interests

The authors declare that they have no financial or personal relationship(s) that may have inappropriately influenced them in writing this article.

Authors' contributions

P.P. (University of Pretoria) was the veterinary clinician responsible for this clinical case and wrote the case report. R.M.K. (University of Pretoria) provided intellectual and practical contributions regarding the imaging study and writing of the description. S.T. (University of Pretoria) was responsible for pathology descriptions and review of the article content.

References

Bailey, W.S., 1972, *'Spirocerca lupi*: a continuing inquiry', *Journal of Parasitology* 58, 3–22. http://dx.doi.org/10.2307/3278233, PMid:5012526

Bailey, W.S., Cabrera, D.J. & Diamond, D.L., 1963, 'Beetles of the family Scarabaeidae as intermediate hosts for *Spirocerca lupi*', *Journal of Parasitology* 49, 485–488. http://dx.doi.org/10.2307/3275823, PMid:13969028

Bindal, R.K., Sawaya, R.E., Leavens, M.E., Taylor, S.H. & Guinee, V.F., 1994, 'Sarcoma metastatic to the brain: results of surgical treatment', *Neurosurgery* 35, 185–190. http://dx.doi.org/10.1227/00006123-199408000-00002, PMid:7969824

Du Plessis, C.J., Keller, N. & Millward, I.R., 2007, 'Aberrant extradural spinal migration of *Spirocerca lupi*: four dogs', *Journal of Small Animal Practice* 48, 275–278. http://dx.doi.org/10.1111/j.1748-5827.2006.00262.x, PMid:17425698

Dvir, E., Clift, S.J. & Williams, M.C., 2010, 'Proposed histological progression of the *Spirocerca lupi*-induced oesophageal lesion in dogs', *Veterinary Parasitology* 168, 71–77. http://dx.doi.org/10.1016/j.vetpar.2009.10.023, PMid:19963322

Dvir, E., Kirberger, R.M. & Malleczek, D., 2001, 'Radiographic and computed tomographic changes and clinical presentation of spirocercosis in the dog', *Veterinary Radiology and Ultrasound* 42, 119–129. http://dx.doi.org/10.1111/j.1740-8261.2001.tb00914.x, PMid:11327359

Dvir, E., Kirberger, R.M., Mukorera, V., Van der Merwe, L.L. & Clift, S.J., 2008, 'Clinical differentiation between dogs with benign and malignant spirocercosis', *Veterinary Parasitology* 155, 80–88. http://dx.doi.org/10.1016/j.vetpar.2008.04.006, PMid:18534758

JiHyun, H., YoungHwan, G., BoKyung, B., MiHyeon, Y., EulSoo, C., DaeYong, K. *et al.*, 2007, 'Extraskeletal osteosarcoma of the mammary gland in a dog', *Journal of Veterinary Clinics* 24, 663–666.

Kaewpitoon, N., Kaewpitoon, S.J., Pengsaa, P. & Sripa, B., 2008, '*Opisthorchis viverrini*: the carcinogenic human liver fluke', *World Journal of Gastroenterology* 14, 666–674. http://dx.doi.org/10.3748/wjg.14.666, PMid:18205254

Kuntz, C.A., Dernell, W.S., Powers, B.E. & Withrow, S., 1998, 'Extraskeletal osteosarcomas in dogs: 14 cases', *Journal of the American Animal Hospital Association* 34, 26–30. PMid:9527426

Lindsay, N., Kirberger, R.M. & Williams, M., 2010, 'Imaging diagnosis – spinal cord chondrosarcoma associated with spirocercosis in a dog', *Veterinary Radiology and Ultrasound* 51, 614–616. http://dx.doi.org/10.1111/j.1740-8261.2010.01718.x, PMid:21158232

Marina, N.M., Pratt, C.B., Shema, S.J., Brooks, T., Rao, B. & Meyer, W.H., 1993, 'Brain metastases in osteosarcoma. Report of a long-term survivor and review of the St. Jude Children's Research Hospital experience', *Cancer* 71, 3656–3660. http://dx.doi.org/10.1002/1097-0142(19930601)71:11<3656:AID-CNCR2820711130>3.0.CO;2-L

Mazaki-Tovi, M., Baneth, G., Aroch, I., Harrus, S., Kass, P.H., Ben-Ari, T. *et al.*, 2002, 'Canine spirocercosis: clinical, diagnostic, pathologic, and epidemiologic characteristics', *Veterinary Parasitology* 107, 235–250. http://dx.doi.org/10.1016/S0304-4017(02)00118-8

McNeill, C.J., Overley, B., Shofer, F.S., Kent, M.S., Clifford, C.A., Samluk, M. *et al.*, 2007, 'Characterization of the biological behaviour of appendicular osteosarcoma in Rottweilers and a comparison with other breeds: a review of 258 dogs', *Veterinary and Comparative Oncology* 5, 90–98. http://dx.doi.org/10.1111/j.1476-5829.2006.00116.x, PMid:19754792

Misdorp, W., Cotchin, E., Hampe, J.F., Jabara, A.G. & Von Sandersleben, J., 1971, 'Canine malignant mammary tumours', *Veterinary Pathology* 8, 99–117. PMid:4367432

Mulvenna, J., Sripa, B., Brindley, P.J., Gorman, J., Jones, M.K., Colgrave, M.L. *et al.*, 2010, 'The secreted and surface proteomes of the adult stage of the carcinogenic human liver fluke *Opisthorchis viverrini*', *Proteomics* 10, 1063–1078. PMid:20049860

Patnaik, A.K., 1990, 'Canine extraskeletal osteosarcoma and chondrosarcoma: a clinicopathologic study of 14 cases', *Veterinary Pathology* 27, 46–55. http://dx.doi.org/10.1177/030098589002700107, PMid:2309381

Patnaik, A.K., Liu, S. & Johnson, G.F., 1976, 'Extraskeletal osteosarcoma of the liver in a dog', *Journal of Small Animal Practice* 17, 365–370. http://dx.doi.org/10.1111/j.1748-5827.1976.tb06972.x, PMid:1065784

Ranen, E., Dank, G., Lavy, E., Perl, S., Lahav, D. & Orgad, U., 2008, 'Oesophageal sarcomas in dogs: histological and clinical evaluation', *Veterinary Journal* 178, 78–84. http://dx.doi.org/10.1016/j.tvjl.2007.06.024, PMid:17804268

Ranen, E., Lavy, E., Aizenberg, I., Perl, S. & Harrus, S., 2004, 'Spirocercosis-associated esophageal sarcomas in dogs: A retrospective study of 17 cases (1997–2003)', *Veterinary Parasitology* 119, 209–221. http://dx.doi.org/10.1016/j.vetpar.2003.10.023, PMid:14746980

Ridgway, R.L. & Suter, P.F., 1979, 'Clinical and radiographic signs in primary and metastatic esophageal neoplasms of the dog', *Journal of the American Veterinary Medical Association* 174, 700–704. PMid:429231

Ringenberg, M.A., Neitzel, L.E. & Zachary, J.F., 2000, 'Meningeal osteosarcoma in a dog', *Veterinary Pathology* 37, 653–655. http://dx.doi.org/10.1354/vp.37-6-653, PMid:11105956

Salm, R., 1959, 'A case of primary osteogenic sarcoma of extraskeletal soft tissues', *British Journal of Cancer* 13, 614–617. http://dx.doi.org/10.1038/bjc.1959.66, PMid:14441040

Salm, R. & Mayes, S.E., 1969, 'Retroperitoneal osteosarcoma in a dog', *Veterinary Record* 85, 651–653. PMid:5261205

Schena, C.J., Stickle, R.L., Dunstan, R.W., Trapp, A.L., Reimann, K.A., White, J.V. *et al.*, 1989, 'Extraskeletal osteosarcoma in two dogs', *Journal of the American Veterinary Medical Association* 194, 1452–1456. PMid:2722641

Smout, M.J., Laha, T., Mulvenna, J., Sripa, B., Suttiprapa, S., Jones, A. *et al.*, 2009, 'A granulin-like growth factor secreted by the carcinogenic liver fluke, *Opisthorchis viverrini*, promotes proliferation of host cells', *PLoS Pathogens* 5, e1000611, viewed 18 February 2012, from http://www.plospathogens.org/article/info%3Adoi%2F10.1371%2Fjournal.ppat.1000611

Spodnick, G.J., Berg, J., Rand, W.M., Schelling, S.H., Couto, G., Harvey, H.J. *et al.*, 1992, 'Prognosis for dogs with appendicular osteosarcoma treated by amputation alone – 162 cases (1978–1988)', *Journal of the American Veterinary Medical Association* 200, 995–999. PMid:1577656

Stefanowicz, J., Izycka-Swieszewska, E., Szurowska, E., Bien, E., Szarszewski, A., Liberek, A. *et al.*, 2011, 'Brain metastases in paediatric patients – characteristics of a patient series and review of the literature', *Folia Neuropathologica* 49, 271–281. PMid:22212917

Turnwald, G.H., Smallwood, J.E. & Helman, R.G., 1979, 'Esophageal osteosarcoma in a dog', *Journal of the American Veterinary Medical Association*174, 1009–1011. PMid:285065

Van der Merwe, L.L., Kirberger, R.M., Clift, S., Williams, M., Keller, N. & Naidoo, V., 2008, '*Spirocerca lupi* infection in the dog: a review', *Veterinary Journal* 176, 294–309. http://dx.doi.org/10.1016/j.tvjl.2007.02.032, PMid:17512766

Vennervald, B.J. & Polman, K., 2009, 'Helminths and malignancy', *Parasite Immunology* 31, 686–696. http://dx.doi.org/10.1111/j.1365-3024.2009.01163.x, PMid:19825108

Wandera, J.G., 1976, 'Further observations on canine spirocercosis in Kenya', *Veterinary Record* 99, 348–351. http://dx.doi.org/10.1136/vr.99.18.348, PMid:1069399

Chapter 5

Pathophysiology

Kirberger RM, Clift S, van Wilpe E, Dvir E. *Spirocerca lupi*-associated vertebral changes: A radiologic-pathologic study. *Veterinary Parasitology* 2013;195:87-94.

The mechanism by which spondylitis develops in spirocercosis and whether inflammation is in fact present has not been elucidated to date. The above paper attempts to answer some of these questions. It disproves some old theories of aberrantly migrating larvae being responsible[1, 2] and emphasizes the need for further work to clarify the pathomechanisms of spondylitis formation and the disease process as a whole, particularly the neoplastic transformation of the oesophageal nodule.

References

1 Bailey WS. Parasites and cancer: sarcoma associated with *Spirocerca lupi*. Ann NY Acad Sci 1963;108:890-923.

2 Bailey WS. 1972. *Spirocerca lupi:* A continuing enquiry. Vet Parasitol 1972;58:3-22.

Veterinary Parasitology 195 (2013) 87–94

Contents lists available at SciVerse ScienceDirect

Veterinary Parasitology

journal homepage: www.elsevier.com/locate/vetpar

Spirocerca lupi-associated vertebral changes: A radiologic-pathologic study☆

Robert M. Kirberger[a,*], Sarah J. Clift[b], Erna van Wilpe[c], Eran Dvir[a]

[a] Department of Companion Animal Clinical Studies, Faculty of Veterinary Science, University of Pretoria, Private Bag X04, Onderstepoort, South Africa
[b] Department of Paraclinical Sciences, Faculty of Veterinary Science, University of Pretoria, Private Bag X04, Onderstepoort, South Africa
[c] Electron Microscopy Unit, Department of Anatomy and Physiology, Faculty of Veterinary Science, University of Pretoria, Private Bag X04, Onderstepoort, South Africa

ARTICLE INFO

Article history:
Received 13 November 2012
Received in revised form
13 December 2012
Accepted 15 December 2012

Keywords:
Dog
Radiology
Histopathology
Spirocerca lupi
Spondylosis deformans
Spondylitis
Thoracic vertebrae

ABSTRACT

Spirocerca lupi causes a caudal esophageal mass in dogs which may be accompanied by aortic changes and caudal thoracic spondylitis. Previous literature hypothesized that the spondylitis was caused by either aberrant larval migration or was secondary to the inflammation caused by the aortic migration. The current study aimed to evaluate these hypotheses. Ten dogs of various breeds and ages with radiographic evidence of spondylitis, which were necropsied, had the affected vertebrae removed and prepared for light and transmission electron microscopy examination. Transverse and sagittal sections of the ventral vertebrae were taken from 27 spondylitis and 8 spondylosis deformans lesions as well as from 8 normal vertebrae. Early spondylitis changes were characterized by periosteal woven new bone covered by hyperplastic periosteum with some involvement of the ventral longitudinal ligament. More mature lesions were characterized by nodules of denser trabecular bone and cartilage, also covered by hyperplastic periosteum and involved the ventral longitudinal ligament. It was difficult to distinguish the spondylitis and spondylosis deformans new bone. Inflammation was seen in five spondylitis cases (edema, lymphocytes, plasma cells, eosinophils and fibrin fibers). Spirocerca eggs were seen in one histologic section. This study shows that inflammation is mild and inconsistent in spirocercosis-induced spondylitis and that aberrant migration of the larvae or adults did not appear to be a predominant cause. Inflammatory mediators or osteoproliferative growth factors, which may be related to the primary esophageal lesion or to the worm itself, could be involved. This requires further investigation.

1. Introduction

Spirocerca lupi (*S. lupi*) is a nematode of dogs that become infected by ingesting the intermediate host (coprophagous beetles) or paratenic host such as lizards (van der Merwe et al., 2008). After ingestion the larvae migrate from the stomach, via the gastric arteries, to the aorta from where they migrate intramurally to the caudal thoracic aorta. From here they penetrate the adjacent esophagus, mature to adults and form an inflammatory fibroblastic nodule or nodules which may progress to an esophageal sarcoma (Dvir et al., 2010). The disease has a worldwide distribution in tropical and subtropical areas. In certain areas of South Africa the prevalence of the disease can reach 80–100% (Kok et al., 2010). In up to 25% of long standing cases the esophageal nodule may

☆ An abstract of this work was presented at the 16th International Veterinary Radiology Association meeting at Bursa, Turkey, 27–31 August 2012.

* Corresponding author. Tel.: +27 12 529 8270; fax: +27 12 529 8306.
E-mail addresses: robert.kirberger@up.ac.za, robert@vetimagingspecialists.co.za (R.M. Kirberger).

0304-4017/$ – see front matter © 2012 Elsevier B.V. All rights reserved.
http://dx.doi.org/10.1016/j.vetpar.2012.12.039

undergo neoplastic transformation to sarcoma (Dvir et al., 2001), illustrating the clinical significance of this disease in endemic areas and its scientific significance as a natural model for helminth-induced cancer.

Clinically the diagnosis of spirocercosis might be challenging as the presenting complaints are non specific (e.g. weight loss and pyrexia) and more typical signs such as regurgitation appear only in about 60% of cases (Dvir et al., 2001; Mazaki-Tovi et al., 2002).

The diagnosis may be confirmed by finding the characteristic eggs in the feces, but sensitivity is not high (Christie et al., 2011). In these circumstances, radiology has a major role in screening for this disease, as it has 86% sensitivity and 100% specificity. Pathognomonic thoracic radiographic changes for spirocercosis are spondylitis and aorta aneurysm formation (Dvir et al., 2001; Mazaki-Tovi et al., 2002; van der Merwe et al., 2008). Observing one of these signs together with a caudodorsal mediastinal mass confirms the diagnosis. Computed tomography (CT) is also a very useful modality to evaluate esophageal, spinal and aortic pathology, particularly early spondylitis and aortic mineralization (van der Merwe et al., 2008). Endoscopy is the gold standard diagnostic modality to detect the esophageal nodule.

Caudal thoracic vertebral spondylitis in *S. lupi* infection is observed on radiographs in up to 53% of cases (Bailey, 1972; Dvir et al., 2001). Spondylitis is either an infectious or non-infectious inflammatory reaction of the vertebral body with no involvement of the vertebral end plate and disc space. Infectious spondylitis has classically been associated with migrating inhaled grass awns involving the mid lumbar vertebra or secondarily to penetrating foreign bodies (Horne, 1981; Brennan and Ihrke, 1983). Spondylitis of the caudal lumbar vertebra has also been associated with *Hepatozoon americanum* (*H. americanum*) infection (Panciera et al., 2000). As non-spirocercosis related thoracic spondylitis is extremely rare, it can be regarded as pathognomonic for this disease in spirocercosis endemic areas.

Radiographically, spondylitis must be distinguished from spondylosis deformans as their incidence and clinical significance differs markedly. Spondylosis deformans is a benign vertebral change which typically involves aging dogs. It is characterized by osteophytic new bone formation ventrally and laterally at the vertebral end plate and is believed to be due to breakdown of the peripherally located annulus fibrosus fibers. These osteophytes grow by endochondral ossification which cannot be distinguished from normal bone and will eventually bridge the disc space (Morgan, 1967a,b; Romatowski, 1986; Morgan et al., 1989).

To date there has not been much written on the pathology of vertebral new bone formation in animals, particularly so for spondylitis, with limited histopathologic information and even less information on the pathogenesis of the lesion. Radiographically the typical spirocercosis thoracic vertebral lesions have been termed spondylitis, but the presence of an inflammatory reaction has not been proven to date to warrant this description. It has been postulated that the spondylitis reaction is due to aberrant larval migration (van der Merwe et al., 2008), as Bailey (1972) reported that a few worms were recovered from the muscles and the connective tissue area between the aorta and the thoracic vertebrae. There have also been isolated observations of aberrant migrating larva entering the associated vertebral canal to result in extradural spinal cord compression (du Plessis et al., 2007) or intramedullary larval migration (Dvir et al., 2007; Chai et al., 2008). The progression of the osseous lesions of *H. americanum* typically involves osteoproliferative lesions of the proximal long bone diaphyses and less commonly the lateral surfaces of the vertebral bodies and dorsal spinous processes. There was no evidence of an inflammatory response in the *H. americanum* affected bones or surrounding musculature and humoral factors were postulated as the possible cause (Panciera et al., 2000).

The objective of this study was to describe the microscopic changes seen in the new bone formation in canine spirocercosis and to determine if inflammation and aberrant migration were components of *S. lupi* associated vertebral changes and obtain a greater understanding of the underlying pathophysiologic mechanisms involving the osseous proliferative lesions by means of histology and electron microscopy of the affected vertebrae.

2. Materials and methods

2.1. Patient data

Ten dogs that were euthanized between 2008 and 2011 as result of *S. lupi* infection were enrolled in the study. These dogs formed part of an ongoing prospective spirocercosis study within our faculty. All dogs had radiologic evidence of caudal thoracic spondylitis, seen as ventral vertebral body new bone formation. Some dogs had associated spondylosis deformans and aortic changes. All dogs had typical esophageal lesions associated with spirocercosis at necropsy. Of the 10 dogs, all but one of the esophageal lesions had undergone neoplastic transformation. The dog breeds were 2 boxers, 2 Jack Russell terriers, 2 German shepherd dogs and one each of Rottweiler, Labrador retriever, boerboel and bull terrier. The age was 5.4 ± 1.96 (mean $\pm$ standard deviation) years (median = 5) and the mean weight was 22 ± 9.9 kg (median = 24 kg). There were 6 females and 4 males of which 2 and 2 were sterilized respectively.

At necropsy the affected vertebral column was removed and reradiographed. Thereafter the spinal segment was placed in a 10% formalin solution and stored until all the samples could be processed at the same time.

2.2. Histologic preparation

Vertebral segments were compared to radiographic changes and 1 cm thick blocks cut of the required regions and identified. The affected vertebral blocks were again placed in 10% buffered formalin for 2 weeks and then in an 8% nitric acid solution made up in 10% neutral buffered formalin for tissue fixation and decalcification. The solution was replaced every 7–10 days to optimize decalcification, until all the vertebral segments floated in the solution, which was at eight weeks. Thereafter, vertebral samples were again compared to their equivalent radiographs in

order to determine the location of lesions. In cases 1–6 the entire affected vertebral column was harvested and transverse sections were cut, whilst in cases 7–10 the spine was collected after having been sectioned in the sagittal plane and sagittal vertebral sections were cut. Samples were sectioned at normal, spondylosis deformans and spondylitis regions as determined radiographically. Toluidine blue and HE-stained sections were examined by routine light microscopy.

2.3. Histologic evaluation

Histologic sections were taken from 8 normal vertebra, 8 spondylosis deformans and 27 spondylitis lesions with where possible normal, spondylosis deformans and spondylitis sections taken at multiple levels in each dog. Sections were examined for histopathology, with specific attention paid to periosteal new bone formation related to the radiologic spondylitis and spondylosis deformans reactions. The following changes were specifically looked for: whether the osteoproliferation was early (microscopic reactions, moderately cellular and pale staining with some edema between collagen fibers and displacement of the adjacent ligament) or mature (macronodular, less cellular, wide trabeculae with embedded ligamentous fibers and strongly staining); if there was ongoing new bone formation; osteoproliferative disruption or impingement of the ventral longitudinal ligament; proximity of bone marrow (specifically megakaryocytes) to new bone; the presence of cartilage in or near new bone; evidence of osteoblasts and osteoclasts; the nature of the junction between new bone and periosteum (specifically the presence of fibroblasts and/or fibrous connective tissue in or near new bone); the presence of adult worms, larvae and/or larvated eggs and if inflammatory cells were present in the region of periosteal new bone.

2.4. Transmission electron microscopy

Decalcification using a strong acid solution for a period of 8 weeks led to mild impairment of Hematoxylin staining of nuclei. Therefore, to further elucidate cell and tissue identification and to detect subtle ultrastructural changes not visible light microscopically (Sheehan and Hrapchak, 1987), a limited number of additional samples from 5 cases were also examined using a transmission electron microscope (Phillips CM10 FEI, Eindhoven, Netherlands) operated at 80 kV.

2.5. Statistical analyses

The study was descriptive with only radiographic and histologic changes compared.

3. Results

Vertebrae affected by spondylitis, as seen on radiographs ranged from T5-L1. There were 35 vertebrae affected with most involving T8 (T5 = 1, T6 = 4, T7 = 6, T8 = 9, T9 = 5, T10 = 8, T11 = 2). Representative radiographs

Fig. 1. Case No. 4; three-year-old male Boxer with neoplastic esophageal mass. Debulked necropsy lateral radiograph of T5-11. Note normal concave ventral surface of T11 vertebral body with remainder of vertebrae being more block shaped (white arrow head) due to the spondylitis reaction ventrally over the vertebral body. Note additional active ventral new bone formation at T7, 9 and 10 (white arrows). Note prominent spondylosis deformans type lesion (white asterisks) at T6 pointing caudally and crossing the intervertebral disc space.

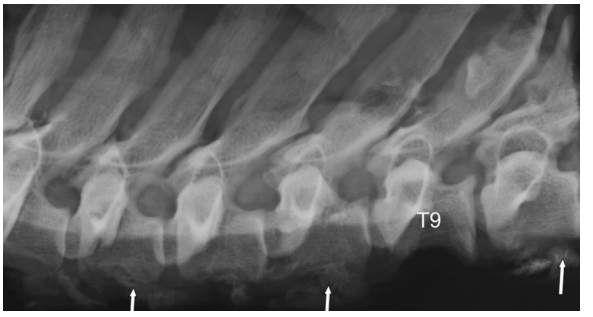

Fig. 2. Case No. 8; eight-year-old Boerboel with neoplastic esophageal mass. Debulked necropsy lateral radiograph of T5-10. Note normal concave ventral surface of T9 vertebral body with remainder of vertebra having active ventral new bone formation indicative of spondylitis (white arrows).

of Cases 4, 8 and 10, which also had photomicrograph and electron micrograph images, are illustrated in Figs. 1–3.

Light microscopic examination showed that 18 out of the 27 spondylitis sections had unequivocal histologic lesions. The remaining sections had no significant pathology, most likely due to early pathology being lost during

Fig. 3. Case No. 10; five-year-old Jack Russell with neoplastic esophageal mass. Debulked necropsy lateral radiograph of T5-10. Note normal concave ventral surface of T10 with vertebra T5-9 being more block shaped due to the spondylitis reaction ventrally over the vertebral body. Note spondylitis lesions more cranially mimicking spondylosis deformans (white arrows).

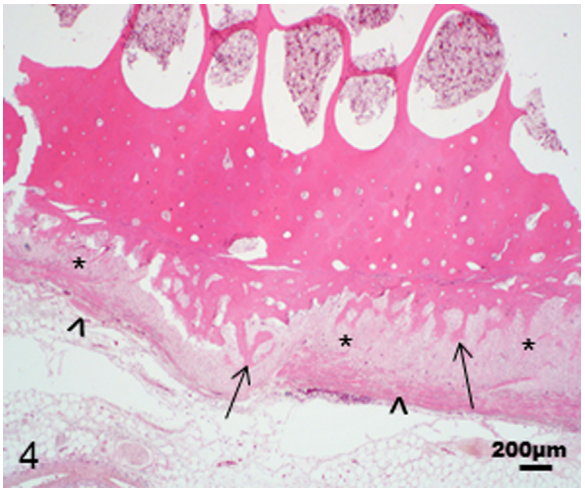

Fig. 4. Vertebra, case 4 (transverse section taken at mid T8); photomicrograph of an early lesion characterized by new bone formation (trabeculae perpendicular to underlying cortical bone) (arrows) and overlying thickened periosteum (asterisks). Note also the apparent interruption of the underlying ventral longitudinal ligament fibers (arrowheads). HE.

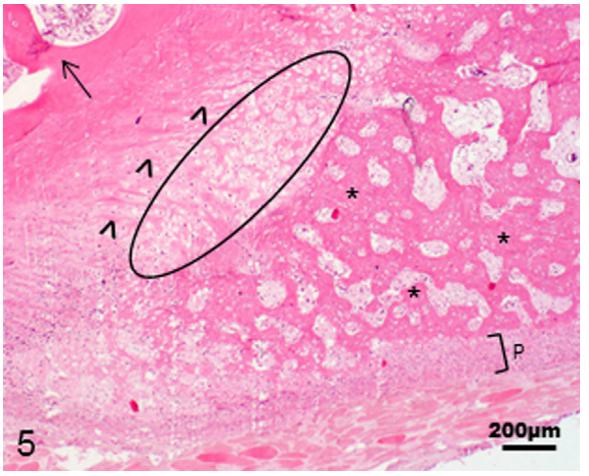

Fig. 5. Vertebra, case No. 6 (transverse section taken at mid T9); photomicrograph of a band of immature cartilage (encircled) can be seen immediately adjacent to mature cortical bone (arrow) with traversing dense collagen bundles (ligament) (arrowheads) and an outer nodule of new bone (asterisks) surrounded by thickened periosteum (P) in a lesion of intermediate maturity. HE.

slide preparation. Eight of the 10 cases with radiographic evidence of spondylitis had at least one section with obvious associated histologic lesions.

Immature or early histologic lesions of spondylitis were characterized by microscopic foci of irregular, periosteal woven new bone oriented perpendicularly to, but continuous with, the surface of the underlying mature cortical bone of the ventral vertebral bodies. The new bone spicules and trabeculae were frequently lined by plump, pyriform and occasionally stellate osteoblasts. Variable numbers of osteoclasts were also observed. The spaces between the bone spicules contained fibrous connective tissue and congested blood vessels lined by plump endothelial cells and surrounded by mild to moderate edema. Mature bone marrow containing hemopoeitic progenitor cells, including megakaryocytes, was usually located within marrow cavities in the adjacent mature vertebral bone. The periosteal new bone was covered by moderately thickened periosteum due to fibroblast and fibrous connective tissue proliferation (Fig. 4). There often was some outward displacement of and/or incorporation of the adjacent ventral longitudinal ligament's dense collagen bundles into the osteoproliferative foci (Fig. 4). As the lesions became more mature cartilaginous foci started in close proximity to the periosteal new bone nodules in 2 cases (Fig. 5).

Mature spondylitis lesions included macroscopic nodules of variably remodeled, denser trabecular bone with peripheral ongoing new bone formation, moderate to severe hyperplasia of the overlying periosteum and foci of cartilage within or immediately adjacent to the nodules (Fig. 6). The greatest proportion of intervening matrix within the thickened periosteum was composed of numerous intermittent oblique bundles of dense regular collagen (ligamentous insertions) that traversed the more irregular, loose collagen of the hyperplastic periosteum to embed in the new bone or cartilage. No obvious hemopoietic precursors were seen in the nodules of new bone, but typical bone marrow was observed in the adjacent mature cortical bone. Mature and immature changes overlapped in 2 cases with mature lesions usually having ongoing new bone formation indicative of a chronic active process.

In three dogs there was convincing evidence of inflammation associated with periosteal new bone formation. These all had prominent multifocal, usually perivascular, accumulations of lymphocytes and plasma cells, especially at the junction between the periosteoproliferative lesions and the adjacent tissues (Figs. 7 and 8).

Within, and sometimes also in the tissues adjacent to the thickened periosteum (composed of loose fibrous connective tissue, adipose tissue and skeletal muscle), there

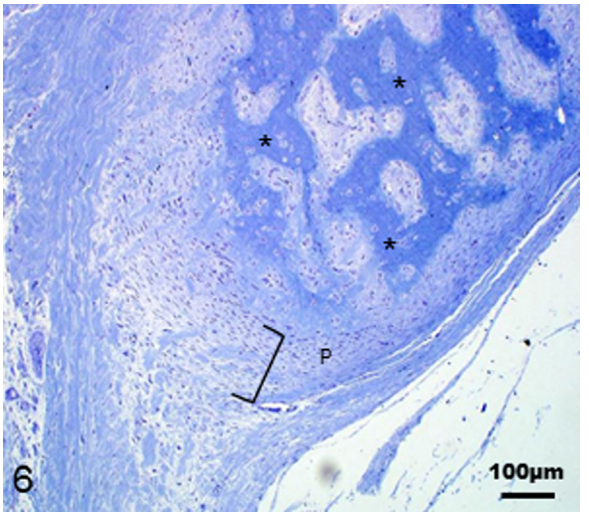

Fig. 6. Vertebra, case No. 10 (sagittal section taken at T9); low-magnification photomicrograph of mature lesion showing new bone proliferation (asterisks) adjacent to periosteal thickening (P). Toluidine blue.

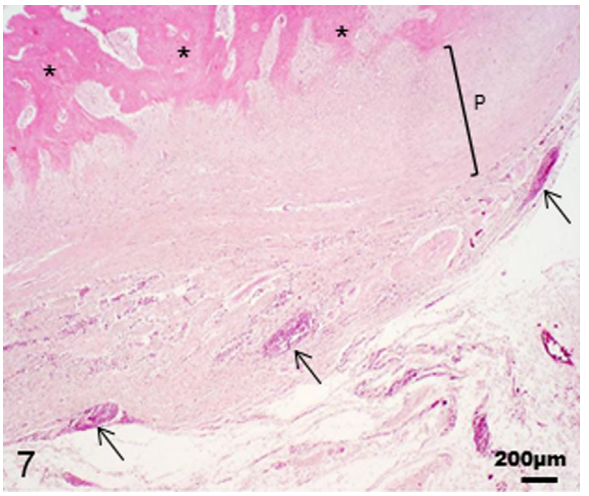

Fig. 7. Vertebra, case No. 8 (sagittal section taken at T7); Low-magnification photomicrograph of mature new bone proliferation (asterisks), overlying periosteal hyperplasia (P) and adjacent perivascular lymphoplasmacytic inflammation (arrows). HE.

were numerous markedly congested neocapillaries lined by plump endothelial cells. Mild to marked perivascular edema was also noted within and adjacent to the hyperplastic periosteum.

Sections through obvious spondylosis deformans lesions ventrally to the intervertebral disc spaces in 4 cases showed nodular new bone formation that was associated with cartilaginous foci, periosteal thickening (mainly fibroblasts and collagen) and disruption and incorporation of dense regular collagen bundles from adjacent ligaments. Spondylitis lesions were, however, occasionally also seen to extend to the ventral aspect of intervertebral discs as ongoing new bone formation on the periphery of the osteoproliferative nodules and could not be distinguished from spondylosis deformans reactions. However, inflammation

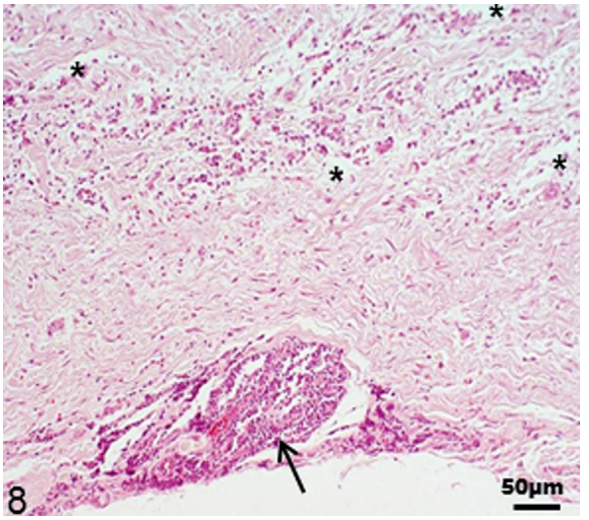

Fig. 8. Vertebra, case No. 8; higher magnification of Fig. 7 showing perivascular lymphoplasmacytic inflammation (arrow) and edema (asterisks) in the connective tissue adjacent to the osteoproliferation. HE.

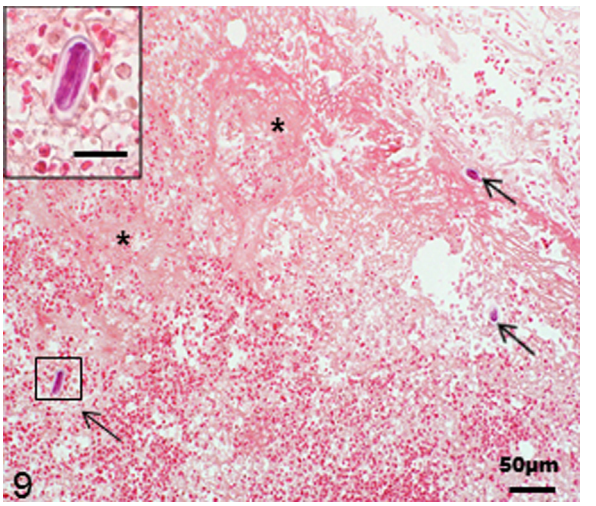

Fig. 9. Vertebra, case No. 7 (transverse section taken at cranial T9); low-magnification photomicrograph of three larvated *Spirocerca lupi* eggs (arrows) amidst a focally extensive area of hemorrhage and fibrin exudation (asterisks) Inset: Higher magnification of one *Spirocerca lupi* egg. Bar = 20 µm. HE.

was never observed in the spondylosis deformans sections. In essence, histopathology alone could not differentiate between mature spondylitis and spondylosis deformans lesions in the absence of inflammation in the adjacent connective tissue.

In no specimen were adult worms or larvae seen. However in one case, on a single section only, several *S. lupi* larvated eggs were present within a focally extensive area of hemorrhage and extravascular fibrin-like fibrillary protein in the adipose tissue adjacent to the ventral vertebral body. These eggs were not obviously associated with new bone formation or inflammation (Fig. 9).

Transmission electron microscopy examination revealed, adjacent to new bone formation, woven bone formation characterized by haphazard arrangement of collagen fibrils (Fig. 10), surrounding islands of cartilage

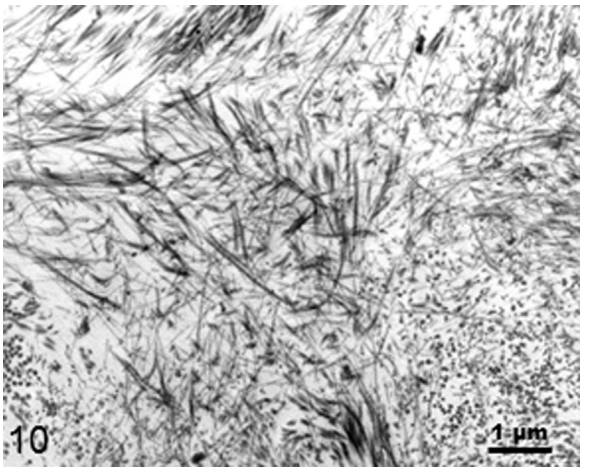

Fig. 10. Vertebra, case No. 10; high magnification electron micrograph showing the haphazard arrangement of collagen fibrils depicting woven bone in a mature lesion.

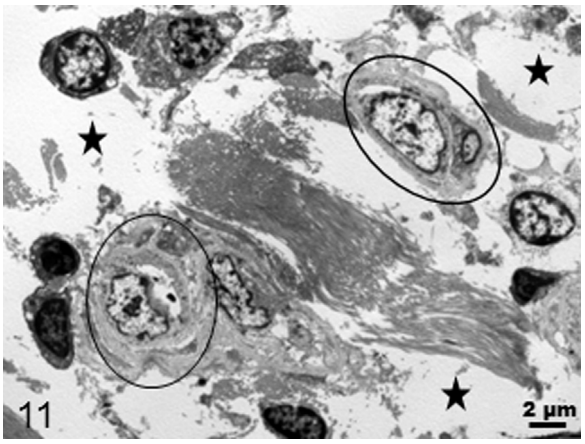

Fig. 11. Vertebra, case No. 8; low magnification electron micrograph showing extravascular inflammatory cells and oedematous areas (stars) in a mature lesion. Note capillaries with endothelial cell hypertrophy (encircled) and surrounding lymphocytes.

in some cases. In one case, fibroblasts and chondroblasts displayed dilated granular endoplasmic reticulum with secretion of collagen ground substance. In 2 cases angiogenesis was prominent within the thickened periosteum with obvious endothelial cell hypertrophy and perivascular edema (Figs. 11 and 12). In 2 cases electron-dense fibrin fibers with a characteristic striated periodicity could be identified (Figs. 13 and 14). In 4 cases interstitial accumulations of edema and inflammatory cells were noted in immature and mature lesions. The cells were lymphocytes (Fig. 11), plasma cells and, intra- or extravascular eosinophils (Fig. 15). Surprisingly only 2 out of these 4 cases also showed inflammation on histopathology indicating the greater sensitivity of EM to detect minimal changes. Thus, combining the EM and histopathology, 5 of the 10 cases showed evidence of inflammation.

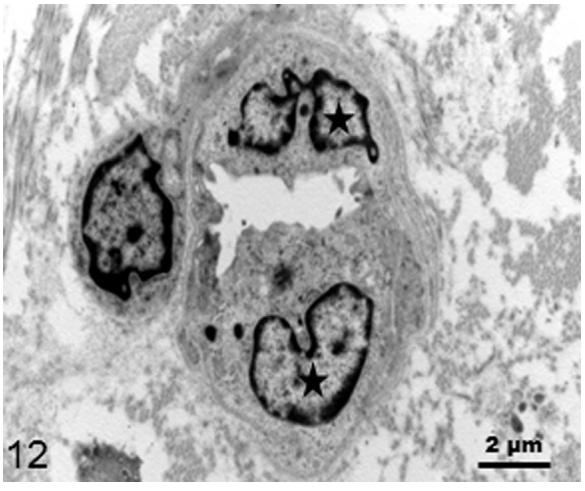

Fig. 12. Vertebra, case No. 10; higher magnification electron micrograph showing a capillary with endothelial cell hypertrophy (stars).

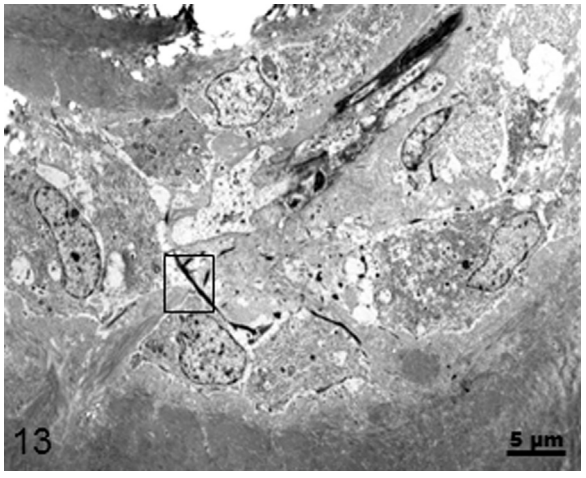

Fig. 13. Vertebra, case No. 10; low magnification electron micrograph of extravascular fibrin.

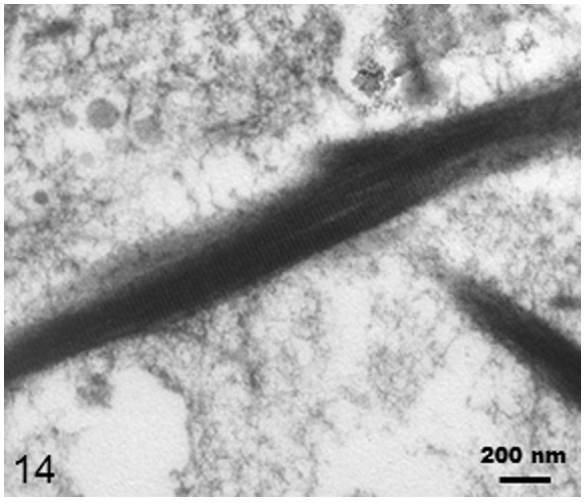

Fig. 14. Vertebra, case No. 10; higher magnification of fibrin fiber (boxed in Fig. 13) showing characteristic periodicity.

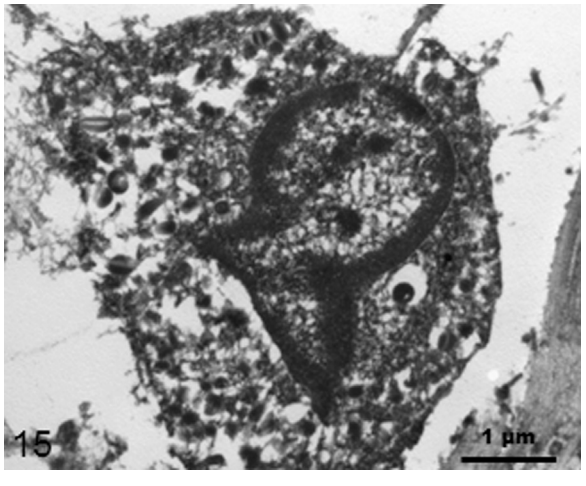

Fig. 15. Vertebra, case No. 4; high magnification electron micrograph of an extravascular eosinophil showing typical granules.

4. Discussion

The commonly used radiographic term spondylitis as compared to spondylosis deformans implies an inflammatory reaction of the vertebral body but to date this has not been proven. Our initial hypothesis was that the osteoproliferative vertebral lesion seen in spirocercosis, termed spondylitis, was an inflammatory reaction. This study showed that local inflammation associated with the vertebral changes was present but to a lesser extent than expected.

Our hypotheses that the inflammation originated either from the programmed larval migration in the thoracic aorta running adjacent to the thoracic vertebra and the subsequent periaortitis, or alternatively, as a result of aberrant larval migration via the intercostal arteries was not proven. Aberrant migration of larvae is a well described phenomenon in spirocercosis (van der Merwe et al., 2008) including the spinal area (du Plessis et al., 2007; Dvir et al., 2007; Chai et al., 2008), but clinically, it is far rarer then the prevalence of spondylitis. We assumed that non-clinical aberrant migration close to the aorta with its associated bony proliferation may be more common and would be detected histologically but the distinct absence of larval material or evidence of migrating tracts in our study questions this hypothesis. This is contrary to the thoughts of Bailey (1963, 1972) who suggested that the periosteal tissue may have been irritated by migrating larvae after leaving the aorta as he had found worms (presumably larvae) in the connective tissue and muscle between the aorta and the vertebra. He did however concede that other factors could also have been involved. In these early studies spondylitis could be present as early as 90 days post infection. It may thus be that in our clinical cases, which were euthanized much later than 90 days post infection, all evidence of the presence of larvae may have disappeared. However the progressive nature of the periosteal reaction still makes the presence of larvae an unlikely cause for the osseous reaction. The presence of *S. lupi* eggs in one histologic slide remains unexplained. The adult worms only lay eggs once encased in the esophageal nodule with an opening to the lumen and to date only aberrantly migrating larvae have been found and not adult worms.

To the best of the authors' knowledge this is the first study to describe the microscopic changes seen in the new bone formation and the inflammatory changes adjacent to the ventral caudal thoracic vertebral bodies in spirocercosis. The local inflammatory changes may well contribute to the vertebral new bone formation but the mild nature of this inflammation raises the suspicion that other osteogenic mediators, such as growth factors (GF), may stimulate such proliferation. Alternatively, inflammatory mediators secondary to systemic or distant inflammation, especially cytokines, also need to be considered as osteoproliferative stimulators. The new bone formation was typical of that seen with hypertrophic osteopathy and *H. americanum* (Panciera et al., 2000). The exact etiopathogenesis of the new bone formation for these well described conditions however also remains speculative. Irrespective of the etiopathogenesis of the thoracic vertebral new bone formation, an inflammatory reaction is present in 50% of cases and potentially may have been missed in adjacent soft tissues in other cases due to the histologic sample preparation concentrating on the osseous changes. Whilst the osseous changes are similar to the proliferative changes seen in spondylosis deformans and hypertrophic osteopathy, implying that the term spondylitis may not be appropriate, the adjacent inflammatory reaction allows the term spondylitis to remain for the vertebral changes described in spirocercosis. Radiological terminology can thus maintain the *status quo* of spondylosis deformans, which usually has no clinical significance, versus spondylitis, which has marked clinical implications regarding diagnosis and treatment, be it in spirocercosis, hepatozoonosis or primary vertebral infection.

Spirocercosis is associated with a moderate to severe local (esophageal) and systemic inflammatory reaction. The systemic response in spirocercosis has pro-inflammatory features such as increased circulatory C-reactive protein (Mukorera et al., 2011a,b), and IL-8 (Dvir et al., 2012). Proinflammatory response is strongly associated with the pathophysiology of new bone formation (Kapoor et al., 2011). The role of GFs in new bone formation is widely recognized, particularly for bone morphogenetic proteins (BMPs), fibroblast growth factor (FGF), insulin-like growth factors (IGFs), platelet-derived growth factor (PDGF), transforming growth factor-β (TGF-β) and vascular endothelial growth factor (VEGF) (Devescovi et al., 2008). TGF-β is of specific interest as it is regarded as the typical cytokine in helminth-induced immune response (Maizels et al., 2009) and its association with spirocercosis-induced bone formation warrants further investigation. FGF and VEGF have been expressed in *S. lupi*-associated esophageal neoplasia (Dvir and Clift, 2010), and serum and plasma levels of VEGF are markedly increased in malignant *S. lupi* nodule cases (Mukorera et al., 2011a, b). These growth factors have marked effects on bone modeling in general (Kacena et al., 2006) and their involvement in the etiopathogenesis of vertebral changes certainly needs to be considered, especially as they play central role in the etiopathogenesis of another bony proliferative lesion that is present is spirocercosis, namely hypertrophic osteopathy (Atkinson and Fox, 2004). Recent data suggests that megakaryocytes (or their platelet products), which were seen in our study, secrete multiple bone matrix proteins and growth factors crucial for bone remodeling and thus play a role in skeletal homeostasis by stimulating osteoblast proliferation and inhibiting osteoclast formation, thus favoring new bone deposition (Ciovacco et al., 2010). Another possible origin of the osteoproliferative mediators is the aortic pathology. This would explain the changes in the adjacent vertebra as the arterial blood supply to these vertebrae originate directly from the aorta via the intercostal arteries (Crock, 1960) with the larger ventral vertebral body branch possibly being the reason for the ventral new bone proliferation if the various growth factors originate somewhere upstream.

Spirocercosis produces three lesions that involve uncontrolled mesenchymal proliferation, namely hypertrophic osteopathy, spondylitis and sarcoma. No other infection in the dog produces this set of lesions and the mesenchymal proliferation is thus more likely to

have common features that are uniquely related to this disease and its pathogen. Our hypothesis is that the *S. lupi* nematode directly secretes or induces secretion of humoral factors that stimulate the mesenchymal cells. If such a factor is induced, we speculate that it might be through unique inflammatory response or positive feedback stimulation of the mesenchymal tissue. In dogs that have spondylitis and that were successfully treated for spirocercosis, the spondylitis reaction appears to remain static on follow up radiographs confirming that active infection is required for the reactive spondylitis lesions.

Conflict of interest statement

The authors declare no potential conflict of interest with respect to financial, personal or institutional matters that could inappropriately influence our work.

Funding

The senior author received funding from the National Research Foundation of South Africa

Acknowledgements

We express our gratitude to the staff of the histopathology laboratory (P. Mokonoto, R. Phaswane and N. Timmerman), Section of Pathology, University of Pretoria, for their careful preparation of tissue sections.

References

Atkinson, S., Fox, S.B., 2004. Vascular endothelial growth factor (VEGF)-A and platelet-derived growth factor (PDGF) play a central role in the pathogenesis of digital clubbing. J. Pathol. 203, 721–728.
Bailey, W.S., 1963. Parasites and cancer: sarcoma associated with *Spirocerca lupi*. Ann. N. Y. Acad. Sci. 108, 890–923.
Bailey, W.S., 1972. *Spirocerca lupi:* a continuing enquiry. Vet. Parasitol. 58, 3–22.
Brennan, K.E., Ihrke, P.J., 1983. Grass awn migration in dogs and cats: a retrospective study of 182 cases. J. Am. Vet. Med. Assoc. 182, 1201–1204.
Chai, O., Shelef, I., Brenner, O., Dogadkin, O., Aroch, I., Shamir, M.H., 2008. Magnetic resonance imaging findings of spinal intramedullary spirocercosis. Vet. Radiol. Ultrasound 49, 456–459.
Christie, J., Schwan, E.V., Bodenstein, L.L., Sommerville, J.E., van der Merwe, L.L., 2011. The sensitivity of direct faecal examination, direct faecal flotation, modified centrifugal faecal flotation and centrifugal sedimentation/flotation in the diagnosis of canine spirocercosis. J. S. Afr. Vet. Assoc. 82, 71–75.
Ciovacco, W.A., Cheng, Y.H., Horowitz, M.C., Kacena, M.A., 2010. Immature and mature megakaryocytes enhance osteoblast proliferation and inhibit osteoclast formation. J. Cell. Biochem. 109, 774–781.
Crock, H., 1960. The arterial supply and venous drainage of the vertebral column of the dog. J. Anat. 954, 88–99.
Devescovi, V., Leonardi, E., Ciapetti, G., Cenni, E., 2008. Growth factors in bone repair. Chir. Organi Mov. 92, 161–168.
du Plessis, C.J., Keller, N., Millward, I.R., 2007. Aberrant extradural spinal migration of *Spirocerca lupi*: four dogs. J. Small Anim. Pract. 48, 275–278.
Dvir, E., Clift, S.J., 2010. Evaluation of selected growth factor expression in canine spirocercosis (*Spirocerca lupi*)-associated non-neoplastic nodules and sarcomas. Vet. Parasitol. 174, 257–266.
Dvir, E., Kirberger, R.M., Malleczek, D., 2001. Radiographic and computed tomographic changes and clinical presentation of spirocercosis in the dog. Vet. Radiol. Ultrasound 42, 119–1218.
Dvir, E., Perl, S., Loeb, E., Hirsch, S.S., Chai, O., Mazaki-Tovi, M., Aroch, I., Shamir, H.M., 2007. Spinal intramedullary aberrant *Spirocerca lupi* migration in 3 dogs. J. Vet. Intern. Med. 21, 860–864.
Dvir, E., Clift, S.J., Williams, M.C., 2010. Proposed histological progression of the *Spirocerca lupi*-induced oesophageal lesion in dogs. Vet. Parasitol. 168, 71–77.
Dvir, E., Mellanby, R.J., Kjelgaard-Hansen, M., Schoeman, J.P., 2012. Plasma IL-8 concentrations are increased in dogs with spirocercosis. Vet. Parasitol., http://dx.doi.org/10.1016/vetpar.2012.06.007.
Horne, R.D., 1981. Grass awn migration in the dog. Canine Pract. 18, 21–32.
Kacena, M.A., Gundberg, C.M., Horowitz, M.C., 2006. A reciprocal regulatory interaction between megakaryocytes, bone cells, and hematopoietic stem cells. Bone 39, 978–984.
Kapoor, M., Martel-Pelletier, J., Lajeunesse, D., Pelletier, J.-P., Fahmi, H., 2011. Role of proinflammatory cytokines in the pathophysiology of osteoarthritis. Nat. Rev. Rheumatol. 7, 33–42.
Kok, D.J., Williams, E.J., Schenker, R., Archer, N.J., Horak, I.G., 2010. The use of milbemycin oxime in a prophylactic anthelmintic programme to protect puppies, raised in an endemic area, against infection with *Spirocerca lupi*. Vet. Parasitol. 174, 277–284.
Maizels, R.M., Pearce, E.J., Artis, D., Yazdanbakhsh, M., Wynn, T.A., 2009. Regulation of pathogenesis and immunity in helminth infections. J. Exp. Med. 2009, 2059–2066.
Mazaki-Tovi, M., Baneth, G., Aroch, A., Harrus, S., Kass, P.H., Ben-Ari, T., Zur, G., Aizenberg, I., Bark, H., Lavy, E., 2002. Canine spirocercosis: clinical, diagnostic, pathologic, and epidemiologic characteristics. Vet. Parasitol. 107, 235–250.
Morgan, J.P., 1967a. Spondylosis derformans in the dog. A morphologic study with some clinical and experimental observations. Acta Orthop. Scand. S96, 7–87.
Morgan, J.P., 1967b. Spondylosis deformans (vertebral osteophytosis) in the dog. A radiographic study from England, Sweden and U.S.A. J. Small Anim. Pract. 8, 57–66.
Morgan, J.P., Hansson, K., Miyabayashi, T., 1989. Spondylosis deformans in the female beagle dog: a radiographic study. J. Small Anim. Pract. 30, 457–460.
Mukorera, V., Kirberger, R.M., Mabeta, P., van der Merwe, L.L., Dvir, E., 2011a. Vascular endothelial growth factor as a marker for neoplastic transformation in canine spirocercosis. In: Abstract ECVIM, September 2011, Seville, Spain.
Mukorera, V., Dvir, E., van der, Merwe, L.L., Goddard, A., 2011b. Serum c-reactive protein concentration in benign and malignant canine spirocercosis. J. Vet. Intern. Med. 25, 963–966.
Panciera, R.J., Mathew, J.S., Ewing, S.A., Cummings, C.A., Drost, W.T., Kocan, A.A., 2000. Skeletal lesions of canine hepatozoonosis caused by *Hepatozoon americanum*. Vet. Pathol. 37, 225–230.
Romatowski, J., 1986. Spondylosis deformans in the dog. Comp. Cont. Ed. 8, 531–534.
Sheehan, D.C., Hrapchak, B.B., 1987. Theory and Practice of Histotechnology. Battelle Memorial Institute, 91 p.
van der Merwe, L.L., Kirberger, R.M., Clift, S., Williams, M., Keller, N., Naidoo, V., 2008. *Spirocerca lupi* infection in the dog: a review. Vet. J. 176, 294–309.

Chapter 6

Review

Dvir E, **Kirberger RM,** Clift SJ, van der Merwe LL. Review: Challenges in diagnosis and treatment of Spirocercosis. *Israel Journal of Veterinary Medicine* 2010;65:5-10.

The second review by Dvir, Kirberger *et al* brought together more recent thoughts of the Onderstepoort study group's experiences on some of the dilemmas still facing clinicians. These include the diagnosis of small or atypically located nodules, emphasizing the value of CT, early cases with no nodules, and non-oesophageal clinical presentation and how to distinguish between benign nodules and malignant tumours.

REVIEW: CHALLENGES IN DIAGNOSIS AND TREATMENT OF CANINE SPIROCERCOSIS

Dvir E[1*]., Kirberger R.M[1]., Clift S.J[2]. and van der Merwe L. L.[1]

[1] The Department of Companion Animal Clinical Studies, Faculty of Veterinary Science, University of Pretoria, Onderstepoort, 0110, Republic of South Africa.
[2] Department of Paraclinical Sciences, Faculty of Veterinary Science, University of Pretoria, Onderstepoort, 0110, Republic of South Africa,
* Corresponding author: Prof. Eran Dvir: eran.dvir@up.ac.za

Spirocerca lupi (S. lupi) is a nematode of worldwide distribution, most commonly found in tropical and subtropical areas (1). Dogs are the definitive hosts and become infested by ingesting the coprophagous beetle intermediate hosts (1) or various paratenic hosts, including poultry, wild birds, lizards, rodents, hedgehogs and rabbits (2). A previous study has revealed that *S. lupi* larvae-infected coprophagous beetles are small and feed within the feces, and dogs probably become infected through coprophagia rather than by catching the beetle (3). After ingestion, the larvae are liberated in the gastric lumen, migrate through the gastric mucosa via the gastric arteries, and reach the caudal thoracic aorta within 10 days. Later they migrate through the thoracic aortic wall to the caudal esophagus within 90 to 109 days (4). The *S. lupi* larvae settle within the esophageal wall, mature to adults and promote nodule formation (1, 2, 5). The nodules are usually incorrectly referred to as granulomas (1, 5). The early nodule is however composed predominantly of fibrocytes (amidst ample mature collagen), that with time (i.e. during nodule maturation), transform into actively dividing fibroblasts that are located between numerous immature capillaries, immediately peripheral to the worms and their migratory tracts (2, 6). The associated inflammatory reaction within the nodule is variable and is not characterized by the presence of macrophages, as in granulomatous inflammation (2, 5). Instead, the predominant infiltrate is lymphoplasmacytic in nature, with pockets of neutrophils specifically associated with the necrotic content of the worms' migratory tract (6). Spirocercosis induces some pathognomonic lesions; aortic scarring with or without osseous metaplasia and/or dystrophic calcification as well as aneurysm formation, caudal thoracic vertebral spondylitis and a characteristic caudal esophageal nodule. The common clinical signs associated with spirocercosis are related to the presence of esophageal nodules and include regurgitation, vomiting and weight loss, with other non-specific signs such as pyrexia (7, 8).

Positive fecal flotation tests show numerous, characteristic, small (35 × 15 µm), thick-shelled, larvated eggs (Fig. 2). However, the sensitivity of fecal flotation is limited because eggs are shed intermittently by the female worms and the eggs are relatively heavy and may require special techniques and solutions such as sodium nitrate solution (specific gravity 1.36), supersaturated 33% zinc sulfate solution and supersaturated sugar solution (9). Recently, a copromicroscopic approach, the FLOTAC technique was reported to improve the sensitivity and increase the number of microscopically detected eggs(10). This method seems to be superior to the previously described techniques / solutions, however it only detected 10 out 31 cases (32%), detected by polymerase chain reaction (PCR), and required specific apparatus and centrifuge. Repeated fecal analysis was found to increase the sensitivity of the test (8). Recently a PCR assay was developed to detect fecal *S. lupi* (10). Such a test can maximize the sensitivity of fecal analysis but also depends on presence of egg-shedding female worms in a patent esophageal nodule. This proviso excludes cases with aberrant migration, extra-luminal nodules, early infestations and late disease with malignant transformation, where the worm is often no longer present.

The clinical diagnosis of spirocercosis largely depends on thoracic radiography, demonstrating a caudodorsal mediastinal mass, caudal thoracic vertebral spondylitis and aortic undulation due to aneurysm formation (with or without aortic mineralization) (7). A caudodorsal mediastinal mass on its own is highly suspicious for spirocercosis in endemic areas but if accompanied by spondylitis and/or aortic aneurysms the radiological changes are pathognomonic for spirocercosis. However, the clinical diagnosis of spirocercosis remains challenging due to several factors; Nodules may be small or atypically located and thus may not be visible on radiographs. Cases may present in early disease stages, prior to the formation of esophageal nodules. Differentiating between a *S. lupi*-induced benign nodule and a neoplastic tumor is sometimes difficult. Atypical cases due to disease related complications or aberrant migration are diagnostically challenging. These difficulties are discussed in this paper.

Diagnosis of small or atypically located esophageal nodules

Positive radiological diagnosis is very reliable, claiming 100% specificity in one study (11). However, the sensitivity of survey radiology is only about 84% (12), because small and atypically located esophageal nodules may not be detected by survey thoracic radiographs (7). Dorsoventral and right lateral recumbent radiographs are recommended to optimize

the masses and aortic aneurysms visibility (12). Small or atypical nodules may, however, readily be detected in contrast radiographic studies, especially pneumo-esophagograms (Fig. 1) (7). In the latter the air filled esophagus provides contrast to enhance the visibility of masses which otherwise tend to be effaced the surrounding esophageal and mediastinal structures. Providing the esophagus is sufficiently distended with air the mural attachment location can usually also be seen allowing for better surgical planning. Additionally the extramural extent of the mass is also highlighted Endoscopy is the most sensitive tool to detect and evaluate *Spirocerca*-induced intra-esophageal nodules (7, 8). It is the only tool that allows direct visualization of the nodule, which its typical appearance contributes to the diagnostic substantially and it is also ideal to monitor response to treatment. Endoscopy does however also have its drawbacks as it provides no information on any other thoracic complications. Additionally the equipment is specialized and expensive and the procedure requires a full general anesthetic.

Computed tomography (CT) is emerging as a very effective tool for detecting small intraluminal nodules, mural and extraluminal nodules, atypically located nodules as well as dystrophic aortic mineralization (7) In CT the cross sectional images avoid superimposition of structures, as is seen on radiographs, enhancing mass detection. The greater sensitivity of CT to detect mineralization is also a great advantage, for example, aortic mineralization is seen in up to 50 % of CT cases whereas on radiographs mineralization is rarely seen.

Diagnosis of early infections when esophageal nodules are absent

The detection of early cases of spirocercosis remains challenging. Computed tomography may detect early spondylitis and aortic mineralization as well as aberrant migration. Although CT will not be done routinely in every sick dog, our institution diagnoses about 8% of our confirmed cases of *S. lupi* incidentally when performing thoracic CT for other reasons. In endemic areas thoracic CT examinations should thus always include specific evaluation of the esophagus, aorta and the spine. Other diagnostic modalities such as endoscopy and fecal examination depend on the presence of an esophageal nodule or a viable egg laying passage respectively. Serology might prove to be a promising modality to detect early infection. Preliminary results of an immunofluorescent antibody test (using the mid-body region of the male worm as an antigen source) showed 100% sensitivity and 80% specificity for *S. lupi* at a titre of 1:640 (13). However, as yet nothing more has been published on this topic.

Differentiating between *S. lupi*-induced esophageal nodules and neoplasms

With time, esophageal nodules may undergo malignant transformation to sarcoma (5, 14). *Ante-mortem* differentiation between non-malignant and malignant cases is challenging yet clinically, therapeutically and prognostically very important. A few studies have tried to investigate criteria that might characterize dogs with *S. lupi*-induced malignant esophageal tumors (5, 14-16). Neoplasia occurs more frequently in older dogs, and in spayed females, while benign nodules are more common in young males, however there is a considerable age and sex overlap between groups. *Ante mortem* indicators of *S. lupi* esophageal neoplasia are non specific and insensitive (15). Hypertrophic osteopathy (HO) occurs in 40% of patients with *S. lupi* induced esophageal sarcoma (15) and is an indicator of neoplastic transformation. Spondylitis was more common and severe in malignant cases (15-17), but the prevalence of spondylitis in benign cases was 38% (15), indicating that spondylitis is initiated early in the disease process and is progressive. Anemia, leukocytosis, and thrombocytosis occur more commonly in malignancy (15), likely due to continuous esophageal irritation, inflammation and blood loss or they may have a paraneoplastic origin.

Radiology has been used to differentiate between esophageal malignancy and benign nodules. The length of esophageal masses was similar in both benign and malignant cases (15). This unexpected finding was probably due to the superimposition of smaller nodules (ranging 1-9) along the caudal length of the esophagus. in survey thoracic radiographs, the height and width of esophageal messes were significantly higher in neoplastic compared to benign masses (62.6 versus 43.4 mm and 73.9 versus 49.3 mm, respectively) and bronchial displacement was more common in the malignant group, probably secondary to the larger mass size (15). Radiographically detectable esophageal mass mineralization was observed in both neoplastic and non-neoplastic cases and could not be used to diagnose malignant transformation. In the non-neoplastic cases it was probably due to osseous metaplasia (15). False positive results may also occur due to entrapped mineralized ingesta. Assessment of esophageal mass mineralization as a differentiating characteristic between benign and malignant conditions using CT is currently being assessed at our institution. Macroscopically, the surface of malignant esophageal neoplasms tend to be cauliflower-like (2). Based on this characteristic appearance, Ranen and others (2004) reported that they were able to make a tentative diagnosis of *S. lupi*–induced sarcoma, using endoscopy, in all 15 cases examined. An ulcerative vegetative growth pattern with necrosis in deeper layers is common in malignancy (Fig. 3A), although malignant nodules may, on occasion ,have a smooth surface. Benign nodules are typically small, smooth and rounded with a nipple-like protuberance (Fig. 3B), (7). Occasionally however, they may ulcerate and undergo necrosis and inflammation, and might be falsely diagnosed as neoplastic (15). Endoscopy-guided biopsy has limitations. As although highly specific, the procedure has very low sensitivity (7, 8, 16), because biopsies frequently include only the necrotic superficial layers of the tumor, rendering a definite diagnosis impossible. Thoracoctomy and surgical resection of the mass

with histology of the entire mass has the highest sensitivity and specificity, but is invasive with increased risk of complications, can be cost-prohibitive and should be reserved for cases that show endoscopic evidence of neoplasia, HO, or mineralization on imaging. Computed tomography may aid in the decision and planning of the surgical procedure (7). Where there is uncertainty about the diagnosis of neoplastic transformation, response to a medical therapy followed by repeated endoscopy might aid in the diagnosis, demonstrating nodule regression in non-neoplastic cases and further proliferation in neoplastic nodules.

Benign esophageal nodules regress with doramectin (Dectomax, Pfizer, France,) treatment, 400 µg/kg SC at 2-week intervals (18). Pharmacokinetic studies of doramectin in dogs showed good absorption results for oral administration (19), suggesting that it could be an effective route of administration, but no clinical results have as yet confirmed this. The pharmacokinetics of doramectin and ivermectin in dogs are similar, rendering the latter a therapeutic option too, but clinical results are also necessary to confirm this (19). In avermectin susceptible breeds such as collies, milbemycin-oxime may be used (20).

In summary, female gender, anemia, leukocytosis, thrombocytosis, spondylitis and bronchial displacement, if found together in a spirocercosis case, should increase the index of suspicion for malignancy. In addition, according to our data, if HO is diagnosed, it is strongly indicative of neoplastic transformation of the esophageal nodule.

Histologically, the malignant neoplasms are classified as osteosarcoma (most common), fibrosarcoma, or undifferentiated sarcoma (16). Osteosarcomas are defined by the presence of osteoid, produced by neoplastic pyriform osteoblasts (21), while fibrosarcomas are characterized by the presence of collagen matrix between interwoven neoplastic or anaplastic spindle shaped cells (22) and undifferentiated sarcomas lack distinctive architectural pattern, cell products / matrix as well as cytoplasmic and nuclear features (23). In areas where spirocercosis does not exist, malignant neoplasms of the esophagus are extremely rare (<0.5% of all malignant cases) (24), making spirocercosis the major cause of malignant esophageal neoplasms in the dog and certainly the primary cause of osteosarcoma, fibrosarcoma, or undifferentiated sarcoma at this site. Spirocercosis-induced sarcoma can metastasize to various locations, most commonly the lung (5, 7, 16). Based on the current knowledge, malignant esophageal neoplasms can only be treated by surgical excision. Advanced sessile tumors that require full circular esophageal resection carry a very poor prognosis, while small pedunculated tumors that require partial esophagectomies have a far better prognosis (16). Chemotherapies suggested for appendicular osteosarcoma, such as carboplatin and doxorubicin, can be used post-surgically, but thus far, their benefit is not clear (16). The average survival of esophagectomy plus doxorubicin was 267 days in one study in dogs with spirocercosis (16). A murine model of *S. lupi*-associated sarcoma showed doxorubicin and pegylated liposomal doxorubicin to be effective, but not carboplatin or cisplatin (25). Because it is less toxic than doxorubicin, pegylated liposomal doxorubicin is recommended for treatment of S. *lupi*-associated sarcoma.

Non-gastrointestinal clinical presentation in spirocercosis: disease-associated complications and aberrant *S. lupi* migration

Atypical clinical signs of spirocercosis can result from larval or adult worm migration, their presence in different organs and from inflammation. Respiratory signs are very common, occurring in 25%-50% of cases (2) and are due to airway tract compression by esophageal masses, aspiration pneumonia secondary to regurgitation, mediastinitis, pleuritis, pyothorax and pulmonary metastasis (7, 8, 26). Pyothorax occurs quite commonly due to esophageal perforation or aberrant migration (26). Although aortic lesions are extremely common in spirocercosis, aortic rupture with consequent hemothorax is observed less commonly, and is almost always fatal (27). Lameness is not uncommon (up to 25% in one report), and results from HO or secondary septic or immune-mediated arthritis (7). Paraparesis and back pain occur occasionally and have been attributed to the presence of spondylitis in the mid thoracic vertebrae (8). Hind quarter paralysis has been described in spirocercosis-associated aortic thromboembolism (28, 29).

Severe intractable dysphagia with firm mandibular salivary adenomegally has been documented in up to 8.5% patients presenting with spirocercosis with fox terriers and Jack Russell terriers over represented (30). The clinical history in these dogs was often prolonged and included retching, coughing, hypersialosis, gulping and choking, worsened with excitement and palpation of the pharyngeal area. No salivary gland biopsies were obtained, but fine-needle aspirate cytology in four cases showed hyperplasia with no evidence of inflammation. These dogs were all treated symptomatically and with doramectin and phenobarbitone (2 mg/kg q12h) and showed marked improvement within 48 hours from initiating phenobarbitone treatment (30). This response to phenobarbitone suggests an underlying central nervous system involvement, most likely continuous vagal stimulation, known as visceral epilepsy (31).

Aberrant migration of *S. lupi* is not uncommon, and has been reported in most thoracic organs including pleura, mediastinum, diaphragm, lung, trachea, bronchi, thymus and heart (32, 33). Non-thoracic aberrant migration was reported in the gastrointestinal and urinary tracts (34, 35) and subcutaneous tissue (33, 36). Recently, aberrant spinal *S. lupi* has been described in dogs (both extradural and intramedullary) (37, 38). Such migration can lead to paraparesis and paraplegia, clinically mimicking disc extrusion and fibrocartilaginous embolism (37). Intramedullary spinal cord migration presents a distinct neurological syndrome of an acute, progressive

asymmetric, mostly painful paresis progressing to paralysis (38). Neurological examination may suggest a focal spinal cord lesion between T3 and S1, but the pathological lesions might be far more extensive due to progressing larval spinal migration. Cerebrospinal fluid (CSF) neutrophilic and eosinophilic pleocytosis is commonly observed and differentiates such cases from fibrocartilaginous embolism and disc disease. Extradural spinal aberrant migration can be diagnosed by myelography. However, the diagnosis of intramedullary migration is far more challenging, because myelography or computed tomography are usually non-diagnostic (38, 39). Magnetic resonance imaging (MRI) can be used to demonstrate intraspinal parasitic lesions in humans (38), and has revealed abnormalities suggestive of myelitis and myelomalecia in two dogs with aberrant spinal intramedullary migration (39).

When characteristic clinical signs of spirocercosis are present (e.g. regurgitation, vomiting, weight loss and dysphagia) and are supported by specific radiographic and endoscopic findings a diagnosis of spirocercosis is fairly straightforward even if atypical clinical signs of aberrant migration or complications are concurrently present. However, in cases of aberrant migration or complications and in the absence of any of the typical abnormalities, the *ante mortem* diagnosis of spirocercosis is extremely difficult. Therefore, in endemic areas, spirocercosis should be included as a differential diagnosis in dogs presenting abnormal soft tissue masses, hypersalivation with sialoadenomegaly, pyothorax, hemothorax, mediastinal effusion, asymmetric spinal cord neurological signs and aortic thromboembolism.

It is difficult to treat the aberrant migration cases and conventional doramectin treatment is not always effective in these cases. In dogs presenting with pyothorax, conservative medical treatment, including drainage and antibiotics together with doramectin treatment, was found relatively successful (26). In cases of extradural spinal cord migration, removal of the worm was successful in only 1 of 3 cases (37), while in intramedullary spinal cord migration, the prognosis was always grave (38). In humans with spinal schistosomiasis, surgical removal of the worm and the surrounding damaged tissue was very successful (40). Such radical therapy was only attempted twice in dogs, so far without success (39).

This review outlines challenging aspects pertaining to the diagnosis of spirocercosis. At present, the diagnosis of typical cases is routinely achieved. With advances made in diagnostic modalities and in identifying the clinical presentation of atypical spirocercosis such diagnostic challenges can be met.

REFERENCES

1. Bailey, W. S.: Spirocerca lupi: a continuing inquiry. J. Parasitol. 58: 3-22, 1972.
2. van der Merwe, L. L. Kirberger, R. M. Clift, S. Williams, M. Keller, N. and Naidoo V.: Spirocerca lupi infection in the dog: A review. Vet. J. 176: 294-30, 2007.
3. Du Toit, C. A. Scholtz, C. H. and Hyman, W. B.: Prevalence of the dog nematode Spirocerca lupi in populations of its intermediate dung beetle host in the Tshwane (Pretoria) Metropole, South Africa. Onderstepoort J. Vet. Res. 75: 315-321, 2008.
4. Sen, K. and Anantaraman, M.: Some observations on the development of Spirocerca lupi in its intermediate and definitive hosts. J. Helminthol. 45: 123-131, 1971.
5. Bailey, W. S.: Parasites And Cancer: Sarcoma In Dogs Associated With Spirocerca Lupi. Ann. N. Y. Acad. Sci. 108: 890-923, 1963.
6. Dvir, E. Clift, S. J. and Williams, M. C.: Proposed histological progression of the Spirocerca lupi-induced oesophageal lesion in dogs. Vet. Parasitol. Epub ahead of print. doi:10.1016/j.vetpar.2009.10.02
7. Dvir, E. Kirberger, R. M. and Malleczek, D.: Radiographic and computed tomographic changes and clinical presentation of spirocercosis in the dog. Vet. Radiol. Ultrasound. 42: 119-129, 2001.
8. Mazaki-Tovi, M. Baneth, G., Aroch, I. Harrus, S. Kass, P. H. Ben-Ari, T. Zur, G., Aizenberg, I. Bark, H. and Lavy, E.: Canine spirocercosis: clinical, diagnostic, pathologic, and epidemiologic characteristics. Vet. Parasitol. 107: 235-250, 2002.
9. Markovics, A. and Medinski, B.: Improved diagnosis of low intensity Spirocerca lupi infection by the sugar flotation method. J. Vet. Diagn. Invest. 8: 400-401, 1996.
10. Traversa, D. Avolio, S. Modry, D. Otranto, D. Iorio, R. Aroch, I. Cringoli, G. Milillo, P. Albrechtova, K. Mihalca, A. D. and Lavy, E.: Copromicroscopic and molecular assays for the detection of cancer-causing parasitic nematode Spirocerca lupi. Vet. Parasitol. 157: 108-116, 2008.
11. Fisher, M. M. Morgan, J. P., Krecek, R. C. and Kelly, P. J.: Radiography for the diagnosis of spirocercosis in apparently healthy dogs, St. Kitts, West Indies. Vet. Parasitol. 160: 337-339, 2009.
12. Kirberger, R. M. Dvir, E. and van der Merwe, L. L.: The effect of positioning on caudodorsal mediastinal masses. Vet. Radiol. Ultrasound. 50:294-309
13. Coskun, S. Z.: Diagnosis of Spirocerca lupi infections by IFAT in naturally infected dogs. Türkiye Parazitoloji Dergisi. 19: 541-549, 1995.
14. Seibold, H. R. Bailey, W. S., Hoerlein, B. F. Jordan, E. M. and Schwabe, C. W.: Observations on the possible relation of malignant esophageal tumors and Spirocerca lupi lesions in the dog. Am. J. Vet. Res. 16: 5-14, 1955.
15. Dvir, E. Kirberger, R. M. Mukorera, V. van der Merwe, L. L. and Clift, S. J.:Clinical differentiation between dogs with benign and malignant spirocercosis. Vet. Parasitol. 155: 80-88, 2008.
16. Ranen, E. Lavy, E. Aizenberg, I. Perl, S. and Harrus, S.: Spirocercosis-associated esophageal sarcomas in dogs. A retrospective study of 17 cases (1997-2003). Vet. Parasitol. 119: 209-221, 2004.

17. Brodey, R. S. Thomson, R. G. Sayer, P. D. and Eugster, B.: Spirocerca lupi infection in dogs in Kenya. Vet. Parasitol. 3: 49-59, 1977.
18. Lavy, E. Aroch, I. Bark, H. Markovics, A. Aizenberg, I. Mazaki-Tovi, M. Hagag, A. and Harrus, S.: Evaluation of doramectin for the treatment of experimental canine spirocercosis. Vet. Parasitol. 109: 65-73, 2002.
19. Gokbulut, C. Karademir, U. Boyacioglu, M. and McKellar, Q. A.: Comparative plasma dispositions of ivermectin and doramectin following subcutaneous and oral administration in dogs. Vet. Parasitol. 135: 347-354, 2006.
20. Kelly, P. J. Fisher, M. Lucas, H. and Krecek, R. C.: Treatment of esophageal spirocercosis with milbemycin oxime. Vet. Parasitol. 156: 358-360, 2008.
21. Thompson, K. G. and Pool, R. R.: Tumors of bones. *In:* D. J. Meuten (ed.), Tumors in Domestic Animals, 4th edition, pp. 245-317. Ames, Iowa: Iowa State Press, USA, 2002.
22. Head, K. W. Else, R. W. and Dubielzig, R. R.: Tumors of the alimentary tract. In: Meuten, D. J. (ed.): Tumors in Domestic Animals, 4th edition. Iowa State Press, Ames, Iowa, USA, pp. 401-481, 2002.
23. Undifferentiated and anaplastic sarcoma. In: C. M. Kahn (ed.): The Merck Veterinary Manual, 9th edition. Merk & Co., Whitehouse Station, N.J., USA, pp. 782, 2005.
24. Ridgway, R. L. and Suter, P. F.: Clinical and radiographic signs in primary and metastatic esophageal neoplasms of the dog. J. Am. Vet. Med. Assoc. 174: 700-704, 1979.
25. Stettner, N. Ranen, E., Dank, G. Lavy, E. Brenner, O. and Harmelin, A.:Chemotherapeutic treatment of xenograft Spirocerca lupi-associated sarcoma in a murine model. Comp. Med. 57: 267-271, 2007.
26. Klainbart, S. Mazaki-Tovi, M. Auerbach, N. Aizenberg, I. Bruchim, Y. Dank, G. Lavy, E. Aroch, I. and Harrus, S.: Spirocercosis-associated pyothorax in dogs. Vet. J. 173: 209-214, 2007.
27. Hamir, A. N.: Perforation of thoracic aorta in a dog associated with Spirocerca lupi infection. Aust. Vet. J. 61: 64, 1984.
28. Gal, A. Kleinbart, S. Aizenberg, Z. and Baneth, G.: Aortic thromboembolism associated with Spirocerca lupi infection. Vet. Parasitol. 130: 331-335, 2005.
29. Kirberger, R. M. and Zambelli, A.: Imaging diagnosis-aortic thromboembolism associated with spirocercosis in a dog. Vet. Radiol. Ultrasound. 48: 418-420, 2007.
30. van der Merwe, L. L.: Mandibular salivary gland sialoadenosis in dogs infected with *Spirocerca lupi*: a retrospective study. *In:* 17th European College of Veterinary Internal Medicine Companion Animal (ECVIM-CA) & 9th European Society of Veterinary Clinical Pathology (ESVCP) Congress, Budapest - Hungary, 2007, pp. 212.
31. Schroeder, H. and Berry, W. L.: Salivary gland necrosis in dogs: a retrospective study of 19 cases. J. Small Anim. Pract. 39: 121-125, 1998.
32. Babero, B. B. Fawzi, A. H., and Al-Dabagh, M. A.: Zoonoses In Iraq. Further Studies On Spirocerciasis. Br. Vet. J. 121: 183-190, 1965.
33. Harrus, S. Harmelin, A., Markovics, A. and Bark, H.: Spirocerca lupi infection in the dog: aberrant migration. J. Am. Anim. Hosp. Assoc. 32: 125-130, 1996.
34. Georgi, M. E. Han, H. and Hartrick, D. W.: Spirocerca lupi (Rudolphi, 1809) nodule in the rectum of a dog from Connecticut. Cornell Vet. 70: 42-49, 1980.
35. Wandera, J. G.: Further observations on canine spirocercosis in Kenya. Vet. Rec. 99: 348-351, 1976.
36. Turk, R. D.: Occurrence of the nematode Spirocerca lupi in unusual locations. J. Am. Vet. Med. Assoc. 137: 721-722, 1960.
37. Du Plessis, C. J. Keller, N. and Millward, I. R.: Aberrant extradural spinal migration of Spirocerca lupi: four dogs. J. Small Anim. Pract. 48: 275-278, 2007.
38. Dvir, E. Perl, S. Loeb, E. Shklar-Hirsch, S. Chai, O. Mazaki-Tovi, M. Aroch, I. and Shamir, M. H.: Spinal intramedullary aberrant Spirocerca lupi migration in 3 dogs. J. Vet. Intern. Med. 21: 860-864, 2007.
39. Chai, O. Shelef, I. Brenner, O. Dogadkin, O. Aroch, I. and Shamir, M. H.: Magnetic resonance imaging findings of spinal intramedullary spirocercosis. Vet. Radiol. Ultrasound. 49: 456-459, 2008.
40. Saleem, S. Belal, A. I. and el-Ghandour, N. M.: Spinal cord schistosomiasis: MR imaging appearance with surgical and pathologic correlation. AJNR. Am. J. Neuroradiol. 26: 1646-1654, 2005.

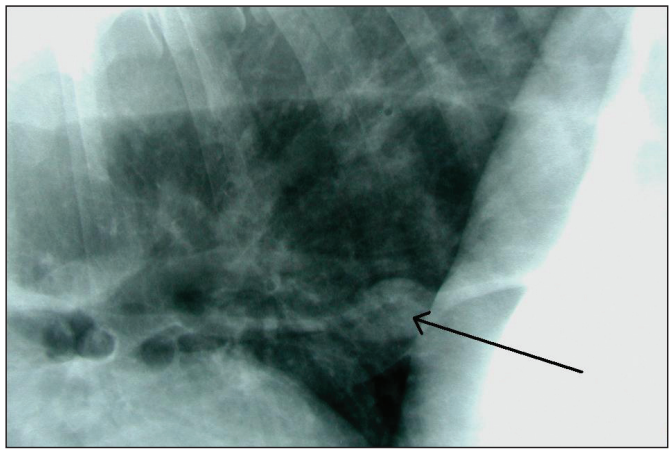

Fig. 1
Collimated right lateral view of the caudodorsal thorax of a dog after pneumo-esophagography. An oval ventral esophageal nodule is highlighted by esophageal gas (arrow). This nodule could not be seen in survey radiographs.

Fig. 2
A typical, elongated, oval, thick-shelled *Spirocerca lupi* egg. The eggs are small (35 × 15 µm) and contain the first-stage larva.

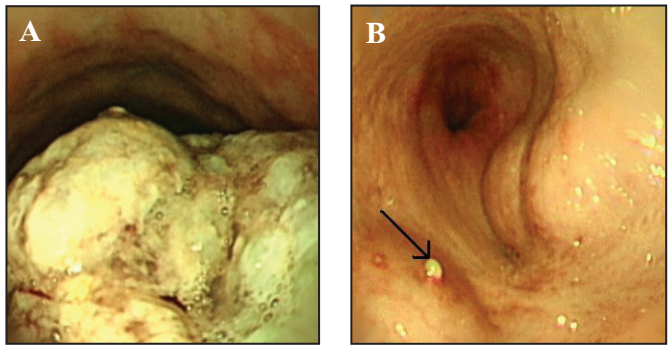

Fig. 3
Esophageal endoscopic photos of a neoplastic mass (A) and three benign nodules (B) in two different dogs. The neoplastic mass is proliferative and lobulated and presents black discolouration due to ulceration and necrosis. This mass is large (15 centimetres in length) and occupies most of the esophageal lumen. The benign nodules have a smooth, round appearance and show a typical protuberance (operculum, arrow). The esophageal mucosa has a normal, healthy appearance. The nodules are small in relation to the oesophageal lumen.

Chapter 7

Discussion and conclusion

Thoracic radiography remains the initial imaging modality of choice to diagnose spirocercosis. The aorta and oesophagus are primarily involved and pathology thereof needs to be optimized on survey radiographs. The oesophagus is not routinely seen on survey films but we have proven that the terminal oesophagus may be seen in large breed dogs in LLR and may thus be confused with a possible caudodorsal mediastinal mass on this view. We have shown that the normal descending aorta is best seen on DV and LLR projections. From the above we concluded that the initial thoracic radiographs should be a DV and RLR view to avoid mistaking normal visibility of the aorta in LLR for pathology. In our further study on the visibility of *S. lupi* associated caudodorsal mediastinal masses, the masses were seen equally well on DV and VD views and there was no difference in visibility between LLR and RLR views. However the DV/VD views identified 86% of masses, whereas RLR/LR only detected 50% of masses, emphasizing the need for orthogonal views. Combining the above information a DV and RLR view are thus the optimal views to make. In cases where sophisticated imaging and other diagnostic tools are not available, or where there are financial constraints, pneumoesophagography was investigated to further elucidate oesophageal pathology characteristics. In this study the lateral views had greater sensitivity than DV/VD views to detect intraluminal pathology with no significant differences in pathology detection between DV and VD views or RLR and LLR views. However in the RLR view, the gastric gas is visible in the fundus of the stomach, potentially allowing easier detection of *S. lupi* associated gastric masses in this view. Pneumoesophagography also allowed the nodule's mural location to be determined and enabled the assessment of nodule surface characteristics to some extent. This is important for possible surgical removal or as an indicator of malignant transformation respectively.

Where available, alternative imaging techniques must also be considered. As most of spirocercosis associated pathology is in the thorax, diagnostic ultrasound has limited use. However, oesophageal masses located adjacent to the diaphragm can, in experienced hands, be visualized transabdominally via a transhepatic approach and may even be biopsied taking special care to avoid the hepatic vasculature, caudal vena cava and aorta. In dogs presented with a history of vomiting and undergoing abdominal ultrasound, the terminal oesophagus should thus be evaluated in endemic *S. lupi* areas. Additionally, in endemic areas, abdominal ultrasound should routinely examine the abdominal aorta, cranial mesenteric and coeliac arteries to screen for potential aneurysm or thrombus formation secondary to the migrating larvae. In our experience, and from unpublished data, abdominal changes are rare but should be looked for. Additionally, *S. lupi* induced iliac thromboembolism must be considered in endemic areas in patients presented with hind quarter paresis or paralysis.

The greater availability of CT in veterinary teaching institutions and specialist veterinary practices has revolutionised the approach to spirocercosis imaging. Computed tomography is much more sensitive than radiographs for aortic mineralization and aneurysm detection and is particularly useful where large aneurysms result in difficult to interpret radiographs.

Aortic thrombus formation, secondary to intimal scarring by migrating larvae, can also be detected using CT angiography. Additionally, mass detection and location is markedly enhanced using CT which is essential for surgical planning. The much greater sensitivity of CT *versus* radiographs to detect metastasis is important in prognostication when considering treatment. Atypical thoracic presentations of spirocercosis are also more readily evaluated using CT, for example, oesophageal perforation with mediastinitis or pyothorax, as well as aberrant migratory secondary haematomas or abscess formation. Dogs in endemic areas presented with neurological deficits originating from the thoracolumbar region should have aberrantly migrating larvae entering the vertebral canal as a differential diagnosis. Although extremely rare, there are several described cases of extradural as well as intramedullary located larvae causing clinical signs. These changes can best be defined using magnetic resonance imaging.

Malignant transformation of spirocercosis-associated oesophageal lesions is well-described and has grave implications for the patient, usually resulting in expensive surgery and possible chemo- or radiation therapy, or alternatively, euthanasia. This thesis contains a number of clinical, clinical pathological and imaging parameters that have been evaluated in order to detect malignant transformation. From a radiographic perspective, larger masses in older dogs are more likely to be malignant, hypertrophic osteopathy is a very specific indicator of malignancy, but lacks sensitivity and spondylitis may be more prevalent in malignant cases. These findings can also be extrapolated to CT findings. Additionally on CT the prevalence of aortic mineralization is significantly higher in malignant transformation cases.

Metastasis of the spirocercosis-induced oesophageal sarcoma, usually osteosarcoma or fibrosarcoma, is well-recognised and may involve multiple body sites. Any dog in endemic areas that has metastatic disease, and that does not have an obvious primary neoplasm, must have a primary *S. lupi*-associated caudal oesophageal neoplasm ruled out. Metastatic sites most commonly reported include the lungs, tracheobronchial lymph nodes, liver, heart, pleura and kidney less frequent spread to the omentum, peritoneum, pancreas, diaphragm, spleen, mediastinum and subcutis. We have described two new metastatic locations of *S. lupi*-associated tumours: oesophageal chondrosarcoma that spread to the spinal cord and oesophageal osteosarcoma that spread to the brain and spinal cord. This implies that the clinician must consider brain or spinal cord metastasis as well as extradural and intramedullary aberrant larval migration in any dog presenting with neurological deficits.

This thesis has defined radiographic procedures to maximise their diagnostic accuracy. In addition the value of CT has been demonstrated in further defining the pathology and the limited benefits of diagnostic ultrasound and MRI have been elucidated. Future spirocercosis-associated research should now be directed at the earlier and more specific detection of malignant transformation of the benign nodule as well as determining the pathomechanisms of neoplastic transformation and spondylitis reactions. Here the CT characteristics of the oesophageal mass and in particular vascularisation patterns during early and late arterial and venous flow after contrast administration may be beneficial.

Spirocercosis produces three lesions that involve uncontrolled mesenchymal proliferation, namely hypertrophic osteopathy, spondylitis and sarcoma. No other infection in the dog produces this set of lesions and the mesenchymal proliferation is thus more likely to have common features that are uniquely related to this disease and its pathogen. It may be that the *S. lupi* nematode directly secretes or induces secretion of humoral factors that stimulate mesenchymal cells. If such a factor is induced, it may be through a unique inflammatory response or positive feedback stimulation of the mesenchymal tissue. This needs to be proven and its effect on lesion characteristic should be investigated by means of sophisticated imaging techniques and other methodologies.